SYNTHESIS OF GUEST MOLECULES FOR STUDIES OF UREA INCLUSION COMPOUNDS

by

ANGELA DEE ADAMS

B.S., Winona State University, 2009

A THESIS

submitted in partial fulfillment of the requirements for the degree

MASTER OF SCIENCE

Department of Chemistry
College of Arts and Sciences

KANSAS STATE UNIVERSITY
Manhattan, Kansas

2011

Approved by:

Major Professor
Mark D. Hollingsworth

Abstract

Most urea inclusion compounds (UICs) are known to share a common packing arrangement in which the urea host forms helical ribbons held together by hydrogen bonds to form a series of linear, hexagonal tunnels. Because UICs can encapsulate a wide variety of linear guest molecules, they serve as useful model systems for probing mechanisms of crystal growth and molecular recognition. In this thesis, the syntheses (or attempts thereof) of six compounds that will serve as consequential guest molecules in studies of UICs are presented. These compounds are (5*S*,6*S*)-2,9-decanedione-d_2, 1,6-dicyanohexane-1,1,6,6-d_4, 1,11-undecanedioic acid, bis(3-oxobutyl) adipate, 2,16-heptadecanedione, and 2-eicosanone. With the exception of (5*S*,6*S*)-2,9-decanedione-d_2, whose synthesis remains incomplete, detailed synthesis and crystal growth of the UICs of these compounds are discussed. Ongoing studies with the UICs containing these guests include the determination of the absolute configuration of UICs, the study of guest conformer population changes via solid-state NMR, the development and identification of novel ferroelastic UICs, and the classification of guest ordering in a series of alkanedione UICs.

Table of Contents

List of Figures

Acknowledgements

I would like to acknowledge Dr. Mark Hollingsworth for all of his help and support. I greatly appreciate everything he has done and I feel honored to have worked in his group. I would also like to acknowledge the members of the Hollingsworth group that I had the privilege of working with: Shane Nichols, Bo Wang, Dr. Farhod Nozirav, Dr. Eric Chan, Dr. Roman Gajda, Jithma Abeykoon, and Clayton Galloway. Also, I want to thank my committee members, Dr. Stefan Bossmann and Dr. Vikas Berry for their time and feedback. Lastly, I would like to thank many of the students and faculty in the Kansas State Chemistry Department for their help and guidance.

Dedication

This work has been dedicated to my family, as they have provided constant love and support throughout my life. I want to thank my fiancé, Nihar, for everything he has done for me. He is truly an inspiration to me and I am extremely proud of him for everything that he has accomplished. I also want to thank my parents for always being there for me. They are the most dedicated and hard working people I know, and I appreciate everything they have taught me. Finally, I would like to thank my brother, Anthony, for his support. I couldn't ask for anyone better as a brother or as a friend.

CHAPTER 1 - General Introduction

Urea Inclusion Compounds

Since the discovery of the first urea inclusion compounds (UICs) in 1940 by M. F. Bengen,[1] urea has been extensively studied as a host molecule owing to its ability to form multiple hydrogen-bonded networks.[2] In its pure form, urea crystallizes as a tetragonal structure in which each oxygen is tethered to four hydrogens. However, when a suitable guest is present, the urea molecules spontaneously form channel structures that surround the guest. The structures of conventional UICs comprise a series of linear, hexagonal tunnels containing helical ribbons of hydrogen bonded urea molecules.[3,4] These helical ribbons run in opposite directions (Figure 1-1A), much like the double helix of DNA, and repeat every six urea molecules (11.0 Å).[4] Unlike physiological DNA, most UICs can exist as either right-handed or left-handed helices. However, when incorporating certain classes of guest molecules, urea can form a non-helical hydrogen-bonded network described as a stacked loop.[5] These stacked loops are generally characterized as low symmetry (biaxial) systems, and are usually adopted for guests with the formula $X(CH_2)_6Y$ (X, Y = Br, Cl, CN, NC).[5]

The hexagonal tunnels of UICs are found to be stable only when filled with a suitable guest. Because these tunnels are narrow, UICs can only accommodate guests of long n-alkane chains (and analogs) with a small degree of substitution.[2,6] Owing to the relatively smooth, yet rigid, urea channels, guests are often held loosely within the channels and frequently undergo torsions, librations, and translations.[6] This disorder of the guests about the channel axis helps maintain the hexagonal symmetry of the host structure. However, in the case of guests containing suitably placed hydrogen bond acceptors, urea molecules can break their hydrogen-bonded network by turning toward the guest molecule to form new host-to-guest hydrogen bonds.[6] In some cases, such as with some diketones, the urea channel is distorted away from its usual hexagonal symmetry due to host-to-guest hydrogen bonding.

Most UICs are incommensurate, that is they have a non-stoichiometric relationship between the periodic repeat distances of the host ($\boldsymbol{c}_h$) and guest ($\boldsymbol{c}_g$). In other words, the host may have its own periodic repeat that is separate from the guest such that there are no reasonably small integers m and n for which $n\boldsymbol{c}_h = m\boldsymbol{c}_g$ (Figure 1-1C).[4] In some cases, however,

commensurate UICs can be formed such that a reasonably small integer is defined for *m* and *n* for which $n\boldsymbol{c}_h' = m\boldsymbol{c}_g'$ (the primes are introduced to differentiate the host and guest repeats from the true ***c*** axis for a commensurate system).[6] In general, much less motional freedom of guest molecules is seen in commensurate UICs.[6]

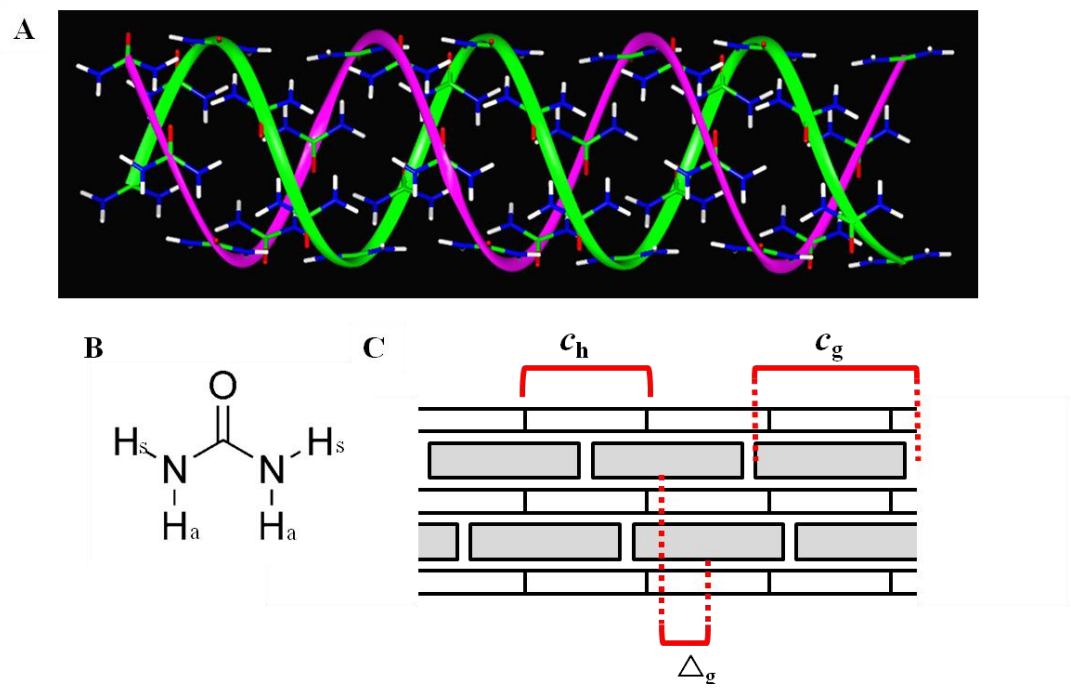

Figure 1-1: (A) The helix structure of one host channel of a UIC. (B) Chemical structure of urea molecule, with the syn and anti hydrogen denoted as H_s and H_a, respectively. (C) A 2D view of an incommensurate UIC, defining c_g and $\boldsymbol{c}_h$. Note that for a urea host, $\boldsymbol{c}_h$ represents one turn of the helix, or six urea molecules. The symbol $\triangle_g$ denotes the offset between guests in adjacent channels of a UIC. [Adapted with permission from M. D. Hollingsworth, *et al.*, *Science*. **273**, 1355-1359 (1996)]

Applications of Urea Inclusion Compounds

Since their discovery, UICs have been utilized in a variety of applications in both research and industry. One such application that has been well studied since the 1960s is the production of linear macromolecules via polymerization within the channels of UICs.[7] High-energy radiation (such as gamma- or X-rays) can serve as initiators, thus allowing monomers within the urea channels to polymerize. A major benefit of inclusion polymerization is the ability to produce entirely unbranched polymers. In addition, the formation of byproducts is

generally limited and the macromolecular nature of the polymeric product makes it easy to separate the urea host from the guest by selective dissolution.[7] For example, in 1960 D. M. White reported that 1,3-butadiene could be polymerized to polybutadiene by irradiating with X-rays.[8]

Orienting molecules for spectroscopic research has also been a common use of UICs, as in the case of electron spin resonance (ESR) spectroscopic studies.[9] ESR detects the presence of paramagnetic guest species (i.e., species having unpaired electrons). As a result, ESR is commonly used to investigate free radicals. Since UICs can accommodate guest molecules within the channels, irradiating these inclusion compounds with either X-rays or gamma-rays can generate free radicals.[9] Because these free radicals are trapped within the urea structure, they remain intact for longer durations and provide a convenient medium for ESR studies. For example, O. H. Griffith was able to generate several free radicals from single crystals of inclusion compounds formed between long-chain alkyl esters and urea by irradiating with X-rays at room temperature.[10] Additionally, because guest molecules are known to fit only loosely in the urea channels, Griffith was able to investigate the orientation and molecular motion of these ester radicals.[10]

Given the limited size of UIC hexagonal tunnels (approximately 5.5 to 5.8 Å),[6] urea prefers to form inclusion compounds with straight chain hydrocarbons rather than guests containing side chains or large substituents.[6] Thus, UICs make molecular separation possible by distinguishing linear from branched hydrocarbons. This becomes important for the separation of branched from unbranched fatty acids. It has been shown that by utilizing liquid chromatography techniques, fatty acids of linear chains were incorporated into inclusion compounds while their branched analogs were eluted from the column. For example, Cason and co-workers were able to separate and identify a saturated fatty acid from an unsaturated ester isolated from bacterial extracts.[6]

A unique application of UICs that has not received much attention involves the resolution of enantiomers. Urea is an achiral molecule; however, it is able to form chiral inclusion compounds upon crystallization with a guest. The chiral environment of the guest is created by the helical packing of the urea host, enabling a single crystal to have either a right-handed or left-handed host spiral.[11,12] The chirality of the urea tunnel is generated spontaneously during crystal growth;[3] thus, spontaneous resolution of UICs can lead to chiral discrimination between guest

enantiomers.[13] Studies have shown that there is a correlation between the chirality of the guest and the helical configurations of the host.[12] This makes it possible to obtain a UIC crystal containing a guest of preferred configuration by simply seeding a crystallizing solution with a crystal of the desired configuration. For example, Schlenk and co-workers utilized this seeding technique to obtain 95.6% of a single enantiomer ((+)-2-chlorooctane) from a racemic mixture.[12]

The final application that will be discussed is the use of UICs to better understand domain switching in ferroelastic and ferroelectric materials. Ferroelectricity refers to materials that have different domain orientations that can be switched by application of an external electric field. Similarly, ferroelasticity is observed in compounds that exhibit different domain orientations that can be interconverted through the application of an external mechanical stress (Figure 1-2).[14,15] Ferroelasticity and ferroelectricity are closely related, and many crystals display both properties. Single crystals of simple molecular materials that undergo observable elastic phenomena, such as UICs, can provide a route for probing the elastic properties of solids, which are relevant in the domain switching of ferroelectrics.[15] Although most ferroelectrics in industry are made of inorganic materials, organic materials provide advantages, such as: low molecular mass, flexibility, low toxicity, and low expense.[16] A better understanding of domain switching processes in organic solids is important for the development of all-organic (i.e. carbon based) electronic and photonic devices.[16]

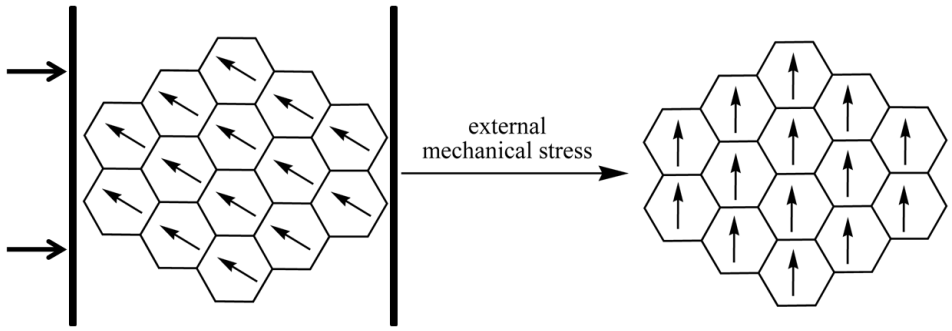

Figure 1-2: An example of stress induced domain reorientation of guest molecules within a UIC, demonstrating the effects of ferroelasticity. Guest molecules typically undergo 60° rotations within the hexagonal channels.

The synthesis of six compounds (or attempts thereof), which will serve as consequential guest molecules in the studies of UICs, will be presented in this thesis. These compounds include: (5*S*,6*S*)-2,9-decanedione-d_2, 1,6-dicyanohexane-1,1,6,6-d_4, 1,11-undecanedioic acid,

bis(3-oxobutyl) adipate, 2,16-heptadecanedione, and 2-eicosanone. The importance, synthesis, and crystal growth of these six compounds will be discussed. The relevant studies that will be examined for UICs containing these compounds include, but are not limited to: the determination of the absolute configuration of UICs, the characterization of molecular recognition, the development and identification of novel ferroelastic UICs, and the classification of guest ordering in a series of related structures.

Chapter 1 References

1 Bengen, M., F. OZ 123438 Mar. 18, 1940; German Patent 869,070 (1953); Technical Oil Mission Reel, 1945, 143, 135; CA: 48:11479c. *German Patent Appl.*, (1940).

2 Li, Q. and Mak, T. C. W. Hydrogen-bonded urea-anion host lattices. 4. Comparative study of inclusion compounds of urea with tetraethylammonium and tetraethylphosphonium chlorides. *J. Inclusion Phenom. Mol. Recognit. Chem.* **28**, 151-161, (1997).

3 Yeo, L. and Harris, K. D. M. Temperature-dependent structural properties of a solid urea inclusion compound containing chiral guest molecules: 2-bromotetradecane/urea. *Can. J. Chem.* **77**, 2105-2118, (1999).

4 Hollingsworth, M. D., Brown, M. E., Hillier, A. C., Santarsiero, B. D. and Chaney, J. D. Superstructure control in the crystal growth and ordering of urea inclusion compounds. *Science* **273**, 1355-1359, (1996).

5 Hollingsworth, M. D., Peterson, M. L., Pate, K. L., Dinkelmeyer, B. D. and Brown, M. E. Unanticipated guest motion during a phase transition in a ferroelastic inclusion compound. *J. Am. Chem. Soc.* **124**, 2094-2095, (2002).

6 Hollingsworth, M. D. and Harris, K. D. M. in *Comprehensive Supramolecular Chemistry* Vol. 6 (eds. D. D. MacNicol, F. Toda, and R. Bishop) pp. 177-237 (Elsevier Science Ltd., Oxford, 1996).

7 Farina, M. in *Inclusion Compounds* Vol. 3 (eds. J. L. Atwood, J. E. D. Davies, and D. D. MacNicol) pp. 297-329 (Academic, London, 1984).

8 White, D. M. Stereospecific polymerization in urea canal complexes. *J. Am. Chem. Soc.* **82**, 5678-5685, (1960).

9 Davies, J. E. D. in *Inclusion Compounds* Vol. 3 (eds. J. L. Atwood, J. E. D. Davies, and D. D. MacNicol) pp. 37-68 (Academic, London, 1984).

10 Griffith, O. H. Electron spin resonance and molecular motion of the $RCH_2CHCOOR'$ radical in X-irradiated ester-urea inclusion compounds. *J. Chem. Phys.* **41**, 1093-1105, (1964).

11 Brown, M. E., Chaney, J. D., Santarsiero, B. D. and Hollingsworth, M. D. Superstructure topologies and host-guest interactions in commensurate inclusion compounds of urea with bis(methyl ketone)s. *Chem. Mater.* **8**, 1588-1591, (1996).

12 Schlenk, W., Jr. Asymmetric urea inclusion lattice. I. Separation of racemates. *Justus Liebigs Ann. Chem* **7**, 1145-1155, (1973).

13 Hollingsworth, M. D., Brown, M. E., Dudley, M., Chung, H., Peterson, M. L. and Hillier, A. C. Template effects, asymmetry, and twinning in helical inclusion compounds. *Angew. Chem. Intl. Ed. Engl.* **41**, 965-969, (2002).
14 Brown, M. E. and Hollingsworth, M. D. Stress-induced domain reorientation in urea inclusion compounds. *Nature (London)* **376**, 323-327, (1995).
15 Hollingsworth, M. D., Peterson, M. L., Rush, J. R., Brown, M. E., Abel, M. J., Black, A. A., Dudley, M., Raghothamachar, B., Werner-Zwanziger, U., Still, E. J. and Vanecko, J. A. Memory and perfection in ferroelastic inclusion compounds. *Cryst. Growth Des.* **5**, 2100-2116, (2005).
16 Horiuchi, S. and Tokura, Y. Organic ferroelectrics. *Nat. Mater.* **7**, 357-366, (2008).

CHAPTER 2 - (5*S*,6*S*)-2,9-Decanedione-d_2/urea

Introduction

As previously mentioned, UICs have the capability of resolving racemic mixtures; however, the difficulty with this application is that it is currently impossible to identify which configuration (i.e. handedness) of the urea host structure is present.[1] It is known that *R*-guest/(right-handed)-host and *S*-guest/(right-handed)-host systems are diastereomeric and have different energies.[2-4] Therefore, one enantiomeric guest usually favors inclusion into a urea host with a particular handedness. (Although such UICs are most properly termed "diastereomorphs," the host structures are enantiomorphic.) For example, through extensive research on stereoselective UIC formation, Schlenk and co-workers discovered that one enantiomorphic host configuration ("A") selectively incorporated (-)-2-butyldecanoate, whereas the other enantiomorph ("B") incorporated (+)-2-butyldecanoate.[3] However, the absolute configurations of "A" and "B" are unknown. From this work, Schlenk proposed a model that compared the relative fits of guest molecules within the available space in a given UIC channel. This model was based on the known crystal structure of the urea host and an examination of the space available to a chiral guest (Figure 2-1).[1,5,6] Unfortunately, this model lacks rigor due to the lack of structural information. That is, no crystal structures have been reported for the systems Schlenk has studied. Lenné's work using photographic methods[7] suggests that Schlenk's principal model compound ((*S*,*S*)-3-21-dimethyltetracosane/urea) is commensurate with $\boldsymbol{c}_g$ = 33.04 Å ($1\boldsymbol{c}_g' = 3\boldsymbol{c}_h'$), but without high-resolution crystallographic data, there is no way of knowing if this system is commensurate or incommensurate. If this system is incommensurate, then the guest molecules are located in a multitude of different host environments along the urea channels. Thus, if Schlenk had studied an incommensurate system, then his model is unreliable. Even if his systems had been commensurate, the full structure would still be needed to test his structural models. To interpret Schlenk's results more clearly, it would be beneficial to determine the absolute configuration of a UIC, which will in turn validate (or refute) his proposed model.

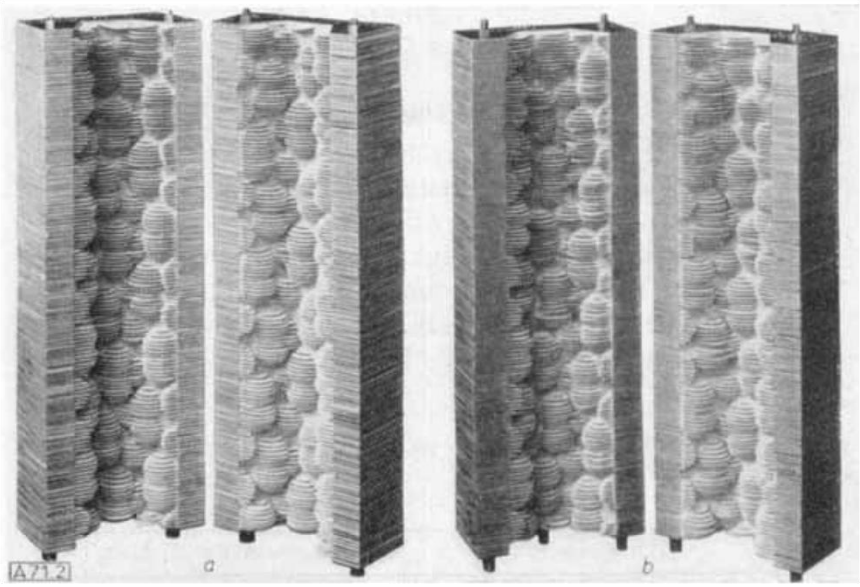

Figure 2-1: Space filling model used by Schlenk to predict relative fits of guest molecules within the available space in a given UIC channel. Left-handed (left image) and right-handed (right image) helices are shown. [Taken with permission from W. Schlenk. *Angew. Chem.* **72**, 845-849 (1960)]

More recently, Hollingsworth has developed a crystal growth model that can be used to disentangle the complex optical textures of optically anomalous UICs containing mixtures of guests. This model accounts for recognition patterns and can be used to predict major features of stable crystal packing arrangements for UIC hosts and guests.[8] However, the absolute configuration of a UIC is still needed to provide a benchmark for this crystal growth model. A more detailed description of Hollingsworth's crystal growth model will be discussed in the following paragraphs.

Crystal Growth Model and Molecular Recognition

To understand the dynamics of host-guest relationships in crystal growth, it is important to investigate the molecular recognition phenomena (i.e. the specific interactions) involving the host and guest molecules. Molecular recognition events between hosts and guests can be easily visualized by examining McBride's schematic representation of the "packing of ducks" (Figure 2-2A).[9] This model contains host and guest ducks, in which the guest ducks have projections behind their heads that generate repulsive contacts with any adjacent ducks. Because a repulsive contact would be generated if it were to lead with its head, guest ducks are only incorporated "head-up" on the top face of the crystal and "head-down" on the bottom face of the crystal.

Once the guest ducks bind, "head-up" for example, then the host ducks can easily lock the guest in place by coming in from behind, as shown at the top of the diagram in Figure 2-2A. However, guest ducks are not easily locked into position on the right and left edges of the crystal due to slow overgrowth by the host molecules.[9] Because guest ducks are only incorporated by the top and bottom surfaces, a division of the crystal into four triangular sectors may result.[9] These processes represent the growth face-specific incorporation of impurities and can be used to explain the sectoring observed in many UIC crystals (Figure 2-2B).

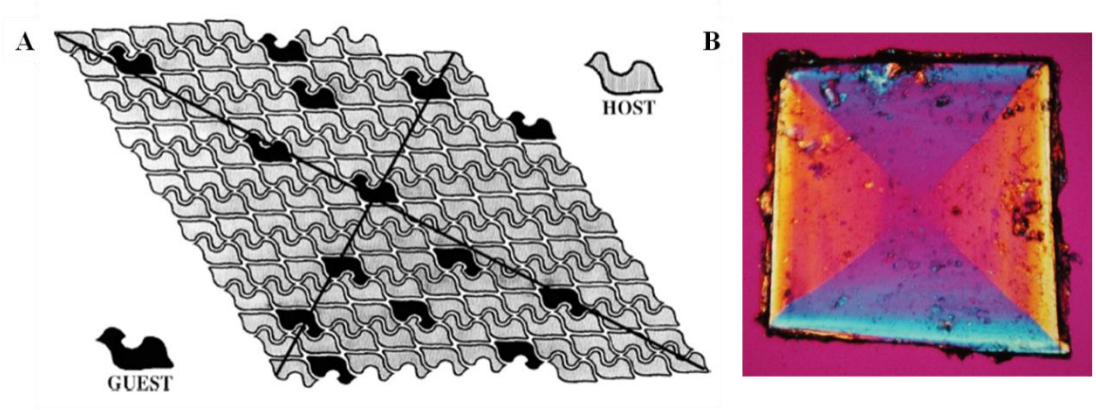

Figure 2-2: (A) McBride's "packing of ducks" model illustrating growth face-specific incorporation of impurities, in which the lines are a guide to the eye showing the division of the crystal into sectors. (B) Photomicrograph showing sectoring and anomalous birefringence of a mixed crystal. [Fig. A adapted with permission from J. M. McBride, *Angew. Chem. Intl. Ed.*, **28**, 377-379 (1989); Fig. B adapted with permission from J. M. McBride and S. B. Bertman, *Angew. Chem. Intl. Ed.*, **28**, 330-333 (1989)]

In addition to growth face-specific incorporation of impurities, UICs have also been observed to undergo template-directed growth.[10] Figure 2-3 illustrates the template-directed mechanism proposed for UICs. Protrusion of guest molecules from the urea host channel (Figure 2-3B) causes host molecules to wrap around the guests, resulting in the formation of new ledges (Figure 2-3C). Guest molecules then bind to ledge and kink sites (Figure 2-3D), once again allowing more host molecules to wrap around the guests (Figure 2-3E). The guest-directed addition of urea seen in Figure 2-3E forms a terrace, and successive additions of guest and host cause rapid buildup of the terrace in two dimensions.[10] It is plausible that after the initiation events shown here, further growth can occur in a spiral fashion, thus causing left-handed or

right-handed spiral growths. Indeed, such growth spirals have been observed in certain crystals of 2,9-decanedione/urea.[11]

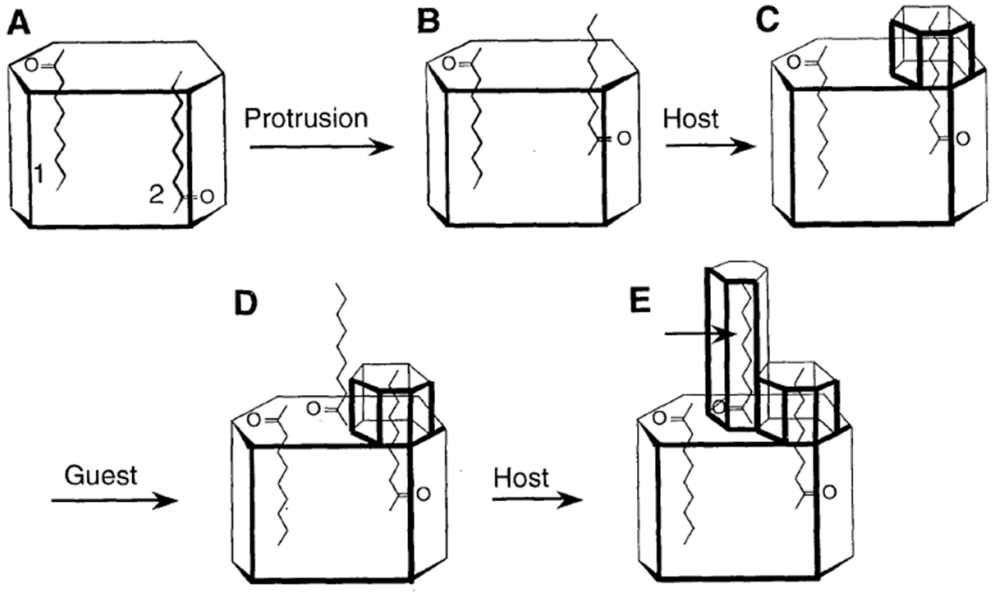

Figure 2-3: Template-directed mechanism for nucleation and crystal growth along channel axes of UICs. (A) Starting position. (B) Guest 2 protrudes from its starting position. (C) Urea molecules add to surface site. (D) A third guest attaches itself to kink site. (E) Templated addition of urea forms a terrace, allowing further growth to occur. [Taken with permission from M. D. Hollingsworth, *et al*., *Science*, **273**, 1355-1359 (1996)]

Upon combination of the concepts of both face-specific incorporation and template-directed growth, the framework for Hollingsworth's crystal growth model begins to emerge. If, for example, a UIC with a right-handed helix grows in a clockwise spiral direction, it can be inferred that this system will contain different recognition sites (i.e., guest binding sites) than a left-handed helix with a clockwise growth spiral. For further discussion of this crystal growth model, a UIC system containing a mixture of 90% 2,9-decanedione and 10% 2-decanone will be used as the model system.

With 2,9-decanedione/urea, the stoichiometry is $3\boldsymbol{c}_g' = 4\boldsymbol{c}_h'$. In other words, the guest is 4/3 the length of the urea helix repeat, so a commensurate structure is obtained by applying a threefold screw axis to the guest. The crystal exists in either of two enantiomorphous space groups, $P3_112$ or $P3_212$, which have right and left handed helices, respectively. Guests are

related by a threefold screw axis, so along the channel, each unit cell (four urea repeats) contains three guest molecules.

For alkanedione/urea inclusion compounds such as 2,9-decanedione/urea, guest carbonyl groups serve as readily available hydrogen bond acceptors for the syn N-H groups of the urea molecules.[4] (See Figure 2-4C.) Urea molecules that serve as available recognition sites will be represented as red wedges, such that the larger end of the wedge points in the direction of the recognition site (Figure 2-4D).

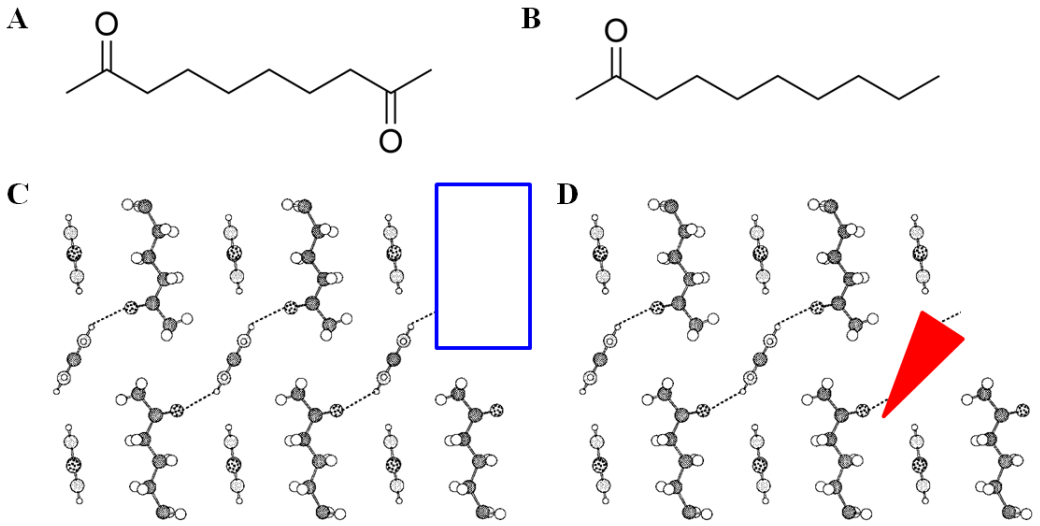

Figure 2-4: (A) Chemical structure of 2,9-decanedione. (B) Chemical structure of 2-decanone. (C) Cutaway view illustrating the rotation of ureas to form hydrogen bonds with diketone-containing guests. The blue box indicates an available recognition for a guest molecule to bind. (D) Red wedge symbolizing a urea molecule that is available for hydrogen bonding with a guest's carbonyl group. [Figs. C and D adapted with permission from M. E. Brown, *et al.*, *Chem. Mater.* **8**, 1588-1591 (1996)]

If we were to examine one underlayer of a UIC crystal containing a 9:1 mixture of 2,9-decanedione and 2-decanone (Figure 2-5), the recognition sites available for new guest molecules can be classified by the different orientations of the hydrogen bond donating ureas in the kink sites. Because 2,9-decanedione/urea has a threefold screw axis ($3\boldsymbol{c}_g' = 4\boldsymbol{c}_h'$), the recognition sites for the crystal growth model are identified for three underlayers. The urea helix rotates 120 degrees as each additional layer is added; thus, the addition of three layers will result

in a net rotation of 360 degrees. As a result, the fourth layer will have the same recognition sites defined by the first layer.

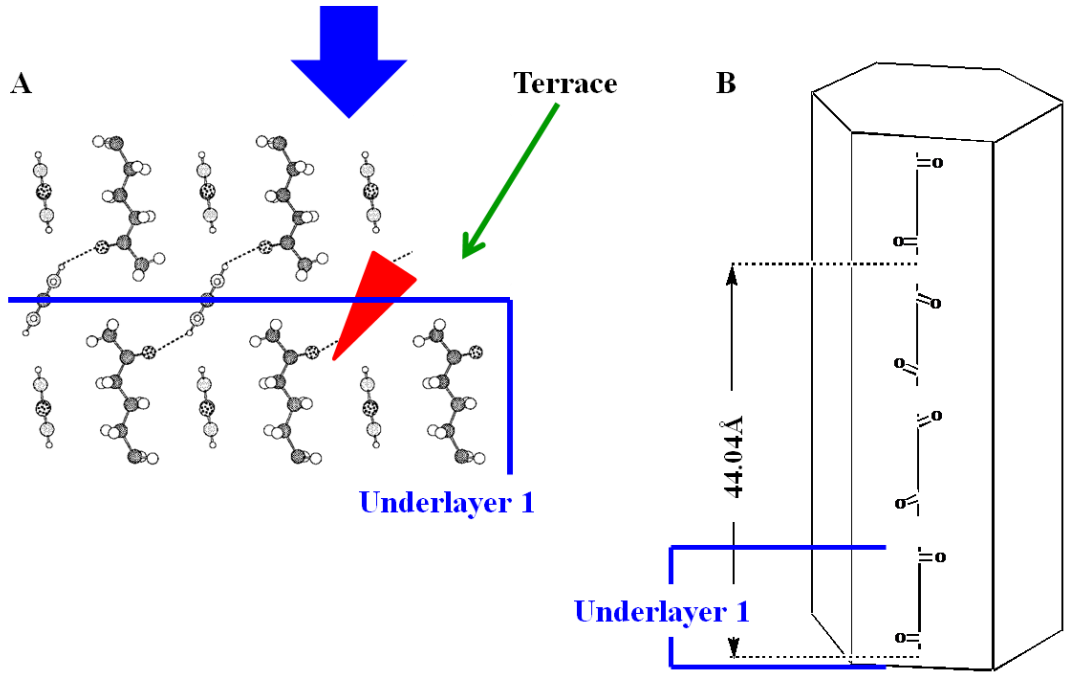

Figure 2-5: (A) A terrace with an available recognition site is illustrated by looking down the urea channel axis (large blue arrow) at underlayer 1. (B) Urea channel containing 2,9-decanedione with one underlayer of the crystal indicated in blue. Underlayers 2, 3, etc. would continue vertically up the channel as each guest molecule successively adds according to template-directed growth. [Fig. A adapted with permission from M. E. Brown, *et al.*, *Chem. Mater.* **8**, 1588-1591 (1996); Fig. B provided courtesy of M. D. Hollingsworth]

Figure 2-6 illustrates that for a UIC of a 9:1 mixture of 2,9-decanedione and 2-decanone crystal with a right-handed helix and a clockwise growth spiral, "Type 1", "Type 2", "Type 3", and "Type 4" recognition sites can be identified. "Type 1" represents a urea molecule that has turned into the channel in such a way that it is positioned on the leading edge of the clockwise growth spiral. "Type 2" represents a urea molecule that is available for binding, not at the leading edge of the growth spiral, but one channel over. Likewise, "Type 3" is yet one more channel over. "Type 4" represents a terrace that does not contain a urea molecule that can be used as a hydrogen bond donor. These types of recognition sites can be identified for each layer of the crystal as guest molecules add according to the template-directed growth mechanism (Figure 2-6).

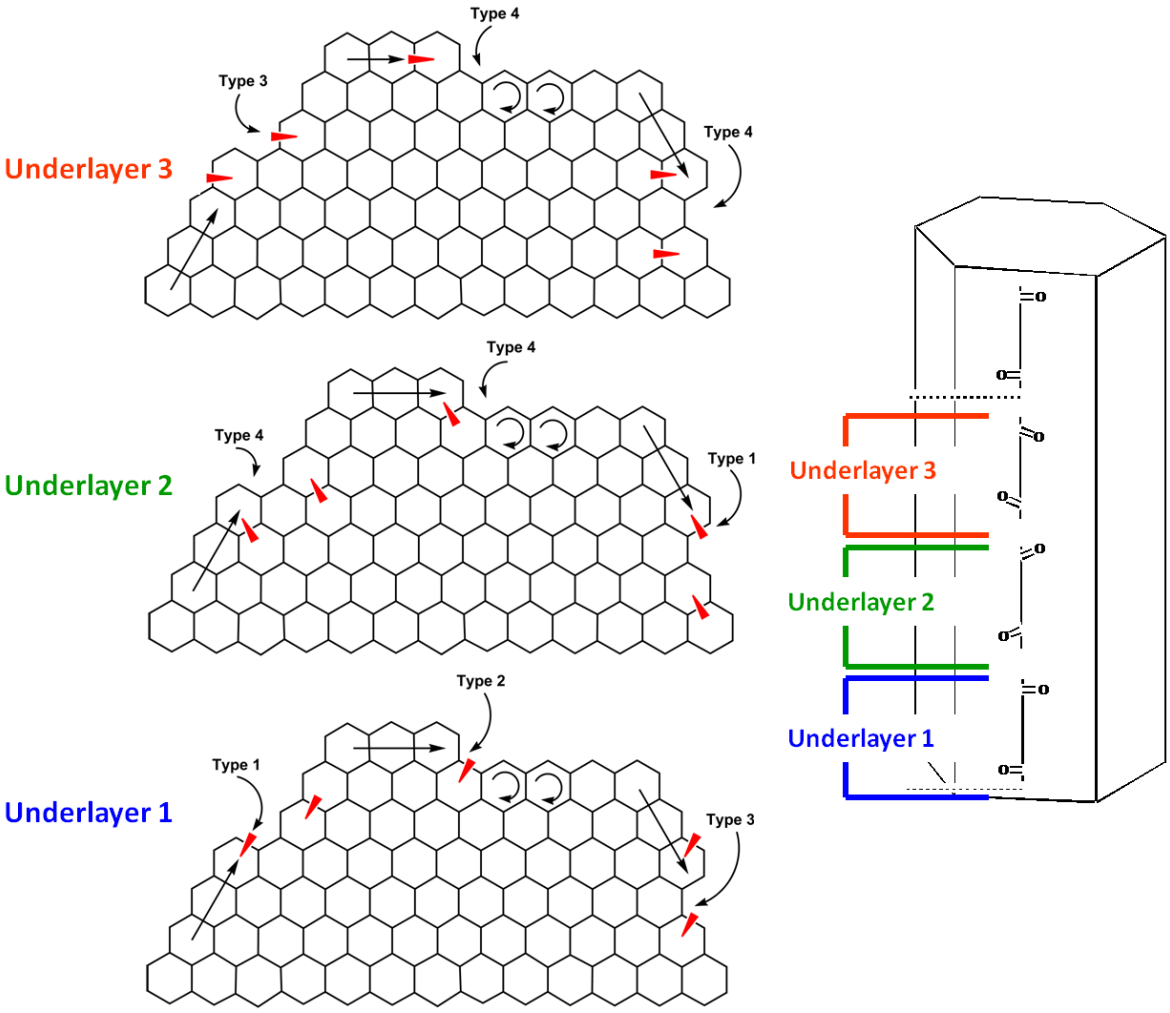

Figure 2-6: Using the crystal growth model to define the available recognition sites for each layer of the crystal. Note that after three layers, the urea helix has rotated by 360 degrees, causing layer 4 to be identical to layer 1. In the diagram, the curved arrows represent the handedness of the helix (right-handed), and straight arrows represent the direction of growth spiral (clockwise). [Provided courtesy of M. D. Hollingsworth]

The types of recognition sites for each layer, for either a right-handed or left-handed urea helix, have been organized in a table (Figure 2-7A), which shows that both the left and right growth faces have the same types of recognition sites, whereas the top face of the crystal is different. For example, with a right-handed helix having a clockwise growth spiral, the left and right sides of the crystal display "Type 1", "Type 3", and "Type 4" recognition sites, whereas the top of the crystal displays "Type 2" and "Type 4" sites. Because every other face has the same recognition sites, crystals are often divided into alternating sectors (Figure 2-7B).

A

Recognition sites available to a crystal from a 9:1 mixture of 2,9-decanedione and 2-decanone with a clockwise growth spiral			
	Left face of crystal	**Top face of crystal**	**Right face of crystal**
Right-handed helix	Type 1 Type 3 Type 4	Type 2 Type 4 Type 4	Type 1 Type 3 Type 4
Left-handed helix	Type 2 Type 4 Type 4	Type 1 Type 3 Type 4	Type 2 Type 4 Type 4

B

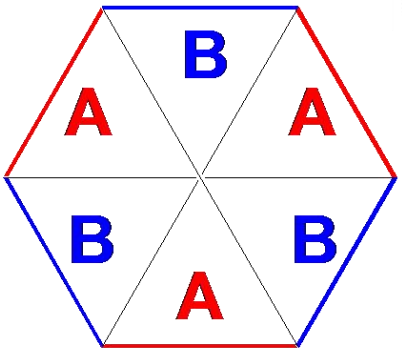

C

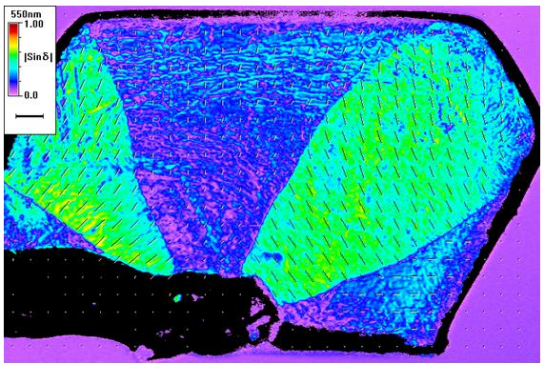

Figure 2-7: (A) Table defining the types of recognition sites for a UIC crystal grown from a 9:1 mixture of 2,9-decanedione and 2-decanone, here with a clockwise growth spiral having either a right-handed or left-handed helix. (B) Figure showing alternating sectors created in crystals as a result of various recognition sites located on different growth faces of crystals. (C) Metripol[12] retardation map for a crystal grown from a solution containing a 9:1 mixture of 2,9-decanedione and 2-decanone. The differences in retardation between sectors illustrate the alternating intersectoral zoning. [Figs. B and C adapted from J. R. Rush. *Ph.D. Dissertation*, Kansas State University (2007)]

Hollingsworth's crystal growth model is useful for unraveling the complex optical textures of optically anomalous UICs containing mixtures of guests.[8] One issue remains however, in that the absolute configuration of one UIC is needed in order to reliably formulate predictions from this model. To accomplish the objective of unambiguously defining the absolute configuration of a UIC, correlations with optical rotation will be utilized.

Correlating Optical Rotation with Absolute Configuration

As previously mentioned, identifying the absolute configuration of a UIC is imperative for the support of several theoretical models. The main objective of this project is to correlate optical rotation with absolute configuration of UICs. This can be accomplished by using single crystal neutron diffraction of UICs containing stereospecifically-deuterated guests. Since it is possible to use polarized light microscopy to image the optical rotation[13] (i.e. dextrorotary or levorotary) of a uniaxial crystal (Figure 2-8), this assignment will allow us to unambiguously establish a relationship between optical rotation and absolute configuration (i.e. left-handed or right-handed helices) of UICs. By using a chiral guest whose optical rotation is essentially zero, there will be no ambiguity about the source of the optical rotation in the UIC.

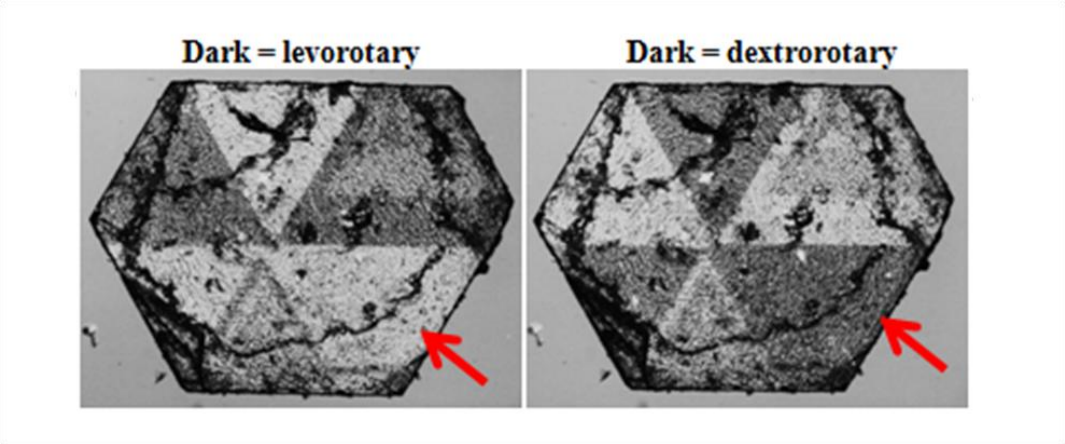

Figure 2-8: Optical images of 2,12-tridecanedione/urea that illustrate how polarized light microscopy can be used to differentiate levorotary and dextrorotary domains in uniaxial crystals. The red arrow points to a domain that is dextrorotary. Polarized light of 546 nm was used, and the analyzer was rotated counterclockwise (left image) and clockwise (right image) by 9° from the crossed position. [Adapted with permission from M. D. Hollingsworth, *et al. Angew. Chem. Intl. Ed.* **41**, 965-969 (2002)]

Previous attempts to assign the absolute configuration of a urea helix utilized several heavy-atom containing guest molecules that had been predicted to give commensurate, uniaxial structures amenable to optical rotation studies.[14] However, these studies proved unsuccessful because the observed structures were either biaxial, centrosymmetric, incommensurate, or had large superstructures. Without specialized equipment, having a biaxial system (i.e., with two

optic axes) prevents optical rotation studies since biaxial systems display linear birefringence, which is typically orders of magnitude larger than optical rotation.

As an alternative to heavy-atom containing guests, we chose to stereospecifically deuterate 2,9-decanedione. Deuterons are known to be efficient neutron scatterers; that is, the difference between the neutron scattering lengths of hydrogen (-3.7046 fm) and deuterium (+6.671 fm) allows these two isotopes to be readily distinguishable in a neutron-scattering experiment.[15] For example, Koetzle and co-workers have shown that neutron diffraction can be used to determine absolute configurations of molecules containing chiral methylene groups (R-CHD-R').[15] By utilizing Koetzle's techniques for identifying chiral methylene groups, we will be able to distinguish the chirality of deuterons placed in the 5- and 6-carbon positions of 2,9-decanedione. Because the chirality of the deuterium labeled guests (i.e. *R,R*, or *S,S*) would already be known, the information gathered from the neutron diffraction experiments will allow us to determine the absolute configuration of the urea helix. In other words, the guest's configuration will serve as a reference point for defining the handedness of the urea helix.

For this project, 2,9-decanedione/urea was chosen as an appropriate guest to study since its crystal structure has already been reported (Figure 2-9B),[10] thus allowing for easy structural characterization of its deuterated analog. The system of 2,9-decanedione/urea is characterized as having a well-defined commensurate structure, with three guests for every four host repeats ($3\boldsymbol{c}_g' = 4\boldsymbol{c}_h'$).[10] This commensurate system is also an ideal candidate for optical rotation studies because it is optically uniaxial (Figure 2-9C), with three guest molecules related along the channel axis by a 3-fold screw axis. In addition, 2,9-decanedione/urea was found to grow as flat, hexagonal plates, which allows one to easily measure optical rotation (Figure 2-9D).

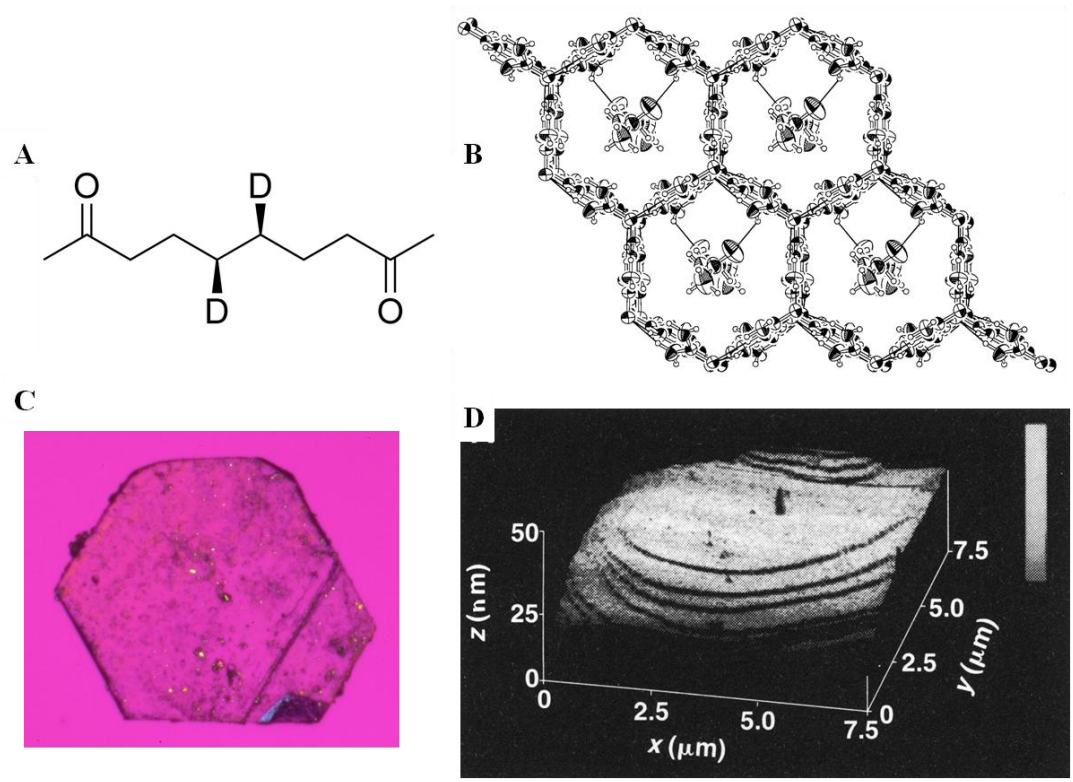

Figure 2-9: (A) Chemical structure of (5*S*,6*S*)-2,9-decanedione-d_2. (B) ORTEP view down the channel axis of 2,9-decanedione/urea, with one layer of guest shown (space group $P3_112$). (C) Photomicrograph of 2,9-decanedione/urea between crossed polars and a lambda plate. (D) AFM image of the {001} face of 2,9-decanedione/urea in air, demonstrating the template-directed growth of smooth ledges. [Figures B and D taken with permission from M. D. Hollingsworth, *et al.*, *Science*. **273**, 1355-1359 (1996); Figure C provided courtesy of M. D. Hollingsworth]

One possible objection to the use of a commensurate structure would be that the 2,9-decanedione guest molecules exist in chiral conformations and in supramolecular chiral arrays when included within the UIC channel. However, one line of evidence to support the idea that the helical host structure dominates the optical rotation of UICs comes from the work of Schlenk, who measured optical rotations for a series of *n*-alkanone UICs that incorporated guests with different chain lengths and substitutional patterns.[13] This work showed that for the UICs studied, at least, the optical rotation was independent of the identity of the guest (Figure 2-10)

Rotationsdispersion von Harnstoff-Einschlußkristallen

Gastmolekül	Untersuchter Kristall Dicke mm	Vorz. der Drehung	Spezif. Drehung [α] (Grad/mm) bei den Wellenlängen (mμ) 578	545	436	405/8	366	334	313	302	297	280	265	254	248	240	235/8	230
Undecanon-(6)	0.525	(−)	8.25	9.25	16.66	20.60	26.1	35.6	43.8	49.3		67.5	88.5	107				
Dodecanon-(3)	0.512	(−)	8.50	9.40	16.80		27.0	37.0		51.0		69.0	79.0	107	119			
	1.300	(+)	8.11	8.91	16.35	19.85	26.8	35.5	43.9	50.3								
	0.500	(+)	8.22	9.13	16.54	20.07	27.1	35.5	44.0	49.6		67.4	86.1	105	117	136	144	153
Dodecanon-(5)	0.950	(−)	8.28	9.27	11.45 *)	20.35	27.4	35.8	44.4	50.0		64.5	83.8	105	118			
Tridecanon-(3)	0.402	(+)	8.28	9.13	16.50	20.10	26.7	35.0	43.2	48.3	51.1	66.0	84.0	102	113	132	138	
Tridecanon-(7)	0.775	(−)	8.27	9.16	16.70	20.40	27.5	36.0	44.6	50.5		67.4	86.9	106	119	139		
Tetradecanon-(3)	0.315	(−)	8.03	8.89	16.56	19.8	26.7	34.9	43.3	48.9	51.0	67.0	85.0	102	114	132	138	
Pentadecanon-(2)	0.275	(+)	8.22	8.80	16.18	19.92	26.8	35.0	43.5	49.3	52.0	66.5	84.6	102	114	130	135	
Hexadecanon-(7)	0.107	(+)	8.08	9.15	17.1	20.0	26.4	34.6	43.2	48.3		65.2	83.6	102	120			
Quarz			22.55	25.40	41.55	48.5	61.2	76.0	87.8	96.3	100.3	115.9	133.1	150.1	158.0	172.9	180.5	190

*) Wahrscheinlich ein Ablesefehler.

Figure 2-10: Reported optical rotations at various wavelengths as a function of crystal thickness for a series of *n*-alkanone urea inclusion compounds. Note how optical rotations of each system remain relatively constant. [Taken with permission from W. Schlenk, *Chem. Ber.*, **101**, 2445-2449 (1968)]

Although two of these UICs (6-undecanone/urea and 7-tridecanone/urea) are known to have strong interchannel ordering of guests,[10] all of them are thought to be incommensurate structures.[7] Because the more highly ordered arrays of guests in commensurate UICs might contribute more significantly to the optical rotation than guests in incommensurate UICs, it would be desirable to measure the optical rotation of UICs containing ordered guests. Measurement of the optical rotations of a series of uniaxial UICs containing diketones will confirm (or refute) the idea that the helical host structure dominates the optical rotation.

Synthesis of (5*S*,6*S*)-2,9-Decanedione-d_2

In this and following sections, a detailed description of the attempted synthesis of (5*S*,6*S*)-2,9-decanedione-d_2 will be discussed. Several synthetic routes were pursued for stereospecific deuteration of 2,9-decanedione at the 5 and 6 positions. All of the synthetic routes attempted produced one common intermediate: (2*S*,3*S*)-1,4-dibromobutane-d_2 (or its 2*R*,3*R* enantiomer). This common intermediate was chosen because a three-carbon unit containing a methyl ketone functional group can easily be added to each side of the chain via reaction with an enolate anion. The enolate anion chosen was that of the commercially available methyl isopropenyl ether, also commonly referred to as 2-methoxypropene. Specifically, this enolate

was chosen over an enolate derived from a ketone (such as an acetone enolate) since ketone enolates are known to react slowly with alkyl halides.[16]

The synthetic method for producing (5*S*,6*S*)-2,9-decanedione-d_2 via this common intermediate is illustrated in Figure 2-11. Initially the methyl isopropenyl ether is metallated, using previously optimized conditions,[16] with *n*-butyllithium and potassium *tert*-butoxide. Subsequently, the resulting metallated methyl isopropenyl ether is treated with the common intermediate, (2*S*,3*S*)-1,4-dibromobutane-d_2, to yield (5*S*,6*S*)-2,9-dimethoxydeca-1,9-diene-d_2. The expected (5*S*,6*S*)-2,9-decanedione-d_2 is then obtained after acid hydrolysis. This method has been shown to give the desired product efficiently and in high yields.[16]

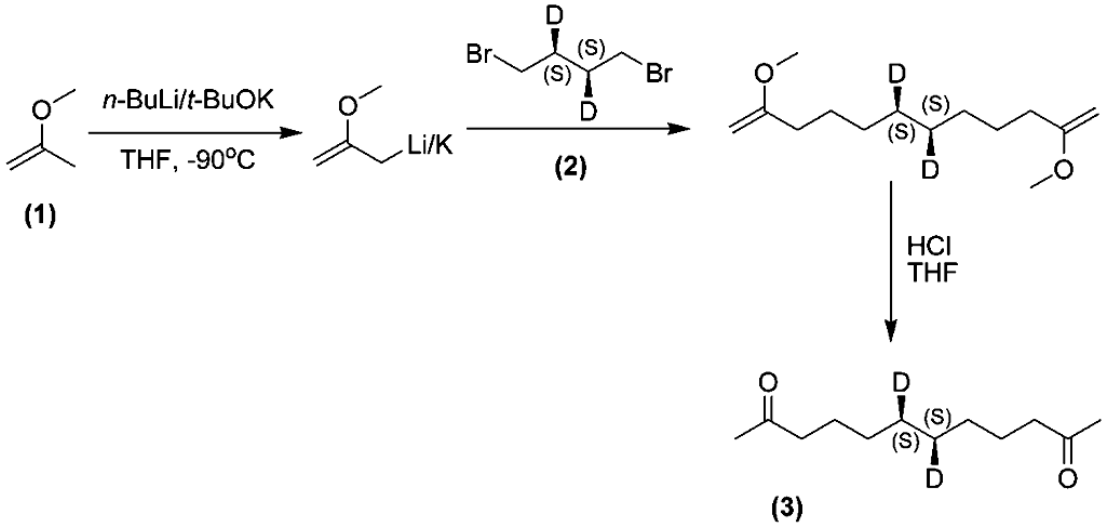

Figure 2-11: Synthetic procedure for converting the common intermediate (2*S*,3*S*)-1,4-dibromobutane-d_2 (2) via metallation of methyl isopropenyl ether (1) into the desired (5*S*,6*S*)-2,9-decanedione-d_2 (3).

Synthetic Routes Attempted in the Past

Previous members of the Hollingsworth group have attempted to synthesize the common intermediate by resolving the enantiomers of racemic *dl*-2,3-dibromo-1,4-butanediol through the use of yohimbine-dihemisuccinate adducts. This approach, shown in Figure 2-12, was adapted from procedures used by both P. W. Feit[17] and J. S. Chickos and co-workers.[18]

For this approach, the commercially available *dl*-2,3-dibromo-1,4-butanediol can be treated with succinic anhydride to form a racemic dihemisuccinate ester. This dihemisuccinate ester then crystallizes in the presence of yohimbine to form diastereomeric salts. A single

diastereomeric salt can be isolated and treated with acid to yield a single enantiomer of the dibromobutanediol ((2*R*,3*R*)-dibromo-1,4-butanediol for example). Reduction with lithium aluminum deuteride ($LiAlD_4$), would then afford (2*R*,3*R*)-1,4-butanediol-d_2. $LiAlD_4$ was chosen because it appeared to be one of the only reliable ways to stereospecifically reduce an alkyl bromide to an alkane. Other reagents, such as $NaBD_4$, can undergo electron transfer reactions that are not stereospecific.[19] The terminal alcohols can then be replaced with bromines via carbon tetrabromide and triphenylphosphine, thus forming the common intermediate (2*R*,3*R*)-1,4-dibromobutane-d_2.

Unfortunately, this method was unsuccessful because of problems in resolving the enantiomers via yohimbine. Previous members of the Hollingsworth group were unable to crystallize the yohimbine adduct and were therefore unable to separate the enantiomers.

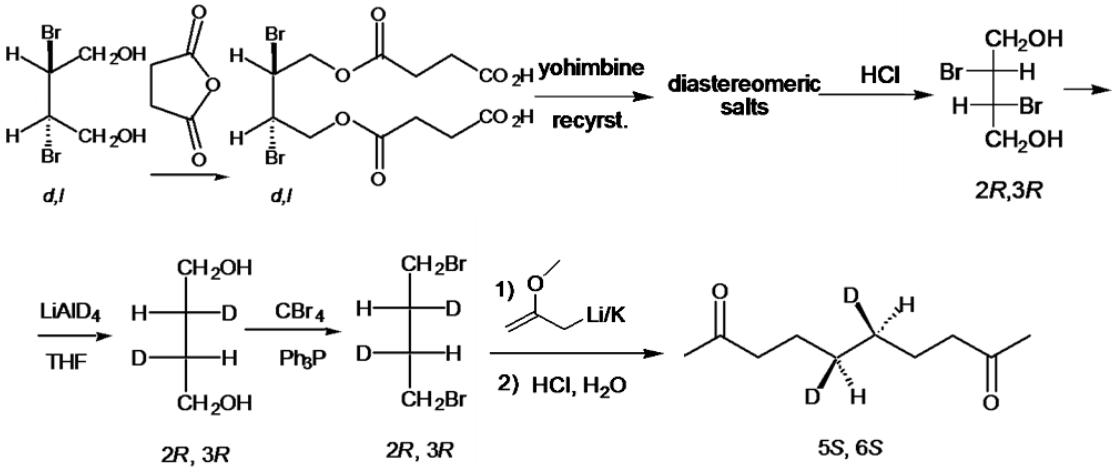

Figure 2-12: Previously attempted synthesis of (5*S*,6*S*)-2,9-decanedione-d_2, via resolution with yohimbine. [The first part of synthesis was adapted from P. W. Feit, *Chemische Berichte-Recueil*, **93**, 116-127 (1960) and J. S. Chickos, *et al.*, *J. Org. Chem.* **46**, 3559-3562 (1981)]

Resolution of enantiomers via bis(acetylmandelate ester) diastereomers

In the previous attempt of using yohimbine to resolve enantiomers, yohimbine's function was to act as a resolving agent to create diastereomeric salts. Because diastereomers have different physical properties, they can be separated by means of crystallization or chromatography.[20] Resolution via crystallization was unsuccessful, however, so an alternative

method was designed in which diastereomers could be separated with column chromatography. The chiral auxiliary, (*S*)-(+)-O-acetylmandelic acid, was chosen because it is a robust resolving agent that can easily be removed after the separation of the diastereomers.[21]

The use of (*S*)-(+)-O-acetylmandelic acid as a resolving agent is illustrated in Figure 2-13. The commercially available *dl*-2,3-dibromo-1,4-butanediol can first be esterified in the presence of (*S*)-(+)-O-acetylmandelic acid. The corresponding bis(acetylmandelate ester) diastereomers can then be separated via column chromatography before ester hydrolysis is used to produce one enantiomer of the dibromobutanediol (for example, (2*S*,3*S*)-dibromo-1,4-butanediol). As in the earlier synthesis, the introduction of deuterium in a stereospecific fashion is accomplished by reduction with $LiAlD_4$ to afford (2*S*,3*S*)-1,4-butanediol-d_2. The terminal alcohols can then be replaced with bromines, thus again forming the common intermediate.

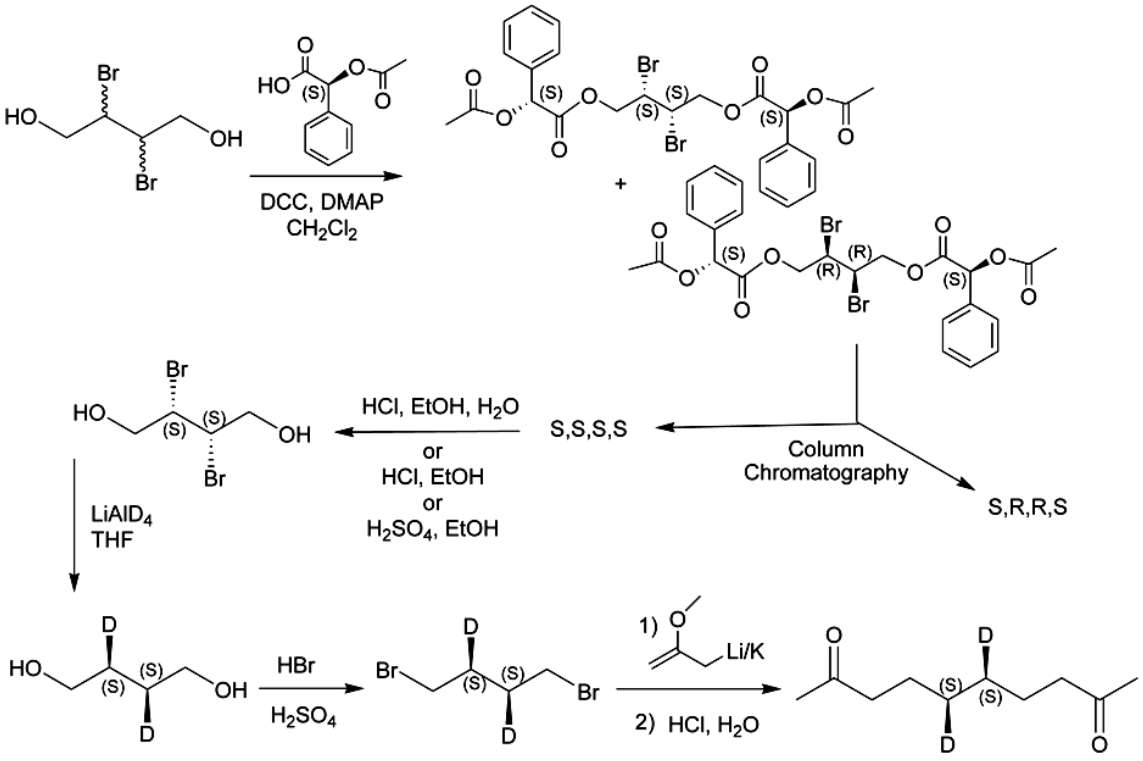

Figure 2-13: Synthesis of (5*S*,6*S*)-2,9-decanedione-d_2, via resolution with the chiral auxiliary, (*S*)-(+)-O-acetylmandelic acid, utilizing a vicinal dibromide compound.

Although this method looked promising, it was proven unsuccessful due to complications during ester hydrolysis. Initially when performing this synthesis, a single diastereomer (the high R_f diastereomer) was successfully isolated with column chromatography. Ester hydrolysis in the presence of HCl, ethanol, and water afforded what was thought to be one enantiomer of 2,3-dibromo-1,4-butanediol. This diol was immediately crystallized and then examined with X-ray diffraction by Dr. Roman Gajda. Because the molecule contains bromine, the technique of anomalous dispersion[22] was used to show that the crystal chosen for the determination of the absolute configuration had the 2*R*,3*R* configuration (Figure 2-14).[23] Surprisingly, however, optical rotation measurements and melting points did not agree with the crystallographic data. The experimental[24] optical rotation ($[\alpha]^{20}_D$ = +7.80°, ***c*** 0.02 MeOH) and melting point (mp 93-96 °C) were more similar to the literature[17] values of *dl*-2,3-dibromo-1,4-butanediol ($[\alpha]^{20}_D$ = 0°, mp 89.5-90.5 °C) than to those of the expected single enantiomer ($[\alpha]^{20}_D$ = +40.0° (*c* 2, MeOH), mp 114-115 °C). This clearly demonstrates that the single crystal selected for crystallographic studies was not representative of the entire sample. By chance, a crystal of (2*R*,3*R*)-dibromo-1,4-butanediol was chosen from the batch, but the majority of the sample had racemized.

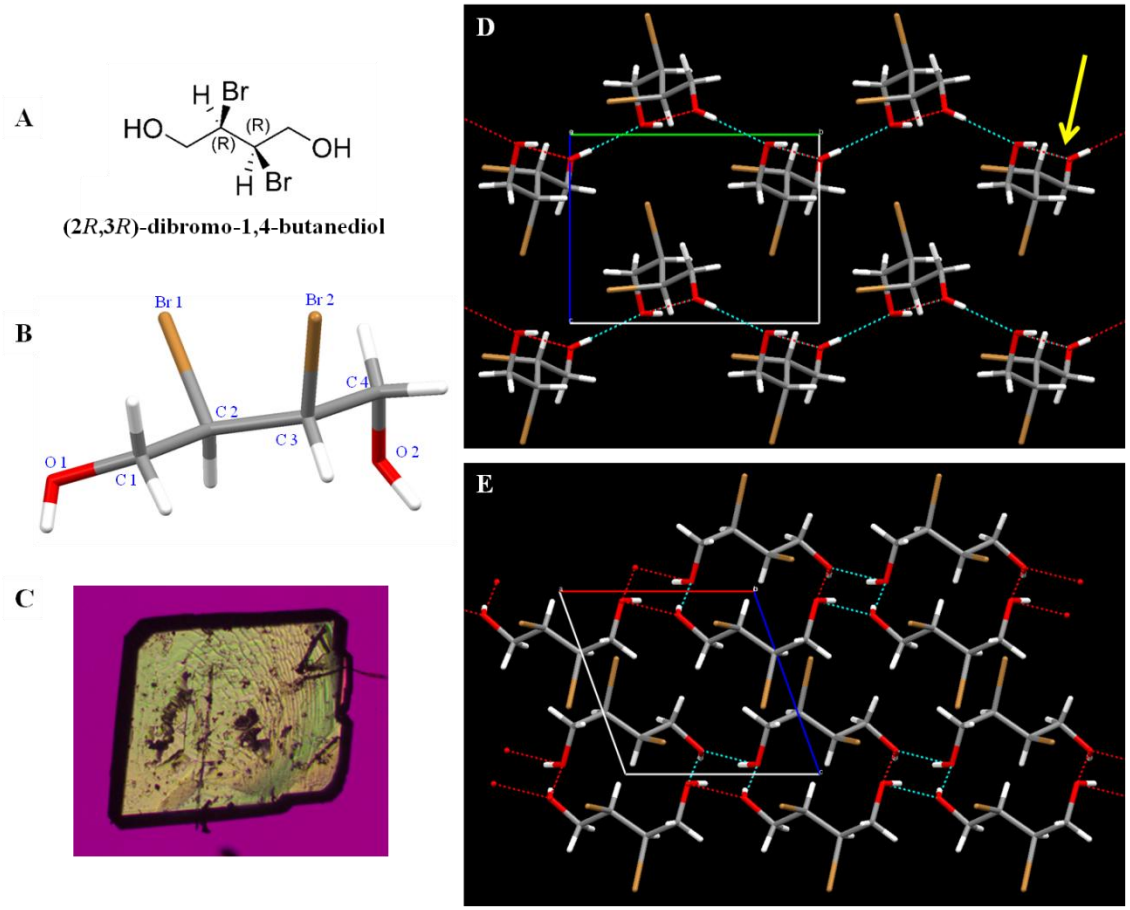

Figure 2-14: (A) Chemical structure of (2*R*,3*R*)-dibromo-1,4-butanediol. (B) Molecular structure of (2*R*,3*R*)-dibromo-1,4-butanediol showing the absolute configuration of the molecule, as determined from the crystal structure (space group $P2_1$). (C) Photomicrograph of (2*R*,3*R*)-dibromo-1,4-butanediol crystal, grown as a thin prismatic plate, used for X-ray studies. (D) Crystal packing of (2*R*,3*R*)-dibromo-1,4-butanediol, viewed along the ***a*** axis. Note the blue dashed lines designate H-bonding between molecules in a zigzag pattern. The yellow arrow points to the dashed red line, which designates H-bonding to a molecule behind the observed molecule. (E) Packing diagram, viewed along the ***b*** axis. [Figs. B, D, E provided courtesy of M. D. Hollingsworth; Fig. C provided courtesy R. B. Gajda]

After conducting an extensive literature search, it was discovered that vicinal dibromides are very sensitive towards neighboring group participation in polar solvents.[25] Because the racemization is thought to proceed through the charged bromonium ion, it was proposed that if the dielectric constant of the solvent were kept low, racemization could be minimized. As previously stated, ester hydrolysis was initially attempted with an HCl/ethanol/water mixture. Assuming that water's dielectric constant ($\varepsilon = 80.4$)[26] was too high, ester cleavage was then attempted with two different approaches: (1) with dry HCl/ethanol, and (2) with H_2SO_4/ethanol.

However, racemization of the vicinal dibromides still occurred in both cases (Figure 2-15). This reveals the extreme sensitivity of vicinal dibromides towards neighboring group participation. As a result, the method of resolving enantiomers via vicinal dibromide-containing bis(acetylmandelate ester) diastereomers was proven to be ineffective.

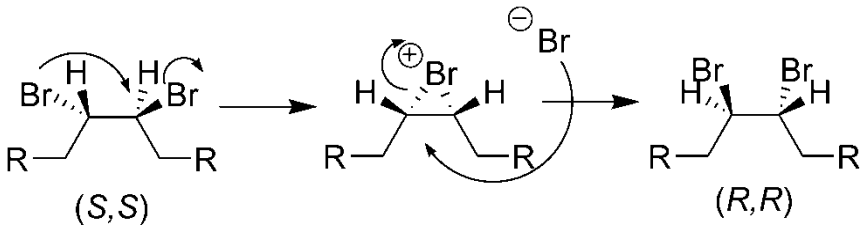

Figure 2-15: Proposed mechanism for the racemization of vicinal dibromides.

As an alternative to diastereomer separations, isolation of a single enantiomer of 2,3-dibromo1,4-butanediol was attempted via HPLC using a chiral column.[27] However, the separation of *d,l*-2,3-dibromo-1,4-butanediol with chiral HPLC was unsuccessful.

Dibromo-bis(acetylmandelate ester) diastereomers:

To a round bottom flask equipped with a dropping funnel, racemic *d,l*-2,3-dibromo-1,4-butanediol (0.338 g, 1.36 mmol, Aldrich, 99%), dicyclohexylcarbodiimide (0.505 g, 2.45 mmol, Aldrich, 99%), and 4-dimethylaminopyridine (0.033 g, 0.272 mmol, Aldrich, 99%) were added under an argon atmosphere. Dry CH_2Cl_2 (15 mL) was then added to the flask, and the reaction mixture was cooled to -15 °C. A mixture of (*S*)-(+)-O-acetylmandelic acid (0.529 g, 2.73 mmol, Aldrich, 99%) in CH_2Cl_2 (3 mL) was added dropwise to the reaction mixture. After the addition was completed, the reaction mixture was warmed to room temperature and stirred for 24 hours. The reaction mixture was filtered to remove the dicyclohexylurea byproduct and was then concentrated on a rotary evaporator to yield a crude mixture of the dibromo-bis(acetylmandelate ester) diastereomers. The diastereomers were separated by flash column chromatography. The high R_f diastereomer (0.566 g, 136% yield, contaminated with DCU) and low R_f diastereomer (0.100 g, 24.5% yield) were isolated as colorless oils.

Physical Data: R_f = 0.68 for high R_f and 0.52 for low R_f diastereomer (1:1 EtOAc/hexanes v/v, PMA stain as indicator). ^{1}H NMR for high R_f diastereomer (400 MHz, $CDCl_3$, ADA-A163-fr69-75): δ2.22 (6H, s, C**H**$_3$COOR), 3.98 (1H, m, C**H**Br), 4.15 (1H, m,

C**H**Br), 4.29 (2H, two sets of dd, α-C**H**$_2$OCOR, $J_{a^*b^*}$ = 11.2 Hz, $J_{a^*c^*}$ = 4.8 Hz, $J_{a_\blacktriangle b_\blacktriangle}$ = 11.6 Hz, $J_{a_\blacktriangle c_\blacktriangle}$ = 6.4 Hz), 4.43 (2H, two sets of dd, α-C**H**$_2$OCOR, $J_{a^*b^*}$ = 11.2 Hz, $J_{b^*c^*}$ = 8.4 Hz, $J_{a_\blacktriangle b_\blacktriangle}$ = 11.6 Hz, $J_{b_\blacktriangle c_\blacktriangle}$ = 7.6 Hz), 5.90 (2H, s, α-C**H**COOR), 7.43 (10H, m, phenyl-C**H**). All coupling constants for this data set are treated as if they were first order systems, even though there are distortions. The * and ▲ symbols refer to the two conformations of the diastereomers. These conformations, which are thought to differ by rotation about the central C-C bond, are concentration dependent. The coupling constants J_a and J_b refer to the methylene protons (α-C**H**$_2$OCOR), and J_c refers to the methine proton (C**H**Br). In one conformer (triangles), the system has an ABX spectrum. In the other conformer (asterisks), the system behaves more like an ABM spin system. See Appendix B for peak identification and 2D COSY NMR results (400 MHz, $CDCl_3$, ADA-A145-16-dry-COSY). In addition to COSY, peak assignments relied on the concentration dependence of conformer populations (c.f. spectrum ADA-A145-16-dry, in which the ratio of peaks at 4.15 and 3.98 ppm had an intense ratio of 1:1.2.) ^{1}H NMR for low R_f diastereomer (400 MHz, $CDCl_3$, ADA-A163-fr105-115): δ2.22 (6H, s, C**H**$_3$COOR), 3.84 (2H, m, C**H**Br), 4.41 (2H, m, α-C**H**$_2$OCOR), 4.56 (2H, m, α-C**H**$_2$OCOR), 5.87 (2H, s, α-C**H**COOR), 7.45 (10H, m, phenyl-C**H**). Some of the high R_f diastereomer may be present in the ^{1}H NMR for the low R_f diastereomer.

Notebook pages: ADA-A143, ADA-A161, ADA-A167

(2R,3R)-Dibromo-1,4-butanediol (hydrolysis with HCl/water/ethanol):

A stock solution of HCl in a 1:1 mixture of water and ethanol was prepared by adding HCl (1 mL, 12 M) to water (10 mL) and absolute ethanol (10 mL, Decon Labs). This stock solution (17 mL) was added to a round bottom flask containing the high R_f dibromo-bis(acetylmandelate ester) diastereomer (1.60 g, 2.67 mmol). After refluxing for 4 hours, the reaction mixture was quenched with water (50 mL) and extracted with diethyl ether (6 x 50 mL). The organic layer was washed with 1M $NaHCO_3$ (1 x 50 mL) and saturated aq. NaCl (1 x 50 mL) before it was dried over $MgSO_4$, filtered, and concentrated on a rotary evaporator. The crude product was purified with flash column chromatography and recrystallized from a solution of 4:1 hexanes to ethyl acetate to yield mostly (2*R*,3*R*)-dibromo-1,4-butanediol (0.226 g, 66.2% yield) as a white solid, with an optical purity of 19.5% *ee*.

Physical data: R_f = 0.41 (1:1 EtOAc/hexanes v/v, PMA stain as indicator). Melting point: 93-96 °C (Lit. mp for racemate: 89.5-90.5 °C, Lit. mp for single enantiomer: 114-115 °C).[17] Optical rotation: $[\alpha]^{20}_D$ = +7.80° *c* 0.02, MeOH (Lit. optical rotation for single enantiomer: $[\alpha]^{20}_D$ = +40.0° *c* 2, MeOH).[17] ^{1}H NMR (400 MHz, DMSO-d_6, ADA-A156-14-fr93-120): δ3.69 (4H, m, C**H**$_2$), 4.45 (2H, t, C**H**Br, *J* = 6.8 Hz), 5.49 (2H, t, O**H**, *J* = 6.3 Hz).

Notebook pages: ADA-A147, ADA-A155[28]

(2R,3R)-Dibromo-1,4-butanediol (hydrolysis with HCl/ethanol):

A solution of dry 1.218 M HCl in ethanol (8 mL) was added to a round bottom flask containing the high R_f diastereomer (0.081 g, 0.135 mmol) under an argon atmosphere. After heating at 30 °C for 20 hours, the reaction mixture was quenched with water (30 mL) and extracted with diethyl ether (5 x 30 mL). The organic layer was washed with 1M $NaHCO_3$ (1 x 50 mL) and saturated aq. NaCl solution (1 x 50 mL). It was then dried over $MgSO_4$, filtered, and concentrated on a rotary evaporator. The crude product was purified with flash column chromatography and recrystallized from a solution of 4:1 hexanes to ethyl acetate to give mostly racemic 2,3-dibromo-1,4-butanediol (0.025 g, 74.5% yield) as a white solid.

Physical data: R_f = 0.41 (1:1 EtOAc/hexanes v/v, PMA stain as indicator). Melting point: 88-89 °C (Lit. mp for racemate: 89.5-90.5 °C, Lit. mp for single enantiomer: 114-115 °C).[17] No optical rotations were measured.

Notebook pages: ADA-A179

(2R,3R)-Dibromo-1,4-butanediol (hydrolysis with H_2SO_4/ethanol):

A stock solution of H_2SO_4 in water and ethanol was prepared by adding concentrated H_2SO_4 (22 mL) to water (5 mL) and absolute ethanol (13 mL, Decon Labs). This stock solution (5 mL) was added to a round bottom flask containing the high R_f diastereomer (0.1043 g, 0.174 mmol). The reaction mixture was sonicated for 10 minutes to dissolve the diastereomer and was then heated at 38 °C for 8 hours. Following this, the reaction mixture was quenched with water (20 mL) and extracted with diethyl ether (5 x 30 mL). The organic layer was washed with 1 M $NaHCO_3$ (2 x 25 mL) and saturated aq. NaCl (1 x 50 mL). It was then dried over $MgSO_4$, filtered, and concentrated on a rotary evaporator. The crude product was purified with flash

column chromatography and recrystallized from a solution of 4:1 hexanes to ethyl acetate to give primarily racemic 2,3-dibromo-1,4-butanediol (0.0203g, 47.0% yield) as a white solid.

Physical data: $R_f = 0.41$ (1:1 EtOAc/hexanes v/v, PMA stain as indicator). Melting point: 87-90 °C (Lit. mp for racemate: 89.5-90.5 °C, Lit. mp for single enantiomer: 114-115 °C).[17] Optical rotation: $[\alpha]^{20}_D = +0.735°$ *c* 0.004, MeOH (Lit. optical rotation for single enantiomer: $[\alpha]^{20}_D = +40.0°$ *c* 2, MeOH).[17]

Notebook pages: ADA-A171

Dimesylate Synthetic Approach

Having excluded vicinal dibromides as synthetic intermediates, we devised an alternative synthetic method using the mesylate group, which is known to be an excellent leaving group. Mesylate esters have been shown to undergo reduction via $LiAlD_4$[29] even more rapidly than alkyl bromides.[25] As a starting material, the most practical, commercially available option, based on availability and cost, was that of (2*S*,3*S*)-(-)-1,4-dimethoxy-2,3-butanediol. Therefore, this starting material was utilized in a newly modified synthetic method shown in Figure 2-16.

By following an optimized procedure reported in literature,[30] (2*S*,3*S*)-(-)-1,4-dimethoxy-2,3-butanediol was first mesylated with methanesulfonyl chloride to give (2*S*,3*S*)-dimethanesulfonate-1,4-dimethoxybutane. This dimesylate can then be reduced with $LiAlD_4$ to yield (2*R*,3*R*)-1,4-dimethoxybutane-d_2. Following that, the dimethoxybutane can be converted, using HBr and H_2SO_4,[31] to the common intermediate described above ((2*S*,3*S*)-1,4-dibromobutane-d_2).

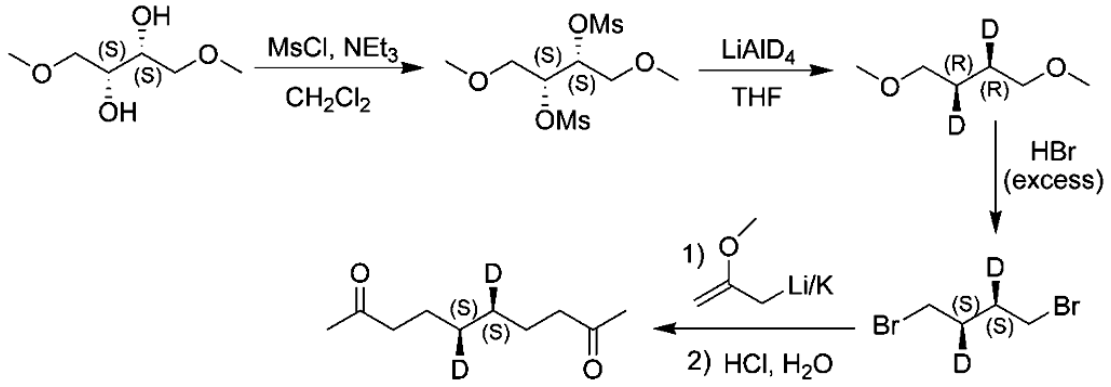

Figure 2-16: Dimesylate synthetic approach towards the synthesis of (5*S*,6*S*)-2,9-decanedione-d_2, using the commercially available (2*S*,3*S*)-(-)-1,4-dimethoxy-2,3-butanediol as starting material.

While implementing this dimesylate synthetic approach, several roadblocks were encountered. The first was learning how to handle (2*R*,3*R*)-1,4-dimethoxybutane-d_2. Because 1,4-dimethoxybutane has such a low molecular weight and boiling point (40-45 °C),[32] it was found to be very difficult to isolate and handle. Numerous attempts were made to synthesize this compound before finding a successful solution. Initially several reactions were carried out by treating 1,4-butanediol with sodium hydride and methyl iodide in either diethyl ether or THF (Figure 2-17A).[33] These reactions were ineffective because it was impossible to separate 1,4-dimethoxybutane from either solvent. However, when conducting a literature survey for the synthesis of methyl ethers, an interesting procedure was discovered. This involved treating 1,4-butanediol with methyl iodide and potassium hydroxide in DMSO (Figure 2-17B).[34] Luckily, this method was discovered to be an excellent choice, since the desired 1,4-dimethoxybutane can be distilled quite easily from the high-boiling DMSO solvent.[35]

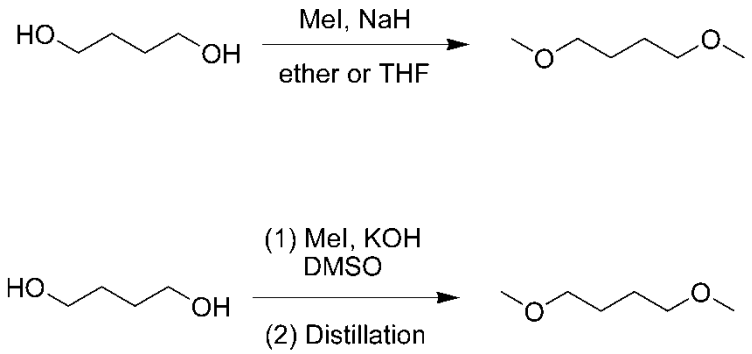

Figure 2-17: (A) First attempt to make 1,4-dimethoxybutane: this was found to be unsuccessful since 1,4-dimethoxybutane is difficult to separate from both diethyl ether and THF. (B) Second attempt to make 1,4-dimethoxybutane: this worked because the desired product can be distilled from DMSO.

The second major roadblock encountered in the dimesylate synthetic approach was the discovery of anchimeric effects in the $LiAlD_4$ reductions of vicinal dimesylate esters. It has been reported in some cases[36,37] that compounds undergoing S_N2 substitution of vicinal dimesylate esters (or tosylate esters) can undergo anchimeric assistance, thus causing an unexpected inversion of configuration. The proposed mechanism of this process is illustrated in Figure 2-18. The S_N2 substitution of one mesylate group by deuteride ion causes displacement of the vicinal

mesylate group by the departing mesylate ion.[36] This causes an inversion of configuration at this site. A second inversion of configuration would then occur at this site by substitution of the remaining mesylate group by another deuteride. As a result, the dimesylate synthetic approach for the synthesis of (5*S*,6*S*)-2,9-decanedione-d_2 was not pursued due to anchimeric effects that were anticipated during the reduction of vicinal dimesylate esters.

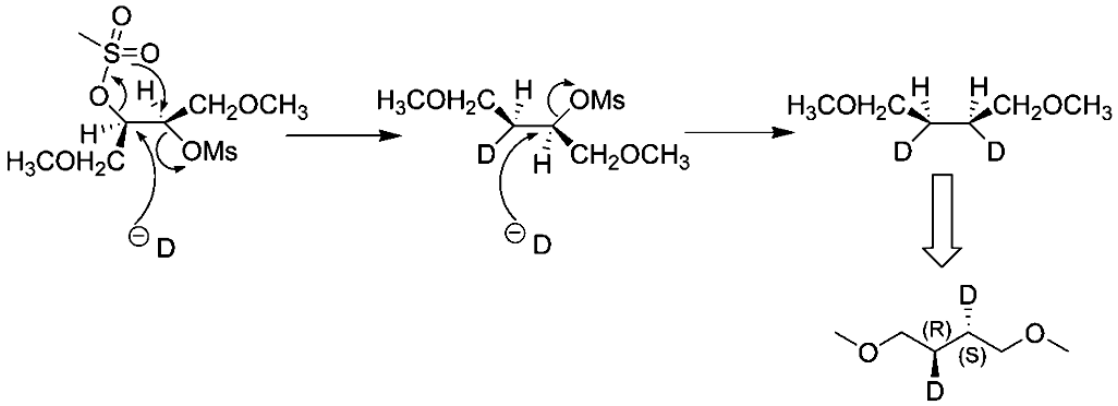

Figure 2-18: Proposed mechanism for anchimeric assistance of vicinal dimesylate esters. Deuteride ion originates from $LiAlD_4$. Note that the *meso* stereochemistry is different from what is expected in Figure 2-16. [Adapted from I. Navarro, *et al.*, *Angew. Chem. Int. Ed.*, **38**, 164-166 (1999)]

1,4-Dimethoxybutane:

To a round bottom flask equipped with a dropping funnel was added 1,4-butanediol (1.4 g, 15.5 mmol, Aldrich, 99%), potassium hydroxide (5.67 g, 106.4 mmol, MCB), and dry DMSO (10 mL, ACS grade, Fischer Scientific) under an argon atmosphere. After 15 minutes, methyl iodide (5.67 g, 39.9 mmol, Mallinckrodt) was added dropwise to reaction mixture. After stirring at room temperature for 18 hours, the desired product was removed via fractional distillation to yield 1,4-dimethoxybutane (0.973 g, 53.1% yield) as a colorless liquid.

Physical data: ^{1}H NMR (400 MHz, $CDCl_3$, ADA-A239-7a-toplayer): δ1.63 (4H, m, β-C**H**$_2$), 3.34 (6H, s, C**H**$_3$), 3.39 (4H, m, α-C**H**$_2$). ^{13}C NMR (100.57 MHz, $CDCl_3$, ADA-A239-7a-C13): δ26.47 (β-**C**H$_2$), 58.70 (**C**H$_3$), 72.76 (α-**C**H$_2$).

Notebook pages: ADA-A237, ADA-A239

1,4-Dibromobutane from 1,4-dimethoxybutane:

To a round bottom flask equipped with a dropping funnel, reflux condenser, and bubbler was added 1,4-dimethoxybutane (0.973 g, 8.24 mmol). Concentrated HBr (85 mL, 1.56 mol, Aldrich, 46%) was slowly added to the ice-cold reaction flask, followed by the dropwise addition of concentrated H_2SO_4 (42.9 mL, 0.805 mol, Fisher Scientific). Evolution of gas was observed upon addition of H_2SO_4. After 10 minutes, the ice bath was removed, and the reaction mixture was heated to 70 °C. Yellow fumes were emitted from the reaction mixture for 20 minutes. After stirring at 70 °C for 16 hours, the yellow reaction mixture was quenched with water (100 mL) and then neutralized with 1 M $NaHCO_3$ until a pH of 7 was reached. This mixture was extracted with CH_2Cl_2 (4 x 80 mL), and the organic layer was washed with 1 M $NaHCO_3$ (1 x 25 mL) and saturated aq. NaCl (1 x 25 mL). The organic layer was dried over Na_2SO_4, filtered, and concentrated on a rotary evaporator. The desired product was purified via a simple distillation, yielding 1,4-dibromobutane (1.12 g, 63.1% yield) as a colorless liquid.

Physical data: $R_f = 0.85$ (1:4 EtOAc/hexanes v/v, iodine chamber as indicator). ^{1}H NMR (400 MHz, $CDCl_3$, ADA-A244-16b-trap): δ2.01 (4H, m, β-C**H**$_2$), 3.45 (4H, m, α-C**H**$_2$-Br).

Notebook pages: ADA-A243, ADA-A245

(2S,3S)-Dimethanesulfonate-1,4-dimethoxybutane:

To a round bottom flask equipped with a dropping funnel was added dry CH_2Cl_2 (5 mL), triethylamine (0.203 g, 2.01 mmol, Fisher Scientific, 99%), and (2*S*,3*S*)-(-)-1,4-dimethoxy-2,3-butanediol (0.1 g, 0.67 mmol, Aldrich, 99%) under an argon atmosphere. To this ice-cold reaction mixture, methanesulfonyl chloride (0.191 g, 1.67 mmol, Aldrich, 99.7%) was added dropwise, causing the reaction mixture to turn white. After stirring in an ice bath for one hour, the reaction mixture, now a light yellow color, was quenched with water (50 mL) and extracted with ethyl acetate (4 x 40 mL). The organic layer was washed with saturated aq. NaCl (1 x 50 mL), dried over $MgSO_4$, filtered, and concentrated on a rotary evaporator to yield a yellow oil. After the product was chilled to -2 °C for 16 hours, pure (2*S*,3*S*)-dimethanesulfonate-1,4-dimethoxybutane (0.225 g, quantitative yield) was collected as a yellow solid.

Physical data: R_f = 0.55 (3:2 EtOAc/Pet. Ether v/v, PMA stain as indicator). Melting point: 36-40 °C (Lit. mp: 42-44 °C).[30] ^{1}H NMR (400 MHz, $CDCl_3$, ADA-A215-10): δ3.13 (6H, s, C**H**$_3$-MsOR), 3.41 (6H, s, C**H**$_3$-OR), 3.69 (4H, m, C**H**$_2$), 4.94 (2H, m, C**H**-OMs).

Notebook pages: ADA-A203, ADA-A215

Bis(acetylmandelate ester) Diastereomers with Vicinal Dichlorides

Since both vicinal dibromides and vicinal dimesylate esters had been ruled out due to neighboring group participation, this mandated yet another literature survey to find an appropriate substituent. Although chlorine is a poorer leaving group than either bromide or mesylate,[25] reduction of a vicinal dichloride seemed to be the most viable option since vicinal dichlorides are much less susceptible to neighboring group effects than bromides or mesylates.[38]

Analogous to the scheme shown in Figure 2-13 for the dibromide, a method for the preparation of bis(acetylmandelate ester) diastereomers was attempted with a vicinal dichloride. This seemed the most appropriate option to try first since the physical data for a single enantiomer of 2,3-dichloro-1,4-butanediol had been reported in literature.[17,39] Given that *d,l*-2,3-dichloro-1,4-butanediol was not commercially available, it was first synthesized via chlorination of *cis*-2-butene-1,4-diol (see Figure 2-20). In addition, chlorine gas was currently unavailable at the time, so this was produced by slowly dripping 31% HCl solution over potassium permanganate ($KMnO_4$), as described by the schematic in Figure 2-19.

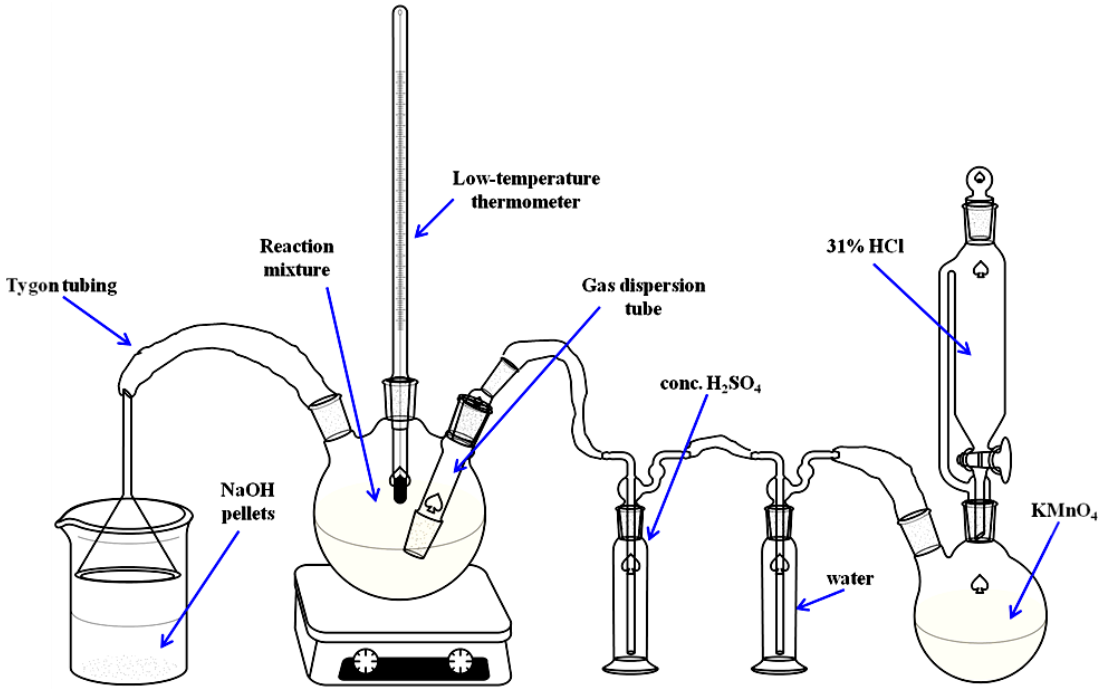

Figure 2-19: Schematic illustrating how chlorine gas was produced. First, 31% HCl was slowly dripped over $KMnO_4$. The Cl_2 gas that was generated was then bubbled through water, concentrated sulfuric acid, and finally through the reaction mixture via a gas dispersion tube. Excess gas was released through an outlet tube and passed over NaOH pellets.

After producing *dl*-2,3-dichloro-1,4-butanediol, the plan was to couple it with the chiral auxiliary, (*S*)-(+)-O-acetylmandelic acid. The resulting diastereomers were then to be separated via column chromatography, followed by ester hydrolysis of a single diastereomer to yield one enantiomer of the dichlorobutanediol, (2*S*,3*S*)-dichloro-1,4-butanediol for example. Following that, the diol would be reduced with $LiAlD_4$, and the terminal alcohols would be replaced with bromides, thus forming the common intermediate.

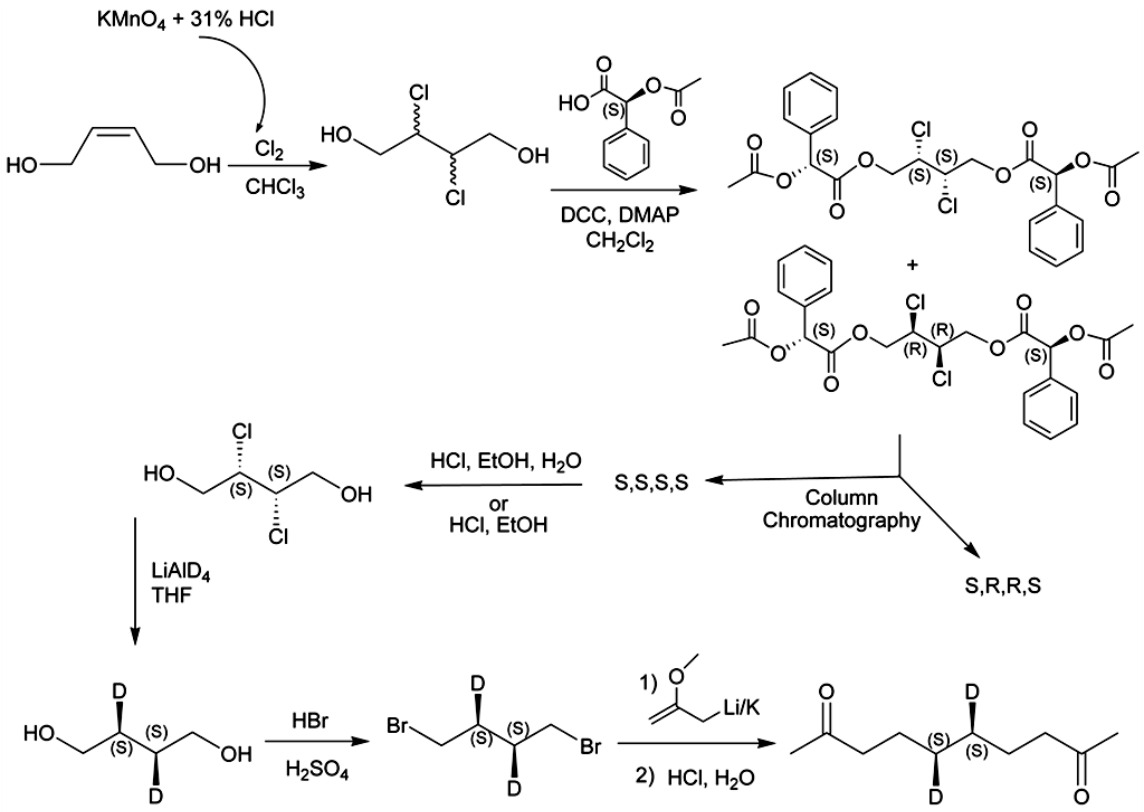

Figure 2-20: Synthesis of (5*S*,6*S*)-2,9-decanedione-d_2, via resolution with the chiral auxiliary, (*S*)-(+)-O-acetylmandelic acid, utilizing a vicinal dichloride compound.

Unfortunately this method was unsuccessful due to complications in separation of the diastereomeric esters. It was discovered that unlike their dibromide analogs, the bis(acetylmandelate ester) diastereomers containing vicinal dichlorides, were inseparable via column chromatography. High-performance liquid chromatography (HPLC) was also attempted, but again separation did not occur.[40]

dl-2,3-Dichloro-1,4-butanediol:

For this procedure, an apparatus shown in Figure 2-19 was assembled. To the 3-neck round bottom flask was added *cis*-2-butene-1,4-diol (4.00 g, 45.4 mmol, Aldrich, 97%) and dry $CHCl_3$ (30 mL). After cooling the reaction mixture to 0 °C, chlorine gas was produced by slowly dripping 31% HCl (300 mL) over $KMnO_4$ (25.0 g, J.T. Baker). The chlorine gas was bubbled through water and concentrated H_2SO_4 and then through the reaction mixture via a gas dispersion tube for 3 hours, after which the reaction mixture was quenched with water (60 mL) and saturated aq. NaCl (30 mL). The reaction mixture was extracted with $CHCl_3$ (4 x 50 mL),

then dried over Na_2SO_4, filtered, and concentrated on a rotary evaporator. After extracting the aqueous layer with diethyl ether (3 x 50 mL), the organic layer was dried over Na_2SO_4, filtered, and concentrated a rotary evaporator. The crude products obtained from the $CHCl_3$ extractions were combined and then purified with column chromatography to yield *d,l*-2,3-dichloro-1,4-butanediol (3.34 g, 46% yield) as an off-white solid. The observed melting point did not match the literature value, most likely due to the presence of ethyl acetate, which can be seen in the NMR spectrum.

Physical data: $R_f = 0.65$ (4:1 EtOAc/hexanes v/v, PMA stain as indicator). Melting point: 48-52 °C (Lit. mp: 66-67 °C).[17] ^{1}H NMR (400 MHz, $CDCl_3$, ADA-A267-20-H1): δ2.53 (2H, br s, O**H**), 3.96 (4H, m, C**H**$_2$), 4.35 (2H, m, C**H**Cl). ^{13}C NMR (100.57 MHz, $CDCl_3$, ADA-A267-20-C13): δ62.24 (**C**H_2), 63.59 (**C**HCl).

Notebook pages: ADA-A261, ADA-B23, ADA-B25, ADA-B27

Resolution via Dichloro-Bis(methylbenzylamide) Diastereomers

In a reexamination of the earlier work by Feit and Chickos, who used yohimbine as a resolving agent,[17,18] a new method was developed that utilized (*S*)-(-)-α-methylbenzylamine, along with various other previously discussed techniques. Figure 2-21 outlines this synthetic procedure. To begin this synthesis, *dl*-2,3-dichloro-1,4-butanediol was prepared via chlorination of *cis*-2-butene-1,4-diol. This can subsequently be treated with succinic anhydride to form the familiar racemic dihemisuccinate ester, 4,4'-[(2,3-dichlorobutane-1,4-diyl)bis(oxy)]bis(4-oxobutanoic acid). Diastereomers can then be formed by reaction with the chiral auxiliary (*S*)-(-)-α-methylbenzylamine to give dichloro-bis(methylbenzylamide) diastereomers. After separation with column chromatography, ester hydrolysis can be conducted on a single diastereomer, yielding one enantiomer of the dichlorobutanediol, for example (2*S*,3*S*)-dichloro-1,4-butanediol. The introduction of deuterium in a stereospecific fashion can then be accomplished by reduction with $LiAlD_4$ to afford (2*S*,3*S*)-1,4-butanediol-d_2. After this, the terminal alcohols can be substituted with bromides, resulting in the formation of the common intermediate, (2*S*,3*S*)-1,4-dibromobutane-d_2.

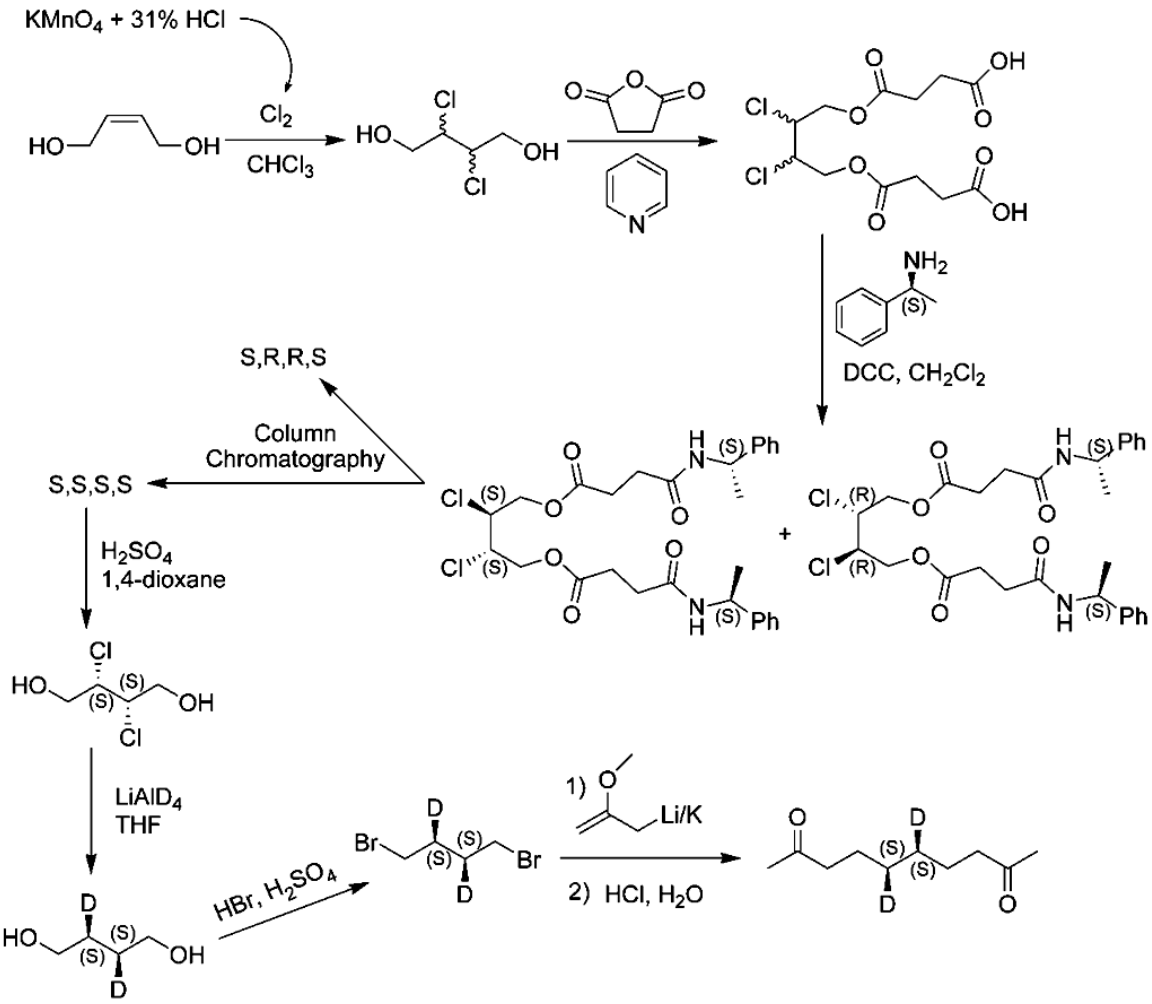

Figure 2-21: Synthesis of (5*S*,6*S*)-2,9-decanedione-d_2, via resolution with the chiral auxiliary, (*S*)-(-)-α-methylbenzylamine, utilizing a vicinal dichloride compound.

For several reasons, the step involving ester hydrolysis was conducted in a 1:1 mixture of 10 M sulfuric acid and 1,4-dioxane. Given its miscibility with water, 1,4-dioxane was utilized as an organic solvent to dissolve the bis(methylbenzylamide) diastereomer, as this diastereomer exhibited low water solubility. This solvent ($\varepsilon = 2.20$)[26] was also used to keep the dielectric constant of the reaction mixture low, so as to avoid the formation of halonium ions. Sulfuric acid was chosen in preference over hydrochloric acid to avoid excess chloride ions in solution. When hydrochloric acid is used, if a chloronium ion happens to form, excess chloride ions in solution could immediately attack to open the chloronium ion, thus causing racemization of the vicinal dichloride. In addition, a highly concentrated acid (10 M sulfuric acid) was chosen since it was discovered that ester functional groups have been reported to undergo specific acid

catalysis.[41] That is, the identity of the acid does not affect the reaction rate. By performing ester hydrolysis with 10 M sulfuric acid, reaction conditions were reduced to a 20-hour reaction time at room temperature, instead of extended periods of heating required for less concentrated solutions of hydrochloric acid.

Much to our surprise, this synthetic method was also proven unsuccessful, again due to neighboring group participation. Although it was thought that vicinal dichlorides would be much less likely to form halonium ions than their dibromide counterparts,[38,42] racemization still occurred during hydrolysis of the bis(methylbenzylamide) diastereomers. As a result, the synthesis of (5*S*,6*S*)-2,9-decanedione-d_2 via resolution of vicinal dichloride-containing bis(methylbenzylamide) diastereomers was no longer pursued.

4,4'-[(2,3-Dichlorobutane-1,4-diyl)bis(oxy)]bis(4-oxobutanoic acid):

Pyridine (Fisher Scientific) was freshly distilled, and succinic anhydride (Aldrich, 99%) was recrystallized prior to use. To a round bottom flask was added *d,l*-2,3-dichloro-1,4-butanediol (2.34 g, 14.63 mmol) and dry pyridine (3.01 g, 38.0 mmol) under an argon atmosphere. Succinic anhydride (3.22 g, 32.19 mmol) was added all at once. After stirring at room temperature for 20 hours, the reaction mixture was cooled to 0 °C before adding ice-cold 5 M HCl (20 mL). Stirring at 0 °C for 30 minutes resulted in the formation of a precipitate. The reaction mixture was filtered, and the precipitate was rinsed with ice-cold water (4 x 5 mL). After recrystallizing the precipitate from water, pure 4,4'-[(2,3-dichlorobutane-1,4-diyl)bis(oxy)]bis(4-oxobutanoic acid) (2.34 g, 44.3% yield) was collected as a white solid.

Physical data: $R_f = 0.19$ (4:1 EtOAc/hexanes v/v, PMA stain as indicator). Melting point: 116-117.5 °C (Lit. mp: 122.5-123 °C).[17] ^{1}H NMR (400 MHz, $CDCl_3$, ADA-B68-15): δ2.69 (8H, m, ROOC-C**H**$_2$-C**H**$_2$-COOH), 4.33 (4H, m, α-C**H**$_2$-OOC-), 4.46 (2H, m, C**H**Cl).

Notebook pages: ADA-B47, ADA-B67, ADA-B75

Dichloro-bis(methylbenzylamide) diastereomers:

To a round bottom flask equipped with a reflux condenser, the dichloro-dihemisuccinate ester (0.583 g, 1.61 mmol), (*S*)-(-)-α-methylbenzylamine (0.43 g, 3.54 mmol, Acros, 99%), and dry CH_2Cl_2 (10 mL) were added under an argon atmosphere. Dicyclohexylcarbodiimide (0.83 g, 4.03 mmol, Aldrich, 99%) was added to the ice-cold reaction mixture. After stirring at ice

temperatures for 30 minutes, the reaction was warmed and heated to reflux (40 °C) for 2 hours, after which it was cooled and filtered to remove the dicyclohexylurea byproduct. The organic filtrate was washed with 1% HCl (1 x 50 mL), 1% $NaHCO_3$ (1 x 50 mL), and saturated aq. NaCl (1 x 50 mL), and was then dried over Na_2SO_4, filtered, and concentrated on a rotary evaporator to yield a crude mixture of the bis(methylbenzylamide) diastereomers. The crude product was purified with flash column chromatography, resulting in the isolation of the high R_f diastereomer (0.615 g, 135% yield, contaminated with DCU) and the low R_f diastereomer (0.198 g, 43.5% yield) as white, sticky solids.

Physical data: $R_f = 0.67$ for high R_f and 0.44 for low R_f diastereomer (4:1 EtOAc/hexanes v/v, PMA stain as indicator). ^{1}H NMR for high R_f diastereomer (400 MHz, DMSO-d_6, ADA-B36-fr20-50): δ1.34 (6H, d, C**H**$_3$, J = 7.0 Hz), 2.44 (4H, m, α-C**H**$_2$-amide), 2.58 (4H, m, β-C**H**$_2$-amide), 4.29 (4H, m, α-C**H**$_2$-OOC), 4.69 (2H, m, C**H**Cl), 4.89 (2H, qd, α-C**H**-amide, J = 7.0 Hz, J = 7.9 Hz), 7.21 (2H, m, phenyl-C**H**), 7.29 (8H, m, phenyl-C**H**), 8.25 (2H, d, N**H**, J = 7.9 Hz). ^{13}C NMR for high R_f diastereomer (400 MHz, DMSO-d_6, ADA-B36-fr20-50-DMSO-C13): δ23.20 (**C**H$_3$), 29.51 (α-**C**H$_2$-amide), 30.98 (β-**C**H$_2$-amide), 50.23 (α-**C**H-amide), 59.17 (**C**HCl), 65.29 (α-**C**H$_2$-OOC), 126.60 (phenyl-**C**H), 127.22 (phenyl-**C**H), 128.87 (phenyl-**C**H), 145.38 (phenyl-**C**), 170.28 (-**C**OOR), 172.55 (-**C**ONR). ^{1}H NMR for low R_f diastereomer (400 MHz, DMSO-d_6, ADA-A289-19-H1): δ1.32 (6H, d, C**H**$_3$, J = 6.9 Hz), 2.44 (4H, m, α-C**H**$_2$-amide), 2.55 (4H, m, β-C**H**$_2$-amide), 4.27 (4H, m, α-C**H**$_2$-OOC), 4.69 (2H, m, C**H**Cl), 4.89 (2H, qd, α-C**H**-amide, J = 6.9 Hz, J = 7.0 Hz), 7.21 (2H, m, phenyl-C**H**), 7.29 (8H, m, phenyl-C**H**), 8.37 (2H, d, N**H**, J = 7.9 Hz). ^{13}C NMR for low R_f diastereomer (400 MHz, DMSO-d_6, ADA-A289-19-C13): δ23.23 (**C**H$_3$), 29.45 (α-**C**H$_2$-amide), 30.33 (β-**C**H$_2$-amide), 48.49 (α-**C**H-amide), 59.16 (**C**HCl), 65.25 (α-**C**H$_2$-OOC), 126.64 (phenyl-**C**H), 127.24 (phenyl-**C**H), 128.85 (phenyl-**C**H), 145.40 (phenyl-**C**), 170.30 (-**C**OOR), 172.64 (-**C**ONR).

Notebook pages: ADA-A287, ADA-B35, ADA-B37, ADA-B73

Attempted synthesis of a single enantiomer of 2,3-dichloro-1,4-butanediol:

To a round bottom flask, the low R_f diastereomer (0.569 g, 1.00 mmol), 1,4-dioxane (10 mL, ACS grade, Fisher Scientific), and 10 M sulfuric acid (10 mL) were added. After stirring at room temperature for 20 hours, the reaction mixture was quenched with water (20 mL) and extracted with diethyl ether (5 x 40 mL). The organic layer was washed with saturated $NaHCO_3$

(3 x 50 mL) and saturated aq. NaCl (1 x 50 mL), and was then dried over $MgSO_4$, filtered, and concentrated on a rotary evaporator. The crude product was purified with flash column chromatography and recrystallized from $CHCl_3$ to yield 2,3-dichloro-1,4-butanediol (0.075 g, 46.5 % yield) as off-white crystals, with an optical purity of 9.28% *ee*.

Physical data: $R_f = 0.39$ (1:1 EtOAc/hexanes v/v, PMA stain as indicator). Melting point: 62-64 °C (Lit. mp for racemic: 67-68 °C, Lit. mp for single enantiomer: 88-89 °C).[17] Optical rotation: $[\alpha]^{20}_D$ = +5.95° *c* 0.06, $CHCl_3$ (Lit. optical rotation for single enantiomer: $[\alpha]^{20}_D$ = +64.1° *c* 0.56, $CHCl_3$).[17,39] ^{1}H NMR (400 MHz, $CDCl_3$, ADA-B83-17): δ2.62 (2H, br s, O**H**), 3.97 (4H, m, C**H**$_2$), 4.35 (2H, m, C**H**Cl).

Notebook pages: ADA-B81 (refer to ADA-B49 for hydrolysis with HCl/water)

$LiAlD_4$ Reduction of Dibromo-Bis(methylbenzylamide) Diastereomers

After performing all of the experiments described above, it was determined that any method involving hydrolysis of esters containing vicinal dihalides could not be used due to the observed racemization. However, instead of starting over, it was decided that the method of forming bis(methylbenzylamide) diastereomers could still be utilized. It was proposed that reduction of a bis(methylbenzylamide) diastereomer containing vicinal dibromides with $LiAlD_4$, prior to performing ester hydrolysis, could result in the formation of the stereospecifically deuterated guest. Initially this approach was avoided because it was unclear if neighboring group participation from the ester or amide functional groups would result during the $LiAlD_4$ reduction. In addition, immediate reduction of a given diastereomer would require a greater amount of $LiAlD_4$ since deuteride may also reduce the ester and deprotonate the amide functional groups in conjunction with reduction of the vicinal dibromides. More importantly, the optical activity and melting point of 2,3-dibromo-1,4-butanediol are known, and the stereospecific reduction of this compound is known to proceed cleanly.[17,18]

In this modified approach (Figure 2-22), *d,l*-2,3-dibromo-1,4-butanediol would be treated with succinic anhydride to form the racemic dihemisuccinate, 4,4'-[(2,3-dibromobutane-1,4-diyl)bis(oxy)]bis(4-oxobutanoic acid). The reaction of this substrate with (*S*)-(-)-α-methylbenzylamine would form dibromo-bis(methylbenzylamide) diastereomers, which can be separated with column chromatography. Reduction of a single diastereomer, (*S,S,S,S*) stereochemistry for example, with $LiAlD_4$ would give (2*S*,3*S*)-1,4-butanediol-d_2. The terminal

alcohols can then be replaced with bromine to form the common intermediate (2*S*,3*S*)-1,4-dibromobutane-d_2.

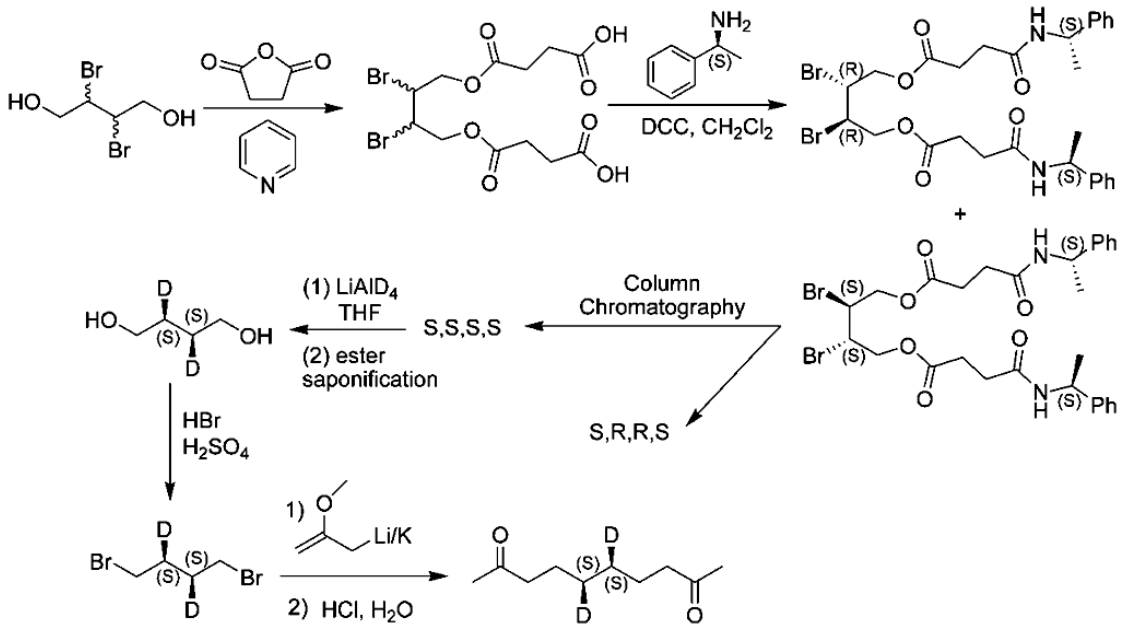

Figure 2-22: Synthesis of (5*S*,6*S*)-2,9-decanedione-d_2, via resolution with the chiral auxiliary, (*S*)-(-)-α-methylbenzylamine, utilizing a vicinal dibromide.

This modified approach is currently in progress. The only roadblock faced thus far is the crystallization of a single bis(methylbenzylamide) diastereomer. A crystal structure for one of the diastereomers is required for this synthesis, as this will allow us to assign the stereochemistry of the vicinal dibromides. This synthetic approach cannot be pursued further unless crystallographic data is obtained for a single diastereomer.

If growing crystals of a single bis(methylbenzylamide) diastereomer is unsuccessful, then an alternative crystal growth method has been proposed. Instead of forming a covalently linked diastereomer, it may be possible to crystallize the dibromo-dihemisuccinate ester with (*S*)-(-)-α-methylbenzylamine in the form of a diastereomeric salt. These diastereomeric salts may preferentially crystallize in one form over the other, allowing for the isolation of a single diastereomer. Mild acid hydrolysis would liberate the amine from the dihemisuccinate, allowing the isolation of a single enantiomer of the dibromo-dihemisuccinate ester. This crystallization method is currently in progress. Several cooling and evaporative growth techniques are being attempted.

4,4'-[(2,3-Dibromobutane-1,4-diyl)bis(oxy)]bis(4-oxobutanoic acid):

This procedure was performed by Angelo Aguilar, a previous member of the Hollingsworth group. To a round bottom flask, *d,l*-2,3-dibromo-1,4-butanediol (50.0 g, 0.20 mol, Aldrich, 99%) and pyridine (42.6 g, 0.54 mol, Fisher Scientific) were added under an argon atmosphere. To this reaction mixture, succinic anhydride (43.8 g, 0.44 mol, Aldrich, 99%) was added all at once. After stirring at room temperature for 18 hours, the reaction was cooled to ice temperatures and was quenched with chilled 2.5 M HCl until a pH of 1 was reached. After stirring for 30 minutes at ice temperatures, a white precipitate had formed in the reaction mixture. The reaction was filtered, and the white precipitate was rinsed three times with cold water. The white precipitate was recrystallized from water, affording the racemic 4,4'-[(2,3-dibromobutane-1,4-diyl)bis(oxy)]bis(4-oxobutanoic acid) (75.039 g, 82.7% yield) as a white solid.

Physical data (all physical data were analyzed by the author): R_f = 0.05 (4:1 EtOAc/hexanes v/v, PMA stain as indicator). Melting point: 95-98 °C (Lit. mp: 96-98 °C).[17] ^{1}H NMR (400 MHz, Acetone-d_6, ADA-B101-2-H1): δ2.65 (8H, m, ROOC-C**H**2-C**H**2-COOH), 4.37 (2H, dd, α-C**H**$_2$-OCOR, *J* = 11.5 Hz, *J* = 7.1 Hz), 4.54 (2H, dd, α-C**H**$_2$-OCOR, *J* = 11.5 Hz, *J* = 6.2 Hz), 4.68 (2H, m, C**H**Br). ^{13}C NMR (100.57 MHz, Acetone-d_6, ADA-B101-3-C13): δ28.37 (ROOC-CH2-**C**H2-COOH), 29.73 (ROOC-**C**H2-CH2-COOH), 50.47 (α-**C**H$_2$-OCOR), 65.91 (**C**HBr), 171.57 (-**C**OOH), 172.99 (-**C**OOR).

Notebook pages: AA-24A for synthetic procedure, ADA-B101 for physical analysis

Dibromo-bis(methylbenzylamide) diastereomers:

In a 3-neck round bottom flask equipped with a reflux condenser, the racemic 4,4'-[(2,3-dibromobutane-1,4-diyl)bis(oxy)]bis(4-oxobutanoic acid) (3.52 g, 7.82 mmol), (*S*)-(-)-α-methylbenzylamine (2.08 g, 17.2 mmol, Acros, 99%), and CH_2Cl_2 (30 mL) were added under an argon atmosphere. The reaction mixture was cooled to ice temperatures prior to the addition of *N,N*'-dicyclohexylcarbodiimide (4.03 g, 19.55 mmol, Aldrich, 99%). The reaction mixture was stirred at ice temperatures for 30 minutes, after which the ice bath was removed, and the reaction mixture was heated to reflux. After refluxing at 40 °C for 4 hours, the reaction mixture was cooled and filtered to remove the excess dicyclohexylurea byproduct. The CH_2Cl_2 filtrate was

washed with 1 M HCl (1 x 50 mL), 1 M $NaHCO_3$ (1 x 50 mL), and saturated aq. NaCl solution (1 x 50 mL). The organic layer was dried over $MgSO_4$, filtered, and concentrated on a rotary evaporator to yield crude dibromo-bis(methylbenzylamide) diastereomers as a yellow oil. The crude product was purified with flash column chromatography to isolate the high R_f diastereomer (3.29 g, 128% yield, contaminated with DCU) and the low R_f diastereomer (1.49 g, 58.4% yield) as sticky white solids. Recrystallizations from acetone, ethyl acetate, and DMSO have been unsuccessful thus far.

Physical data: $R_f = 0.33$ for high R_f and 0.18 for low R_f diastereomer (1:1 EtOAc/hexanes v/v, PMA stain as indicator). ^{1}H NMR for high R_f diastereomer (400 MHz, DMSO-d_6, ADA-A191-23): δ1.33 (6H, d, C**H**$_3$, *J* = 7.0 Hz), 2.44 (4H, m, α-C**H**$_2$-CONR), 2.57 (4H, m, β-C**H**$_2$-CONR), 4.34 (4H, m, α-C**H**$_2$-OOCR), 4.70 (2H, m, C**H**Br), 4.89 (2H, qd, α-C**H**-NCOR, *J* = 7.0 Hz, *J* = 8.1 Hz), 7.21 (2H, m, phenyl-C**H**), 7.29 (8H, m, phenyl-C**H**), 8.25 (2H, d, N**H**, *J* = 8.1 Hz). ^{1}H NMR for low R_f diastereomer (400 MHz, DMSO-d_6, ADA-A191-24): δ1.32 (6H, d, C**H**$_3$, *J* = 7.0 Hz), 2.43 (4H, m, α-C**H**$_2$-CONR), 2.54 (4H, m, β-C**H**$_2$-CONR), 4.32 (4H, m, α-C**H**$_2$-OOCR), 4.68 (2H, m, C**H**Br), 4.89 (2H, qd, α-C**H**-NCOR, *J* = 7.0 Hz, *J* = 8.1 Hz), 7.21 (2H, m, phenyl-C**H**), 7.29 (8H, m, phenyl-C**H**), 8.33 (2H, d, N**H**, *J* = 8.1 Hz).

Notebook pages: ADA-A181, ADA-B85, ADA-B97, (refer to ADA-B103 for recrystallization experiments)

2,3-Dideuterio-1,4-butanediol:

To a round bottom flask was added $LiAlD_4$ (0.81 g, 19.3 mmol, Acros, 98 atom% D) and dry THF (10 mL) under an argon atmosphere. After cooling the reaction mixture to ice temperatures, a solution of the low R_f diastereomer (1.49 g, 2.14 mmol, ADA-B87-fr.66-90) in THF (10 mL) was added. After bubbling ceased, the ice bath was removed, and the reaction mixture was allowed to stir at room temperature for 2 days. The reaction mixture was then slowly quenched with 5 mL water, and 2.5 M HCl (40 mL) was slowly added. The reaction mixture was continuously extracted with diethyl ether for 24 hours before the organic layer was dried over $MgSO_4$, filtered, and concentrated on a rotary evaporator. The crude product was purified with flash column chromatography to afford 2,3-dideuterio-1,4-butanediol (25.0 mg, 12.7% yield) as a colorless oil. The absolute configuration of this will become known only after the crystal structure of the bis(methylbenzylamide) diastereomer has been determined. The low

yield of this reaction could be from the formation of byproducts or decomposition of the desired product. It was observed that when non-deuterated 1,4-butanediol sat in a vial for 1 week, it had changed from a colorless oil to a yellow oil, suggesting that it had started to decompose.

Physical data: $R_f = 0.19$ (4:1 EtOAc/hexanes v/v, PMA stain as indicator). ^{1}H NMR (400 MHz, $CDCl_3$, ADA-B96-fr94-96): δ1.67 (2H, m, C**H**D), 3.69 (4H, m, C**H**$_2$).

Notebook pages: ADA-B89, ADA-B93

Dihemisuccinate-methylbenzylamine diastereomeric salts:

In an Erlenmeyer flask, the dibromo-dihemisuccinate ester (1.0 g, 2.22 mmol) and (*S*)-(-)-α-methylbenzylamine (0.55 g, 4.56 mmol, Aldrich, 98%) were dissolved in a 1:1 mixture of water and ethanol (10 mL). To completely dissolve the dihemisuccinate, the mixture was heated to 40 °C for 15-20 minutes, after which the flask was placed in a 1 L Dewar flask containing 45 °C water/ethanol bath. The Dewar was placed in the freezer and allowed to cool slowly to -26 °C. After 20 hours, no crystals had formed. The Erlenmeyer flask was then placed in a dry ice/ethanol bath and cooled slowly to -50 °C. At -50 °C a white solid precipitated, but it immediately dissolved when the Erlenmeyer flask was removed from the dry ice/ethanol bath.

In a separate Erlenmeyer flask, dibromo-dihemisuccinate ester (3.0 g, 6.67 mmol) and (*S*)-(-)-α-methylbenzylamine (1.68 g, 13.9 mmol, Aldrich, 98%) were dissolved in ethanol (5 mL). To completely dissolve the dihemisuccinate, the mixture was heated to 40 °C for 20-25 minutes, after which the flask was capped with a rubber septum and vented with a needle. A slow stream of argon was blown through the Erlenmeyer flask, allowing slow evaporation of ethanol to occur at room temperature. As of this writing, no crystals had formed.

Notebook pages: ADA-B105

Alternative Approach Through the Stereospecific Formation of an Epoxide

As an alternative to diastereomeric separations, another approach involving the highly stereoselective synthesis of an epoxide intermediate was proposed. This proposed method is illustrated in Figure 2-23.

The inexpensive, commercially available (+)-dimethyl L-tartrate can first be treated with hydrogen bromide in the presence of acetic acid to stereoselectively afford the vicinal acetoxy-

bromide.[43,44] This method has been shown to proceed in high yields and with excellent stereoselectivity.[45] The vicinal acetoxy-bromide can then be deacetylated with HCl and then cyclized in the presence of potassium carbonate to produce (2*R*,3*R*)-dimethyl oxirane-2,3-dicarboxylate epoxy ester.[44] A mild reduction with sodium borohydride can then afford (2*S*,3*S*)-epoxy-1,4-butanediol.[44] Protection of the terminal alcohols with a tetrahydropyranyl (THP) protecting group would be accomplished by reaction with pyridinium *p*-toluenesulfonate (PPTS) and dihydropyran. The THP protecting group was chosen since it can withstand $LiAlH_4$ reductions and can easily be added and removed during any stage of the synthesis.[46] In addition, it has been reported that the THP protecting group can be added under mildly acidic conditions that are compatible with most functional groups. For example, Miyashita *et al.* have shown epoxy functional groups to survive intact during the addition of dihydropyran in the presence of PPTS.[47] After protection of the terminal alcohols with THP, the chiral epoxide can be reduced with $LiAlD_4$. This has been shown to proceed in an S_N2 fashion to give inversion of configuration.[48] The alcohol functional group can then be turned into a better leaving group by reaction with methanesulfonyl chloride, which can subsequently be reduced with $LiAlD_4$. The THP protecting groups can then be removed in the presence of acid, affording the (2*S*,3*S*)-1,4-butanediol-d_2. In the final steps, this diol can easily be converted, using HBr/H_2SO_4, to the common intermediate described previously ((2*S*,3*S*)-1,4-dibromobutane-d_2). The first three steps of this process have successfully been completed.

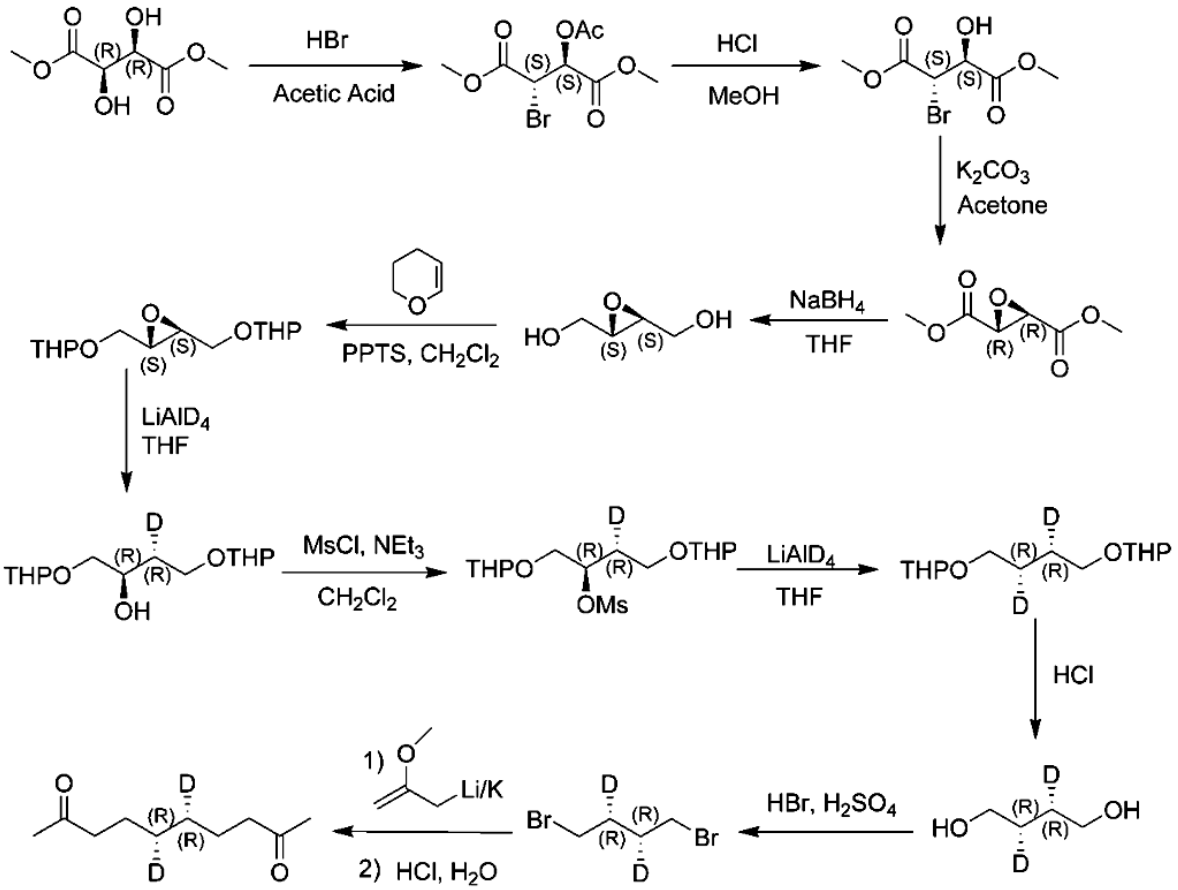

Figure 2-23: Alternative synthesis proposed for the formation of (5*S*,6*S*)-2,9-decanedione-d_2, in which a chiral epoxide intermediate would be formed.

(2S,3S)-Dimethyl-2-acetoxy-3-bromosuccinate:

To a round bottom flask equipped with a dropping funnel was added (+)-dimethyl L-tartrate (1.5 g, 8.42 mmol, Aldrich, 99%) under an argon atmosphere. The flask was placed in an ice bath, after which an HBr solution (3.4 g, 42.10 mmol, Aldrich, 33 wt % in acetic acid) was added dropwise, and the reaction mixture was stirred at 0 °C for 10 minutes. After stirring at room temperature for 11 hours, the reaction mixture was quenched with ice-cold water (25 mL) and extracted with diethyl ether (3 x 100 mL). The organic layer was washed with saturated aq. NaCl (1 x 100 mL), dried over $MgSO_4$, filtered, and concentrated on a rotary evaporator. This yielded the (2*S*,3*S*)-dimethyl-2-acetoxy-3-bromosuccinate (1.67 g, 70% yield) as a colorless liquid, which was used in the next reaction without further purification.

Physical data: $R_f = 0.80$ (1:1 EtOAc/hexanes v/v, PMA stain as indicator). ^{1}H NMR (400 MHz, $CDCl_3$, ADA-A278-11-H1): δ2.10 (3H, s, α-C**H**$_3$-COOR), 3.83 (6H, s, α-C**H**$_3$-OOC), 4.81

(1H, d, C**H**Br, *J* = 5.5 Hz), 5.61 (1H, d, C**H**OAc, *J* = 5.6 Hz). ^{13}C NMR (100.57 MHz, $CDCl_3$, ADA-A278-11-C13): δ20.55 (α-**C**H_3-COOR), 43.33 (**C**HBr), 53.23 (**C**H_3O), 53.94 (**C**H_3O), 72.79 (**C**HOAc), 166.54 (ROO**C**R), 167.14 (ROO**C**R), 169.67 (ROO**C**R).

Notebook pages: ADA-A277, ADA-A299, ADA-B15

(2S,3S)-Dimethyl-2-bromo-3-hydroxysuccinate:

To a round bottom flask equipped with a reflux condenser, (2*S*,3*S*)-dimethyl-2-acetoxy-3-bromosuccinate (1.67 g, 5.93 mmol) and 0.3 M HCl in methanol (59.3 mL) was added. After heating at 60 °C for 5 hours, the reaction mixture was quenched with water (50 mL) and saturated aq. NaCl (50 mL). The aqueous layer was extracted with diethyl ether (4 x 100 mL), and the organic layer was dried over $MgSO_4$, filtered, and concentrated on a rotary evaporator. The crude product was purified with flash column chromatography to yield (2*S*,3*S*)-dimethyl-2-bromo-3-hydroxysuccinate (0.553 g, 39% yield) as a colorless liquid. The yield reported in the literature is 82% after reacting for 46 hours at 22 °C.[44] The present yield could be improved by performing the reaction at a lower temperature for a longer period of time.

Physical data: R_f = 0.63 (1:1 EtOAc/hexanes v/v, PMA stain as indicator). ^{1}H NMR (400 MHz, DMSO-d_6, ADA-A290-17-H1): δ3.71 (6H, s, C**H**$_3$), 4.46 (1H, t, C**H**OH, *J* = 5.1 Hz), 4.59 (1H, d, C**H**Br, *J* = 7.7 Hz), 6.79 (1H, d, O**H**, *J* = 5.3 Hz). ^{13}C NMR (100.57 MHz, DMSO-d_6, ADA-A290-17-C13): δ46.39 (**C**HBr), 52.83 (**C**H_3), 53.80 (**C**H_3), 72.87 (R**C**HOH), 168.03 (R**C**OOR), 170.91 (R**C**OOR).

Notebook pages: ADA-A285, ADA-A303, ADA-B9, ADA-B17

(2R,3R)-Dimethyl oxirane-2,3-dicarboxylate:

To a round bottom flask was added (2*S*,3*R*)-dimethyl-2-bromo-3-hydroxysuccinate (0.553 g, 2.30 mmol), dry acetone (10 mL), and anhydrous potassium carbonate (1.91 g, 13.8 mmol, J.T. Baker) under an argon atmosphere. After stirring at room temperature for 20 hours the acetone was removed on a rotary evaporator at room temperature. The crude reaction mixture was quenched with water (50 mL) and extracted with diethyl ether (3 x 50 mL). The organic layer was washed with saturated aq. NaCl (1 x 50 mL), dried over $MgSO_4$, filtered, and concentrated on a rotary evaporator. The crude product was purified with flash column chromatography to yield pure (2*R*,3*R*)-dimethyl oxirane-2,3-dicarboxylate (0.206 g, 56% yield)

as a white solid, with a measured optical purity of 67.8% *ee.* (The concentration used for polarimetry was lower than that used in literature, so this may explain the apparent loss of optical activity.)

Physical data: $R_f = 0.68$ (1:1 EtOAc/hexanes v/v, PMA stain as indicator). Melting point: 68-71.5 °C (Lit. mp: 70-73 °C). Optical rotation: $[\alpha]^{20}_D = -94.61°$ *c* 0.175, MeOH (Lit. optical rotation: $[\alpha]^{20}_D = -139.6°$ *c* 1.07, MeOH). ^{1}H NMR (400 MHz, $CDCl_3$, ADA-A296-13-H1): δ3.69 (2H, s, epoxy-C**H**), 3.82 (6H, s, C**H**$_3$). ^{13}C NMR (100.57 MHz, $CDCl_3$, ADA-A296-13-C13): δ52.15 (**C**H$_3$ or epoxy-**C**H), 53.18 (**C**H$_3$ or epoxy-**C**H), 167.36 (R**C**OOR).

Notebook pages: ADA-A295, ADA-B7, ADA-B10, ADA-B19

Alternative Approach Through Formation of Diastereomeric Diethers

Another approach for the synthesis of (5*S*,6*S*)-2,9-decanedione-d_2 involving the formation of diastereomeric diethers has been proposed (Figure 2-24). The commercially available (*S*)-2-phenyl-1-propanol could be treated with trifluoromethanesulfonic anhydride to transform the primary alcohol into the triflate, (*S*)-2-phenylpropyl trifluoromethanesulfonate. The triflate has excellent leaving group abilities (10^4 times more reactive than mesylate ester and 10^8 times more reactive than bromide),[41] thus making it an excellent candidate for reacting with an alcohol to form an ether. This can be accomplished by treating (*S*)-2-phenylpropyl trifluoromethanesulfonate with *d,l*-2,3-dibromo-1,4-butanediol, forming a mixture of dibromo-bis(2-phenylpropyl ether) diastereomers. Separation of the diastereomers with column chromatography, followed by $LiAlD_4$ reduction of a single diastereomer would yield a single dideuterio-bis(2-phenylpropyl ether) diastereomer ((*S*,*S*,*S*,*S*) stereochemistry for example). Cleavage of the ether functional groups by treatment with HBr would then form the common intermediate (2*S*,3*S*)-1,4-dibromobutane-d_2. This synthetic approach has yet to be attempted.

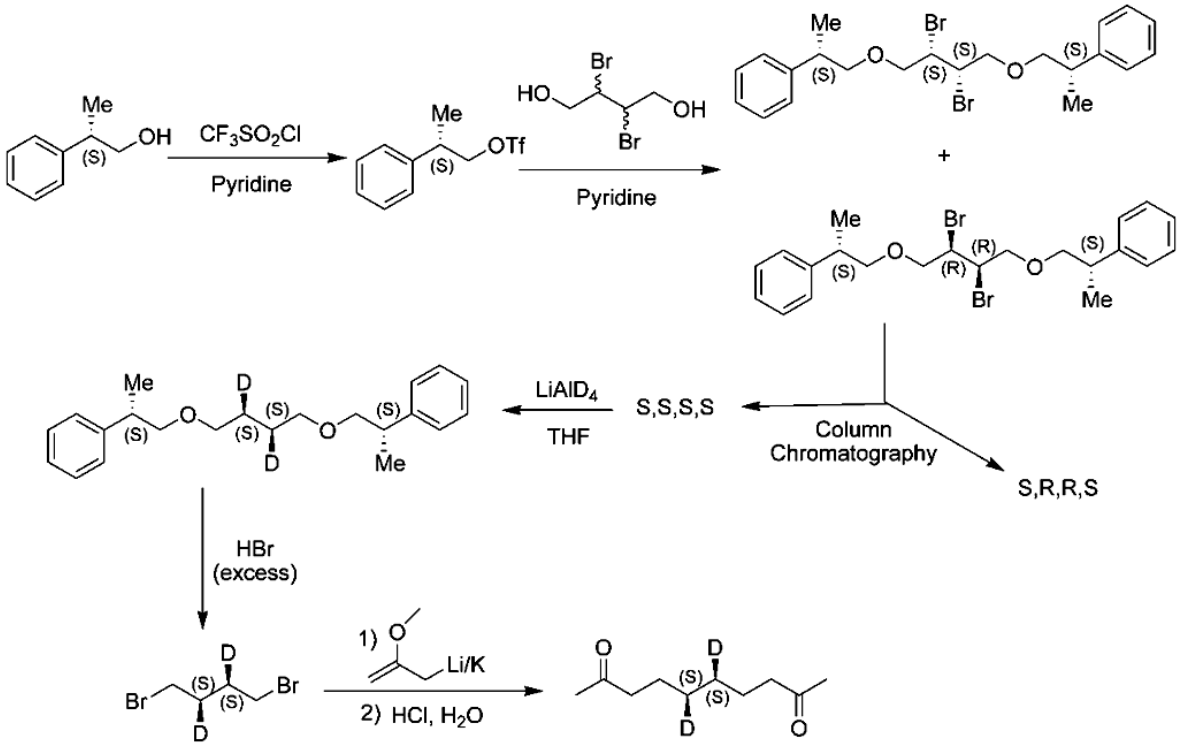

Figure 2-24: Alternative synthetic approach the formation of (5*S*,6*S*)-2,9-decanedione-d_2, involving the separation of dibromo-bis(2-phenylpropyl ether) diastereomers.

Conclusions for Chapter 2

The synthesis of the stereospecifically deuterated guest molecule, (5*S*,6*S*)-2,9-decanedione-d_2, was attempted. This guest molecule is a critical component for determination of the absolute configuration of urea inclusion compounds. Although several synthetic methods were attempted, the successful synthesis of (5*S*,6*S*)-2,9-decanedione-d_2 has yet to be completed. A current strategy involving the stereospecific reduction of a single dibromo-bis(methylbenzylamide) diastereomer with $LiAlD_4$ is still in progress. However, a crystal structure of this diastereomer is needed before proceeding with this synthetic route. Alternative approaches involving a stereospecific epoxide intermediate or the formation of dibromo-bis(2-phenylpropyl ether) diastereomers have been proposed for future research. Future work will consist of successfully preparing (5*S*,6*S*)-2,9-decanedione-d_2/urea and analyzing this system with polarized light microscopy, X-ray topography, and single crystal neutron diffraction. These

studies will allow us to unambiguously define the absolute configuration of urea inclusion compounds.

Chapter 2 References

1 Arad-Yellin, R., Green, B. S., Knossow, M. and Tsoucaris, G. in *Inclusion Compounds* Vol. 3 (eds. J. L. Atwood, J. E. D. Davies, and D. D. MacNicol) 263-295 (Academic, London, 1984).

2 Yeo, L. and Harris, K. D. M. Temperature-dependent structural properties of a solid urea inclusion compound containing chiral guest molecules: 2-bromotetradecane/urea. *Can. J. Chem.* **77**, 2105-2118, (1999).

3 Schlenk, W., Jr. Asymmetric urea inclusion lattice. IV. Absolute configuration of the lattice. *Justus Liebigs Ann. Chem* **7**, 1195-1209, (1973).

4 Hollingsworth, M. D. and Harris, K. D. M. in *Comprehensive Supramolecular Chemistry* Vol. 6 (eds. D. D. MacNicol, F. Toda, and R. Bishop) pp. 177-237 (Elsevier Science Ltd., Oxford, 1996).

5 Schlenk, W. Inclusion diastereoisomerism - Determination of the absolute configuration of the hexagonal urea lattice. *Angew. Chem. Intl. Ed.* **72**, 58-63, (1960).

6 Schlenk, W. Untersuchung uber Einschlu(beta)diastereomerie und bestimmung der absoluten konfiguration des hexagonalen harnstoffgitters. *Angew. Chem.* **72**, 845-849, (1960).

7 Lenné, H. U., Mez, H. C. and Schlenk, W., Jr. Lengths of molecules in inclusion channels of urea and thiourea. *Justus Liebigs Ann. Chem.* **732**, 70-96, (1970).

8 Brown, M. E., Chaney, J. D., Santarsiero, B. D. and Hollingsworth, M. D. Superstructure topologies and host-guest interactions in commensurate inclusion compounds of urea with bis(methyl ketone)s. *Chem. Mater.* **8**, 1588-1591, (1996).

9 McBride, M. J. Symmetry reduction in solid-solutions - a new method for materials design. *Angew. Chem. Intl. Ed. Engl.* **28**, 377-379, (1989).

10 Hollingsworth, M. D., Brown, M. E., Hillier, A. C., Santarsiero, B. D. and Chaney, J. D. Superstructure control in the crystal growth and ordering of urea inclusion compounds. *Science* **273**, 1355-1359, (1996).

11 Alquist, K. Unpublished results regarding growth spirals of 2,9-decanedione/urea have been reported in the Hollingsworth group.

12 Geday, M. A., Kaminsky, W., Lewis, J. G. and Glazer, A. M. Images of absolute retardance LδN, using the rotating polariser method. *J. Microscopy* **198**, 1-9, (2000).

13 Schlenk, W., Jr. Rotation of the plane of polarized light by hexagonal urea inclusion crystals. *Chem. Ber.* **101**, 2445-2449, (1968).

14 Peterson, M. L. Several heavy-atom containing guests studied by Matthew L. Peterson (unpublished work).

15 Bau, R., Schreiber, A., Metzenthin, T., Lu, R. S., Lutz, F., Klooster, W. T., Koetzle, T. F., Seim, H., Kleber, H. P., Brewer, F. and Englard, S. Neutron diffraction structure of (2R,3R)-L-(-)- 2-D carnitine tetrachloroaurate, $(CH_3)(3)N\text{-}CH_2\text{-}CHOH\text{-}CHD\text{-}COOH$ (+) AuCl4 (-): Determination of the absolute stereochemistry of the crotonobetaine-to-

carnitine transformation catalyzed by L-carnitine dehydratase from *Escherichia coli*. *J. Am. Chem. Soc.* **119**, 12055-12060, (1997).

16 Taherirastgar, F. and Brandsma, L. Generation and synthetic application of metallated methyl isopropenyl ether. A substitute for acetone enolate. *Chemische Berichte/Recueil* **130**, 45-48, (1997).

17 Feit, P. W. Synthese der stereoisomeren 1.2-3.4-dioxido-butane. *Chemische Berichte-Recueil* **93**, 116-127, (1960).

18 Chickos, J. S., Bausch, M. and Alul, R. Stereospecific synthesis of optically-active succinic-D2 acid. *J. Org. Chem.* **46**, 3559-3562, (1981).

19 Groves, J. T. and Ma, K. W. Dehalogenations with sodium borohydride - Evidence for a free-radical reaction. *J. Am. Chem. Soc.* **96**, 6527-6529, (1974).

20 Carey, F. A. and Sundberg, R. J. *Advanced Organic Chemistry, Part A: Structure and Mechanisms*. pp. 136-137 (Springer Science & Business Media, New York, NY, 2007).

21 Chatterjee, A., Sasikumar, M. and Joshi, N. N. Preparation of enantiopure trans-1,2-cyclohexanediol and trans-2-aminocyclohexanol. *Synth. Commun.* **37**, 1727-1733, (2007).

22 Bijvoet, J. M., Peerdeman, A. F. and van Bommel, A. J. Determination of the absolute configuration of optically active compounds by means of x-rays. *Nature* **168**, 271-272, (1951).

23 Gajda, R. B. Notebook RBG-C17, RBG-C19; Structure solution MH1024.

24 Adams, A. D. Refer to lab notebook: ADA-A157.

25 Smith, M. B. and March, J. *March's Advanced Organic Chemistry: Reactions, Mechanisms, and Structure*. 6th edn, pp. 446-450 (John Wiley & Sons, Inc., Hoboken, New Jersey, 2007).

26 *Dielectric Constant Values*, <https://www.clippercontrols.com/pages/dielectric-constant-values#D> San Francisco, CA, 2011 Clipper Controls Inc. (June 22, 2011).

27 Adams, A. D. Refer to notebook pages ADA-A187 and ADA-A193 for HPLC experiments.

28 Adams, A. D. Refer to notebook pages ADA-A157 and ADA-A159 for optical rotation measurements of 2,3-dibromo-1,4-butanediol.

29 Abad, J. L., Villorbina, G., Fabrias, G. and Camps, F. Synthesis and use of stereospecifically deuterated analogues of palmitic acid to investigate the stereochemical course of the delta(11) desaturase of the processionary moth. *J. Org. Chem.* **69**, 7108-7113, (2004).

30 Scheurer, A., Mosset, P. and Saalfrank, R. W. Syntheses of C-2-symmetric vicinal diamines derived from tartaric acid. *Tetrahedron-Asymmetry* **10**, 3559-3570, (1999).

31 Newkome, G. R., Gupta, V. K., Griffin, R. W. and Arai, S. Chemistry of micelles series. 4. A convenient synthesis of tetrakis(2-bromoethyl)methane. *J. Org. Chem.* **52**, 5480-5482, (1987).

32 1,4-dimethoxybutane has been reported to have a bp of 131 ^{o}C at 760 Torr [W. Reppe, et. al., *Justus Liebigs Annalen der Chemie*. **596**, 80-158 (1955)]. However, it was experimentally observed that an azeotrope occurs with a mixture of ether and 1,4-dimethoxybutane, lowering its bp.

33 Adams, A. D. Refer to lab notebook: ADA-A207, ADA-A211, ADA-A219, ADA-A225, ADA-A227, & ADA-A233.

34 Johnstone, R. A. W. and Rose, M. E. Rapid, simple, and mild procedure for alkylation of phenols, alcohols, amides, and acids. *Tetrahedron* **35**, 2169-2173, (1979).
35 Adams, A. D. Refer to lab notebook: ADA-A237 & ADA-A239 for synthesis of 1,4-dimethoxybutane in dimethyl sulfoxide.
36 Navarro, I., Fabrias, G. and Camps, F. Insect desaturases as unique analytical tools to unravel the stereochemical course of the reduction of vicinal ditosylates with lithium aluminum deuteride. *Angew. Chem. Intl. Ed. Engl.* **38**, 164-166, (1999).
37 Lin, G. Q. and Shi, Z. C. Enantiomerically pure cage-shaped (1S,4S,5R)-4-hydroxy-2,6-diazabicyclo 3.3.0 octane and (1S,4R,5R)-4-hydroxy-2-oxa-6-azabicyclo 3.3.0 octane: Synthesis and test for enantioselective catalysis. *Tetrahedron* **53**, 1369-1382, (1997).
38 Peterson, P. E. Cyclic halonium ions with 5 membered rings. *Acc. Chem. Res.* **4**, 407-&, (1971).
39 Yoshimitsu, T., Fukumoto, N. and Tanaka, T. Enantiocontrolled synthesis of polychlorinated hydrocarbon motifs: A nucleophilic multiple chlorination process revisited. *J. Org. Chem.* **74**, 696-702, (2009).
40 Adams, A. D. Refer to ADA-A263 for attempted separations of dichloro bis(acetylmandelate ester) diastereomers.
41 Carey, F. A. and Sundberg, R. J. *Advanced Organic Chemistry, Part A: Structure and Mechanisms*. pp. 654-657 (Springer Science & Business Media, New York, NY, 2007).
42 Bellucci, G., Marsili, A., Mastrori.E, Morelli, I. and Scartoni, V. Kinetics of thermal racemization of some 1,2-dihalides. *J. Chem. Soc. - Perkin Trans. 2*, 201-204, (1974).
43 Corey, E. J., Marfat, A. and Hoover, D. J. Stereospecific total synthesis of 12-(R)-forms and 12-(S)-forms of 6-trans leukotriene-B. *Tetrahedron Lett.* **22**, 1587-1590, (1981).
44 Corey, E. J. and Lansbury, P. T. Stereochemical course of 5-lipoxygenation of arachidonate by rat basophil leukemic-cell (RBL-1) and potato enzymes. *J. Am. Chem. Soc.* **105**, 4093-4094, (1983).
45 Golding, B. T., Hall, D. R. and Sakrikar, S. Reaction between vicinal diols and hydrogen bromide in acetic-acid synthesis of chiral propylene-oxide. *J. Chem. Soc., Perkin Trans. 1*, 1214-1220, (1973).
46 Wuts, P. G. M. and Greene, T. W. *Greene's Protective Groups in Organic Synthesis*. 4th edn, pp. 986-1032 (John Wiley & Sons, Inc., Hoboken, New Jersey, 2007).
47 Miyashita, M., Yoshikoshi, A. and Grieco, P. A. Pyridinium p-toluenesulfonate. A mild and efficient catalyst for the tetrahydropyranylation of alcohols. *J. Org. Chem.* **42**, 3772-3774, (1977).
48 Helmkamp, G. K. and Rickborn, B. F. Stereochemistry of some lithium aluminum deuteride reductions. *J. Org. Chem.* **22**, 479-482, (1957).

CHAPTER 3 - 1,6-Dicyanohexane-1,1,6,6-d_4/urea

Introduction

As mentioned in Chapter 1, single crystals of simple molecular materials that undergo observable elastic phenomena can provide a route for probing the mechanical properties of solids. Ordinarily, each system must be considered on a case-by-case basis given that crystal packing is rarely the same.[1] As a result, it is desirable to find materials, such as urea inclusion compounds (UICs), that can be perturbed in predictable ways.[1] Investigations into the elastic properties of UICs help provide a molecular basis for understanding the mechanism of domain switching in ferroelastic UICs.[2] For instance, in ferroelastic UICs, the guest molecules have been observed to distort the urea channel away from its usual hexagonal symmetry. Moreover, specific motions of the guest can also relax the distortion of the urea channel and shift the cell toward hexagonal symmetry.[2]

In the presence of urea, aliphatic α,ω-dinitriles containing three to ten carbon atoms have been observed to display dramatic changes in crystal packing.[3] For example, 1,6-dicyanohexane/urea forms chunky hexagonal prisms, while those of 1,10-dicyanodecane/urea form hexagonal needles, and those of 1,8-dicyanooctane/urea grow as hexagonal-shaped plates.[3] Interestingly, 1,6-dicyanohexane/urea is a commensurate system with a 6:1 ratio of urea to guest; that is, its UIC contains one guest for every repeat of the urea host.[4] The structure of 1,6-dicyanohexane/urea shows no evidence of hydrogen bonding between host and guest, and it has been found that the terminal groups in the guest's chain exist in two gauche conformations[4] that are in equilibrium with each other.[5] In the crystal structures from room temperature to 90 K, two distinguishable gauche conformers can be discerned. (See Figure 3-1B & C.)

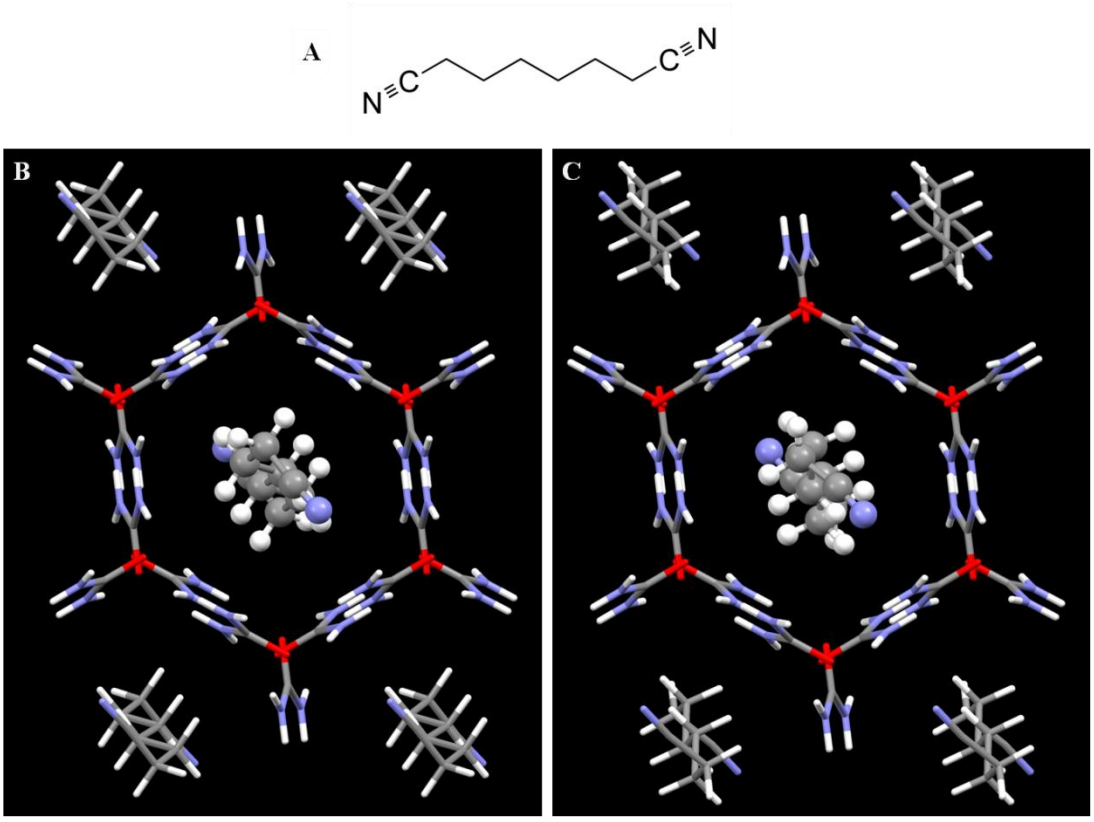

Figure 3-1: (A) Chemical structure of 1,6-dicyanohexane. (B) & (C) Packing view of 1,6-dicyanohexane/urea, at 91 K. The view is along the ***b*** axis, with the ***a*** axis horizontal and ***c**** vertical. At this temperature, these two gauche conformers exist in a B:C ratio of 67.8:32.2. [Provided courtesy of R. B. Gajda (RBG-A73, rbg_5.res)]

In conjunction with crystallographic results, ^{2}H NMR can provide a detailed mechanistic view of guest motions responsible for relaxation of the urea tunnel toward the undistorted structure in UICs.[2] Using methods developed earlier for 1,6-dibromohexane/urea, 1,6-dicyanohexane-1,1,6,6-d_4 was synthesized, in part, so that we could confirm independently that the guests undergo gauche to gauche jumps. Furthermore, investigation of this labeled crystal under uniaxial stress would allow us to examine the effect of external stress on the equilibrium between gauche conformers. Although some crystallographic data have been reported for 1,6-dicyanohexane/urea (Figure 3-1),[4] ^{2}H NMR data for crystals containing labeled guests have never been published, nor have any NMR data been published for this system under stress. Compounds of 1,6-dicyanohexane-2,2,5,5-d_4 and 1,6-dicyanohexane-3,3,4,4-d_4 have already been synthesized and their UICs studied in the Hollingsworth group; however, 1,6-dicyanohexane-1,1,6,6-d_4/urea is critical for this study since this compound alone can distinguish

between gauche to gauche jumps and simple rotations of the guest about the channel axis. In the following sections, a detailed description of the synthesis of 1,6-dicyanohexane-1,1,6,6-d_4 and the formation of its UIC will be discussed. In addition, representative solid-state NMR data for this system will be presented.

Synthesis of 1,6-Dicyanohexane-1,1,6,6-d_4

The synthesis of 1,6-dicyanohexane-1,1,6,6-d_4, completed in three steps, is illustrated in Figure 3-2. The first step involved the introduction of deuterium atoms by reduction of adipoyl chloride with $LiAlD_4$. Reduction of dimethyl adipate was initially attempted, but this substrate was replaced with adipoyl chloride since acid chlorides are known to undergo reduction by $LiAlH_4$ more readily than ester functional groups.[6] After preparing 1,6-hexanediol-1,1,6,6-d_4 via reduction of adipoyl chloride, the terminal alcohols were converted to the corresponding bromides with triphenylphosphine and carbon tetrabromide.[7] The labeled dibromide was then converted to the dinitrile by treatment with sodium cyanide, affording the desired 1,6-dicyanohexane-1,1,6,6-d_4. It should be noted that extra care was taken during the aqueous workup of 1,6-dicyanohexane-1,1,6,6-d_4 since this dinitrile is known to have high water solubility.[8]

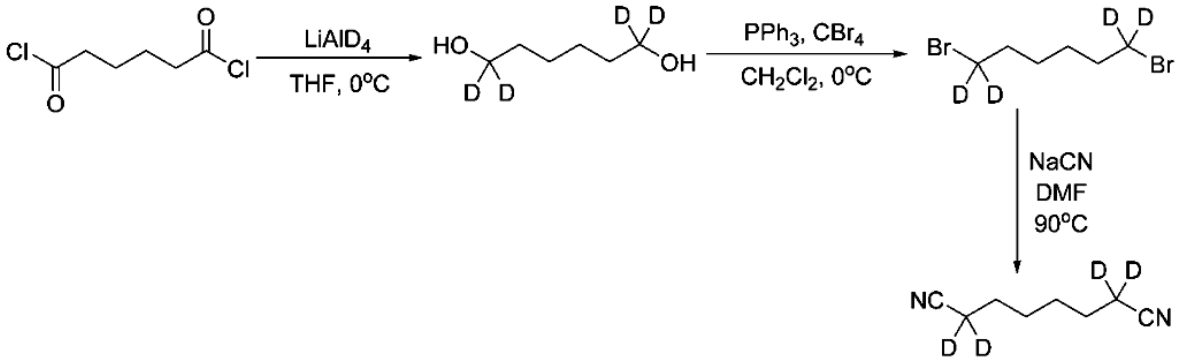

Figure 3-2: Synthesis of 1,6-dicyanohexane-1,1,6,6-d_4 utilizing adipoyl chloride as the starting material.

1,6-Hexanediol-1,1,6,6-d_4:

In a round bottom flask equipped with a dropping funnel, $LiAlD_4$ (1.72 g, 40.97 mmol, Acros, 98 atom % d) was dissolved in dry THF (100 mL) under an argon atmosphere and was cooled to ice temperatures. A solution of freshly distilled adipoyl chloride (5.00 g, 27.3 mmol,

Aldrich, 98%) in dry THF (40 mL) was added dropwise via a dropping funnel, making the reaction mixture very viscous. After stirring at room temperature for 18 hours, the reaction mixture was carefully quenched with water (40 mL) and 1 M NaOH (20 mL) to destroy any alkoxy-aluminate salts. The reaction mixture was filtered to remove excess solid and the filtrate was continuously extracted for 24 hours with diethyl ether (200 mL). The organic layer was dried over $MgSO_4$, filtered, and concentrated on a rotary evaporator. The crude product was purified with flash column chromatography to give pure 1,6-hexanediol-1,1,6,6-d_4 (1.78 g, 53.6% yield) as a white solid.

Physical data: $R_f = 0.28$ (9:1 EtOAc/hexanes v/v, PMA stain as indicator). ^{1}H NMR (400 MHz, $CDCl_3$, ADA-A115-22): δ1.34 (4H, m, γ-C**H**$_2$), 1.57 (4H, m, β-C**H**$_2$).

Notebook Pages: ADA-A77 and ADA-A107.

1,6-Dibromohexane-1,1,6,6-d_4:

In a round bottom flask, 1,6-hexanediol-1,1,6,6-*d_4* (0.1457 g, 1.19 mmol, ADA-A81-20) and triphenylphosphine (0.94 g, 3.58 mmol, Aldrich, 99%) were dissolved in dry CH_2Cl_2 (10 mL) under an argon atmosphere. This solution was cooled to ice bath temperatures prior to the addition of carbon tetrabromide (0.98 g, 2.98 mmol, Aldrich, 99%). After stirring at ice temperatures for one hour, the reaction was quenched with water (10 mL) and extracted with diethyl ether (3 x 30 mL). The organic layer was dried over $MgSO_4$, filtered, and concentrated on a rotary evaporator. The crude product was purified with flash column chromatography to give pure 1,6-dibromohexane-1,1,6,6-*d_4* (0.1859 g, 63% yield) as a colorless liquid.

Physical data: $R_f = 0.83$ (1:1 EtOAc/hexanes v/v, PMA stain as indicator). ^{1}H NMR (400 MHz, $CDCl_3$, ADA-A118-15): δ1.47 (4H, m, γ-C**H**$_2$), 1.87 (4H, m, β-C**H**$_2$).

Notebook pages: ADA-A93 and ADA-A117.

1,6-Dicyanohexane-1,1,6,6-d_4:

In a round bottom flask equipped with a reflux condenser and thermometer, sodium cyanide (0.147 g, 2.99 mmol, Acros, 95+%) and DMF (10 mL, Fisher Scientific) were added under an argon atmosphere. The stirring mixture was heated to 90 °C. When the reaction mixture reached 90 °C, the heat was removed, and 1,6-dibromohexane-1,1,6,6-d_4 (0.1859 g, 0.75 mmol) was added immediately, causing the reaction mixture to turn bright orange. After stirring

at room temperature for 18 hours, DMF was removed via a simple vacuum distillation. To the crude product was added CH_2Cl_2 (20 mL), saturated aq. NaCl (20 mL), and water (25 mL). This mixture was extracted with CH_2Cl_2 (3 x 30 mL). The organic layer was washed with saturated aq. NaCl (2 x 20 mL) before it was dried over K_2CO_3, filtered, and concentrated on a rotary evaporator. To remove traces of DMF, the product was passed through a silica gel column to give pure 1,6-dicyanohexane-1,1,6,6-d_4 (0.0864 g, 82.3% yield) as a yellow oil. According to Mass Spec, the percent of deuteration at the 1 and 6 carbon positions was 96.54%.

Physical data: $R_f = 0.65$ (9:1 EtOAc/hexanes v/v, PMA stain as indicator). ^{1}H NMR (400 MHz, $CDCl_3$, ADA-A119-18): δ1.51 (4H, m, γ-C**H**$_2$), 1.68 (4H, m, β-C**H**$_2$). ^{13}C NMR (100.57 MHz, $CDCl_3$, ADA-A126-23-C13): δ16.71 (α-**C**D_2), 24.99 (γ-**C**H_2), 27.89 (β-**C**H_2), 119.85 (-**C**N). MS *m/z*: 142.1 (11.5%), 141.1 (MH^+, 100%), 140.1 (10.9%), 139.1 (1.2%), 138.0 (0.6%), 137.0 (2.9%). Mass spec shows labeled product contains 88.41% d_4, 9.97% d_3, 0.98% d_2, and 0.64% d_1. The peak at 137.0 is assumed to correlate to the gain of Na^+ plus the loss of cyanide. Since there were relatively low abundances at peaks 138.0 and 139.1, it can be safely assumed that the peak at 137.0 has this correlation.

Notebook pages: ADA-A111 and ADA-A121 (scaled-up synthesis yielding 1.329 g (64.9%)).

Formation of 1,6-Dicyanohexane-1,1,6,6-d_4/urea

The formation of 1,6-dicyanohexane-1,1,6,6-d_4/urea was accomplished via evaporative growth techniques at room temperature.[9] A solution of 1.8 M urea in methanol (10 mL) was used to dissolve a stoichiometric ratio of six urea molecules to one guest molecule (1,6-dicyanohexane-1,1,6,6-d_4) (0.42 g, ADA-A122-fr140-155). After slowly evaporating the methanol at room temperature for six days, thin hexagonal-shaped plates were collected. After an additional one day of evaporation, a second crop of large chunky-prisms, weighing approximately 13-15 mg, were collected (ADA-A139-5, see Figure 3-3). Crystals from the second crop were redissolved and allowed to undergo evaporative growth after adding a small number of seeds from that same batch to generate larger crystals. After three days of evaporation, even larger crystals (31.5 and 38 mg) were formed (ADA-A140-9).

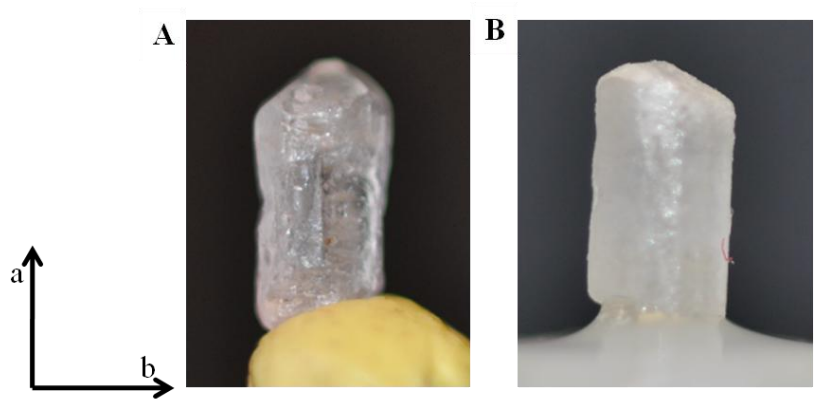

Figure 3-3: (A) 1,6-dicyanohexane-1,1,6,6-d_4/urea crystal, weighing 15.5 mg, mounted along its ***a*** axis on UHU patafix (a form of Blue Tak) for X-ray studies. (B) Same crystal mounted along its ***a*** axis on a goniometer device used for solid-state NMR studies.

Solid-state NMR Results for 1,6-Dicyanohexane-1,1,6,6-d_4/urea

As previously discussed, solid-state ^{2}H NMR can provide a detailed mechanistic view of guest motions within channels of urea inclusion compounds, given that ^{2}H NMR directly probes the C-D bond orientations and dynamics of a molecule.[10] Thus, having the guest specifically deuterated at the 1 and 6 positions will allow us to examine the gauche conformer populations and dynamics of 1,6-dicyanohexane/urea.

A large, single crystal of 1,6-dicyanohexane-1,1,6,6-d_4/urea (shown in Figure 3-3B) was chosen for solid-state NMR studies. This single crystal was oriented in the NMR probe with its ***c*** axis parallel to the magnetic field ($\boldsymbol{B}_0$) and with its ***a*** and ***b*** axes perpendicular to $\boldsymbol{B}_0$ at 0 degree rotation. Figure 3-4 shows this single crystal mounted in a goniometer device. This device allows us to perform a full 360 degree rotation of the crystal about the ***a*** axis within the NMR probe. In addition, stress/strain data for a single crystal can be collected in the NMR probe since this device is able to lock in the applied stress.

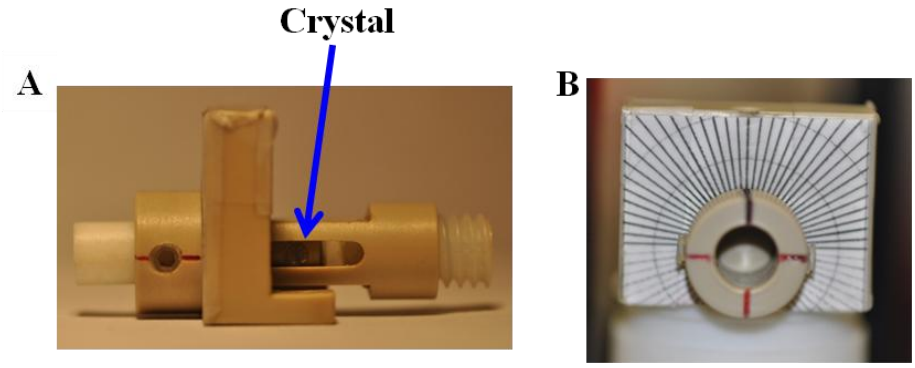

Figure 3-4: (A) Side view of goniometer stress device. Blue arrow indicates where a crystal is positioned. (B) Front view of goniometer device. The black lines indicate 5 degree increments of rotation. [Provided courtesy of M. D. Hollingsworth]

Atomic motions are normally heavily restricted in solids. This enables chemical shifts in solid-state NMR, for example, to depend upon the orientation of the molecule relative to the external magnetic field, $\boldsymbol{B}_0$.[11] Although guest molecules are usually rotating rapidly within the channels of UICs, cooling a crystal to low temperatures limits the guest's motion. Rotational studies of a single crystal of 1,6-dicyanohexane-1,1,6,6-d_4/urea were performed at room temperature, however, since it is not yet feasible to conduct goniometric studies of crystals under stress at low temperatures. Figure 3-5 illustrates the solid-state ^{2}H NMR rotational data collected for 1,6-dicyanohexane-1,1,6,6-d_4/urea in the absence of stress.[12] In these ^{2}H spectra, the signals for individual C-D groups are split into doublets whose relative separations depend on the orientation of the C-D groups in the magnetic field, the jump angle between exchanging C-D groups, and the timescale of such jumps. In the present system, the gauche to gauche exchange process is much more rapid than the frequency separation between peaks, but full goniometric measurements can be used to measure the equilibrium constants for the two conformers.

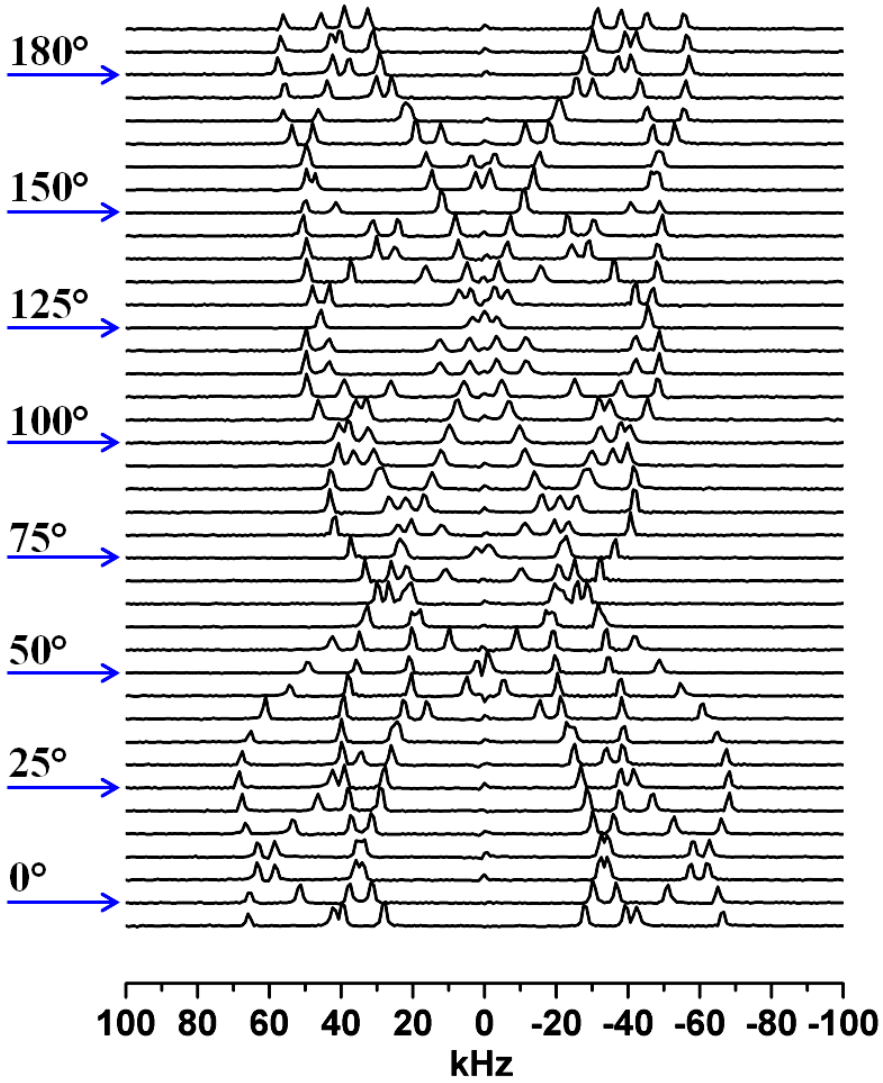

Figure 3-5: Solid-state ^{2}H NMR rotational data collected for a single crystal of 1,6-dicyanohexane-1,1,6,6-d_4/urea. Rotations from 0° to 180° were made. Note that the peak separations at 0° and 180° should be equivalent. However, due to misalignment of the goniometer device in the NMR probe, these splitting were inequivalent. [Provided courtesy of F. Nozirov and M. D. Hollingsworth]

As can be seen in the figure, the single crystal was rotated in five degrees increments from 0 to 180°. After this experiment was completed, it was noticed that the quadrupolar splitting at 0 and 180 degrees did not match each other. It was then discovered that the goniometer was not exactly perpendicular to the $\boldsymbol{B}_0$ axis of the magnet. Unfortunately, this tilt caused misalignment of the rotation axis of the crystal. Since it is not a simple matter to correct for this tilt, this experiment will be repeated once proper alignment of the goniometer is made in

the NMR spectrometer. After repeating this experiment, a similar rotational study will be performed with this crystal under stress. This will allow us to examine how the guest's conformer populations change as a result of stress.

Conclusions for Chapter 3

The specifically labeled guest molecule, 1,6-dicyanohexane-1,1,6,6-d_4, was successfully synthesized and isolated in high purity. Deuterium was introduced into the 1 and 6 carbon positions via reduction of an acyl chloride with $LiAlD_4$. Very large crystals (13-16 mg) of 1,6-dicyanohexane-1,1,6,6-d_4/urea were grown by the author and were studied by others in the Hollingsworth group with ^2H NMR. A solid-state rotational ^2H NMR study was conducted on a crystal of 1,6-dicyanohexane-1,1,6,6-d_4/urea that weighed 15.5 mg at room temperature. Unfortunately, this data set is not publishable because the goniometer was misoriented in the NMR probe. Future work will consist of repeating this exact experiment once proper alignment of the goniometer has been achieved. This rotational experiment will also be repeated for this crystal under stress to assess the changes in gauche conformer populations as a function of stress.

Chapter 3 References

1 Hollingsworth, M. D., Peterson, M. L., Rush, J. R., Brown, M. E., Abel, M. J., Black, A. A., Dudley, M., Raghothamachar, B., Werner-Zwanziger, U., Still, E. J. and Vanecko, J. A. Memory and perfection in ferroelastic inclusion compounds. *Cryst. Growth Des.* **5**, 2100-2116, (2005).

2 Hollingsworth, M. D., Werner-Zwanziger, U., Brown, M. E., Chaney, J. D., Huffman, J. C., Harris, K. D. M. and Smart, S. P. Spring-loading at the molecular level. Relaxation of guest-induced strain in channel inclusion compounds. *J. Am. Chem. Soc.* **121**, 9732-9733, (1999).

3 Hollingsworth, M. D., Santarsiero, B. D., Oumar-Mahamat, H. and Nichols, C. J. New series of 1:1 layered complexes of α,ω-dinitriles and urea. *Chem. Mater.* **3**, 23-25, (1991).

4 Hollingsworth, M. D. and Harris, K. D. M. in *Comprehensive Supramolecular Chemistry* Vol. 6 (eds. D. D. MacNicol, F. Toda, and R. Bishop) pp. 177-237 (Elsevier Science Ltd., Oxford, 1996).

5 Hollingsworth, M. D., Peterson, M. L., Pate, K. L., Dinkelmeyer, B. D. and Brown, M. E. Unanticipated guest motion during a phase transition in a ferroelastic inclusion compound. *J. Am. Chem. Soc.* **124**, 2094-2095, (2002).

6 Smith, M. B. and March, J. *March's Advanced Organic Chemistry: Reactions, Mechanisms, and Structure*. 6th edn, pp. 1788 (John Wiley & Sons, Inc., Hoboken, New Jersey, 2007).

7 Werner-Zwanziger, U., Brown, M. E., Chaney, J. D., Still, E. J. and Hollingsworth, M. D. Deuterium NMR studies of guest motions in urea inclusion compounds of 1,6-dibromohexane with analytical evaluation of spectra in the fast motion limit. *Appl. Magn. Reson.* **17**, 265-281, (1999).
8 Smiley, R. A. and Arnold, C. Aliphatic nitriles from alkyl chlorides. *J. Org. Chem.* **25**, 257-258, (1960).
9 Adams, A. D. Refer to ADA-A127 and ADA-A139 for crystal growth of 1,6-dicyanohexane-1,1,6,6-d_4/urea.
10 Odin, C. and Garcia, P. Single-crystal 2H NMR of deuterated 1,10-decanedicarboxylic acid included in hydrogenated urea channels. *Magn. Reson. Chem.* **42**, 687-694, (2004).
11 Friebolin, H. *Basic One- and Two-Dimensional NMR Spectroscopy, 4th ed.* 4th edn, pp. 353-355 (Germany, 2005).
12 Nozirov, F. Refer to FN-A263 for rotational study of 1,6-dicyanohexane-1,1,6,6-d4/urea at room temp., in the absence of stress.

CHAPTER 4 - 1,11-Undecanedioic acid/urea

Introduction

In certain ferroelastic UICs, when the guest molecules are rigidly held together, domain switching upon mechanical stress can be irreversible. This has proven to be the case for 1,11-undecanedioic acid/urea.[1] As Figure 4-1 illustrates, stress applied to 1,11-undecanedioic acid/urea causes domain reorientation that is mostly irreversible upon release of external stress.

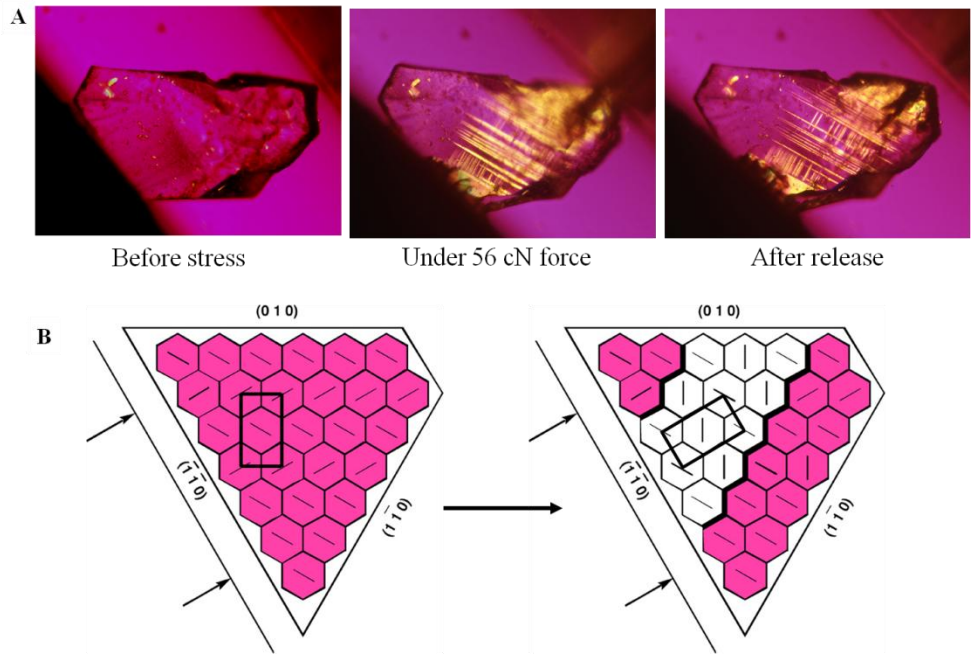

Figure 4-1: (A) Photomicrographs taken for 1,11-undecanedioic acid/urea before, during, and after the release of stress. (B) Schematic representing the irreversible domain switching observed for this crystal. [Provided courtesy of M. D. Hollingsworth]

Crystals of 1,11-undecanedioic acid/urea are commensurate, having $2\boldsymbol{c}_g' = 3\boldsymbol{c}_h'$. That is, there are two guest molecules for every three host repeats. The length of each guest is 1.5 times the length of the urea helix (11.0 Å), so the guest is expected to span 33 Å along the channel axis.[1] However, because these guest molecules are tethered to each other with strong hydrogen bonds, once a given channel starts growing, the guests do not have a chance to adjust their channel axis positions relative to the guests in adjacent channels (Figure 4-2). This results in the

formation of displacive domains. The disorder created from this displacement causes every two out of three layer lines in its X–ray diffraction pattern to be very weak, and it perturbs the intensities of the remaining layer lines. This kind of disorder is not handled well with standard crystallographic packages such as SHELX.

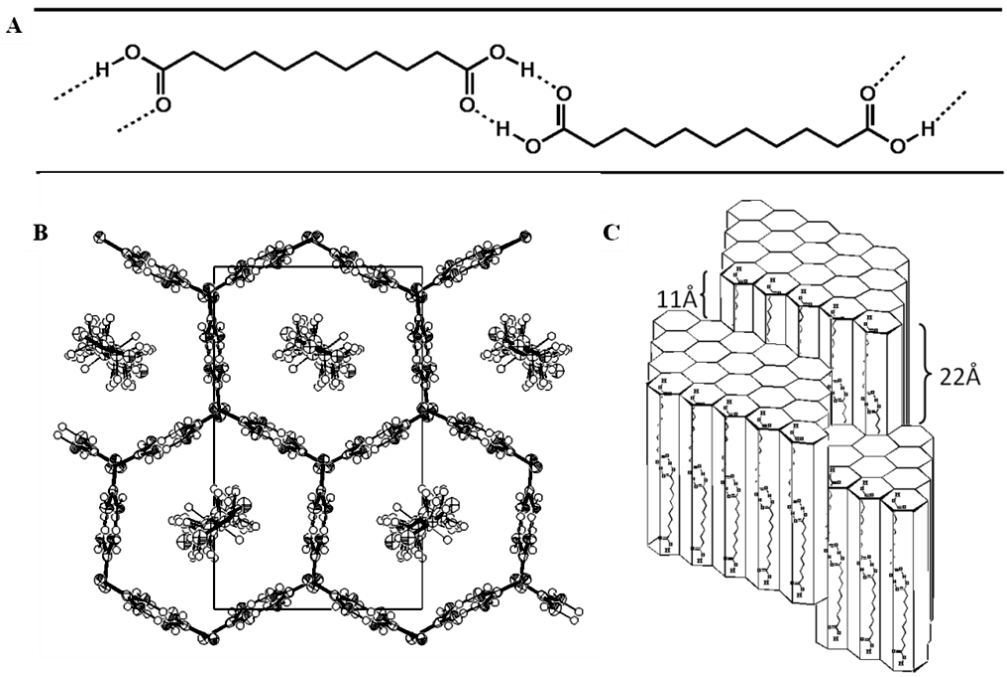

Figure 4-2: (A) Structure of 1,11-undecanedioic acid/urea, illustrating its tethered hydrogen bonding within a channel. (B) Crystal structure of 1,11-undecanedioic acid/urea, using a 33 Å cell (space group $P2_12_12_1$). (C) Schematic illustrating the displacive domains generated by guest translations in adjacent channels. [Provided courtesy of M. D. Hollingsworth]

It has been suggested from other systems studied in the Hollingsworth group, that this displacive disorder may be a general phenomenon in UICs. Therefore, successfully modeling the diffuse scattering in a system with a rigidly anchored guest, such as 1,11-undecanedioic acid, is critical for interpretation of previously unsolvable crystal structures of systems having weak X-ray diffraction data.

Although 1,11-undecanedioic acid is commercially available, it is expensive and of low purity. Previous members of the Hollingsworth group attempted to grow crystals of 1,11-undecanedioic acid/urea from commercially purchased material.[2] However, it was found that high quality crystals for X-ray diffraction studies were difficult to grow. As a result, the

synthesis of pure 1,11-undecanedioic acid was required. Earlier workers in the group also synthesized this guest molecule, but they did not obtain samples of high purity.[3] The synthesis and isolation of highly pure 1,11-undecanedioic acid will be discussed in the following section.

Synthesis of 1,11-Undecanedioic acid

For the synthesis of 1,11-undecanedioic acid (Figure 4-3), the commercially available 1,11-undecanediol was oxidized in the presence of Jones reagent, a mixture of chromic acid and sulfuric acid in water. This reagent has been reported to oxidize primary alcohols rapidly and in high yields.[4] The oxidation is carried out by the addition of Jones reagent to a stirred solution of 1,11-undecanediol in acetone.

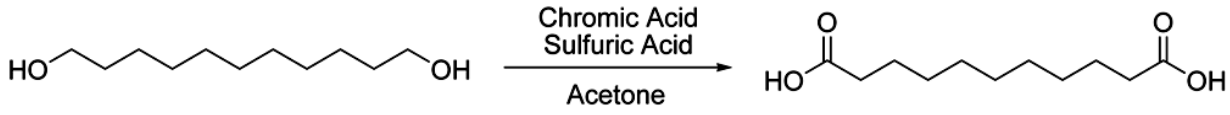

Figure 4-3: Synthesis of 1,11-undecanedioic acid via oxidation of 1,11-undecanediol with Jones reagent.

While evaluating the NMR spectra of the products of this oxidation, it was suspected that esters, along with the desired dicarboxylic acid, were present after working up this reaction (Figure 4-4). Therefore, the crude reaction mixture was treated with sodium hydroxide to saponify the esters that were formed. After performing this saponification, the crude product was reoxidized with Jones reagent. This afforded 1,11-undecanedioic acid in both high purity and high yields.

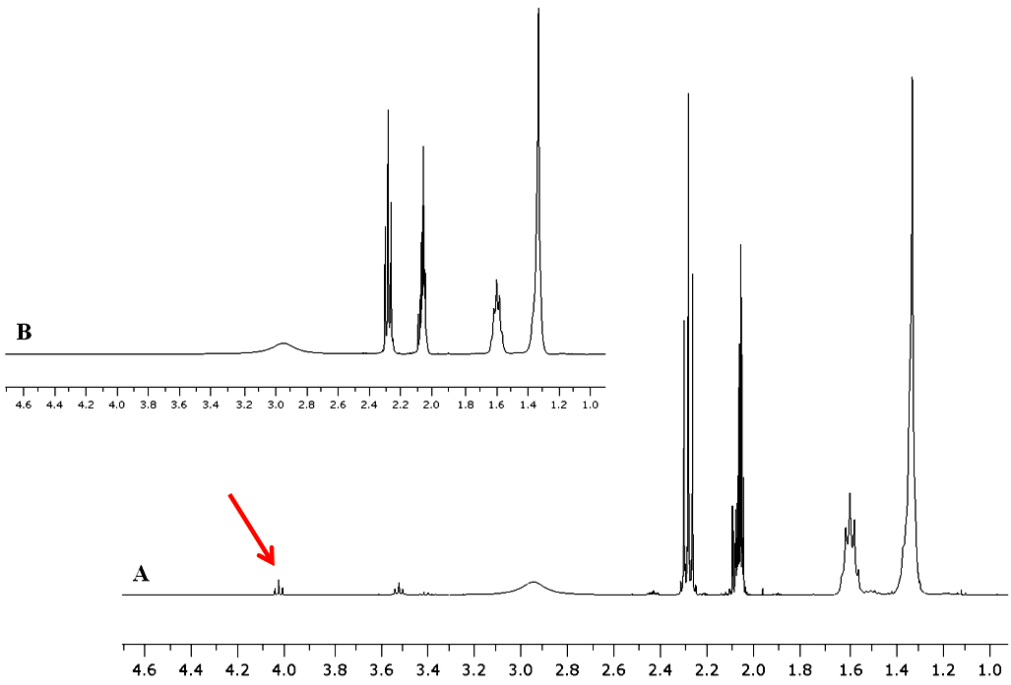

Figure 4-4: (A) ^{1}H NMR spectrum for impure 1,11-undecanedioic acid, after only one oxidation. The red arrow points to a peak that was suspected to be from an ester impurity. (B) ^{1}H NMR for pure 1,11-undecanedioic acid, after the oxidation, saponification, reoxidation sequence.

1,11-Undecanedioic acid:

The Jones reagent was prepared by adding chromium trioxide (26.73 g, 0.267 mol, Fisher Scientific) to a mixture of concentrated H_2SO_4 (23 mL) and water (100 mL), yielding 2.67 M chromic acid. To a round bottom flask containing ice-cold Jones reagent (26.5 mL, 2.67 M), was slowly added a solution of 1,11-undecanediol (5.001 g, 26.6 mmol, Lancaster, 97%) in acetone (250 mL, certified ACS, Fisher Scientific). After stirring at room temperature for 18 hours, the reaction mixture had separated into a green lower layer containing chromium salts and an upper acetone layer containing the oxidized product. The reaction mixture was quenched with enough water to dissolve the chromium salts and was then extracted with diethyl ether (3 x 100 mL). After the organic layer was extracted with 1 M $NaHCO_3$ (3 x 75 mL), the aqueous layer was acidified to pH 2 with 1 M HCl and subsequently extracted again with diethyl ether (3 x 75 mL). The organic layer was dried over $MgSO_4$, filtered, and concentrated on a rotary evaporator. The crude product was dissolved in 1 M NaOH (10 mL) and heated at 50 °C for 2.5 hours to saponify any remaining ester impurities. After cooling to room temperature, the reaction mixture was

acidified to pH 2 with 1 M HCl and extracted with diethyl ether (3 x 50 mL). The organic layer was washed with saturated aq. NaCl (1 x 25 mL), dried over $MgSO_4$, filtered, and concentrated on a rotary evaporator to yield 4.247 g of crude product. This oxidation was repeated by adding a solution of the crude product (4.247 g) in acetone (200 mL) to a round bottom flask containing an ice-cold solution of the Jones reagent (13.25 mL, 2.67 M). After stirring at room temperature for 2 hours, the reaction mixture was quenched with enough water to dissolve the chromium salts and was extracted with diethyl ether (4 x 75 mL). After extracting the organic layer with 1 M $NaHCO_3$ (3 x 75 mL), the aqueous layer was then acidified to pH 2 with 1 M HCl and extracted again with diethyl ether (3 x 75 mL). The organic layer was dried over $MgSO_4$, filtered, and concentrated on a rotary evaporator. This yielded pure 1,11-undecanedioic acid (4.168 g, 72.4% yield) as a white solid.

Physical data: R_f = 0.61 (9:1 EtOAc/hexanes v/v, anisaldehyde as indicator). Melting point: 106.5-108 °C (Lit. mp: 109-111 °C).[5] ^{1}H NMR (400 MHz, acetone-d_6, ADA-A44-29): δ1.32 (10H, s, -C**H**$_2$-), 1.59 (4H, m, β-C**H**$_2$-COOH), 2.28 (4H, t, α-C**H**$_2$-COOH, J = 7.4 Hz), 10.53 (1H, br s, RCOO**H**).

Notebook pages: ADA-A41.

Formation of 1,11-Undecanedioic acid/urea

Crystals of 1,11-undecanedioic acid/urea were grown by a previous member of the Hollingsworth group, Dr. Eric Chan. Although crystals of most urea inclusion compounds can be grown by evaporation or cooling at 0°C and above, temperatures as low as -20 °C are needed for the growth of reasonably formed crystals of 1,11-undecanedioic acid/urea.[6] In a representative procedure, a solution of methanol (4 mL) and isobutyl alcohol (3 mL) was heated to 60 °C to dissolve a mixture of 0.411 g urea and 0.100 g of 1,11-undecanedioic acid. This mixture was placed in a 4 L Dewar flask containing hot ethylene glycol and cooled slowly to -20 °C. After six days, thin plates of 1,11-undecanedioic acid/urea were collected.[7]

Conclusions for Chapter 4

The guest molecule, 1,11-undecanedioic acid, was successfully synthesized in high purity. This was accomplished by oxidizing the commercially available 1,11-undecanediol with Jones reagent. After the first treatment with Jones reagent, ester impurities were saponified and

then oxidized a second time with Jones reagent to obtain 1,11-undecanedioic acid in high purity and reasonable yields. The crystals of 1,11-undecanedioic/urea were used in diffuse scattering experiments that were conducted in the Department of Physics at the University of Rennes, France.[7] Future work will consist of analyzing the data collected and resolving this system's diffuse scattering.

Chapter 4 References

1 Hollingsworth, M. D. Synthesis and Mechanistic Studies of New Series of Ferroelastic Crystals. (NSF CHE - 0809845)

2 Peterson, M. L. MLP-C210, purchased 1,11-undecanedioic acid from Fluka.

3 Peterson, M. L. MLP-C240, attempted synthesis of 1,11-undecanedioic acid.

4 Fieser, L. F. and Fieser, M. *Reagents for Organic Synthesis*. Vol. 1 pp. 142-143 (John Wiley and Sons, Inc., New York, 1967).

5 Cason, J., Taylor, P. B. and Williams, D. E. Branched-chain fatty acids. 20. Synthesis of compounds useful for relating melting point to structure. *J. Org. Chem.* **16**, 1187-1192, (1951).

6 Chan, E. J. Refer to notebook pages EJC-A62, EJC-A68, & EJC-A75 for crystallization of 1,11-undecanedioic acid. Procedure was adapted from Michael E. Brown.

7 Chan, E. J. Refer to EJC-A75 for collection and mounting of 1,11-undecanedioic acid/urea.

CHAPTER 5 - Bis(3-oxobutyl) adipate/urea

Introduction

In the process of generating a series of ferroelastic inclusion compounds, a series of UICs in which $1\boldsymbol{c}_g' = 2\boldsymbol{c}_h'$, that is one guest for every two host repeats, has been developed. The compounds with this stoichiometry, such as 1,10-diacetoxydecane/urea and 2,15-hexadecanedione/urea, for example, are commensurate systems that exhibit ferroelastic properties. In these two UICs, the guest carbonyls form diagonal hydrogen bonds with the urea host, as in 1,10-diacetoxydecane/urea (Figure 5-1). Because this hydrogen bonding generates planar arrays of guest molecules, the unit cells are distorted from hexagonal symmetry, and the crystals are ferroelastic.

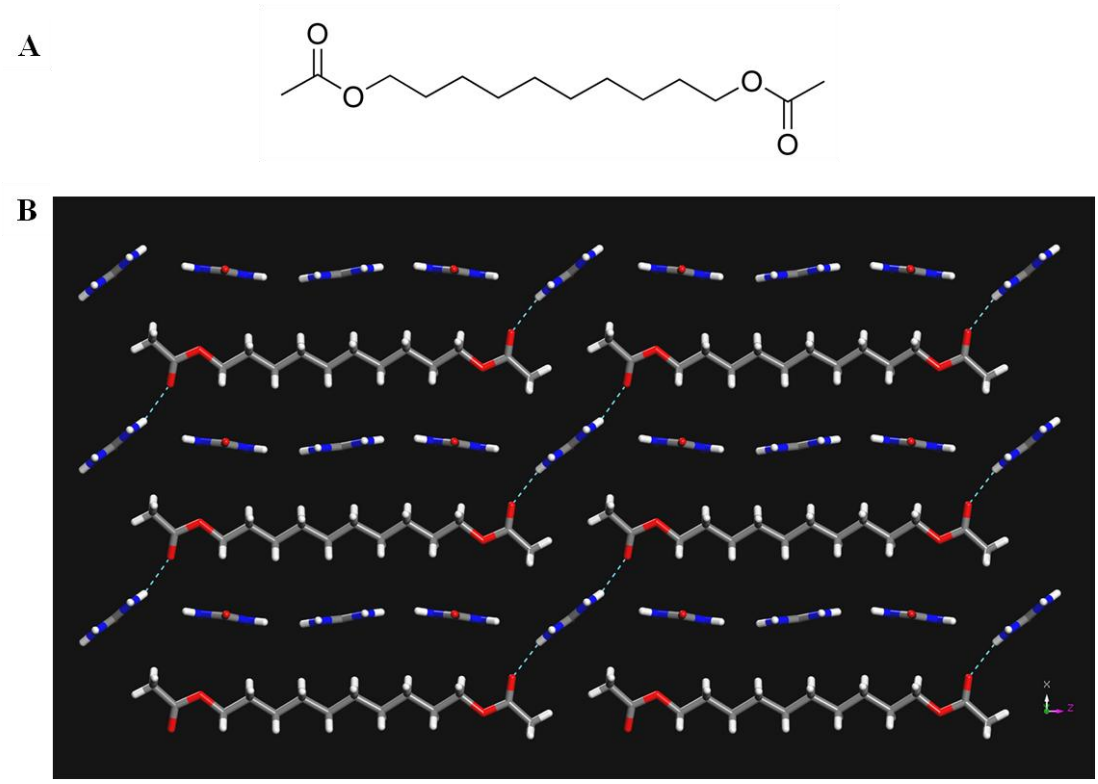

Figure 5-1: (A) Chemical structure of 1,10-diacetoxydecane. (B) Cutaway of the packing of 1,10-diacetoxydecane/urea illustrating the diagonal hydrogen bonds between guest carbonyls and ureas. [Crystal structure solved by Michael E. Brown and M. D. Hollingsworth]

Because the mechanical properties of crystals within this series are related to the host-guest hydrogen bonding, it should be possible to modify these properties by changing the number and kinds of host-guest hydrogen bonds. One can imagine that an extra set of hydrogen bonds that lies along the direction of the applied stress would increase the internal restoring force (or spring constant) that opposes the applied stress during the domain switching process. This notion led to the prediction that ethanediyl bis(5-oxohexanoate)/urea would be a commensurate ferroelastic structure with $1\boldsymbol{c}_g' = 2\boldsymbol{c}_h'$, and that it would undergo extensive host-guest hydrogen bonding (Figure 5-2A). This guest was chosen because the distance between the carbonyl groups in the middle of the molecule was predicted to be almost identical to the distance between adjacent carbonyls at the ends of the molecules. Unexpectedly, however, the host-guest hydrogen-bonding was found only to occur at the ends of the alkyl chains, not in the middle (Figure 5-2B).[1] The most likely reason is shown in Figure 5-2B, in which it is clear that ureas alternate in their "sense" of rotation about the axis perpendicular to this wall of the channel (i.e., clockwise or counterclockwise rotation from the horizontal). In order to form a hydrogen bond with the guest, the third urea from the left, for example, must tilt in the opposite direction from its favored orientation.

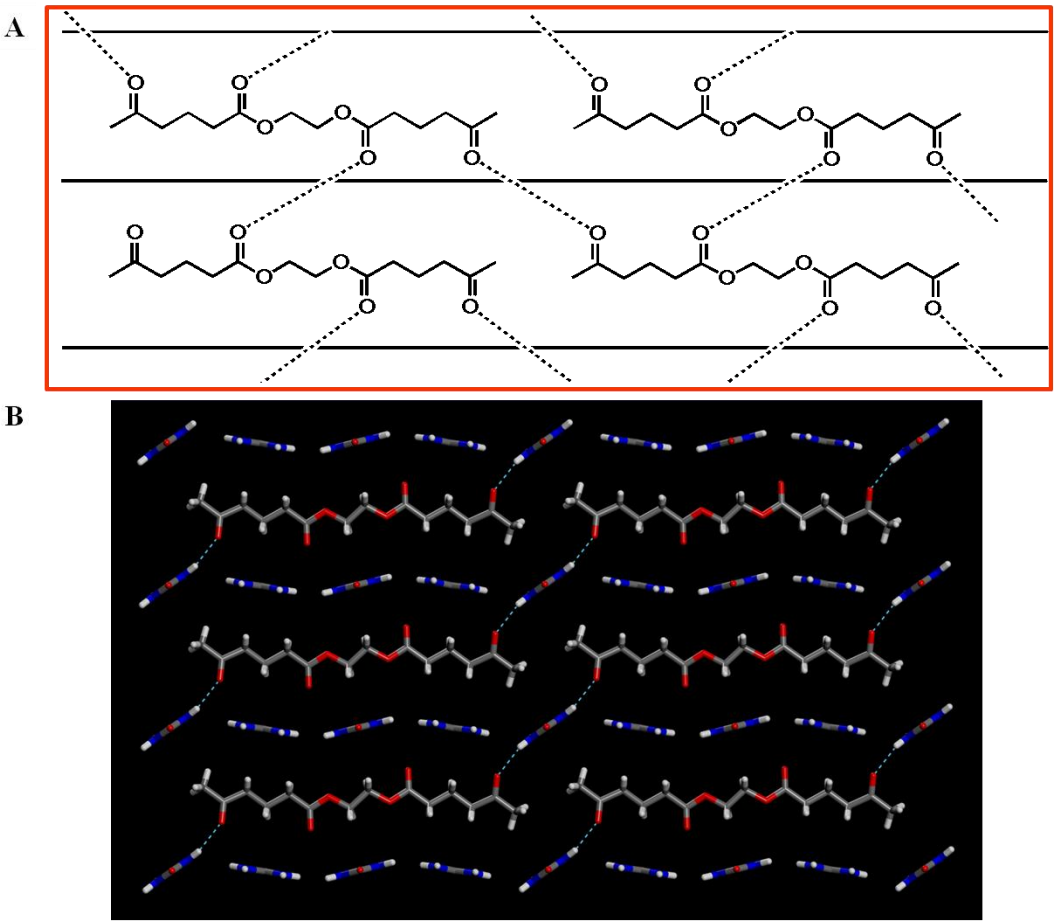

Figure 5-2: (A) Predicted host-guest hydrogen bonding for ethanediyl bis(5-oxohexanoate)/urea. The solid black lines represent urea channel walls, and the dotted black lines represent hydrogen bonding between carbonyl oxygens and urea. (B) Actual hydrogen-bonding motif for ethanediyl bis(5-oxohexanoate)/urea. Internal carbonyl groups do not hydrogen bond to the urea host. [Provided courtesy of M. D. Hollingsworth; the structure shown in Fig. B was solved by J. D. Chaney and M. D. Hollingsworth]

Because subtle features of molecular packing can often change a structure dramatically, an analog of enthanediyl bis(5-oxohexanoate) was considered. One possible explanation for the absence of host-guest hydrogen bonding involving the internal carbonyls was that the distance between internal carbonyl groups was shorter than the optimal distance for host-guest hydrogen bonding. To correct this internal hydrogen-bonding problem, bis(3-oxobutyl) adipate was prepared. This guest has the same overall chain length but a somewhat longer distance between the internal carbonyls (see Figure 5-3). This arises because carbon-carbon bonds are each approximately 0.1 Å longer than carbon-oxygen bonds.

A

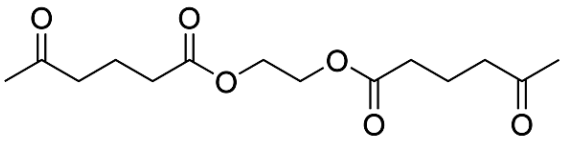

Ethanediyl bis(5-oxohexanoate)

B

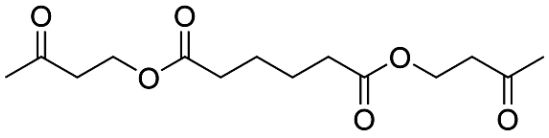

Bis(3-oxobutyl) adipate

Figure 5-3: (A) Chemical structure for ethanediyl bis(5-oxohexanoate). (B) Chemical structure for bis(3-oxobutyl) adipate. Note the distance between the internal carbonyls in (A) is shorter than that in (B).

In preliminary work, it was found that the diffraction patterns for bis(3-oxobutyl) adipate/urea and ethanediyl bis(5-oxohexanoate)/urea had many common features, but also some important differences.[1] Unlike the pattern for ethanediyl bis(5-oxohexanoate)/urea, every other layer line along the reciprocal channel axis was extremely weak in bis(3-oxobutyl) adipate/urea. This suggested that an extended hydrogen-bonding network was not created in the adipate, and instead the guests had undergone a form of displacive disorder, similar to that described in chapter 4, in which some of the guest molecules had rotated and translated along the urea channels (Figure 5-4) by half the length of the guest.

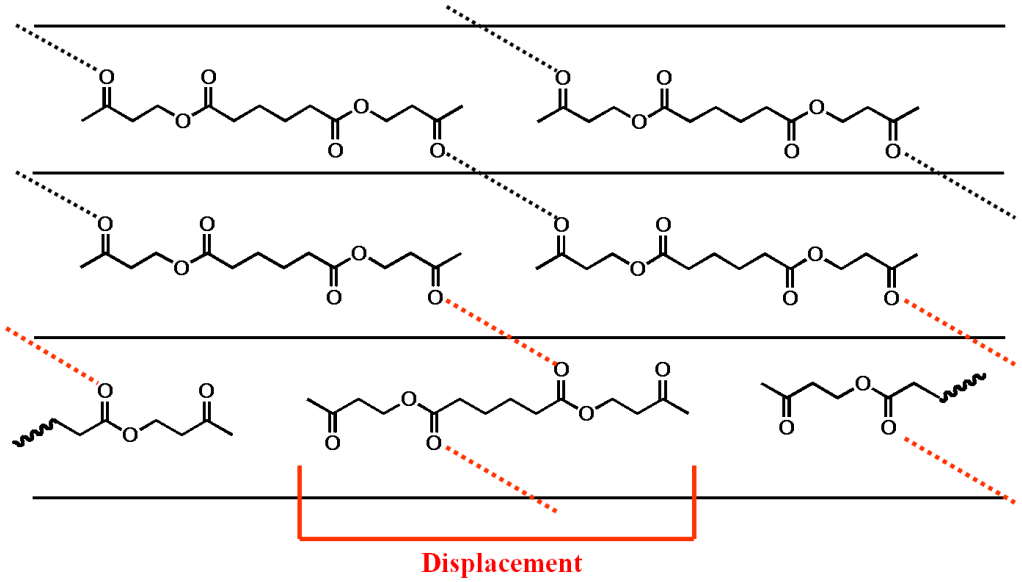

Figure 5-4: Schematic showing the possible displacive disorder in bis(3-oxobutyl) adipate/urea. Such disorder was postulated to explain the intensity alternations in the diffraction pattern of this material. The red dashed lines highlight "new" hydrogen bonds made as a result of the disorder. [Provided courtesy of M. D. Hollingsworth]

Consequently, the synthesis of bis(3-oxobutyl) adipate was desired so that more in-depth crystallographic experiments could be performed on its corresponding UIC crystals. These experiments would thus allow resolution of the structure of bis(3-oxobutyl) adipate/urea. The synthesis and crystal growth of bis(3-oxobutyl) adipate/urea will be discussed in the following section.

Synthesis of Bis(3-oxobutyl) adipate

The synthesis of bis(3-oxobutyl) adipate, shown in Figure 5-4, was completed in a total of four steps, the first two of which were conducted by a previous member of the group (Brian Dinkelmeyer). To begin, the ketone functional group of the commercially available ethyl acetoacetate was protected with ethylene glycol in the presence of *p*-toluenesulfonic acid, yielding the 1,3-dioxolane analogue of ethyl acetoacetate, ethyl (2-methyl-1,3-dioxolan-2-yl) acetate. The 1,3-dioxolane protecting group is one of the most widely used carbonyl protective groups since it is easy to use and because it selectively protects ketones in the presence of esters.[2] After protecting the ketone, the ester functional group of the analogue was reduced with $LiAlH_4$, affording 2-(2-methyl-1,3-dioxolan-2-yl)ethanol. Esterification with adipoyl chloride and two equivalents of 2-(2-methyl-1,3-dioxolan-2-yl)ethanol produced the protected analogue of bis(3-

oxobutyl) adipate, butane-1,4-diyl bis[(2-methyl-1,3-dioxolan-2-yl)acetate]. In the final step, this analogue was deprotected with sulfuric acid on silica gel, giving the desired bis(3-oxobutyl) adipate.

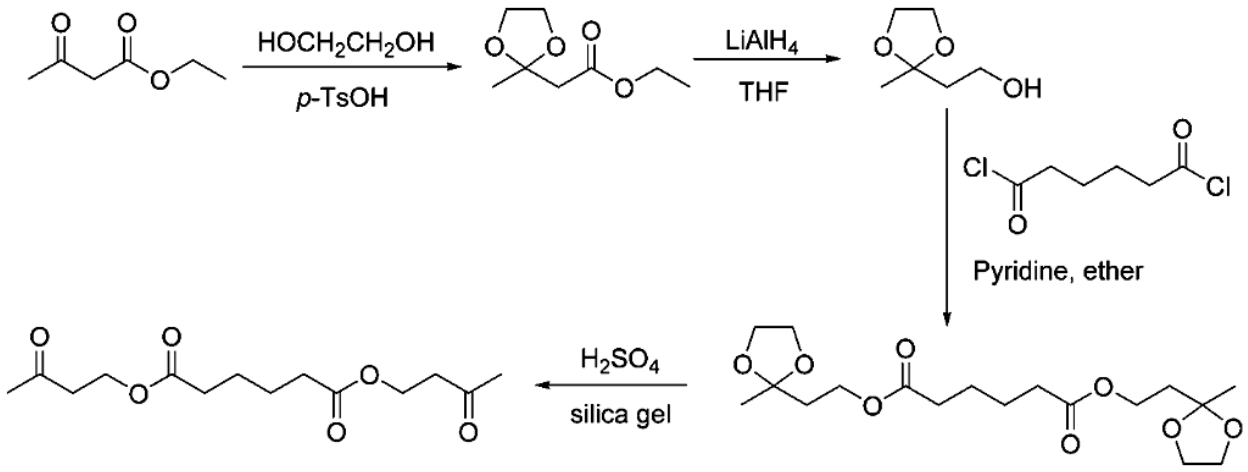

Figure 5-5: Synthesis of bis(3-oxobutyl) adipate, utilizing selective protection and reduction methods to the starting material ethyl acetoacetate.

Ethyl (2-methyl-1,3-dioxolan-2-yl) acetate:

This synthetic procedure was performed by a previous member of the Hollingsworth group, Brian Dinkelmeyer. In a round bottom flask equipped with a Dean-Stark apparatus, benzene (200 mL) was added under a nitrogen atmosphere. Ethyl acetoacetate (30.63 g, 0.235 moles, Aldrich, 99%), ethylene glycol (16.072 g, 0.259 moles, Fisher Scientific), and *p*-toluenesulfonic acid (spatula tip full, catalytic amount, Kodak) were added. After refluxing for 5 hours, the reaction was cooled to room temperature and was washed with saturated $NaHCO_3$ (3 x 50 mL), water (3 x 50 mL), and saturated sodium chloride solution (1 x 50 mL). The organic layer was dried over $MgSO_4$, filtered, and concentrated on a rotary evaporator to yield a crude ethyl (2-methyl-1,3-dioxolan-2-yl) acetate. This was used in the next step without further purification.

Physical data: ^{1}H NMR (400 MHz, $CDCl_3$, BD-A02): δ1.25 (3H, t, $RCH_2C\mathbf{H}_3$, J = 7.2 Hz), 1.49 (3H, s, $C\mathbf{H}_3$), 2.65 (2H, s, α-$C\mathbf{H}_2$-COOR), 3.96 (4H, s, RO-$C\mathbf{H}_2$-$C\mathbf{H}_2$-OR), 4.13 (2H, q, $RC\mathbf{H}_2CH_3$, J = 6.8 Hz).

Notebook pages: BD-A02.

2-(2-Methyl-1,3-dioxolan-2-yl)ethanol:

This synthetic procedure was performed by Brian Dinkelmeyer. To a round bottom flask was added $LiAlH_4$ (6.809 g, 0.179 mols, Aldrich, 97%) and distilled diethyl ether (100 mL) under a nitrogen atmosphere. The crude 1,3-dioxolane analogue of ethyl acetoacetate (20.099 g, 0.115 mols) was added dropwise to the ice-cold reaction mixture. The ice bath was removed after the addition, and the reaction mixture was stirred at room temperature for 2 hours. The reaction mixture was then carefully quenched with water (30 mL), and the ether layer was separated. The organic layer was washed with saturated aq. NaCl solution (1 x 50 mL), dried over $MgSO_4$, filtered, and concentrated on a rotary evaporator. This afforded 2-(2-methyl-1,3-dioxolan-2-yl)ethanol (4.56 g, 31% yield) as a viscous, yellow liquid. This was used in the next step without further purification.

Physical data: $R_f = 0.44$ (9:1 EtOAc/hexanes v/v, PMA stain as indicator). ^{1}H NMR (400 MHz, $CDCl_3$, BD-B41): δ1.35 (3H, s, C**H**$_3$), 1.94 (2H, t, β-C**H**$_2$ to OH, J = 5.2 Hz), 3.75 (2H, t, α-C**H**$_2$ to OH, J = 5.6 Hz), 3.97 (4H, s, RO-C**H**$_2$-C**H**$_2$-OR). ^{13}C NMR (100.57 MHz, $CDCl_3$, BD-B41): δ23.80 (**C**H$_3$), 40.23 (β-**C**H$_2$ to OH), 58.90 (α-**C**H$_2$ to OH), 64.48 (RO-**C**H$_2$-**C**H$_2$-OR), 110.44 (RO-**C**-OR).

Notebook pages: BD-A05.

Butane-1,4-diyl bis[(2-methyl-1,3-dioxolan-2-yl)acetate]:

To a round bottom flask equipped with a dropping funnel and reflux condenser was added dry THF (20 mL), 2-(2-methyl-1,3-dioxolan-2-yl)ethanol (2.34 g, 17.7 mmol)[3], and distilled adipoyl chloride (1.94 g, 10.6 mmol, Aldrich, 98%) under an argon atmosphere. A mixture of pyridine (1.40 g, 17.7 mmol, Fisher Scientific) and THF (15 mL, distilled) was added dropwise to the reaction mixture over a period of one hour. After refluxing at 60 °C for 4 hours, the reaction mixture was quenched with water (50 mL) and extracted with ethyl acetate (3 x 50 mL). The organic layer was washed once with 1 M HCl (20 mL), once with 1 M $NaHCO_3$ (20 mL), and once with saturated aq. NaCl solution (20 mL). The organic layer was dried over $MgSO_4$, filtered, and concentrated on a rotary evaporator to yield butane-1,4-diyl bis[(2-methyl-1,3-dioxolan-2-yl)acetate] (2.43 g, 61.0% yield). This was used in the next step without further purification.[4]

Physical data: R_f = 0.65 (9:1 EtOAc/hexanes v/v, PMA stain as indicator). ^{1}H NMR (400 MHz, $CDCl_3$, ADA-A96-11): δ1.35 (6H, s, C**H**$_3$), 1.66 (4H, m, β-C**H**$_2$-COOR, virtual coupling), 2.01 (4H, t, β-C**H**$_2$-OOCR, *J* = 7.1 Hz), 2.31 (4H, m, α-C**H**$_2$-COOR, virtual coupling), 3.94 (8H, m, RO-C**H**$_2$-C**H**$_2$-OR), 4.19 (4H, t, α-C**H**$_2$-OOCR, *J* = 7.1 Hz).

Notebook pages: ADA-A95.

Bis(3-oxobutyl) adipate:

The crude butane-1,4-diyl bis[(2-methyl-1,3-dioxolan-2-yl)acetate] (2.43 g, 6.45 mmol) in CH_2Cl_2 (20 mL) was added to a round bottom flask containing a slurry of silica gel (38 g, Aldrich, 200-425 mesh) in CH_2Cl_2 (200 mL). A solution of 15% sulfuric acid (3.8 g, 0.1 g/g silica gel) was added dropwise to the reaction mixture. After stirring for 18 hours at room temperature, the reaction was filtered to remove the silica gel. The silica gel was washed with CH_2Cl_2 (3 x 25 mL) and methanol (3 x 25 mL). The filtrate was stirred with 1 M $NaHCO_3$ (20 mL) for 30 minutes before the reaction mixture was transferred to a separatory funnel and the CH_2Cl_2 layer removed. The aqueous layer was extracted with CH_2Cl_2 (3 X 50 mL) before the combined organic layers were washed with saturated sodium chloride solution (1 x 50 mL), dried over Na_2SO_4, filtered, and concentrated on a rotary evaporator. The crude bis(3-oxobutyl) adipate was isolated as a brown oil. After allowing the oil to sit at room temperature for eight days, an off-white solid was isolated and rinsed with hexanes (0.362 g, 19% yield).

Physical data: R_f = 0.55 (9:1 EtOAc/hexanes v/v, PMA stain as indicator). ^{1}H NMR (400 MHz, $CDCl_3$, ADA-A53-30-solid): δ1.63 (4H, m, β-C**H**$_2$-COOR, virtual coupling), 2.19 (6H, s, C**H**$_3$), 2.30 (4H, m, α-C**H**$_2$-COOR, virtual coupling), 2.77 (4H, t, β-C**H**$_2$-OOCR, *J* = 6.2 Hz), 4.33 (4H, t, α-C**H**$_2$-OOCR, *J* = 6.2 Hz).

Notebook pages: ADA-A27, ADA-A57, ADA-A65, and ADA-A97.

Formation of Bis(3-oxobutyl) adipate/urea

A previous member of the Hollingsworth group, Dr. Eric Chan, performed the crystallization of bis(3-oxobutyl) adiapte/urea. Crystals of bis(3-oxobutyl) adipate/urea were formed by gradual cooling.[5] A solution of 2 M urea in methanol (5 mL) was used to dissolve a stoichiometric ratio of twelve urea molecules to one guest molecule (bis(3-oxobutyl) adipate,

0.381 g).[6] After slowly cooling to 2-5 °C overnight in a 4 L Dewar flask, prismatic crystals were collected.

Crystallographic Data for Bis(3-oxobutyl) adipate/urea

Crystallographic results were obtained for bis(3-oxobutyl) adipate/urea, and its structure was solved by Dr. Eric Chan (Figure 5-6). Surprisingly, no host-guest hydrogen bonding was observed in this crystal structure. This contradicts the model of displacive disorder that was postulated earlier. Although strict comparisons are difficult because of the different methods used, high-resolution data collected on different samples by M. D. Hollingsworth and Eric Chan appeared to show significant differences, especially in the diffuse scattering. This suggests that more than one crystal form may exist for bis(3-oxobutyl) adipate/urea. If this system does crystallize in different polymorphs, it may be possible to seed with ethanediyl bis(5-oxohexanoate)/urea or 1,10-diacetoxydecane/urea to generate the polymorph with the desired host-guest hydrogen bonding.

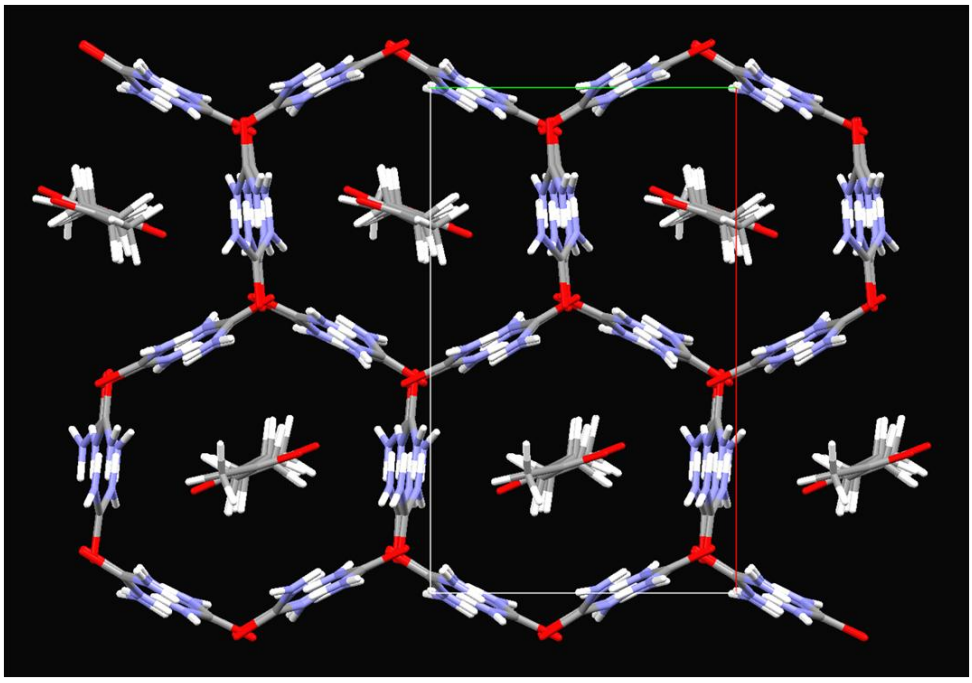

Figure 5-6: Crystal structure of bis(3-oxobutyl) adipate/urea, looking down the channel axis. Notice the absence of host-guest hydrogen bonding. [The structure solved by Eric J. Chan.]

Conclusions for Chapter 5

The guest molecule, bis(3-oxobutyl) adipate, was successfully synthesized by performing esterification of adipoyl chloride with 2-(2-methyl-1,3-dioxolan-2-yl)ethanol. After the removal of the 1,3-dioxolane protecting group, isolation of pure bis(3-oxobutyl) adipate was a challenging task. However, after eight days of waiting for a solid to form, pure bis(3-oxobutyl) adipate was isolated and its corresponding UIC was grown. The bis(3-oxobutyl) adipate/urea crystals were examined at Kansas State University and in the Department of Physics in the University of Rennes.[7] The observed crystal structure exhibits remarkable packing in which host-guest hydrogen bonding is absent. Future work will consist of seeding this system with ethanediyl bis(5-oxohexanoate)/urea or 1,10-diacetoxydecane/urea to promote the formation of the desired polymorph.

Chapter 5 References

1 Hollingsworth, M. D. Synthesis and Mechanistic Studies of New Series of Ferroelastic Crystals. (NSF CHE - 0809845)

2 Wuts, P. G. M. and Greene, T. W. *Greene's Protective Groups in Organic Synthesis*. 4th edn, pp. 454-466 (John Wiley & Sons, Inc., Hoboken, New Jersey, 2007).

3 Dinkelmeyer, B. Refer to BD-B41 for the source of 2-(2-methyl-1,3-dioxolan-2-yl)ethanol.

4 Dinkelmeyer, B. Purification via column chromatography was attempted (refer to BD-A09), but this was found to decompose the product.

5 Chan, E. J. Refer to notebook pages: EJC-A73, EJC-A78, EJC-A79, & EJC-A80.

6 Chan, E. J. In a 25 mL flask was placed 0.381g bis(3-oxobutyl) adipate and 5 mL of 2 M urea in methanol. Refer to EJC-A78.

7 Chan, E. J. Refer to EJC-A97 & EJC-A105 for MAR data collection of bis(3-oxobutyl) adipate/urea. Refer to EJC-A155 for XRD data collected at KSU on the Apex II system.

CHAPTER 6 - 2,16-Heptadecanedione/urea

Introduction

The continuing studies on the alkane/urea, alkanone/urea, and alkanedione/urea series have paved the way for a better understanding of template-directed growth, as was previously mentioned in Chapter 2. Extensive research has gone into developing and analyzing these series. One such series of particular interest is that of alkanediones in urea (Figure 6-1). This chapter deals specifically with 2,16-heptadecanedione/urea, for which the crystal structure and host-guest relationship have yet to be determined.

Guest chain length	Alkanedione/urea	Relationship	Reference
C8	2,7-Octanedione/urea	$6c_g' = 7c_h'$	M. E. Brown, *et al.*, *Chem. Mater.* **8**, 1588-1591 (1996)
C9	2,8-Nonanedione/urea	Unknown	N/A
C10	2,9-Decanedione/urea	$3c_g' = 4c_h'$	M. D. Hollingworth, *et al.*, *Science.* **273**, 1355-1359 (1996)
C11	2,10-Undecanedione/urea	$2c_g' = 3c_h'$	M. E. Brown and M. D. Hollingsworth. *Nature.* **376**, 323-327 (1995)
C12	2,11-Dodecanedione/urea	$7c_g' = 11c_h'$	M. D. Hollingworth, *et al.*, *Science.* **273**, 1355-1359 (1996)
C13	2,12-Tridecanedione/urea	$3c_g' = 5c_h'$	M. D. Hollingworth, *et al.*, *Science.* **273**, 1355-1359 (1996)
C14	2,13-Tetradecanedione/urea	$6c_g' = 11c_h'$	M. E. Brown, *et al.*, *Chem. Mater.* **8**, 1588-1591 (1996)
C15	2,14-Pentadecanedione/urea	Unknown	N/A
C16	2,15-Hexadecanedione/urea	$1c_g' = 2c_h'$	Unpublished work
C17	2,16-Heptadecanedione/urea	Unknown	N/A
C18	2,17-Octadecanedione/urea	Unknown	N/A
C19	2,18-Nonadecanedione/urea	Unknown	N/A
C20	2,19-Eicosanedione/urea	$2c_g' = 5c_h'$	Unpublished work

Figure 6-1: Series of alkanedione/urea systems and their corresponding host-guest relationships.

Investigations of these series allow the construction of models that can be used to predict features of stable crystal packing arrangements of hosts and guests.[1] A model, similar to the helical wheel diagrams employed by biochemists to display amino acid sequences found in α helices of proteins, has been developed that can predict host-guest connectivity and hydrogen-bonding topologies of alkanedione/urea systems (Figure 6-2).[1]

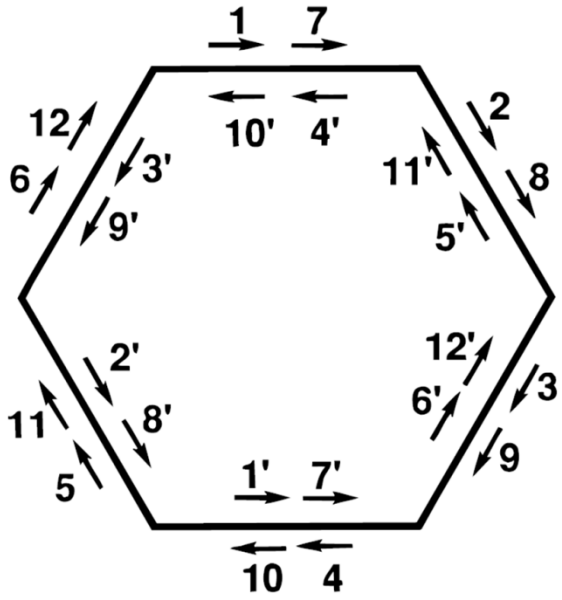

Figure 6-2: General wheel for the helical wheel model, representing two full turns of the urea helix. The arrows show the C=O directions of the urea carbonyl groups. The lowest numbers for each helix (1, 1') represent the ureas closest to the viewer, whereas higher numbers represent ureas that are further down the channel. [Adapted with permission from M. E. Brown, *et al.*, *Chem. Mater.*, **8**, 1588-1591 (1996)]

For this helical wheel model, the two sets of numbers, *N* (helix 1) and *N*' (helix 2), represent the sequences of host molecules in the two urea helices that make up a given channel.[1] Because UICs contain extensive urea-host hydrogen bonded network of helical ribbons running in opposite directions, each urea in helix 1 has another directly across the channel in helix 2 (1 and 1' in Figure 6-2 for example). The arrows in the helical wheel model denote the C=O directions of the urea carbonyl groups, such that helix 1 moves down the channel (1---2---3---4…) by leading with its carbonyl group. Likewise, helix 2 moves down the channel (1'---2'---3'---4'…) leading with its N-H bond.

Lenné,[2] Weber, *et al.*,[3] and Huard[4] have reported guest repeats in heptadecane/urea of 23.912 Å, 23.713(1) and 24.17 Å, respectively. Given that Huard's data was collected with a

high-resolution imaging plate system instead of photographic film, this last number is probably the most reliable. Because alkanediones tend to adopt commensurate structures with high symmetry, it is quite likely that 2,16-heptadecanedione/urea adopts a structure with a host-guest ratio of $6\boldsymbol{c}_g' = 13\boldsymbol{c}_h'$ (one guest for 13 host molecules), which requires a guest repeat length of 23.87 Å. This proposed stoichiometry is based on the idea that alkane, alkanone, and alkanedione molecules have almost identical bond lengths and bond angles,[5] and that a structure with six guest molecules for an integral number of host molecules would necessarily have six-fold symmetry.[1] In examining the helical wheel model, one can predict the topological features of 2,16-heptadecanedione/urea with this stoichiometry. Figure 6-3 illustrates possible combinations of host-guest connectivity for this system, in which the carbonyls of the guest are tethered to the first and fourteenth ureas in the channel. These diagrams represent the possible O=C---C=O torsion angles that the guest must adopt to form a commensurate structure containing a periodic hydrogen-bonded network with urea.[1]

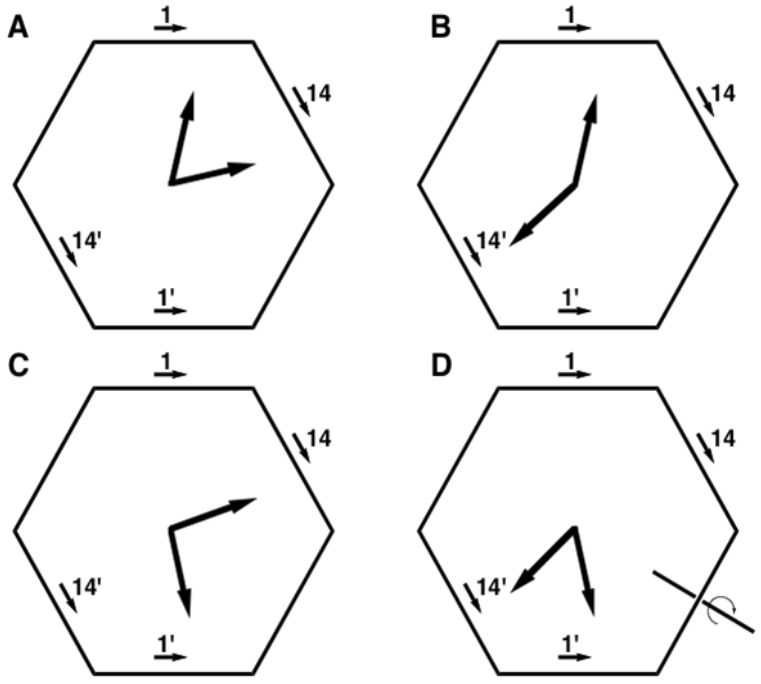

Figure 6-3: Right-handed helical wheel model showing four possible arrangements for host-guest hydrogen bonding in 2,16-heptadecanedione/urea. The *C*2 axis shared by A and D is shown in D. The long arrows in the center of each diagram represent the orientations of the two carbonyls in one guest molecule. [Provided courtesy of M. D. Hollingsworth]

In Figure 6-3A, carbonyls of the guest (represented by large arrows) form hydrogen bonds with the N-H groups of ureas 1 and 14 from the same helix. In other topologies, the guest can form hydrogen bonds to ureas in two different helices (figure 6-3B, C). The topologies represented in Figure 6-3A and D are isoenergetic since they are related by a *C*2 axis of symmetry.[1] Because 2,16-heptadecanedione is an odd chain guest, its carbonyl groups prefer a smaller torsion angle. Thus, it can be predicted that Figure 6-3B would be the least likely topology of this guest. It is impossible to predict whether Figure 6-3A/D or Figure 6-3C would be the most likely topology for 2,16-heptadecanedione/urea, so the answer to this question awaits full structure determination of this UIC. The synthesis and formation of 2,16-heptadecanedione/urea will be discussed in the following section.

Synthesis of 2,16-Heptadecanedione

The synthesis of 2,16-heptadecanedione involved metallation of methyl isopropenyl ether,[6] as previously described in chapter 2. This reagent, created by reaction with potassium *tert*-butoxide and *n*-butyllithium, was reacted with 1,11-dibromoundecane. This afforded 2,16-methoxyheptadeca-1,16-diene (Figure 6-2). The final step involved deprotection with hydrochloric acid and resulted in highly pure 2,16-heptadecanedione.

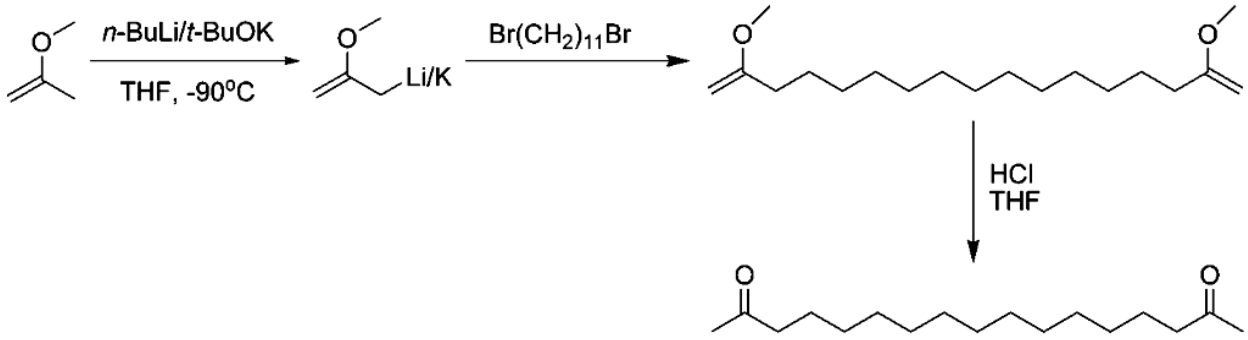

Figure 6-4: Synthesis of 2,16-heptadecanedione via metallation of methyl isopropenyl ether.

Metallation of methyl isopropenyl ether:

Potassium *tert*-butoxide was dried under vacuum for 16 hours before use. A round bottom flask, equipped with a dropping funnel and thermometer and under an argon atmosphere, was cooled to -90 °C in a bath of hexanes and liquid nitrogen. To the cooled flask containing dry THF (5 mL) was added *n*-butyllithium solution (4.10 mL, 6.32 mmol, Aldrich, 1.54 M in

hexanes[7]) and then freshly distilled 2-methoxypropene (1.9 g, 25.3 mmol, Aldrich, 97%). Subsequently, a solution of dry potassium *tert*-butoxide (0.709 g, 6.32 mmol, Aldrich, 95%) dissolved in dry THF (8 mL) was added dropwise at -90 °C to this solution, causing the reaction mixture to turn yellow. The reaction mixture was stirred at -90 °C for one hour and was used without purification for the next step.

Notebook pages: ADA-A85.

2,16-Methoxyheptadeca-1,16-diene:

The aforementioned reaction mixture was warmed to -55 °C before 1,11-dibromoundecane (0.754 g, 2.40 mmol, Aldrich, 98%) was added dropwise at this temperature. After stirring for 10 minutes at -55 °C, the cold bath was removed, and the reaction mixture was allowed to warm to room temperature. After stirring at room temperature for 4 hours, the reaction mixture was quenched with water (50 mL) before extraction with diethyl ether (4 x 50 mL). The combined diethyl ether layers were concentrated using a rotary evaporator, and the crude product was used in the next step without further purification.

Notebook pages: ADA-A86.

2,16-Heptadecanedione:

To a round bottom flask containing the crude 2,16-methoxyheptadeca-1,16-diene was added THF (5 mL) and 10% HCl solution (1.9 mL). After stirring at room temperature for one hour, the white reaction mixture was quenched with water (10 mL) and extracted with diethyl ether (3 x 25 mL). The organic layer was dried over K_2CO_3, filtered, and concentrated on a rotary evaporator, yielding pure 2,16-heptadecanedione (0.428 g, 67% yield) as a white powder.

Physical data: $R_f = 0.43$ (1:9 EtOAc/hexanes v/v, PMA stain as indicator). Melting point: 81-83 °C (Lit. mp: 85-86 °C).[8] ^{1}H NMR (400 MHz, $CDCl_3$, ADA-A89-31): δ1.25 (18H, m, -C**H**$_2$-), 1.56 (4H, br dt, β-C**H**$_2$-COR), 2.14 (6H, s, C**H**$_3$), 2.42 (4H, t, α-C**H**$_2$-COR, J = 7.4 Hz). ^{13}C NMR (100.57 MHz, $CDCl_3$, ADA-A89-31-C13): δ24.10 (-**C**H$_2$-), 29.40 (-**C**H$_2$-), 29.62 (-**C**H$_2$-), 29.67 (-**C**H$_2$-), 29.79 (-**C**H$_2$-), 29.81 (-**C**H$_2$-), 30.07 (**C**H$_3$), 44.06 (α-**C**H$_2$-COR), 209.64 (-**C**O-).

Notebook page: ADA-A88.

Formation of 2,16-Heptadecanedione/urea

The formation of 2,16-heptadecanedione/urea was accomplished via slow cooling techniques. A solution of 2 M urea in methanol containing 1% water (15 mL) and isobutyl alcohol (6 mL) was used to dissolve 2,16-heptadecanedione (0.213 g), with a stoichiometric ratio of thirteen urea molecules to one guest molecule. After slowly cooling from 46 °C to room temperature in a 4 L Dewar flask for 24 hours, thin plates were collected.[9] These crystals were uniaxial as shown by extinction in all positions as the crystal was rotated about the channel axis between crossed polars (Figure 6-5).

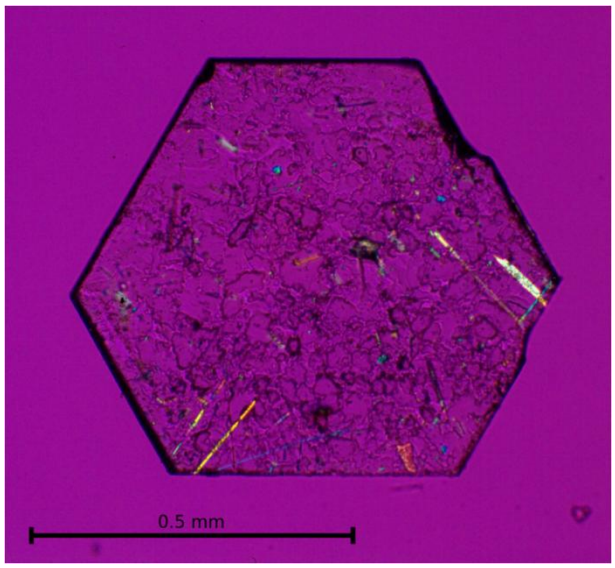

Figure 6-5: Photomicrograph of 2,16-heptadecanedione/urea between crossed polars and a lambda plate. This crystal was extinguished at all stage orientations.

Conclusions for Chapter 6

Synthesis of the guest molecule, 2,16-heptadecanedione, was successfully achieved by utilizing metallated methyl isopropenyl ether. This afforded pure 2,16-heptadecanedione in high yields. Thin, hexagonal plates of 2,16-heptadecanedione/urea were grown, as expected for a commensurate UIC with high symmetry.[5] Future work will consist of the collection of crystallographic data for this system and possible structure solution for this inclusion compound.

Chapter 6 References

1 Brown, M. E., Chaney, J. D., Santarsiero, B. D. and Hollingsworth, M. D. Superstructure topologies and host-guest interactions in commensurate inclusion compounds of urea with bis(methyl ketone)s. *Chem. Mater.* **8**, 1588-1591, (1996).

2 Lenné, H. U., Mez, H. C. and Schlenk, W., Jr. Lengths of molecules in inclusion channels of urea and thiourea. *Justus Liebigs Ann. Chem.* **732**, 70-96, (1970).

3 Weber, T., Boysen, H., Frey, F. and Neder, R. B. Modulated structure of the composite crystal urea n-heptadecane. *Acta Crystallogr.* **B53**, 544-552, (1997).

4 Huard, M. *Instabilités structurales de cristaux moléculaires apériodiques* Ph.D. Thesis, Université de Rennes 1, (2009).

5 Hollingsworth, M. D., Brown, M. E., Hillier, A. C., Santarsiero, B. D. and Chaney, J. D. Superstructure control in the crystal growth and ordering of urea inclusion compounds. *Science* **273**, 1355-1359, (1996).

6 Taherirastgar, F. and Brandsma, L. Generation and synthetic application of metallated methyl isopropenyl ether. A substitute for acetone enolate. *Chemische Berichte/Recueil* **130**, 45-48, (1997).

7 Abeykoon, J. Refer to JPA-A13 for titration of n-butyllithium solution, purchased from Aldrich as 1.6 M in hexanes.

8 Guo, Y., Chen, K. Y., Li, J. L. and Shi, Z. Biomimetic synthesis of twenty-four long-chained diketones as precursors for muscone and further macrocyclic ketones. *Chinese J. Chem.* **26**, 2249-2255, (2008).

9 Nichols, S. M. Refer to SMN-B93-1 for collection of crystals. .

CHAPTER 7 - 2-Eicosanone/urea

Introduction

As mentioned in chapter 6, the studies of alkane/urea, alkanone/urea, and alkanedione/urea have provided many details about UIC crystal growth and molecular recognition. Another significant compound that will aid in extending the alkanone/urea series is that of 2-eicosanone. Of great interest for the alkane/urea series has been the study of eicosane/urea, which was discovered to be a commensurate system (Figure 7-1),[1] having two guest molecules for every five host repeats ($2\boldsymbol{c}_g' = 5\boldsymbol{c}_h'$).[2] However, it has been difficult to obtain a crystal structure for this system due to disorder in the high temperature phase and complicated twinning in the ferroelastic phase. Shane Nichols, a member of the Hollingsworth group, stressed a crystal of eicosane/urea in its high symmetry phase in hopes that upon cooling through the ferroelastic phase transition, a single domain would be populated. This project is currently in progress.[3]

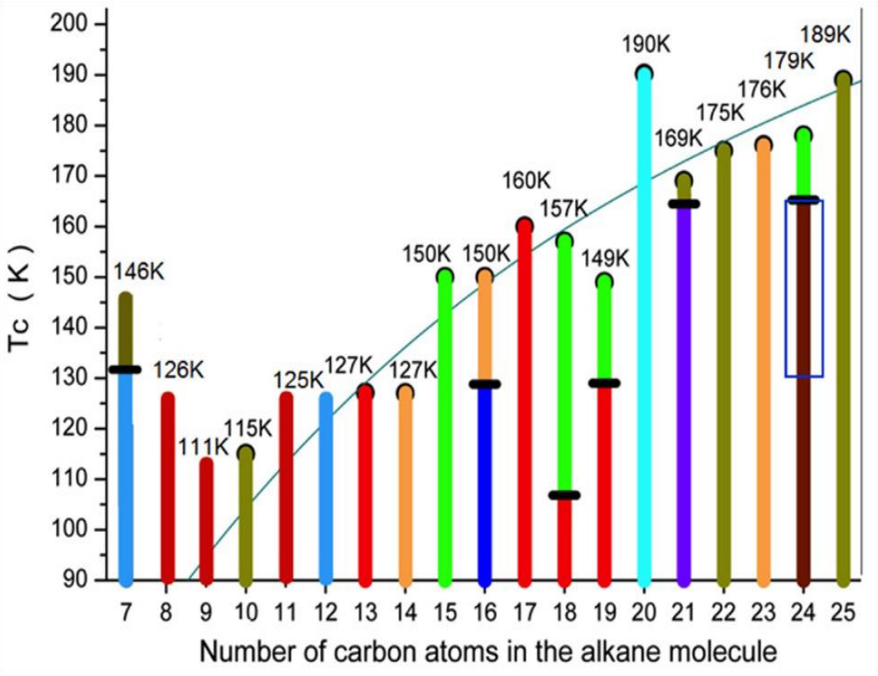

Figure 7-1: Temperature dependent phase transitions of a series of alkane/urea systems. Note how the phase transition for eicosane, a guest having 20-carbons, differs dramatically from the rest of the members of this series. This is because eicosane/urea is a commensurate system. [Adapted from M. Huard, Ph.D. Dissertation, University of Rennes 1 (2009)]

Because of similarities between alkanes, alkanones, and alkanediones, it is desirable to collect XRD data on the corresponding 2-eicosanone/urea and 2,19-eicosanedione/urea systems for comparison with the eicosane/urea. The synthesis and formation of 2-eicosanone/urea will be discussed in the following section.

Synthesis of 2-Eicosanone

2-eicosanone was synthesized in two steps from the commercially available 1-eicosene, as shown in Figure 7-2. The first step involved an oxymercuration-reduction process. Oxymercuration-reduction is useful in that it can quickly hydrate alkenes under mild conditions, giving high yields without producing side products.[4] This procedure involves the addition of OH and HgOAc groups across a double bond, followed by *in situ* treatment with sodium borohydride. This method gives almost exclusively Markovnikov addition.[4] That is, the alcohol functional group is added to the more substituted carbon. In fact, terminal alkenes have been shown to be more than 99% regioselective for Markovnikov addition.[5]

The final step for this synthesis utilized Jones reagent, as previously discussed in Chapter 4, for the oxidation of 2-eicosanol's secondary alcohol to a ketone functional group. This yielded the desired 2-eicosanone.

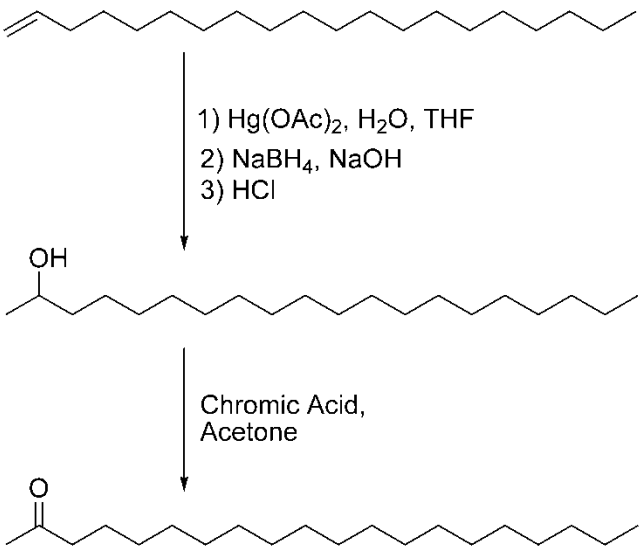

Figure 7-2: Synthesis of 2-eicosanone via oxymercuration-reduction process.

2-Eicosanol:

In a round bottom flask containing ice-cold mercury(II) acetate (1.13 g, 3.56 mmol, Fisher Scientific), was added 15 mL of a 4:1 ratio (v:v) of THF:H_2O. This produced a yellow-colored mixture. At ice temperatures, a solution of 1-eicosene (1.00 g, 3.56 mmol, Aldrich, 90%) dissolved in THF (3 mL) was slowly added to the yellow mixture. When the ice bath was removed, evolution of gas was observed, and then the reaction mixture became a viscous white liquid. After stirring at room temperature for 1 hour, NaOH (6.7 mL, 3 M) was added, followed by the addition of $NaBH_4$ (0.21 g, 5.34 mmol, Aldrich, 99%), making the reaction turn a dark gray color. After stirring at room temperature for 2 hours, HCl (0.5 mL, 6 M) was added dropwise to the reaction mixture, followed by the dropwise addition of 12 M HCl until the reaction mixture reached pH 1. The reaction mixture was extracted with diethyl ether (3 x 40 mL) before the organic layer was washed once with 3 M NaOH (20 mL), once with 50% saturated aq. NaCl solution (40 mL), and finally with saturated aq. NaCl (40 mL). The organic layer was dried over $MgSO_4$, filtered, and concentrated on a rotary evaporator, to yield 2-eicosanol (1.022 g, 96% yield) as a white powder.

Physical data: R_f = 0.81 (1:1 EtOAc/hexanes v/v, PMA stain as indicator). ^{1}H NMR (400 MHz, $CDCl_3$, ADA-A124-17): δ0.88 (3H, t, C**H**$_3$-CH_2R, *J* = 6.7 Hz), 1.19 (3H, d, C**H**$_3$-CHOHR, *J* = 6.2 Hz), 1.26 (32H, s, -C**H**$_2$-), 1.45 (2H, m, α-C**H**$_2$-CHOHR), 3.79 (1H, m, C**H**OH).

Notebook pages: ADA-A123.

2-Eicosanone:

To a round bottom flask containing ice-cold Jones reagent (5.42 mL, 2.67 M), was added crude 2-eicosanol (1.022 g, 3.42 mmol) dissolved in acetone (100 mL, ACS reagent, Fisher Scientific). After stirring at room temperature for 18 hours, the reaction mixture was quenched with enough water to dissolve the chromium salts (approx. 100 mL). The reaction mixture was extracted with diethyl ether (3 x 100 mL) and washed with saturated (1 x 50 mL). The organic layer was dried over $MgSO_4$, filtered, and concentrated on a rotary evaporator. The crude product was purified with flash column chromatography to give pure 2-eicosanone (0.718 g, 70.9% yield) as a white solid.

Physical data: R_f = 0.53 (1:9 EtOAc/hexanes v/v, PMA stain as indicator). Melting point: 55-56 °C (Lit. mp: 58-59 °C).[6] ^{1}H NMR (400 MHz, $CDCl_3$, ADA-A131-17): δ0.88 (3H, t, C**H**$_3$-CH_2R, *J* = 6.4 Hz), 1.25 (32H, s, -C**H**$_2$-), 1.55 (2H, second order multiplet, β-CH_2-COR), 2.13 (3H, s, C**H**$_3$-COR), 2.41 (2H, t, α-C**H**$_2$-COR, *J* = 7.3 Hz). ^{13}C NMR (100.57 MHz, $CDCl_3$, ADA-A131-17-C13): δ14.34 (**C**H_3-CH_2R), 22.92 (CH_3-**C**H_2R), 24.11 (-**C**H_2-), 29.42 (-**C**H_2-), 29.59 (-**C**H_2-), 29.63 (-**C**H_2-), 29.69 (-**C**H_2-), 29.83 (-**C**H_2-), 29.92 (8 overlapping peaks, -**C**H_2-), 30.06 (-**C**H_2-), 32.15 (-**C**H_2-), 44.06 (α-**C**H_2-COR), 209.64 (-**C**O-).

Notebook pages: ADA-A129.

Formation of 2-Eicosanone/urea

Low temperature cooling techniques were utilized for the formation of 2-eicosanone/urea. A solution of 2 M urea in methanol containing 1% water (15 mL), isobutyl alcohol (10 mL), and distilled water (1 mL) was used to dissolve 2-eicosanone (0.196 g), with a stoichiometric ratio of fifteen urea molecules to one guest molecule. After slowly cooling from 45 °C to 0 °C in a 1 L Dewar flask, a mixture of prismatic needles and plate-like crystals were collected (Figure 7-3). Preliminary studies performed at the Advanced Light Source, Lawrence Berkeley National Lab have shown this UIC to commensurate with $2\boldsymbol{c}_g' = 5\boldsymbol{c}_h'$.

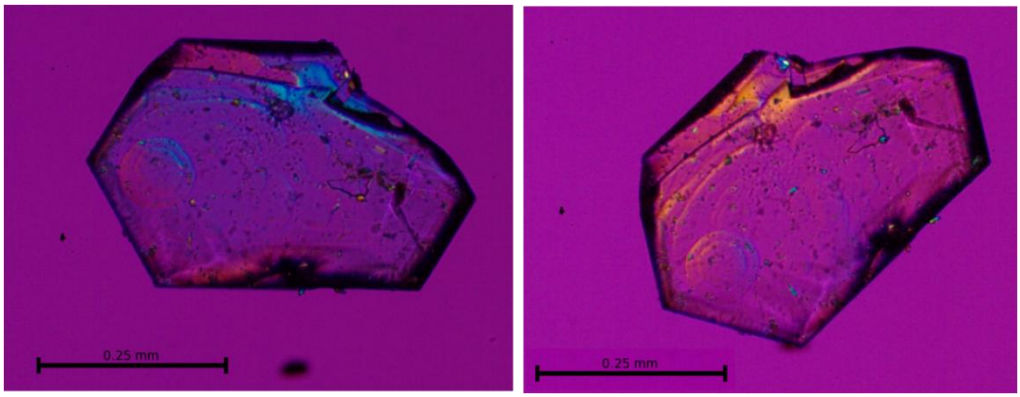

Figure 7-3: Photomicrographs of 2-eicosanone/urea between crossed polars and a lambda plate. Note the different interference colors observed for different orientations of this crystal.

Conclusions for Chapter 7

The synthesis of the guest molecule, 2-eicosanone, was successfully achieved by oxymercuration-reduction, followed by oxidation of the secondary alcohol with Jones reagent. This afforded pure 2-eicosanone in high yields. Crystals of 2-eicosanone/urea were grown, and preliminary crystallographic data were collected at the Advanced Light Source (Lawrence Berkeley Laboratory). Future work will focus on obtaining the full crystal structure of this system.

Chapter 7 References

1 Huard, M. *Instabilités structurales de cristaux moléculaires apériodiques* Ph.D. Thesis, Université de Rennes 1, (2009).

2 Fukao, K. Anomalous behavior in the phase transition and crystal structure of urea adducts with *n*-eicosane. *J. Phys. Condens. Matter*. **8**, 2105-2118, (1996).

3 Nichols, S. M. Refer to SMN-B226, SMN-B237, SMN-B247, SMN-B255, SMN-B261 for eicosane/urea stress experiments.

4 Smith, M. B. and March, J. *March's Advanced Organic Chemistry: Reactions, Mechanisms, and Structure*. 6th edn, pp. 1032-1033 (John Wiley & Sons, Inc., Hoboken, New Jersey, 2007).

5 Carey, F. A. and Sundberg, R. J. *Advanced Organic Chemistry, Part A: Structure and Mechanisms*. 5th edn, pp. 515-520 (Springer Science & Business Media, New York, NY, 2007).

6 Pangborn, M. C. and Anderson, R. J. The chemistry of the lipids of tubercle bacilli. XLI. Part 1. The composition of the *Timothy bacillus* wax. Part 2. The isolation of *d*-eicosanol-2 and *d*-octadecanol-2 from the unsaponifiable matter of the *Timothy bacillus* wax. *J. Am. Chem. Soc.* **58**, 10-14, (1936).

CHAPTER 8 - General Conclusions

To conclude this thesis, the synthesis, crystal growth, and analysis of various urea inclusion compounds have been discussed. Chapter 1 reviewed characteristic details and unique properties of urea inclusion compounds. In addition, industrial and research related applications of urea inclusion compounds were discussed. Some of the applications included using UICs for inclusion polymerization, electron spin resonance (ESR) spectroscopic studies, molecular separation, resolution of enantiomers, and ferroelastic studies.

In Chapter 2, the attempted synthesis of the guest molecule (5*S*,6*S*)-2,9-decanedione-d_2 was described. This guest molecule is a critical component for determination of the absolute configuration of urea inclusion compounds. Although several synthetic methods were attempted, the successful synthesis of (5*S*,6*S*)-2,9-decanedione-d_2 (or its 5*R*,6*R* enantiomer) has yet to be completed. A current strategy involving the stereospecific reduction of a single dibromo-bis(methylbenzylamide) diastereomer with $LiAlD_4$ is still in progress. Alternative approaches such as stereospecific epoxide formation or diether diastereomer separation have also been proposed for future research. Future work will consist of successfully preparing (5*S*,6*S*)-2,9-decanedione-d_2/urea and analyzing this system with polarized light microscopy, X-ray topography, and single crystal neutron diffraction.

The synthesis and preparation of 1,6-dicyanohexane-1,1,6,6-d_4/urea was discussed in Chapter 3. Deuterium was introduced into the 1 and 6 carbon positions via reduction of an acyl chloride with $LiAlD_4$. Very large crystals (13-16 mg) of 1,6-dicyanohexane-1,1,6,6-d_4/urea were grown and were studied by others in the Hollingsworth group with ^2H NMR. Unfortunately, these NMR studies are not publishable because the goniometer was misoriented in the NMR probe. Future work will consist of repeating this exact experiment once proper alignment of the goniometer has been achieved. This rotational experiment will also be repeated for this crystal under stress to assess the changes in gauche conformer populations as a function of stress.

Chapter 4 discussed the synthesis of highly pure 1,11-undecanedioic acid. This was accomplished by oxidizing 1,11-undecanediol twice with Jones reagent. The crystals of 1,11-undecanedioic/urea were used in diffuse scattering experiments that were conducted in the Department of Physics at the University of Rennes, France. Future work will consist of analyzing the data collected and resolving this system's diffuse scattering.

In Chapter 5, the guest molecule bis(3-oxobutyl) adipate was successfully synthesized by performing esterification of adipoyl chloride with 2-(2-methyl-1,3-dioxolan-2-yl)ethanol. Isolation of pure bis(3-oxobutyl) adipate was accomplished, and its corresponding UIC was grown. The bis(3-oxobutyl) adipate/urea crystals were examined at the Department of Physics in the University of Rennes, France and at Kansas State University, Kansas. The crystal structure of this material was surprising since it involved no host-guest hydrogen bonding, even though a nearly isostructural guest exhibited extensive host-guest hydrogen bonding. Future work will involve seeding experiments in attempts to form the hydrogen bonded polymorph.

Chapter 6 discussed the synthesis of the guest molecule 2,16-heptadecanedione. This was successfully achieved by utilizing metallated methyl isopropenyl ether, affording pure 2,16-heptadecanedione in high yields. Thin, hexagonal plates of 2,16-heptadecanedione/urea were grown. This crystal is expected to be a commensurate structure with $6\boldsymbol{c}_g' = 13\boldsymbol{c}_h'$ (one guest molecule for every 13 host molecule repeats). Future work will consist of extensive collection of crystallographic data for this system in an attempt to solve its crystal structure.

In Chapter 7, the synthesis of the guest molecule 2-eicosanone was successfully achieved by means of an oxymercuration-reduction process, followed by oxidation of the secondary alcohol with Jones reagent. This afforded pure 2-eicosanone in high yields. Crystals of 2-eicosanone/urea were grown and preliminary crystallographic data showed that this system was commensurate with $2\boldsymbol{c}_g' = 5\boldsymbol{c}_h'$. Future work will involve the full structure determination of this system above the ferroelastic phase transition temperature.

Appendix A - General Experimental Details

This section outlines experimental details applied for each synthetic procedure performed. All water-sensitive reactions were performed in glassware that had been cleaned and dried overnight in an oven. Solvents such as tetrahydrofuran (THF), diethyl ether, chloroform, methylene chloride, and acetone were distilled before each use. THF and diethyl ether were distilled over sodium metal under an argon atmosphere, with benzophenone as an indicator. Methylene chloride and chloroform were distilled over calcium hydride under an argon atmosphere. Acetone was distilled over anhydrous calcium sulfate under an argon atmosphere. Water was taken from the house distilled water supply. All other solvents were of ACS reagent grade or better, and were used as received, unless otherwise stated. All non-aqueous reactions were carried out under an inert (argon) atmosphere. Argon gas was bubbled through sulfuric acid, and then passed over potassium hydroxide pellets and calcium sulfate before entering the reaction vessel.

Flash column chromatography was performed using 60 Å, 230-400 mesh silica gel (Whatman 4790-050) according to the method reported by Still and co-workers [Still, W. C., Kahn, M., and Mitra, A. Rapid Chromatographic Technique for Preparative Separations with Moderate Resolution. *J. Org. Chem.* **43**, 2923-2925 (1978)]. Thin-layer chromatography was performed using K6F Silica Gel plates, 60 Å, 250 μm thickness (Whatman #4861-820). TLC plates were visualized with the following methods, as specified for each reaction: ultraviolet light (254 nm), iodine chamber (iodine crystals, Mallinckrodt), *p*-anisaldehyde stain, or phosphomolybdic acid stain (PMA).

Melting points were recorded on a Thomas Hoover Melting Point Apparatus and are uncorrected. All NMR spectra were recorded either using a Varian Unity Inova 400 spectrometer operating at 400 MHz or a Varian Mercury-VX spectrometer operating at 400 MHz. ^{1}H and ^{13}C NMR spectra were internally referenced to residual protonated solvent signals: $CDCl_3$ = 7.27 and 77.27 ppm for ^{1}H and ^{13}C resonances, respectively; DMSO-d_6 = 2.50 and 39.5 ppm for ^{1}H and ^{13}C resonances, respectively; acetone-d_6 = 2.05 ppm for ^{1}H, and 29.84 and 206.26 ppm for ^{13}C resonances. NMR spectra were analyzed using Varian VNMRJ or Spinworks (v. 3.1.7, for Windows). All optical rotation measurements were taken with a Perkin-

Elmer 241 Polarimeter, using the following specifications: Sodium lamp, 1 second integration, approximate energy of 70 microamps, and a path length of 1 decimeter. The concentration of samples used for optical rotation measurements were always in the units of grams per milliliter. Mass spectra were taken on an Applied Biosystems API 2000 LC/MS/MS system. Electrospray ionization (ESI), positive polarity, 140 V declustering potential, 400 V focusing potential, 10 V entrance potential were used. A concentration of 10 μM sample in methanol was used for each sample injection.

Crystals were viewed with a Nikon Microphot-SA microscope equipped with crossed polarizers and a 530 nm λ plate. For optical images collected using the Nikon microscope, Nikon M Plan objectives were used with magnifications of 5x and 10x.

Appendix B - Spectral Data for Synthesized Compounds

This section contains ^{1}H and ^{13}C NMR spectra for synthetically prepared compounds. Spectral data are labeled according to the listings in the physical data section for each detailed synthetic procedure. A mass spectrum for 1,6-dicyanohexane-1,1,6,6-d_4 is included as well. The following table lists all spectra included in the subsequent pages, as well as the NMR file name:

^{1}H NMR for High R_f dibromo-bis(acetylmandelate ester) diastereomer

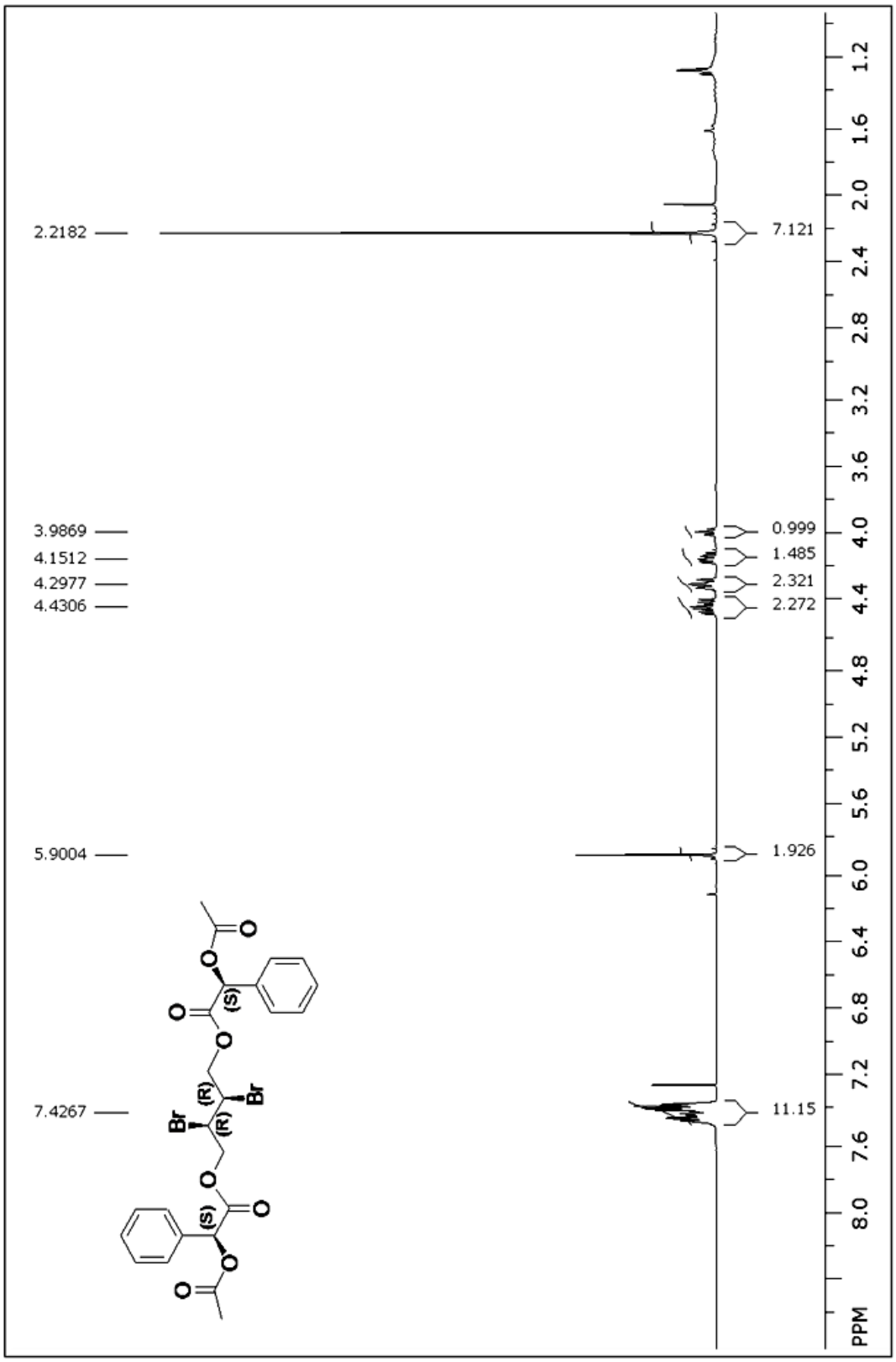

^{1}H NMR for High R_f dibromo-bis(acetylmandelate ester) diastereomer

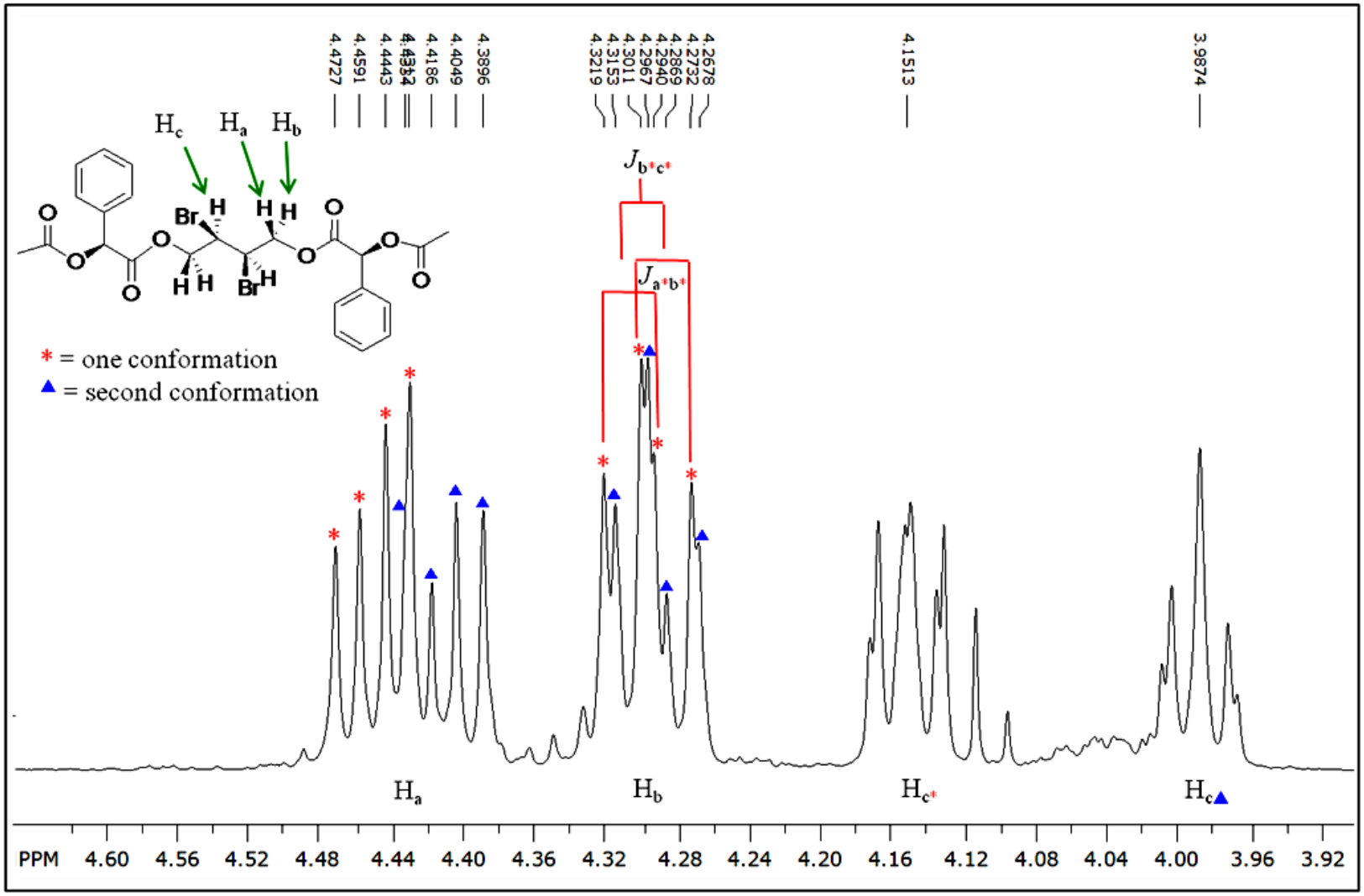

2D COSY NMR for High R_f dibromo-bis(acetylmandelate ester) diastereomer

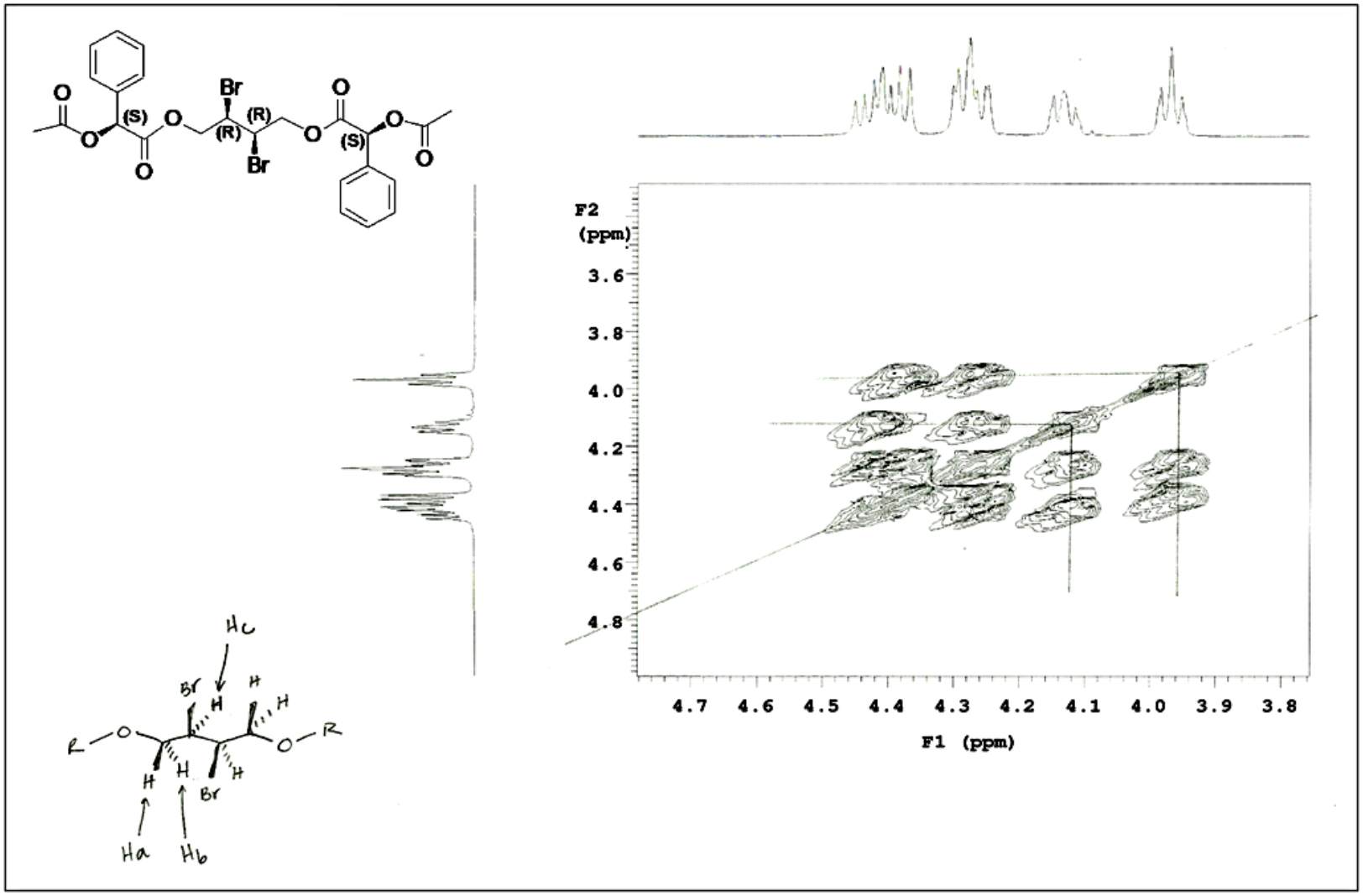

^{1}H NMR for Low R_f dibromo-bis(acetylmandelate ester) diastereomer

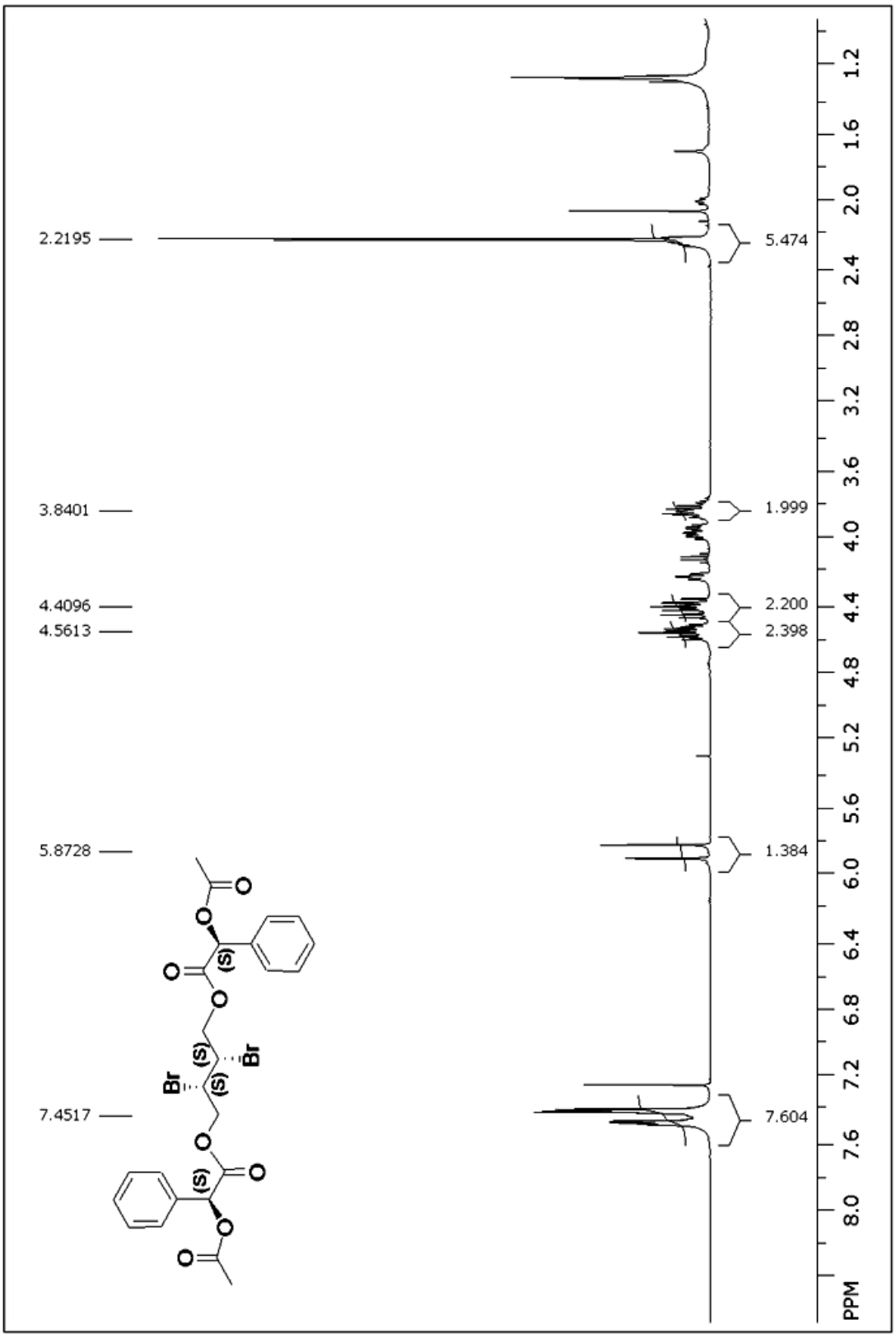

^{1}H NMR for 2*R*,3*R*-dibromo-1,4-butanediol

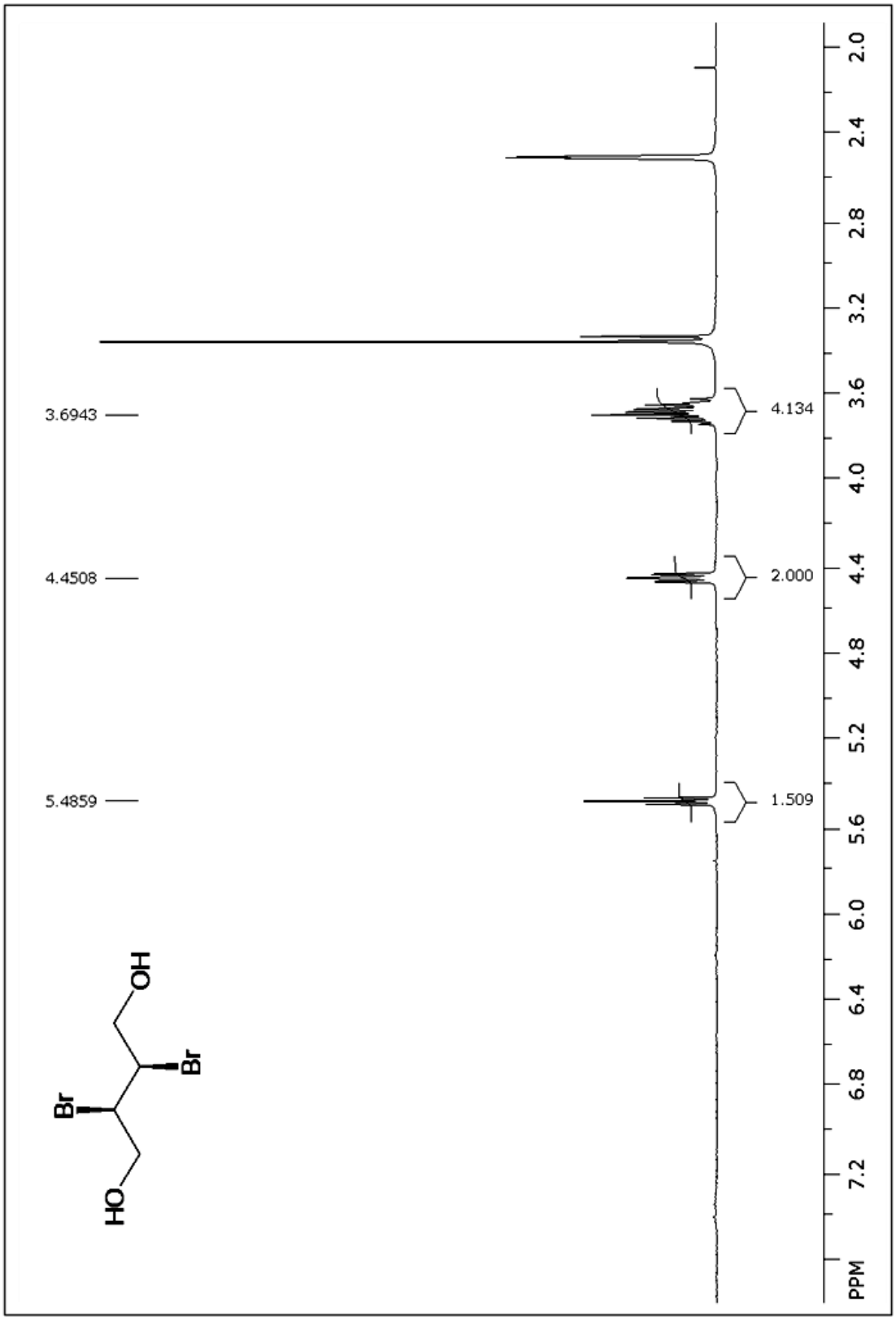

^{1}H NMR for 1,4-dimethoxybutane

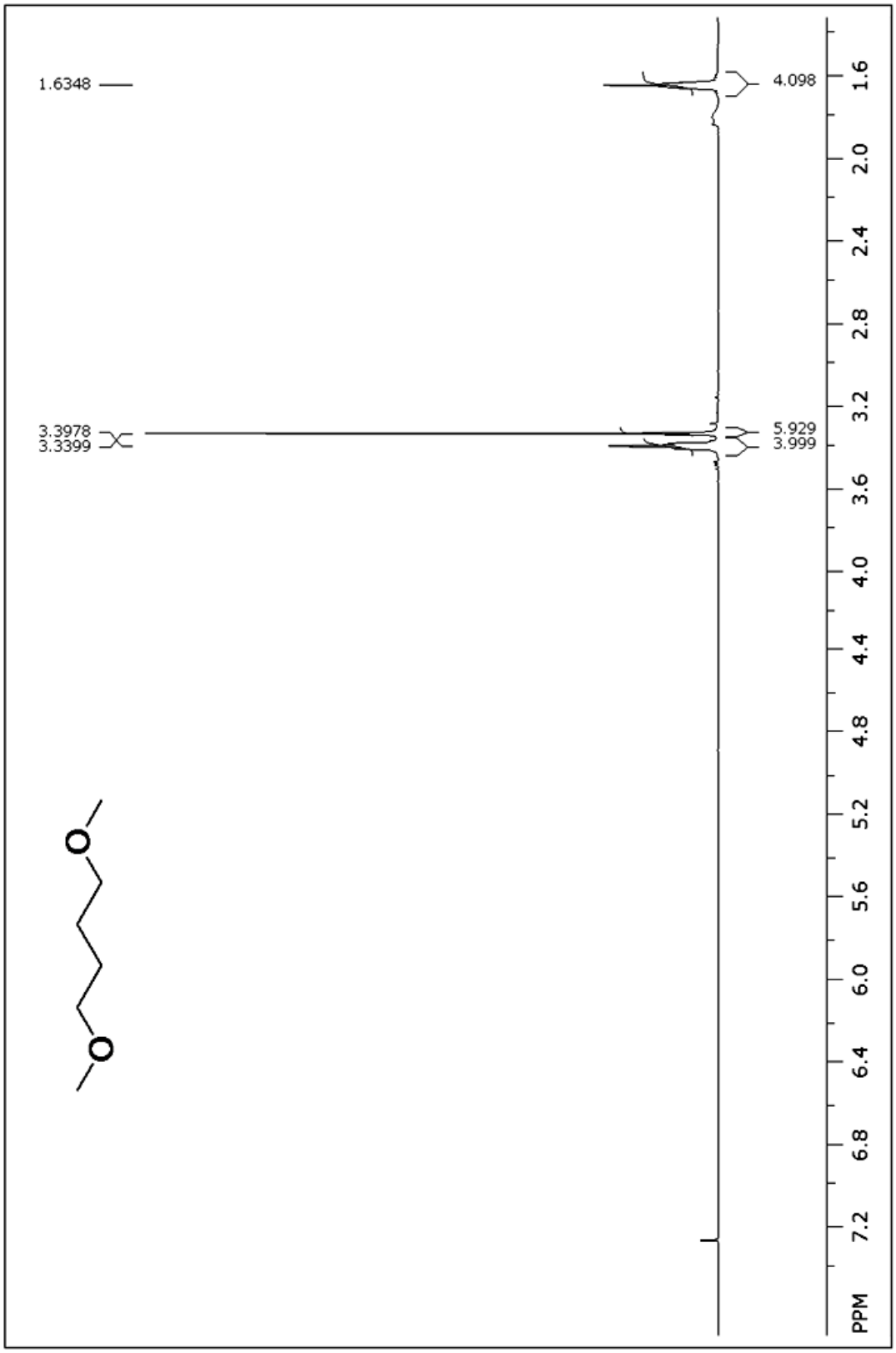

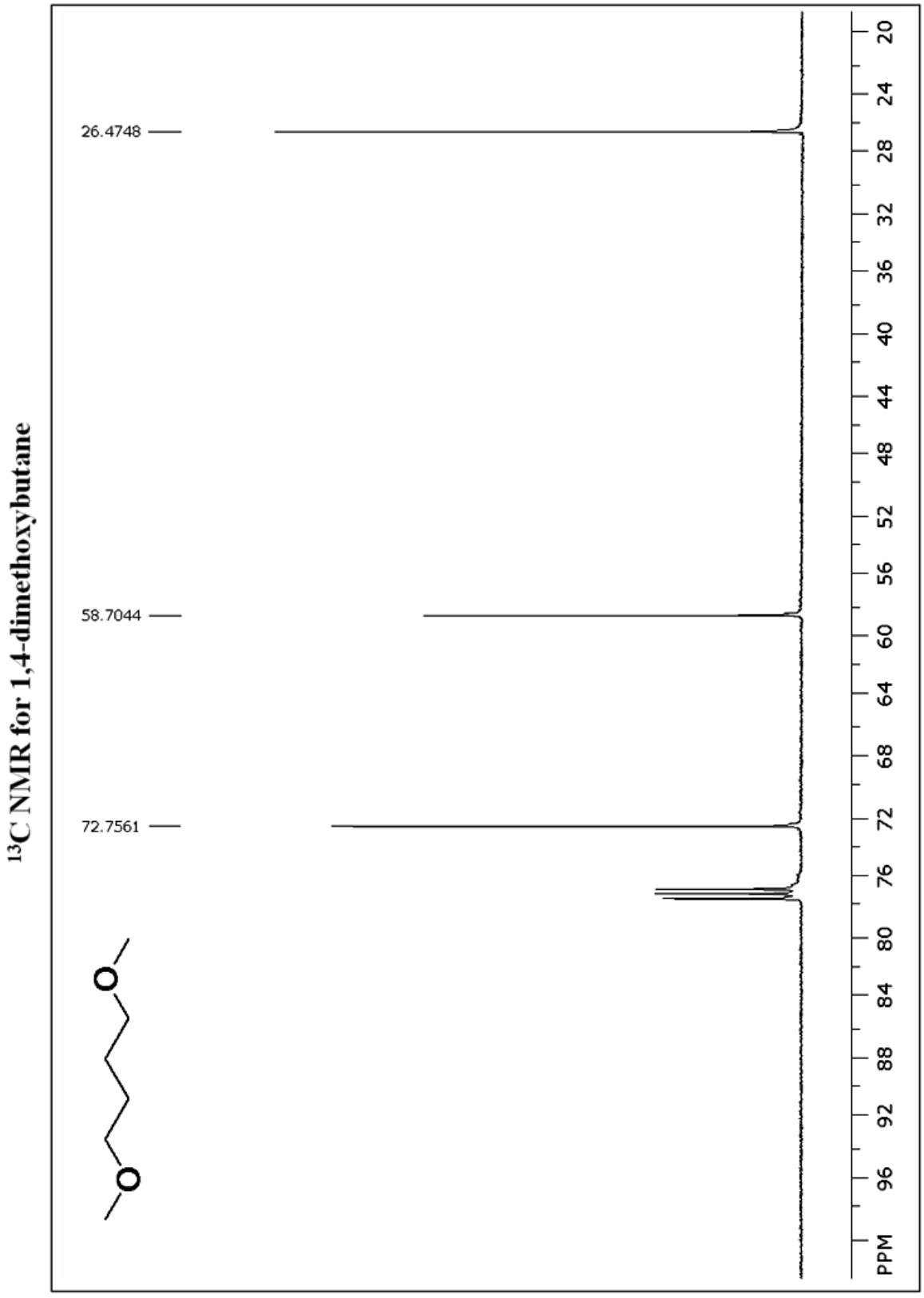
^{13}C NMR for 1,4-dimethoxybutane
26.4748
58.7044
72.7561
PPM
96
92
88
84
80
76
72
68
64
60
56
52
48
44
40
36
32
28
24
20

^{1}H NMR for 1,4-dibromobutane

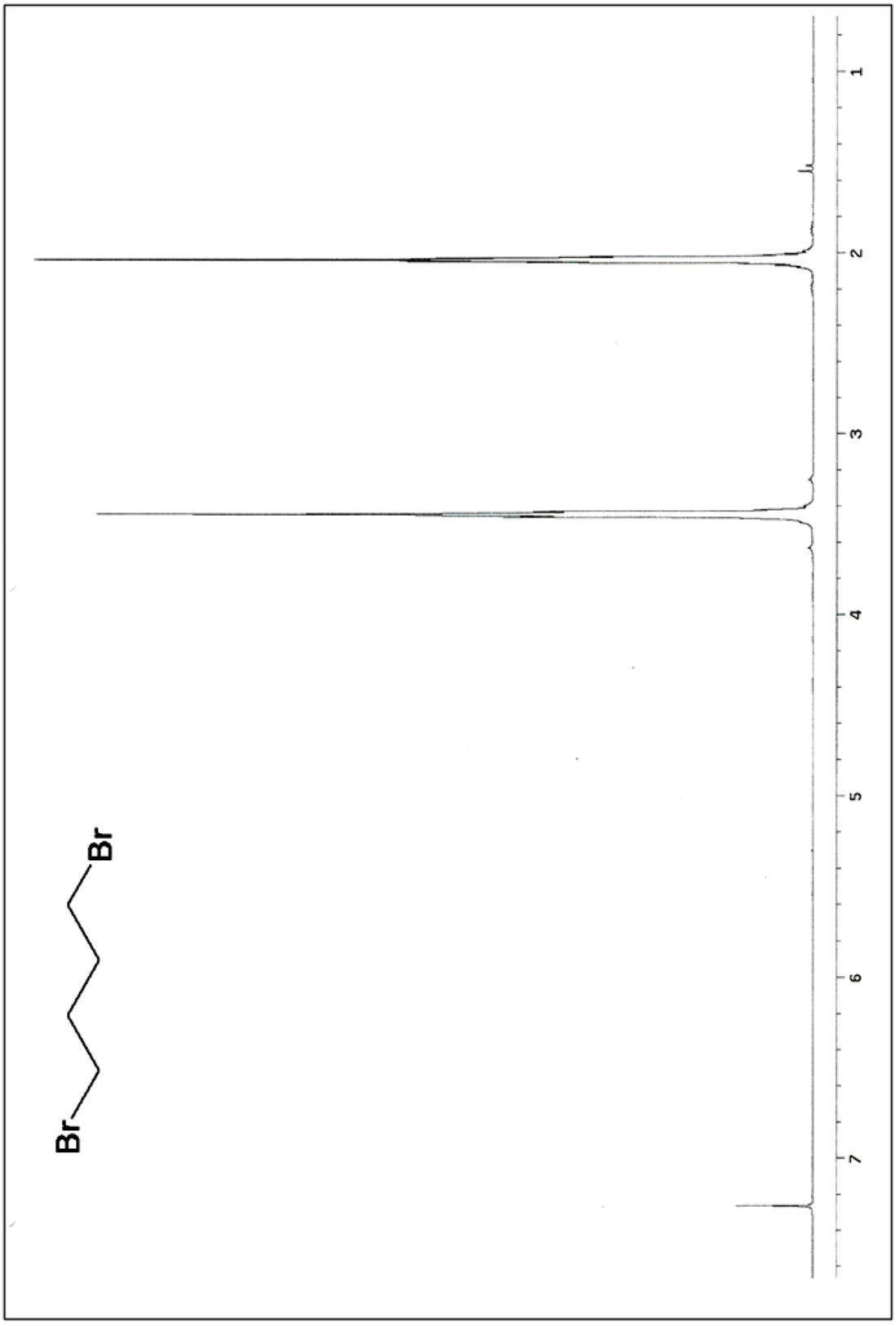

^{1}H NMR for 2*S*,3*S*-dimethanesulfonate-1,4-dimethoxybutane

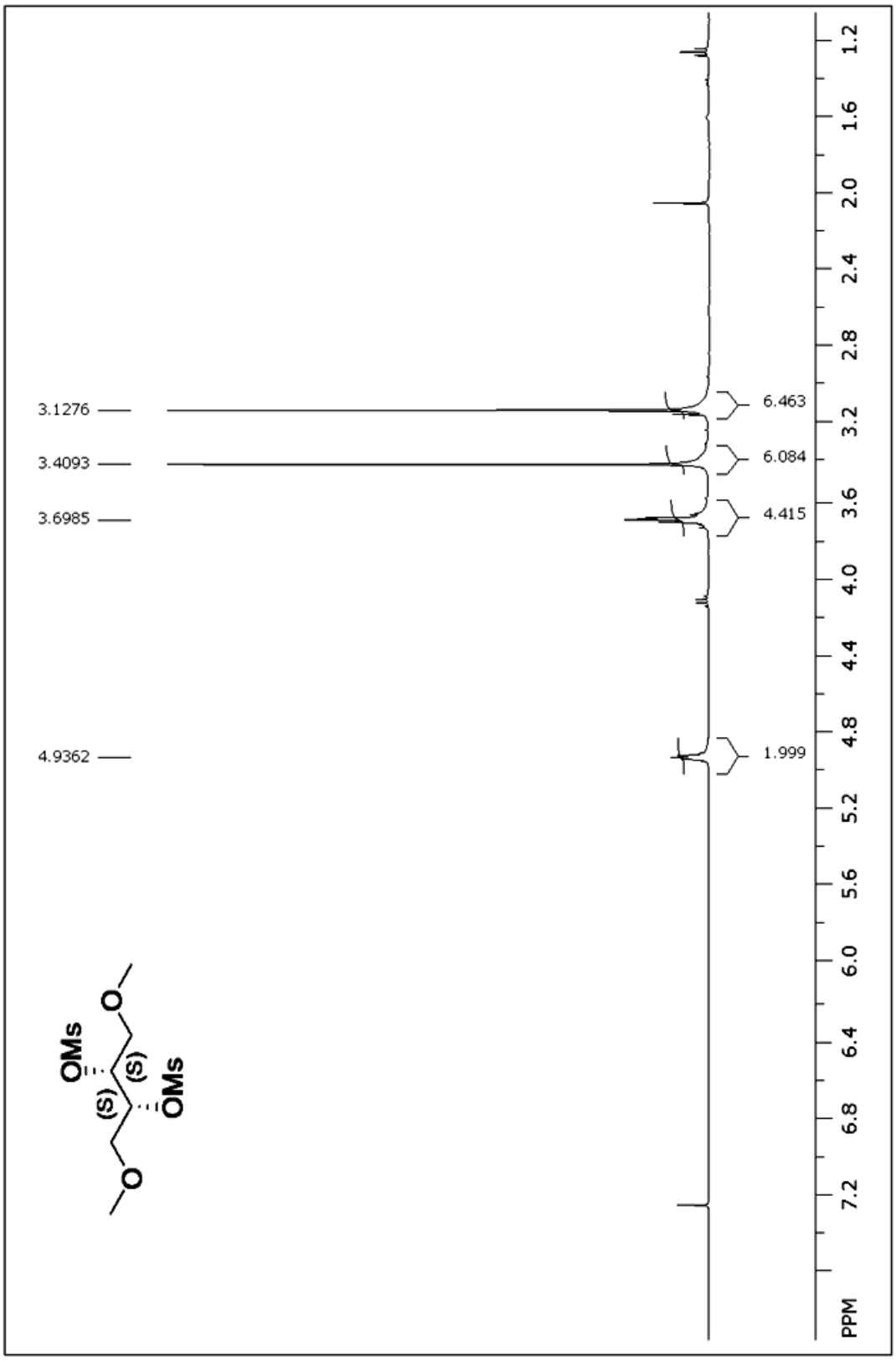

^{1}H NMR for *d,l*-2,3-dichloro-1,4-butanediol

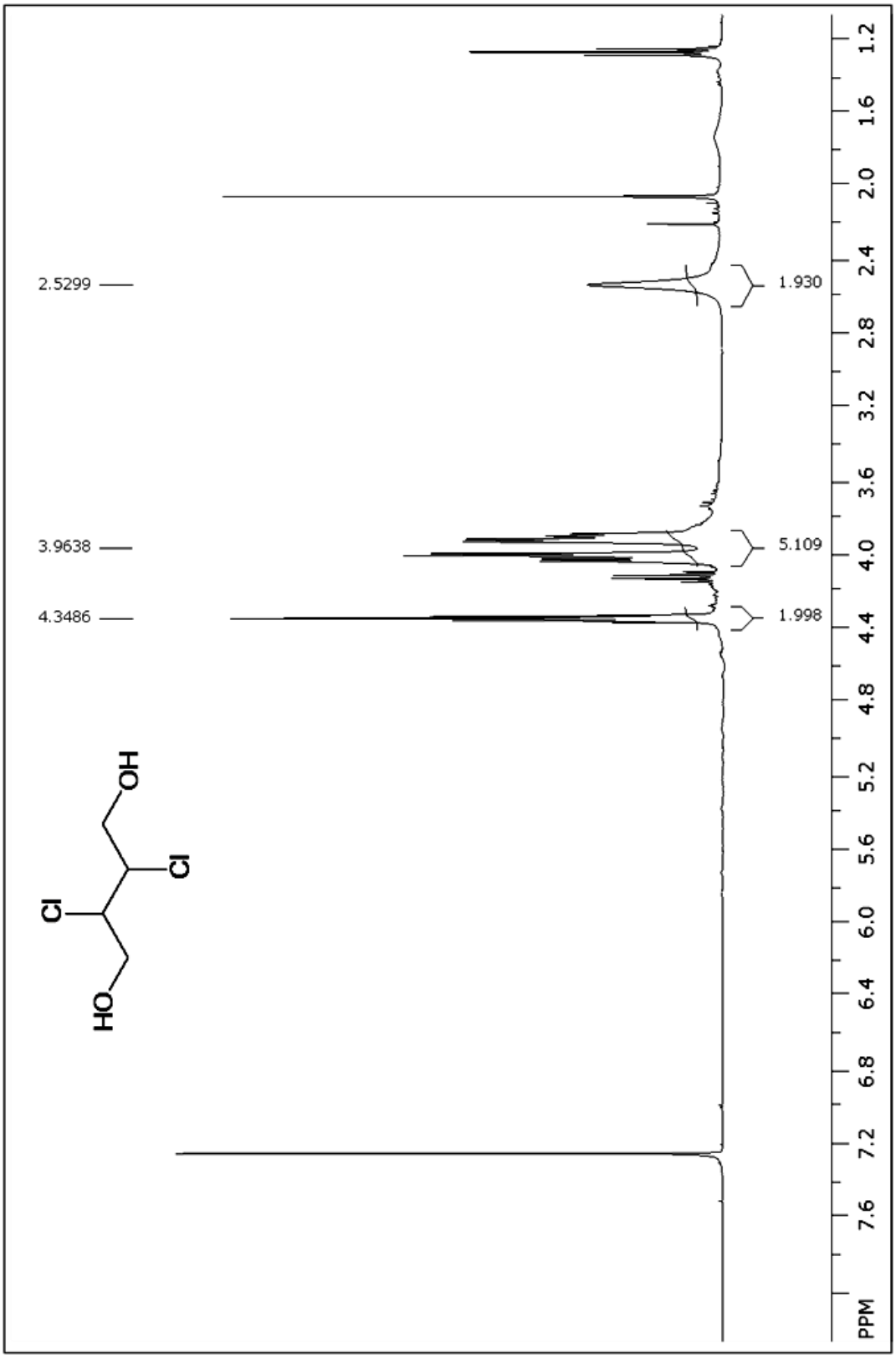

^{13}C NMR for *d,l*-2,3-dichloro-1,4-butanediol

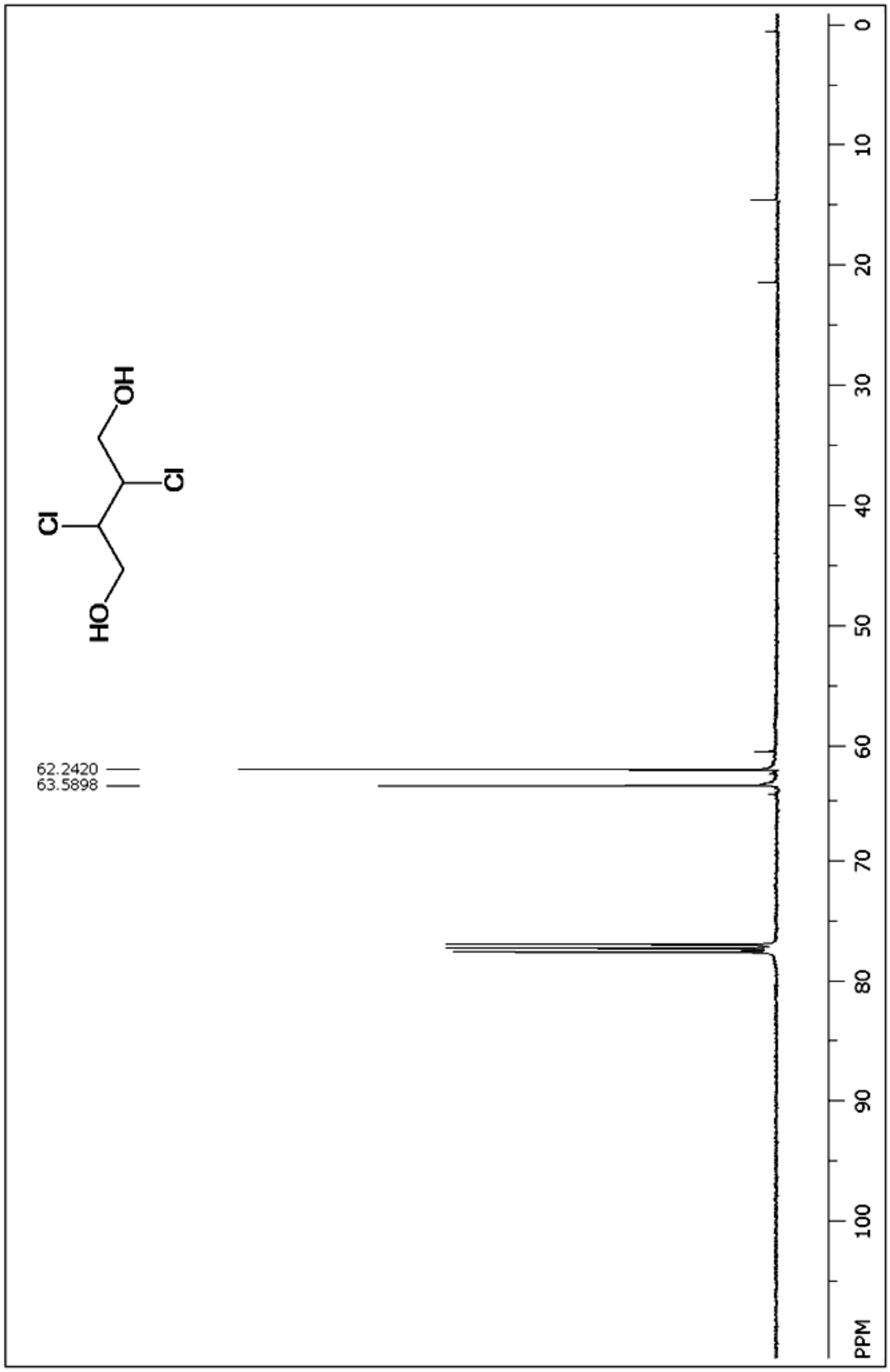

^{1}H NMR for 4,4'-[(2,3-dichlorobutane-1,4-diyl)bis(oxy)]bis(4-oxobutanoic acid)

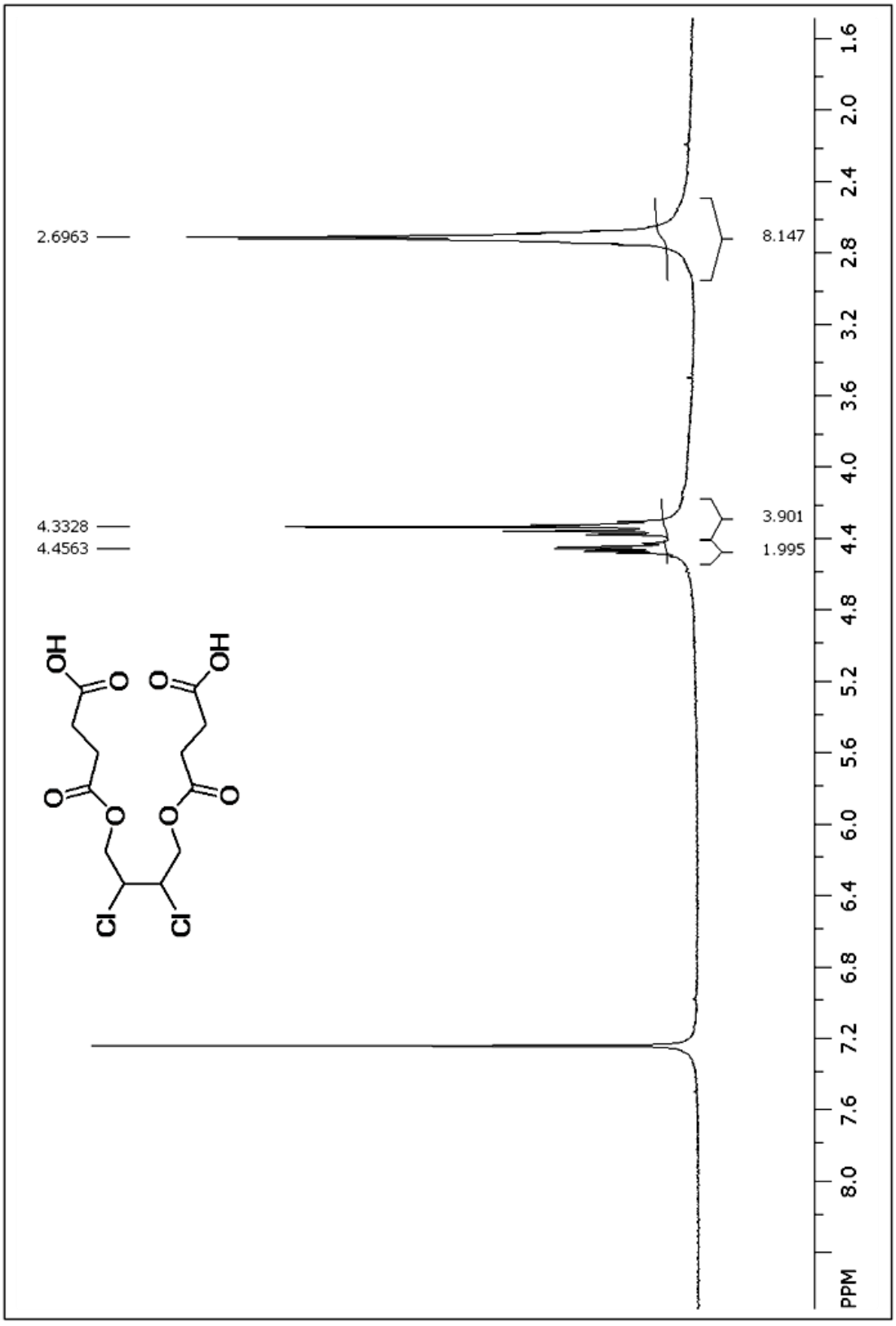

^{1}H NMR for High R_f dichloro-bis(methylbenzylamide) diastereomer

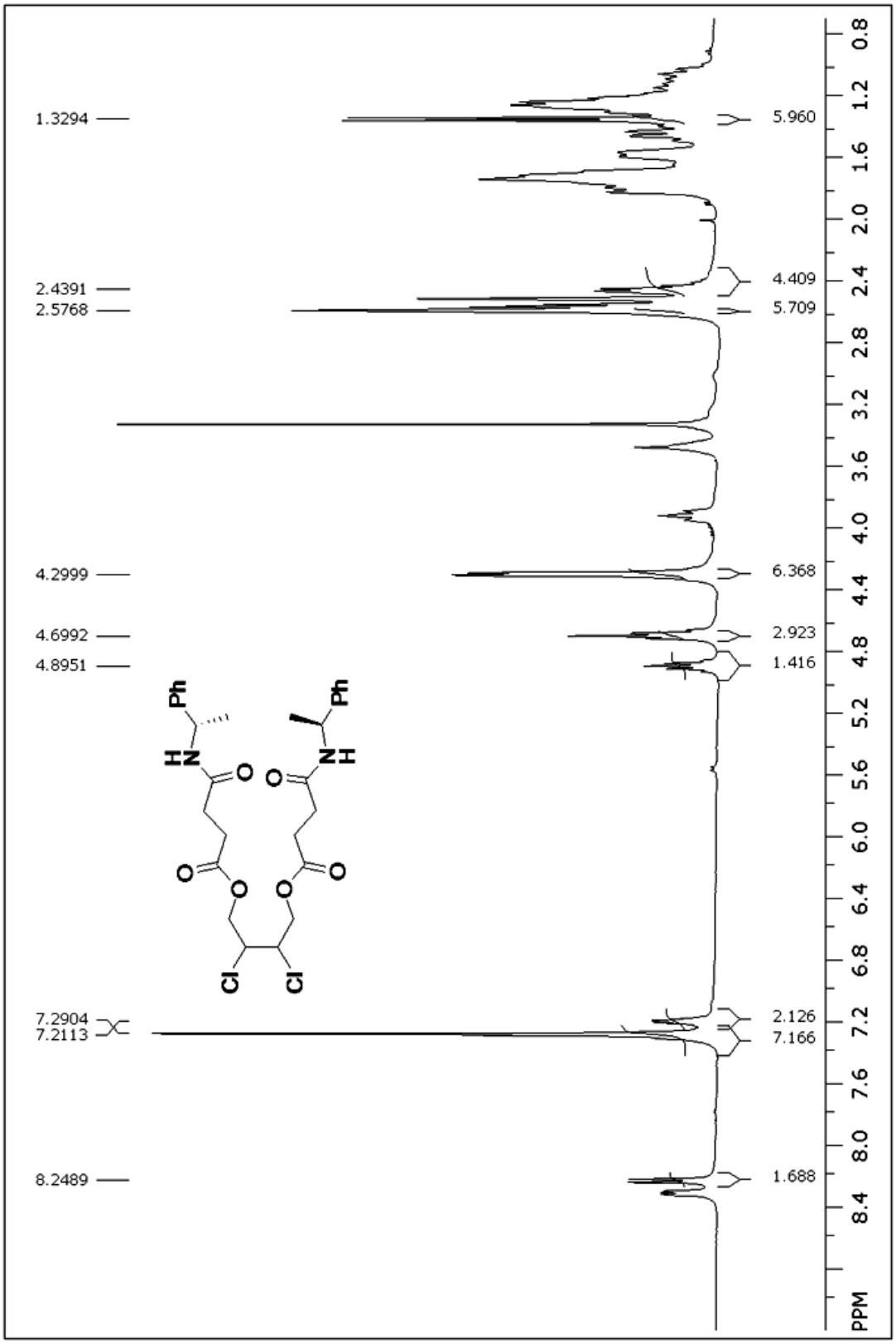

^{13}C NMR for High R_f dichloro-bis(methylbenzylamide) diastereomer

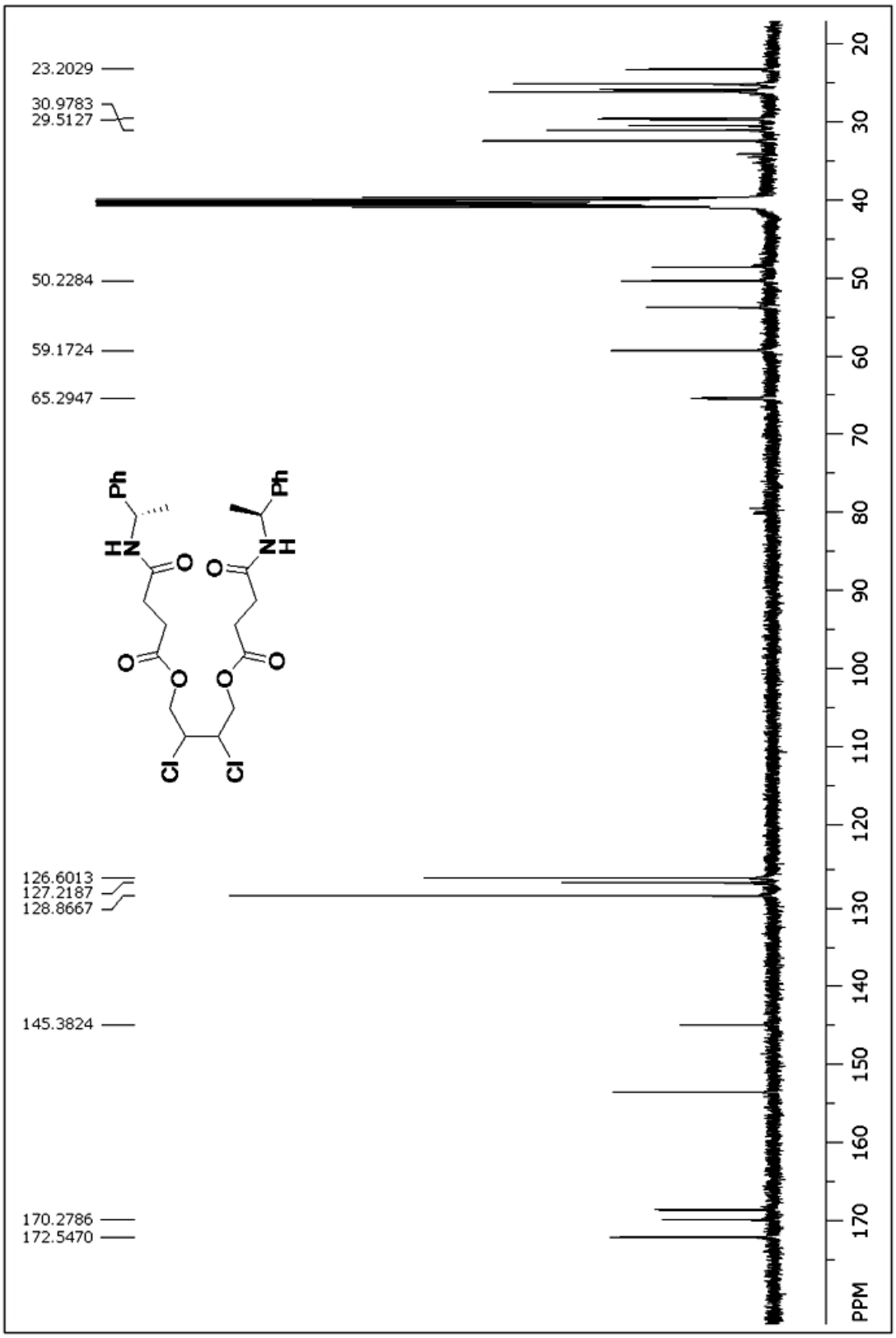

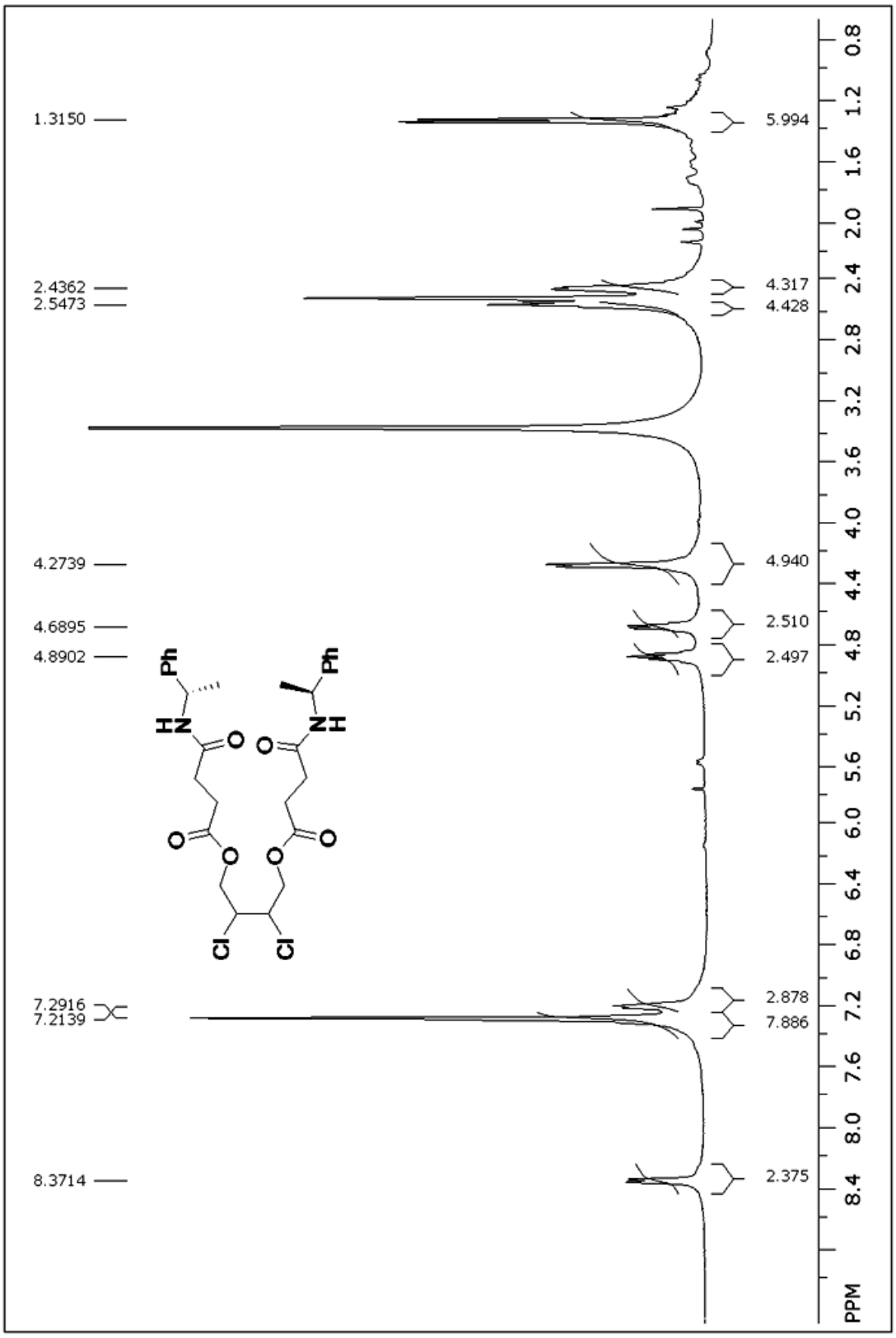

^{1}H NMR for Low R_f dichloro-bis(methylbenzylamide) diastereomer

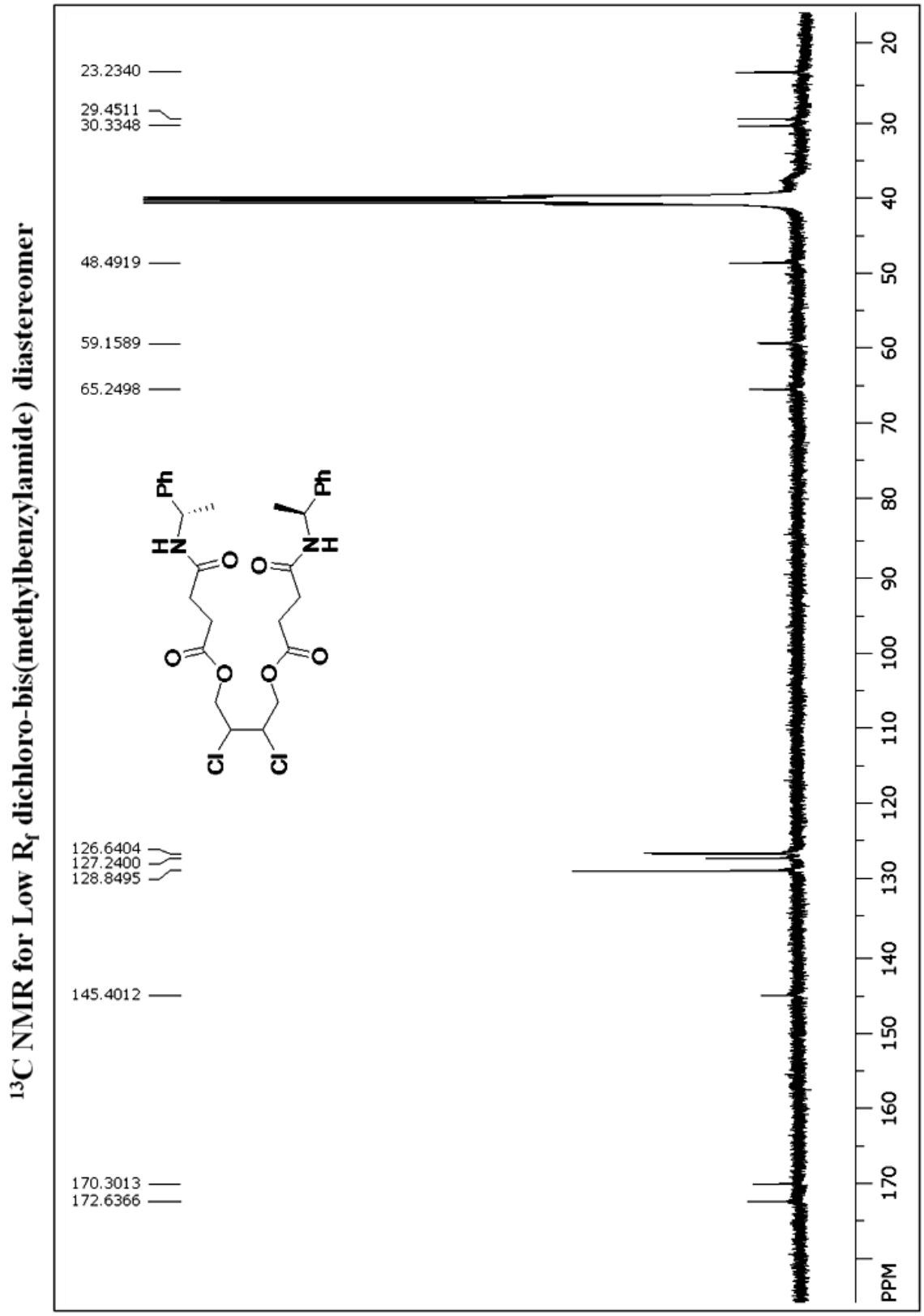

^{13}C NMR for Low R_f dichloro-bis(methylbenzylamide) diastereomer

^{1}H NMR for single enantiomer of 2,3-dichloro-1,4-butanediol

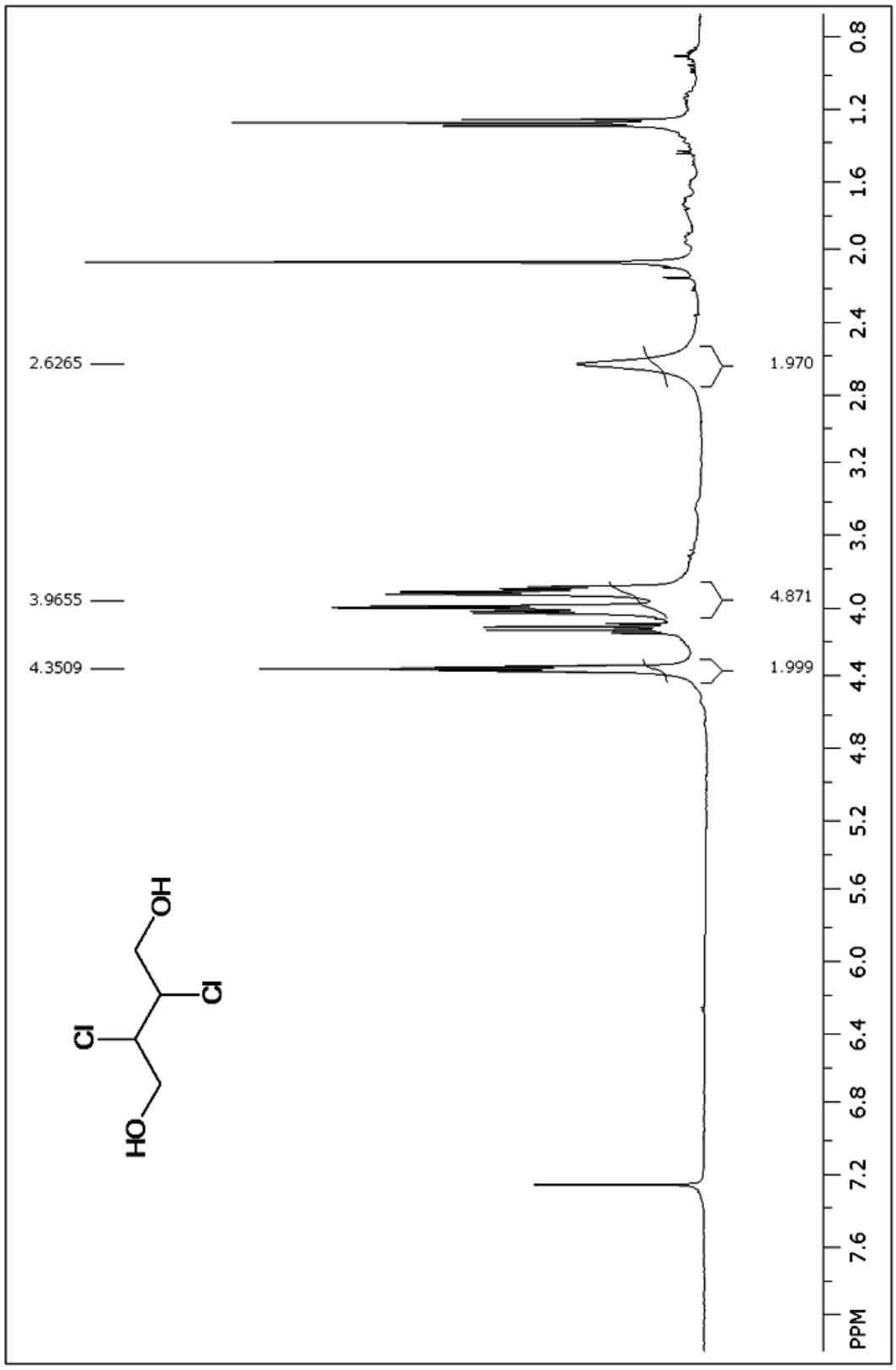

^{1}H NMR for 4,4'-[(2,3-dibromobutane-1,4-diyl)bis(oxy)]bis(4-oxobutanoic acid)

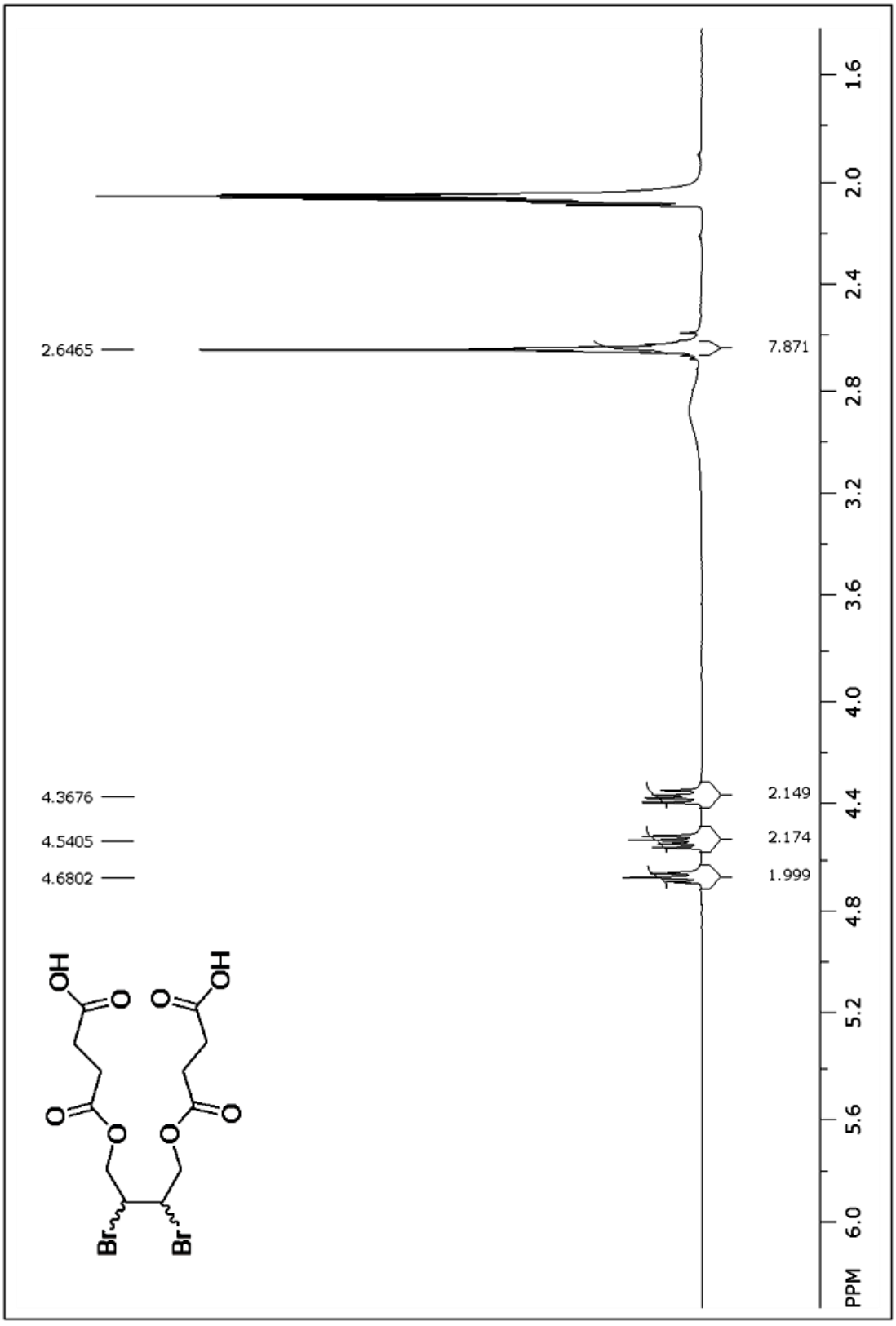

^{13}C NMR for 4,4'-[(2,3-dibromobutane-1,4-diyl)bis(oxy)]bis(4-oxobutanoic acid)

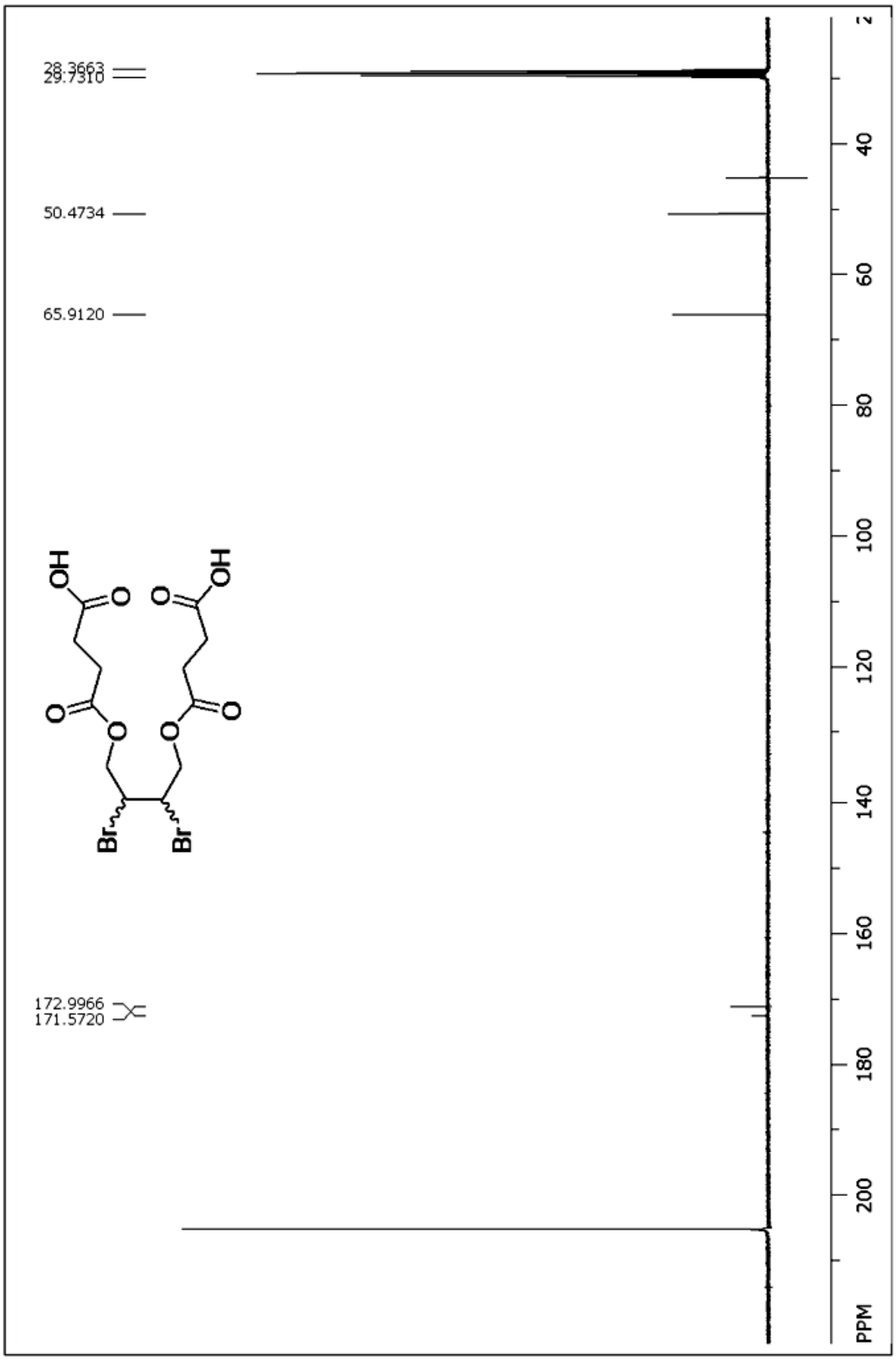

^{1}H NMR for High R_f Dibromo-bis(methylbenzylamide) diastereomer

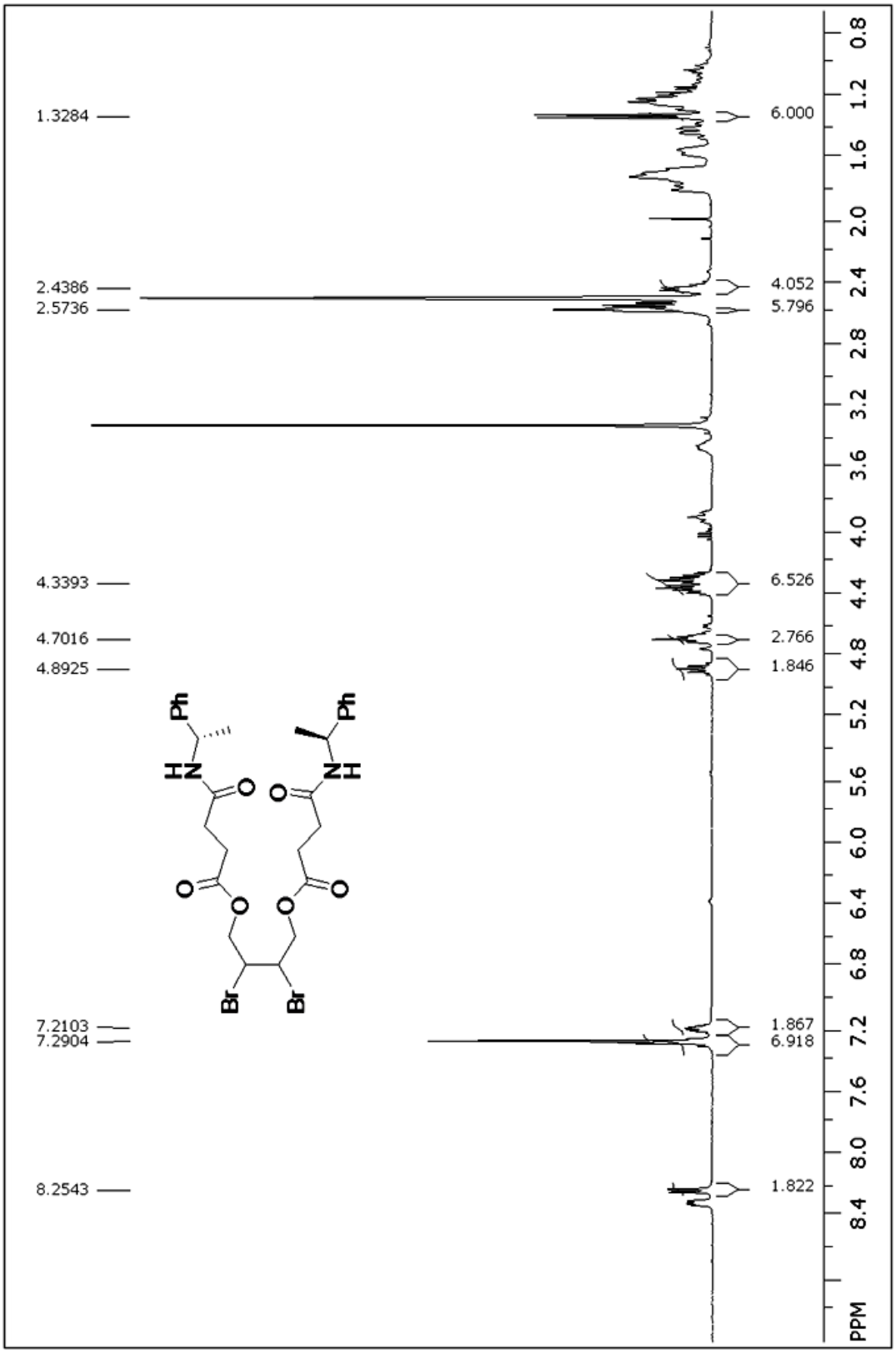

^{1}H NMR for Low R_f Dibromo-bis(methylbenzylamide) diastereomer

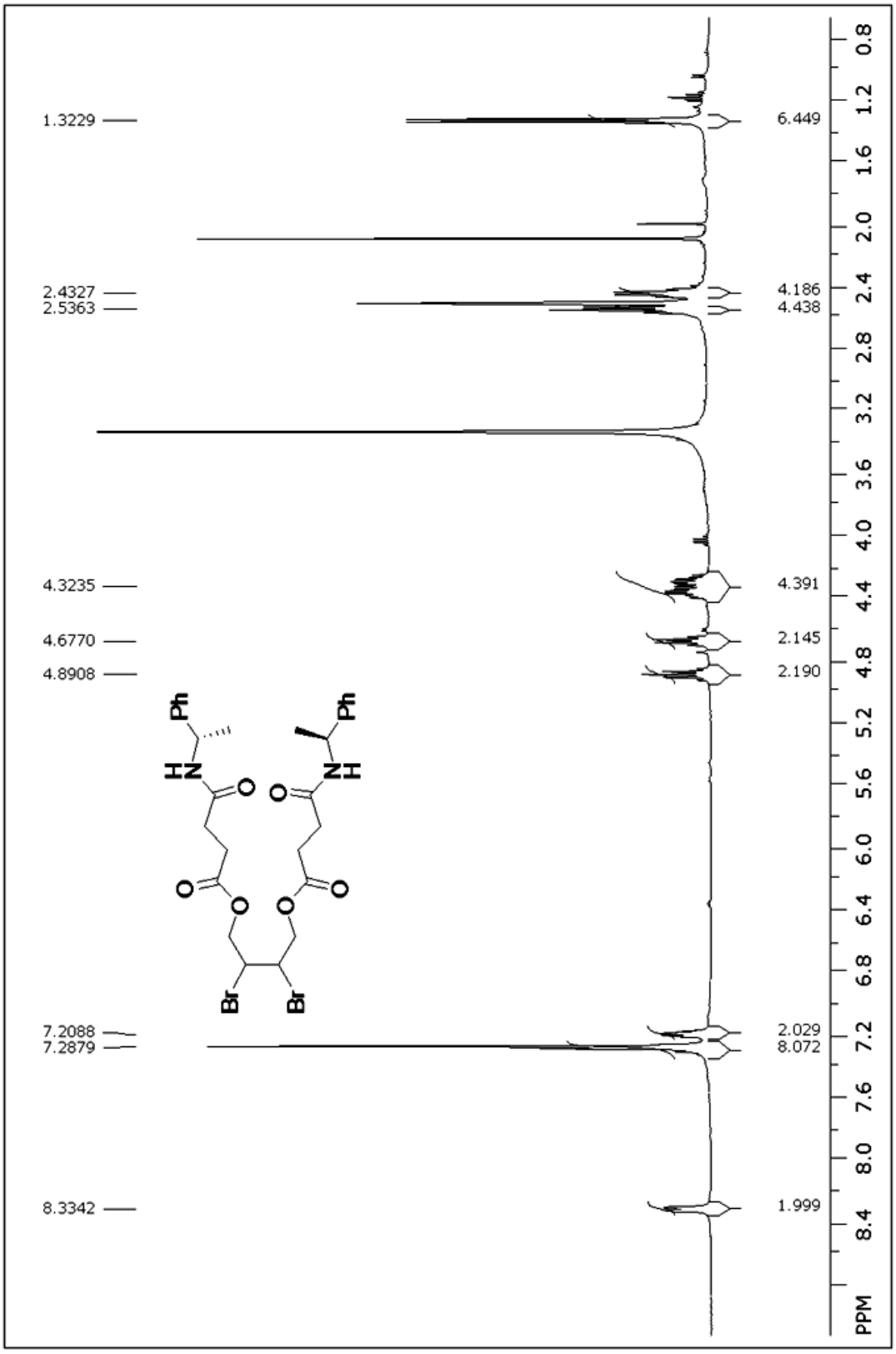

^{1}H NMR for 2,3-dideuterio-1,4-butanediol

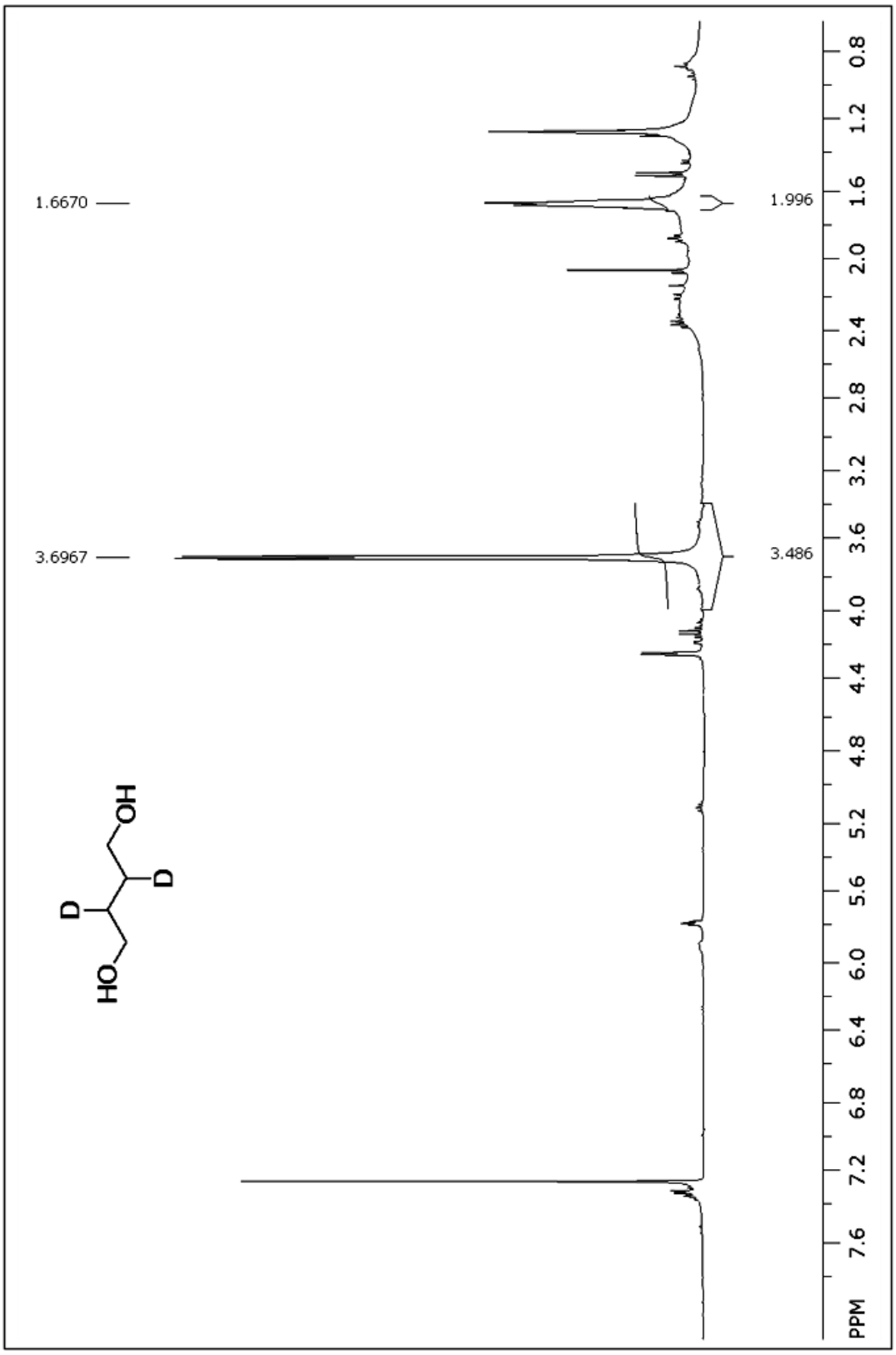

^{1}H NMR for (2*R*,3*S*)-dimethyl-2-acetoxy-3-bromosuccinate

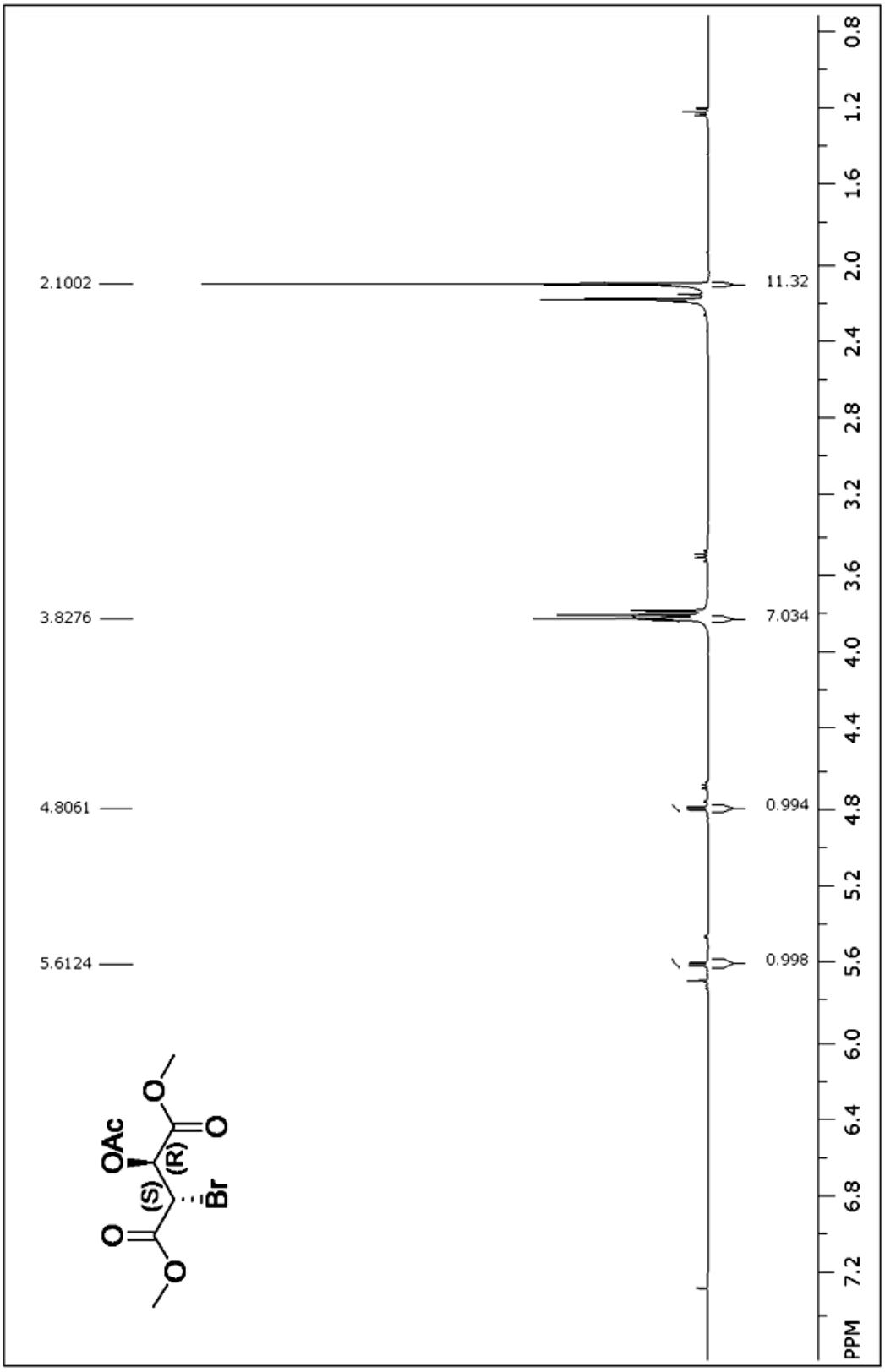

^{13}C NMR for (2*R*,3*S*)-dimethyl-2-acetoxy-3-bromosuccinate

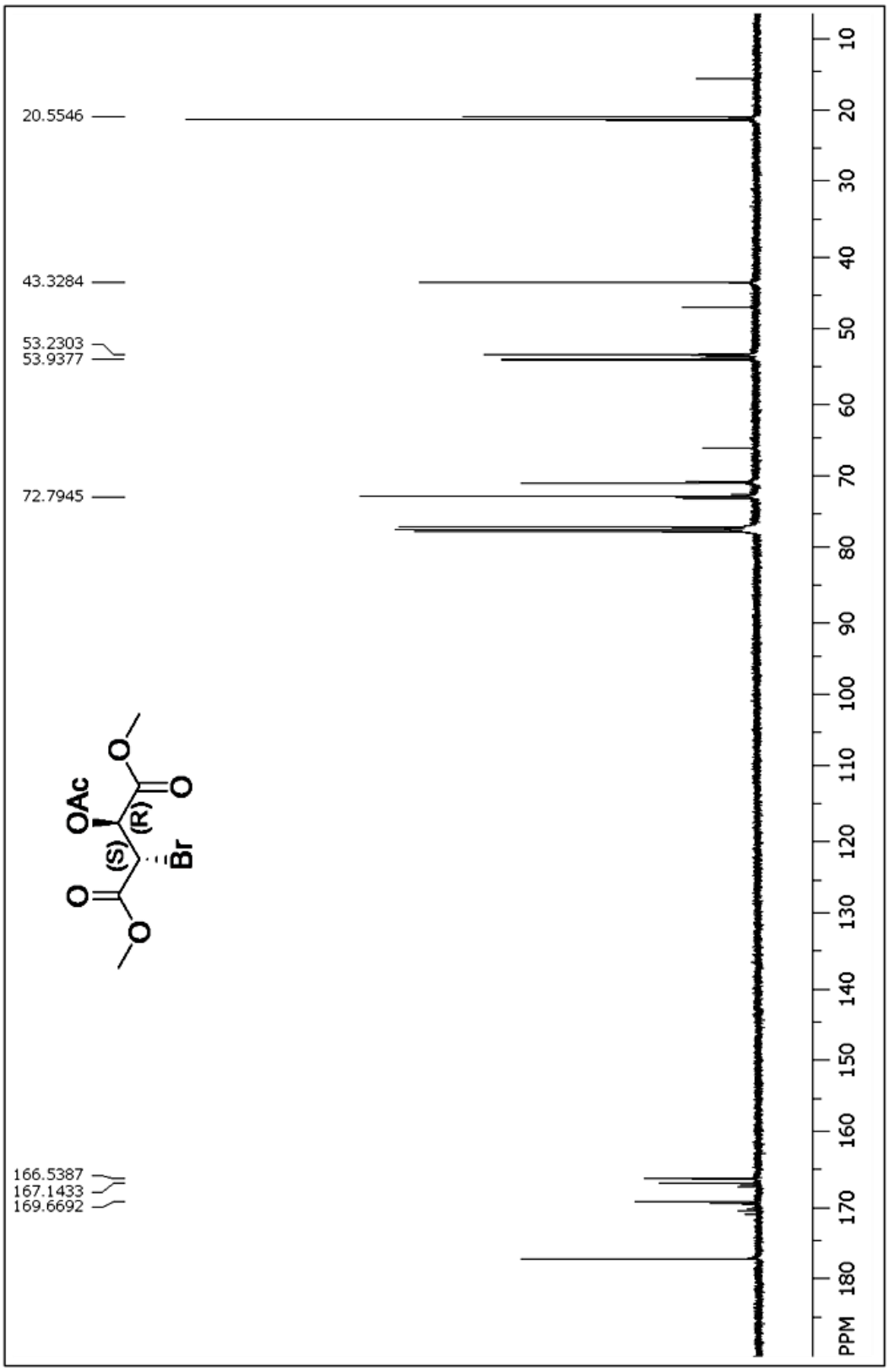

^{1}H NMR for (2*S*,3*R*)-dimethyl-2-bromo-3-hydroxysuccinate

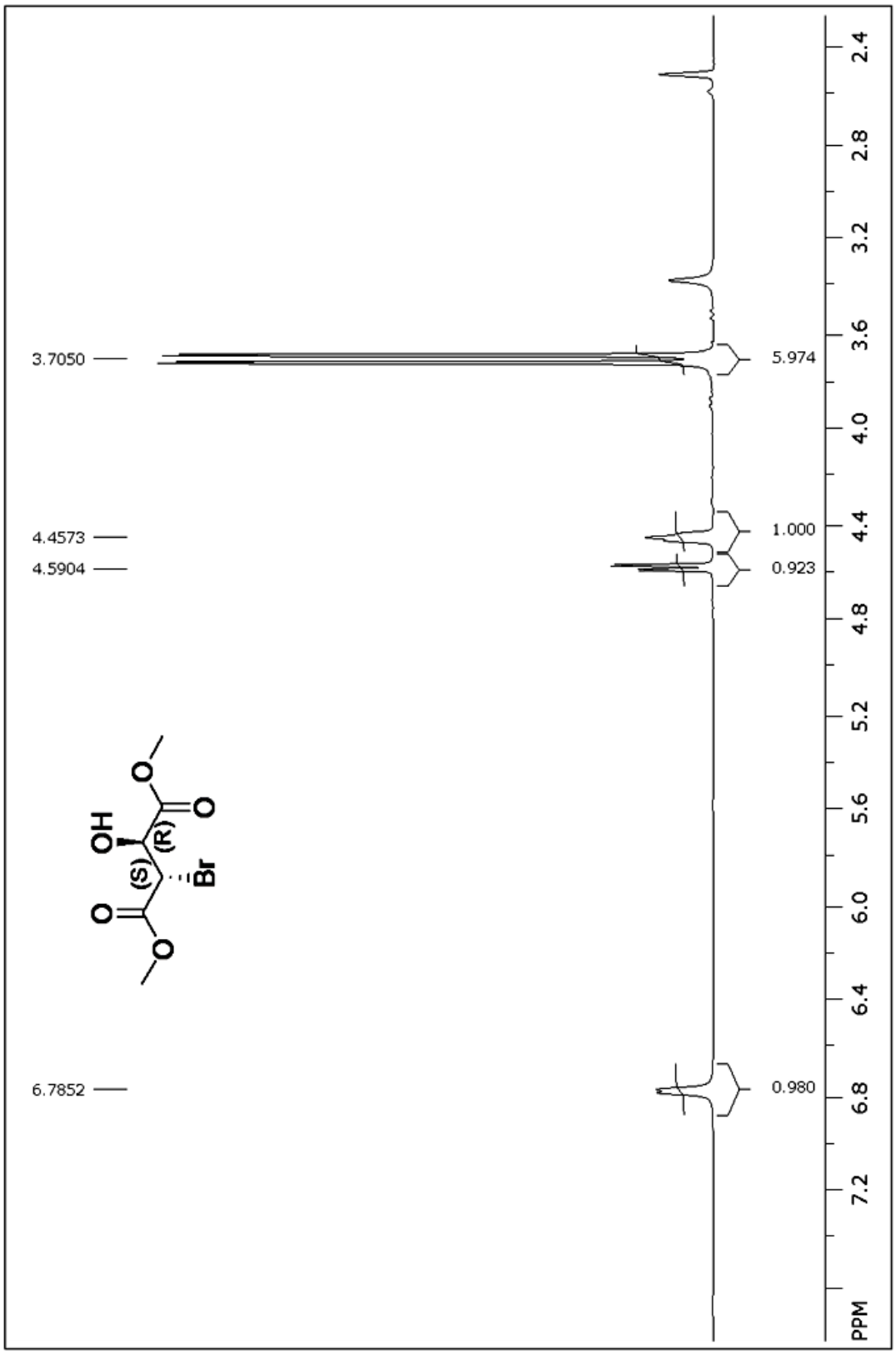

^{13}C NMR for (2*S*,3*R*)-dimethyl-2-bromo-3-hydroxysuccinate

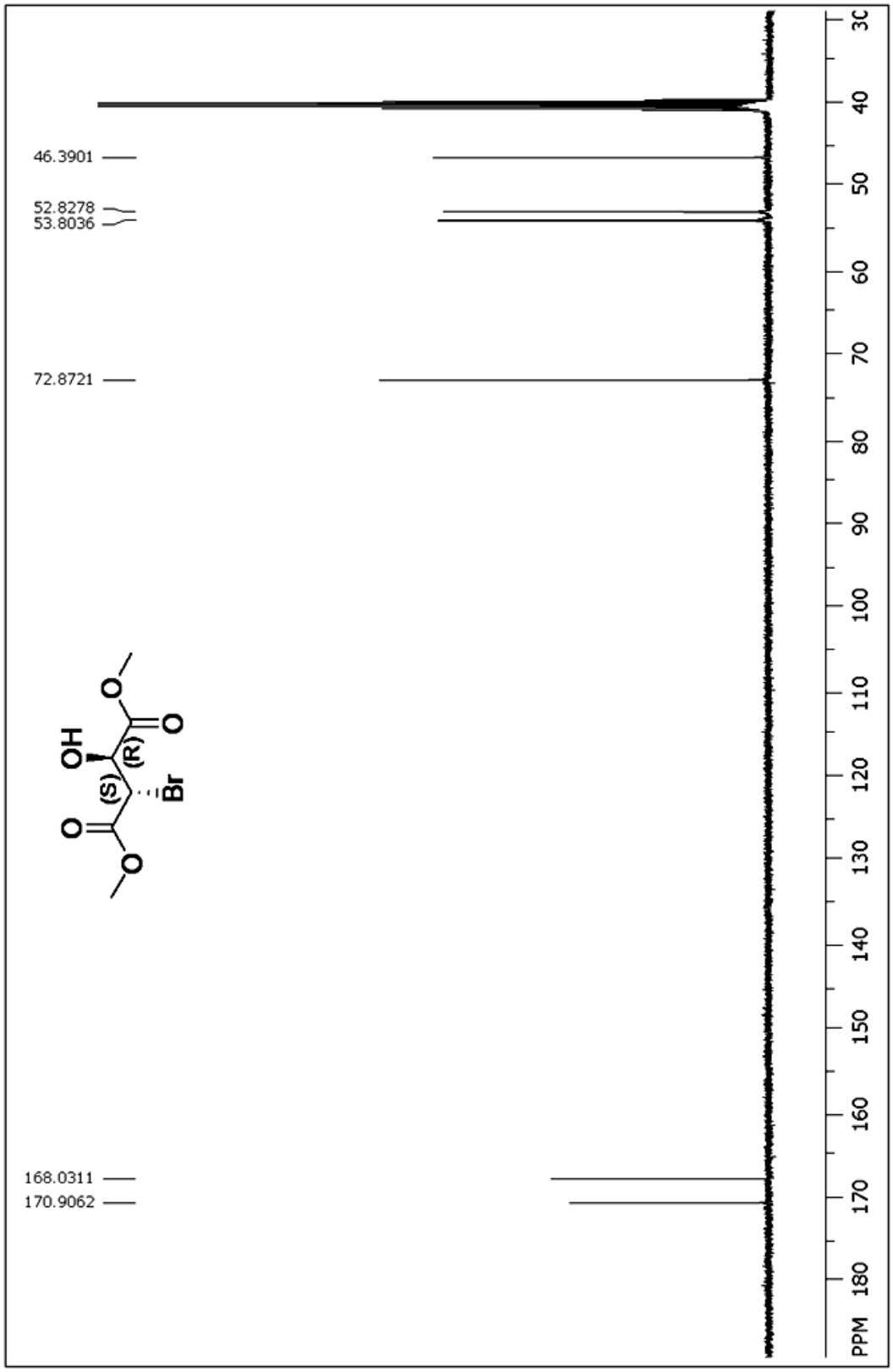

^{1}H NMR for (2*R*,3*R*)-dimethyl oxirane-2,3-dicarboxylate

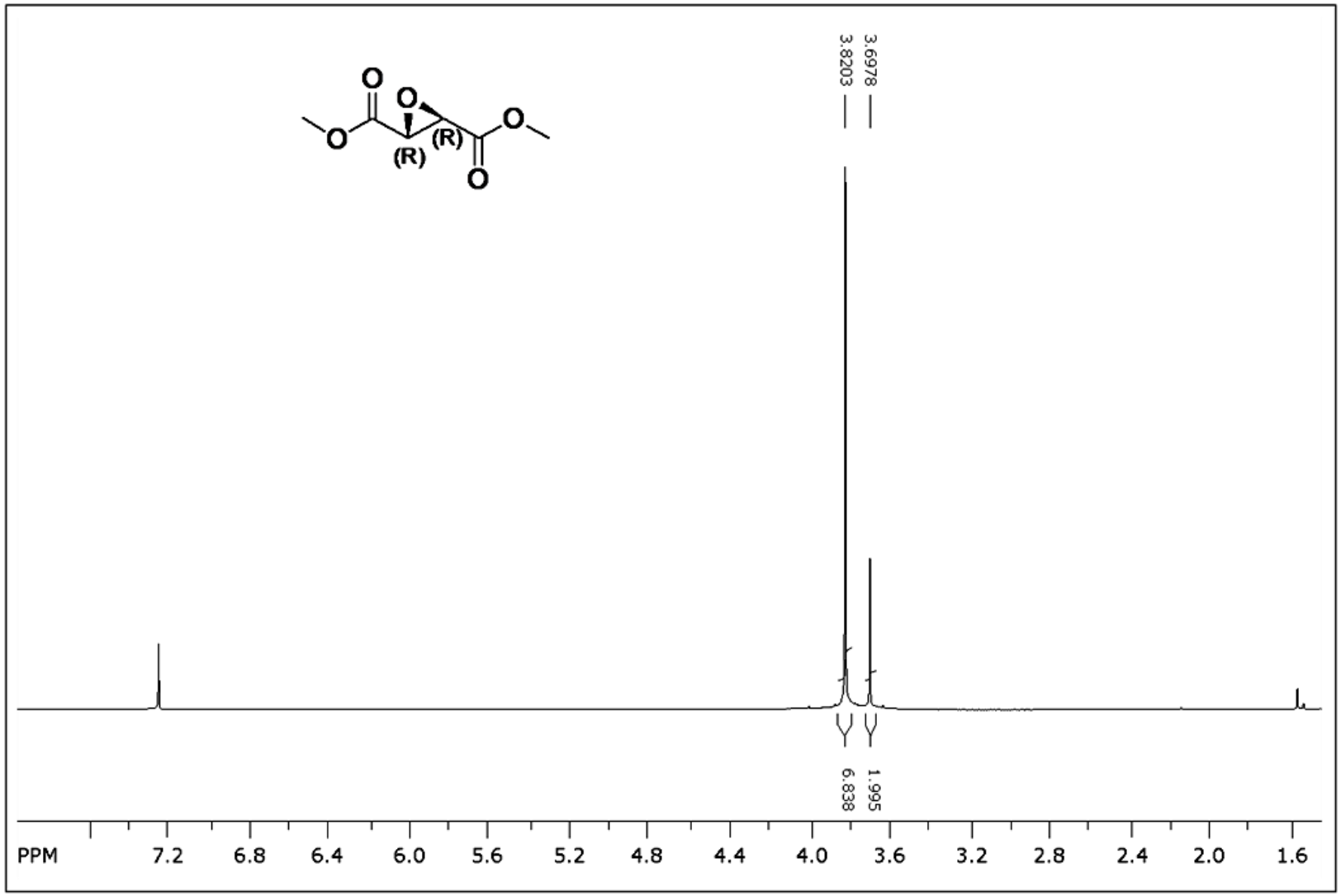

^{13}C NMR for (2*R*,3*R*)-dimethyl oxirane-2,3-dicarboxylate

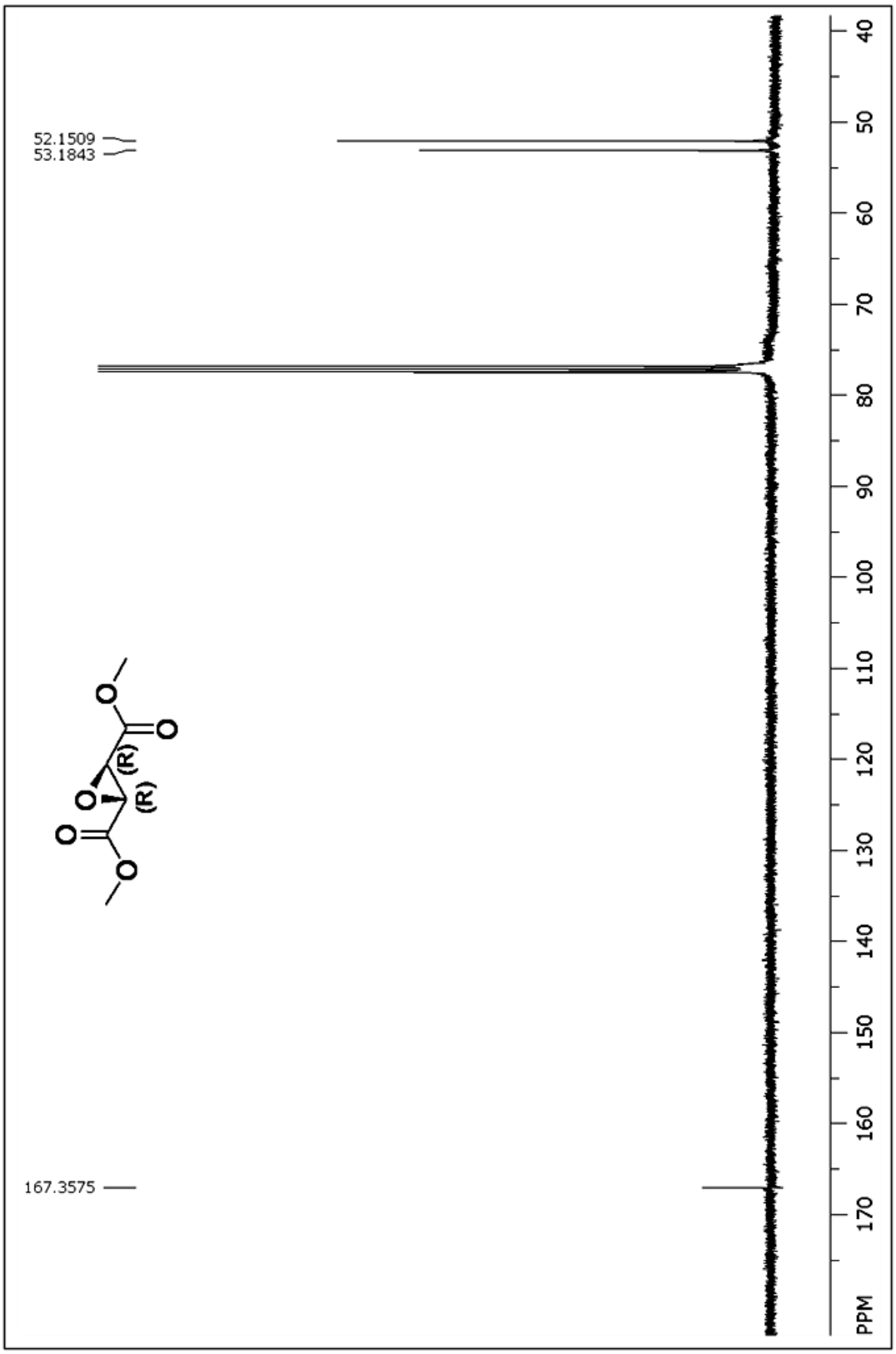

^{1}H NMR for 1,6-Hexanediol-1,1,6,6-d_4

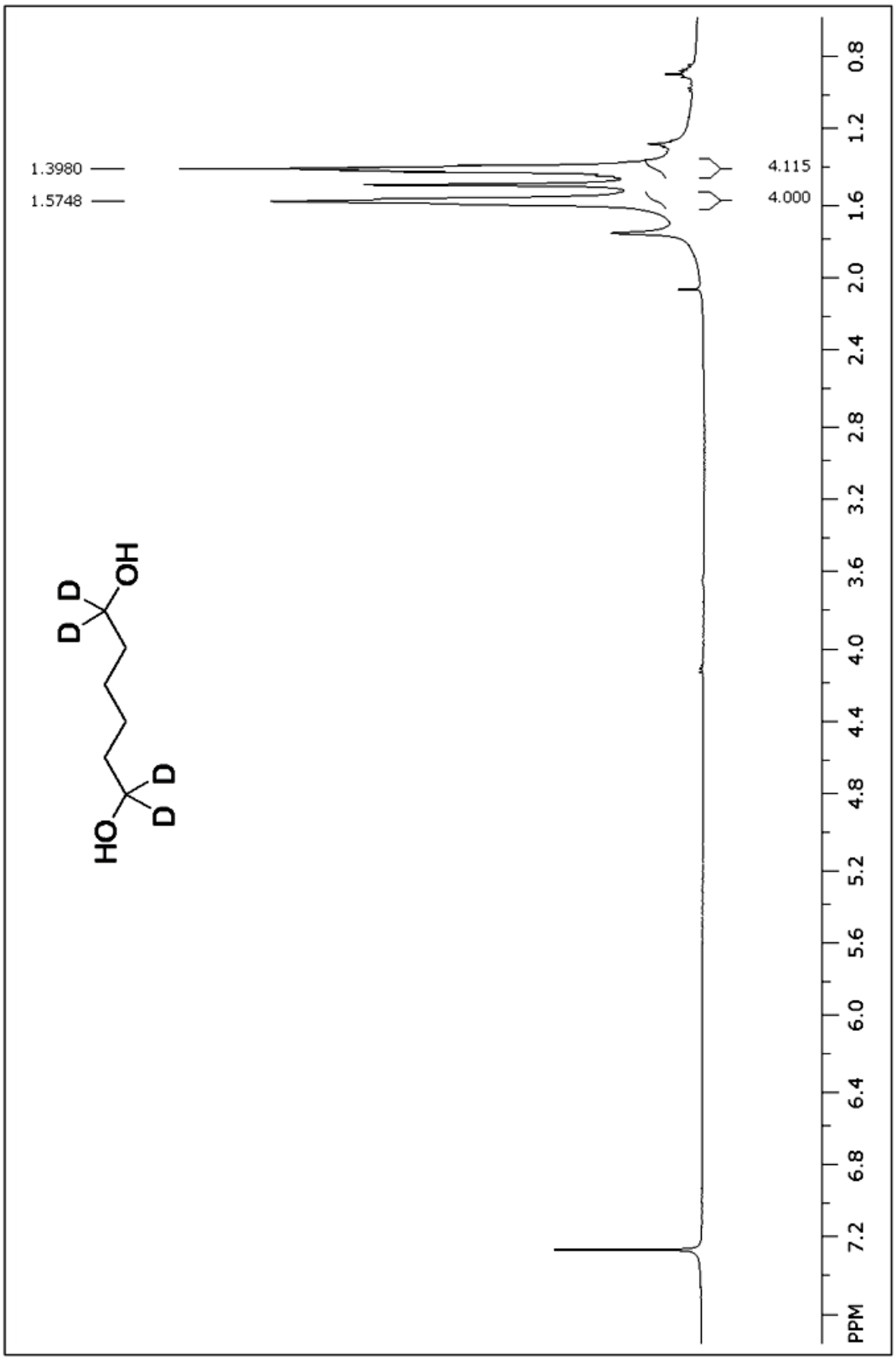

^{1}H NMR for 1,6-Dibromohexane-1,1,6,6-d$_4$

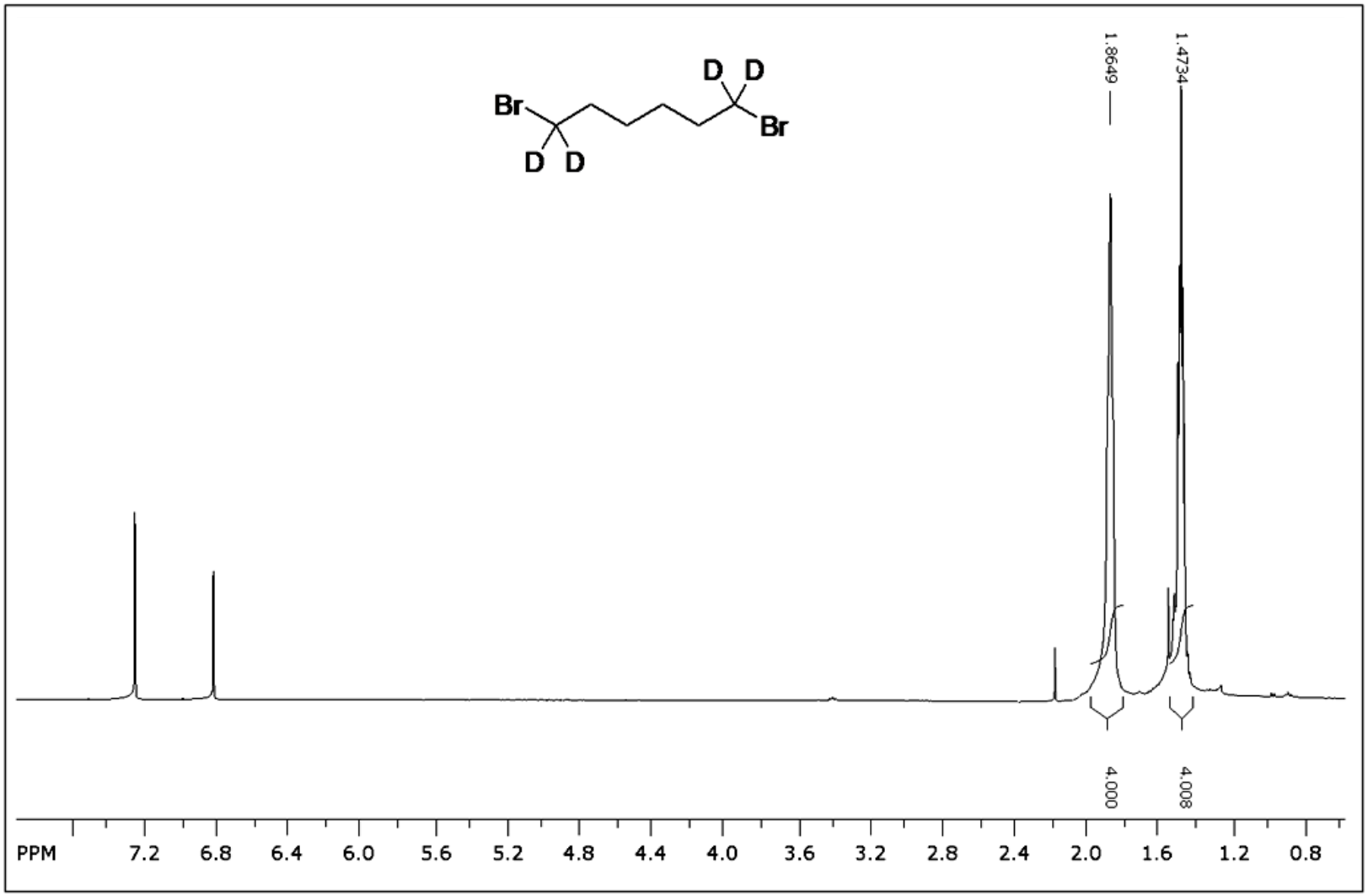

^{1}H NMR for 1,6-Dicyanohexane-1,1,6,6-d$_4$

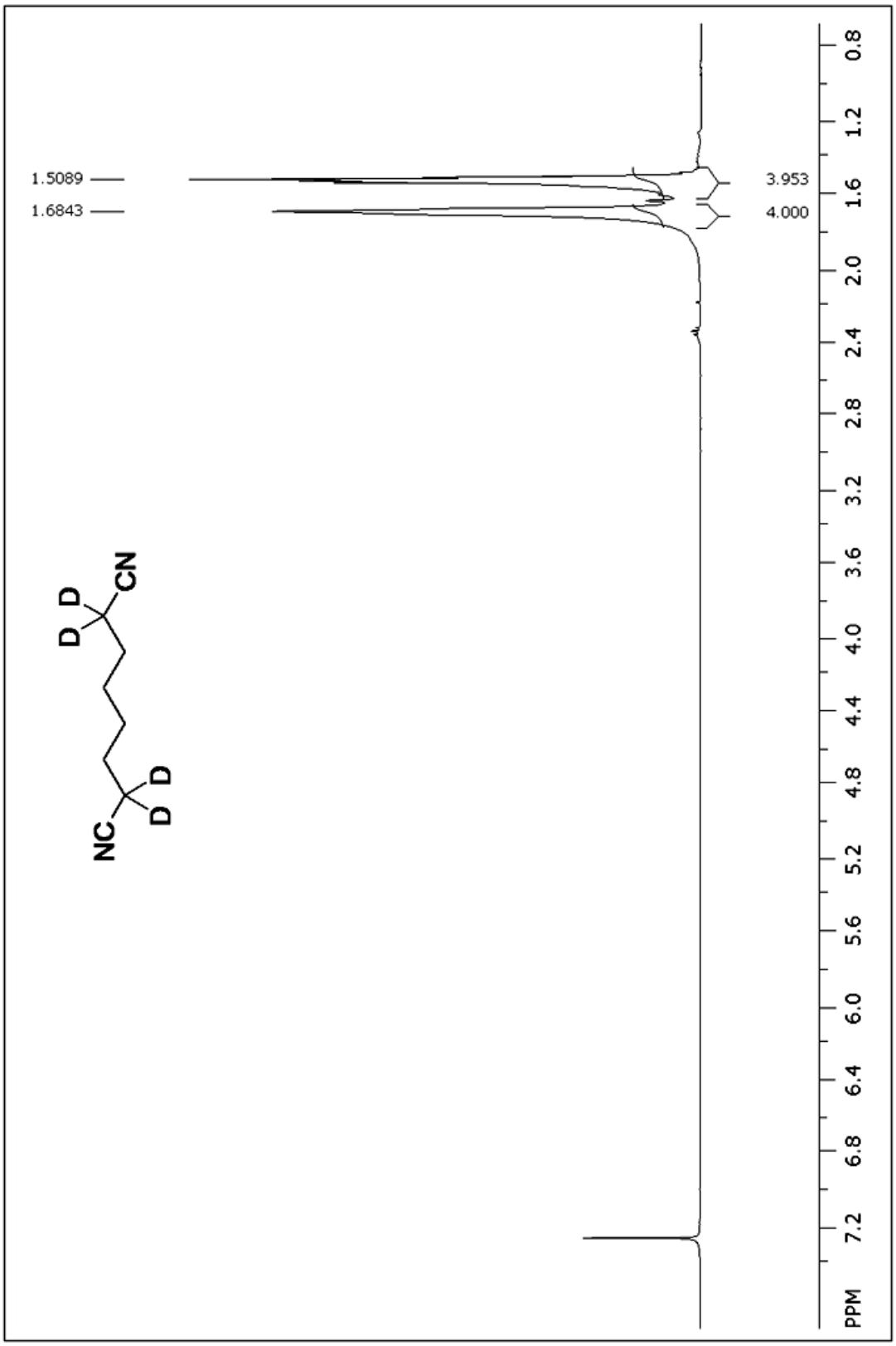

^{13}C NMR for 1,6-Dicyanohexane-1,1,6,6-d_4

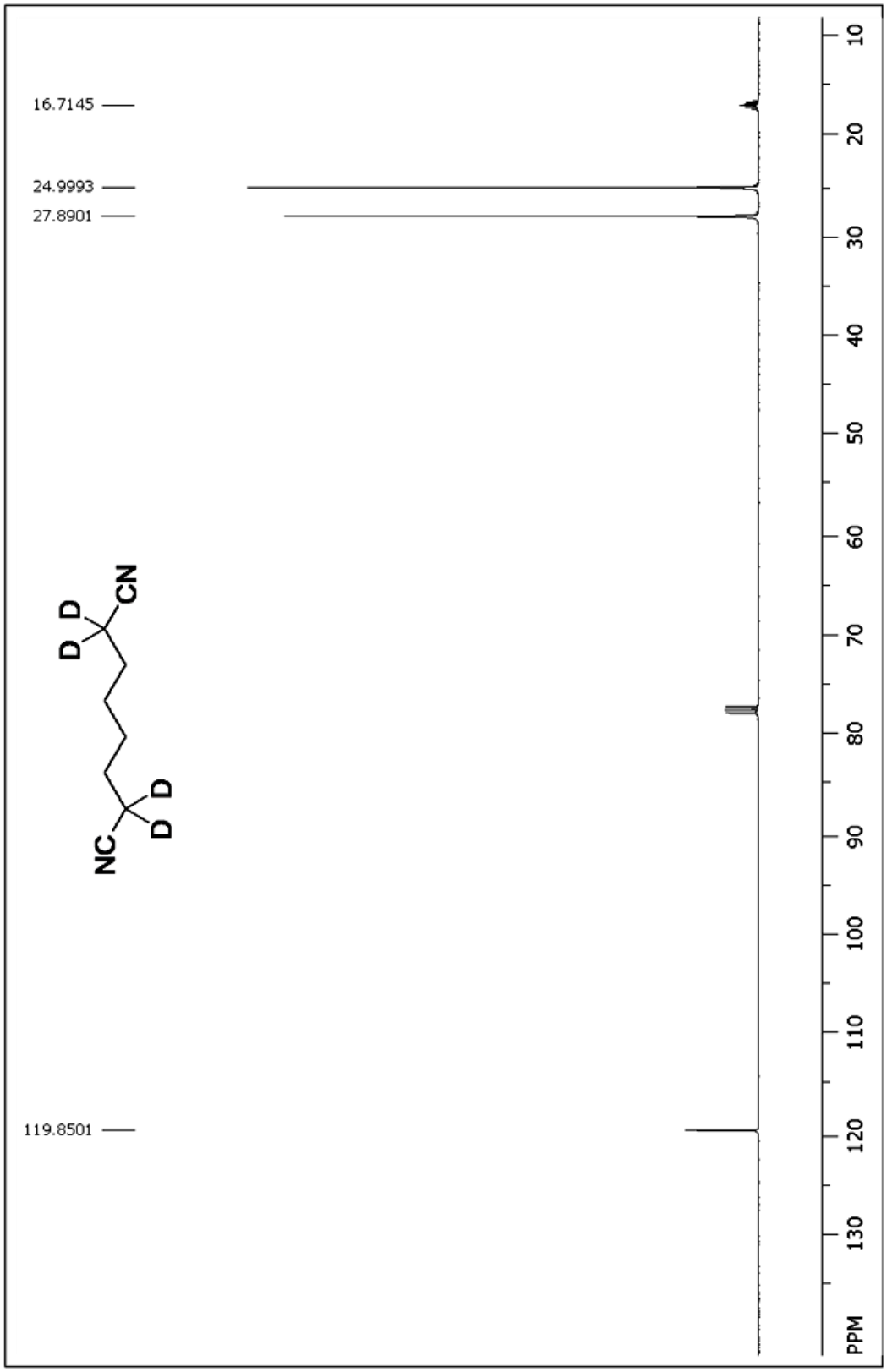

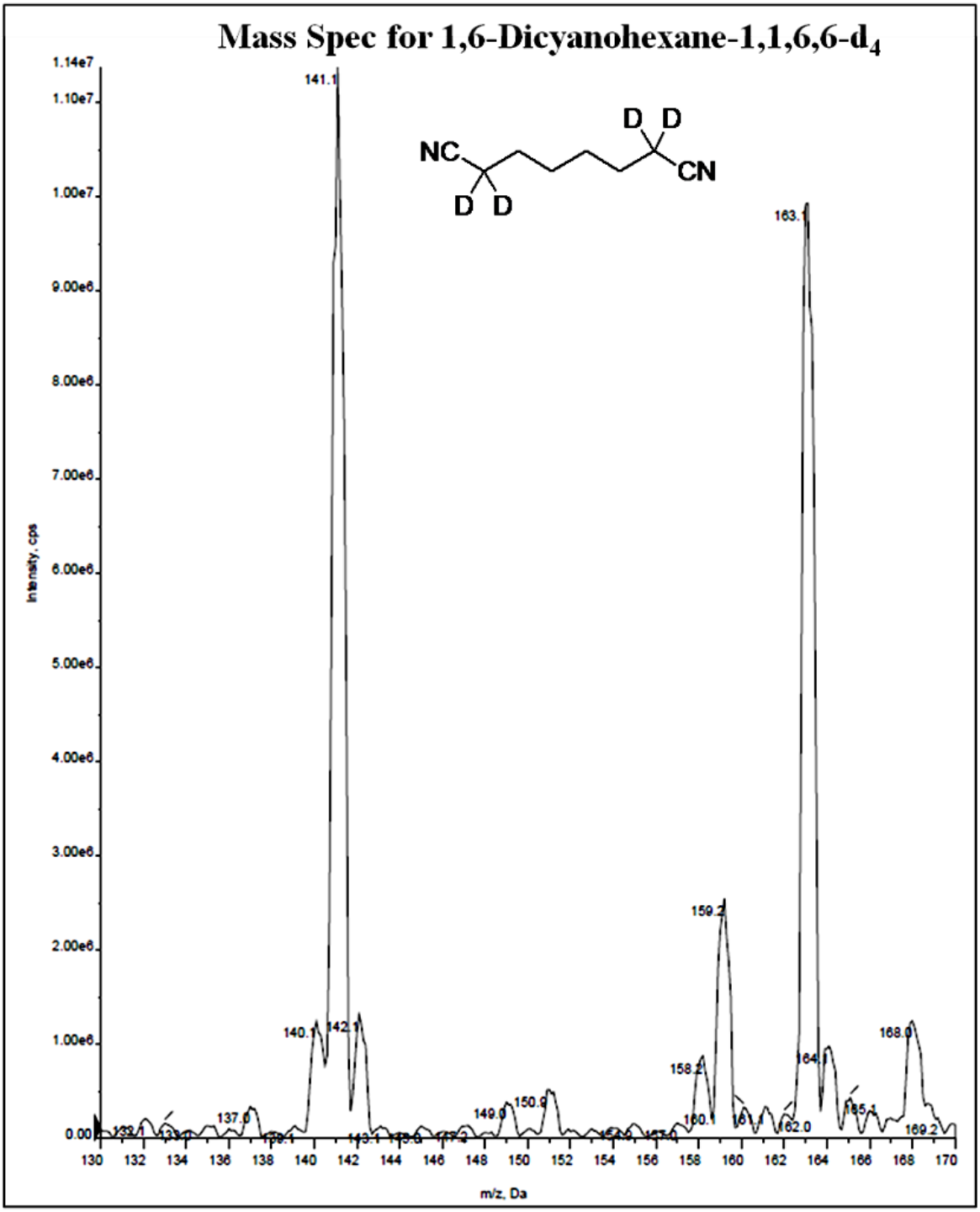
Mass Spec for 1,6-Dicyanohexane-1,1,6,6-d4
NC
D D
D D
CN
Intensity, cps
m/z, Da
141.1
163.1
159.2
140.1
142.1
158.2
168.0
164.1
149.0
150.9
137.0
160.1
162.0
169.2

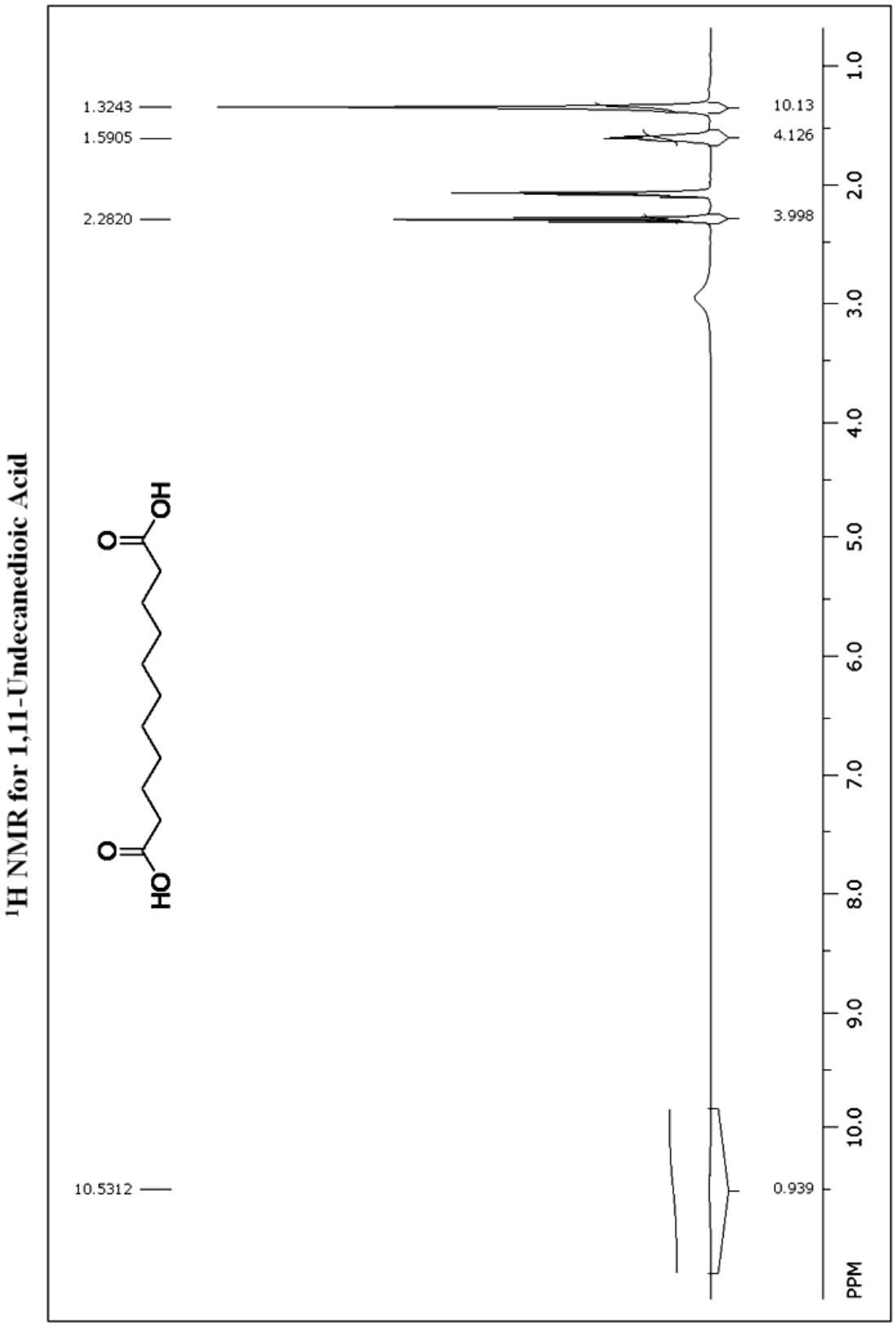

^{1}H NMR for 1,11-Undecanedioic Acid

^{1}H NMR for ethyl (2-methyl-1,3-dioxolan-2-yl) acetate

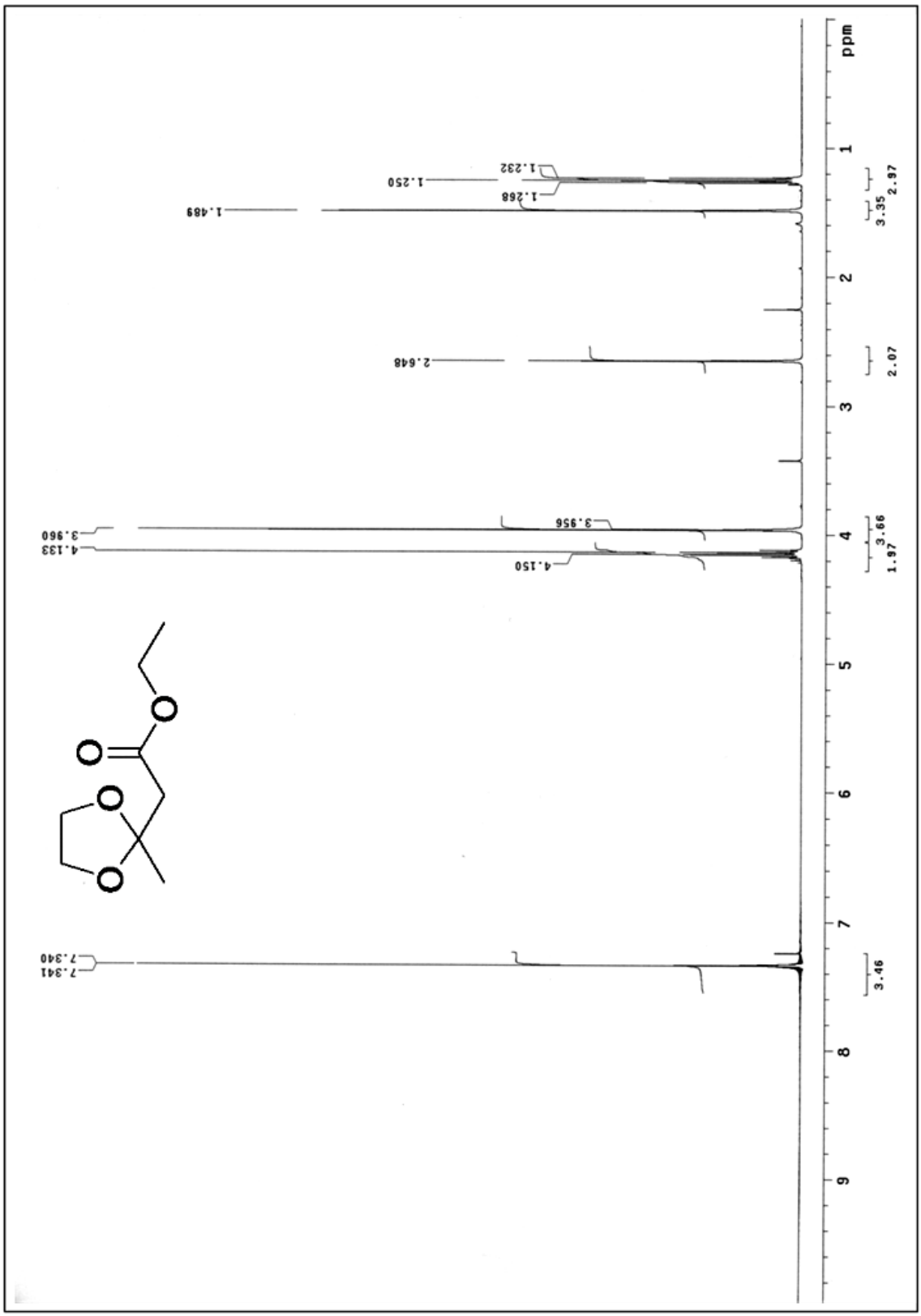

^{1}H NMR for 2-(2-methyl-1,3-dioxolan-2-yl) ethanol

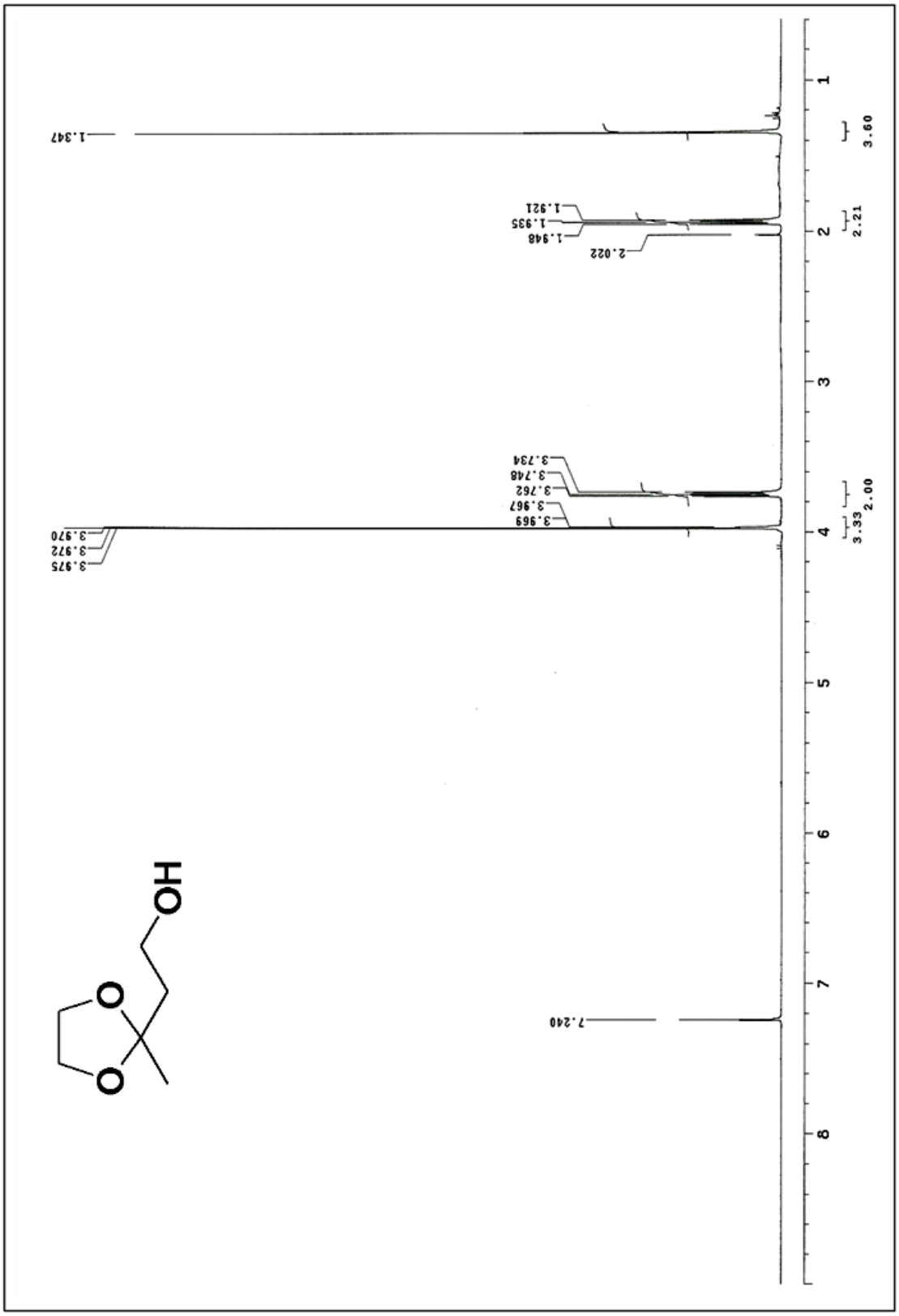

^{13}C NMR for 2-(2-methyl-1,3-dioxolan-2-yl) ethanol

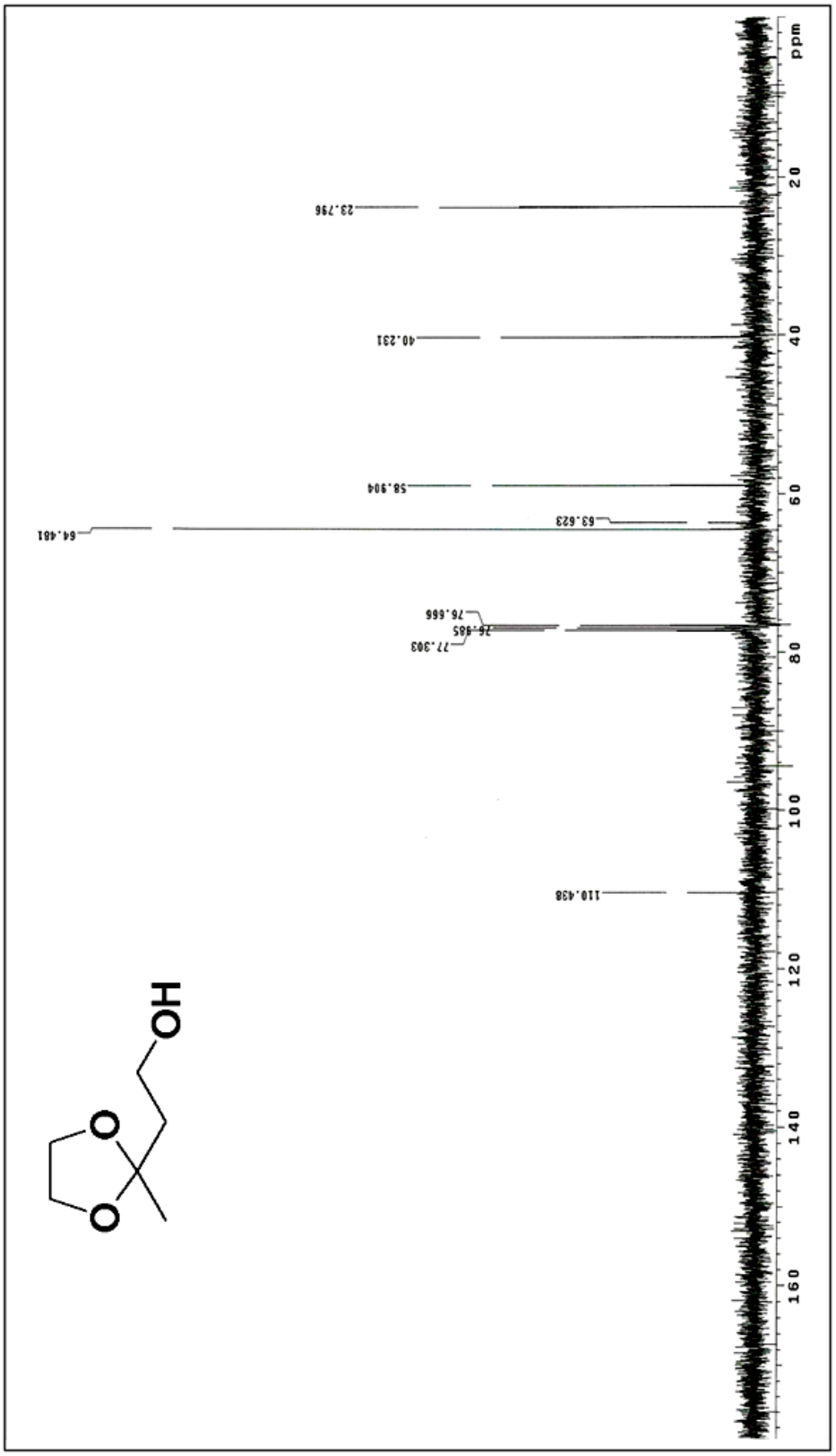

^{1}H NMR for Butane-1,4-diyl bis[(2-methyl-1,3-dioxolan-2-yl)acetate]

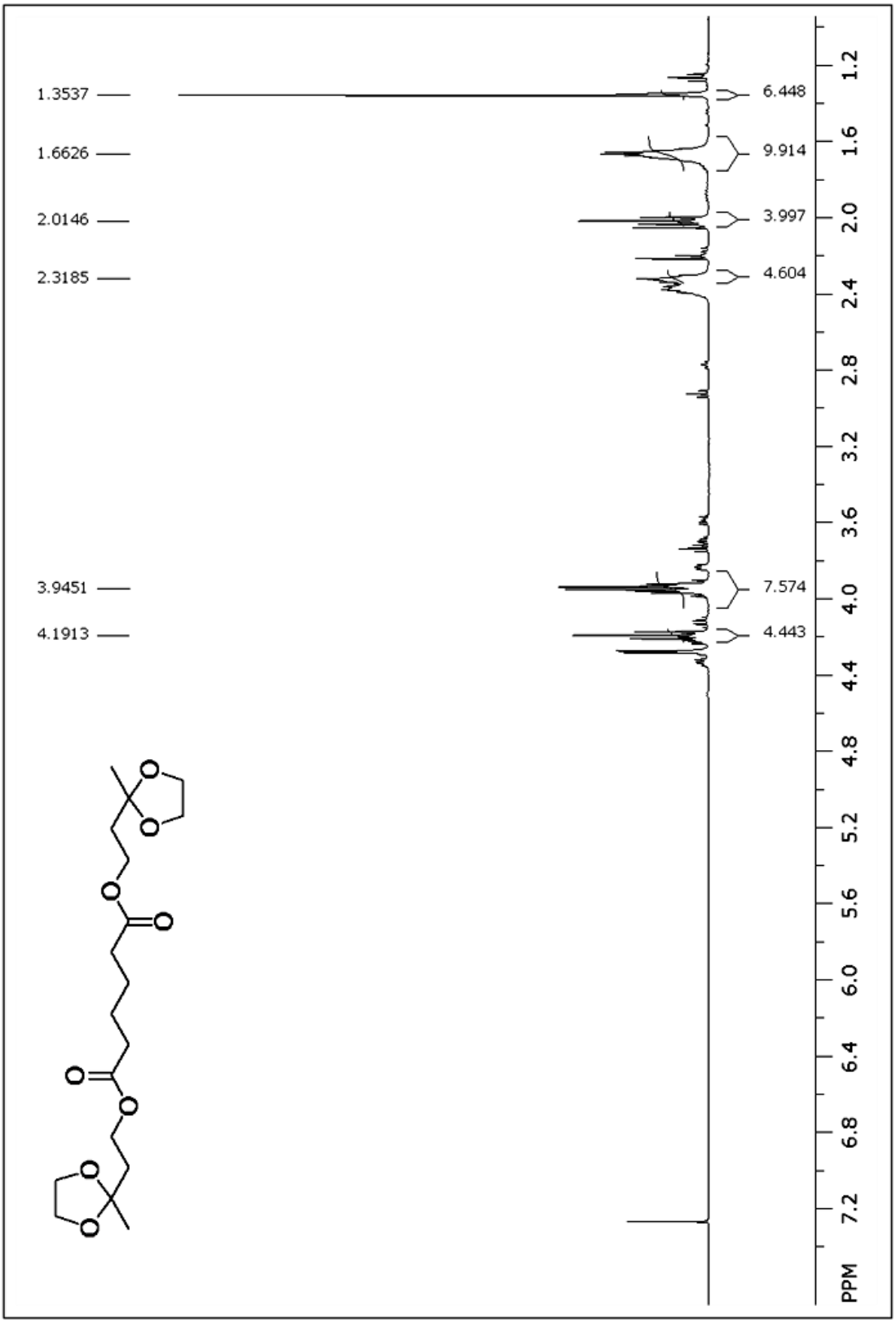

^{1}H NMR for Bis(3-oxobutyl) adipate

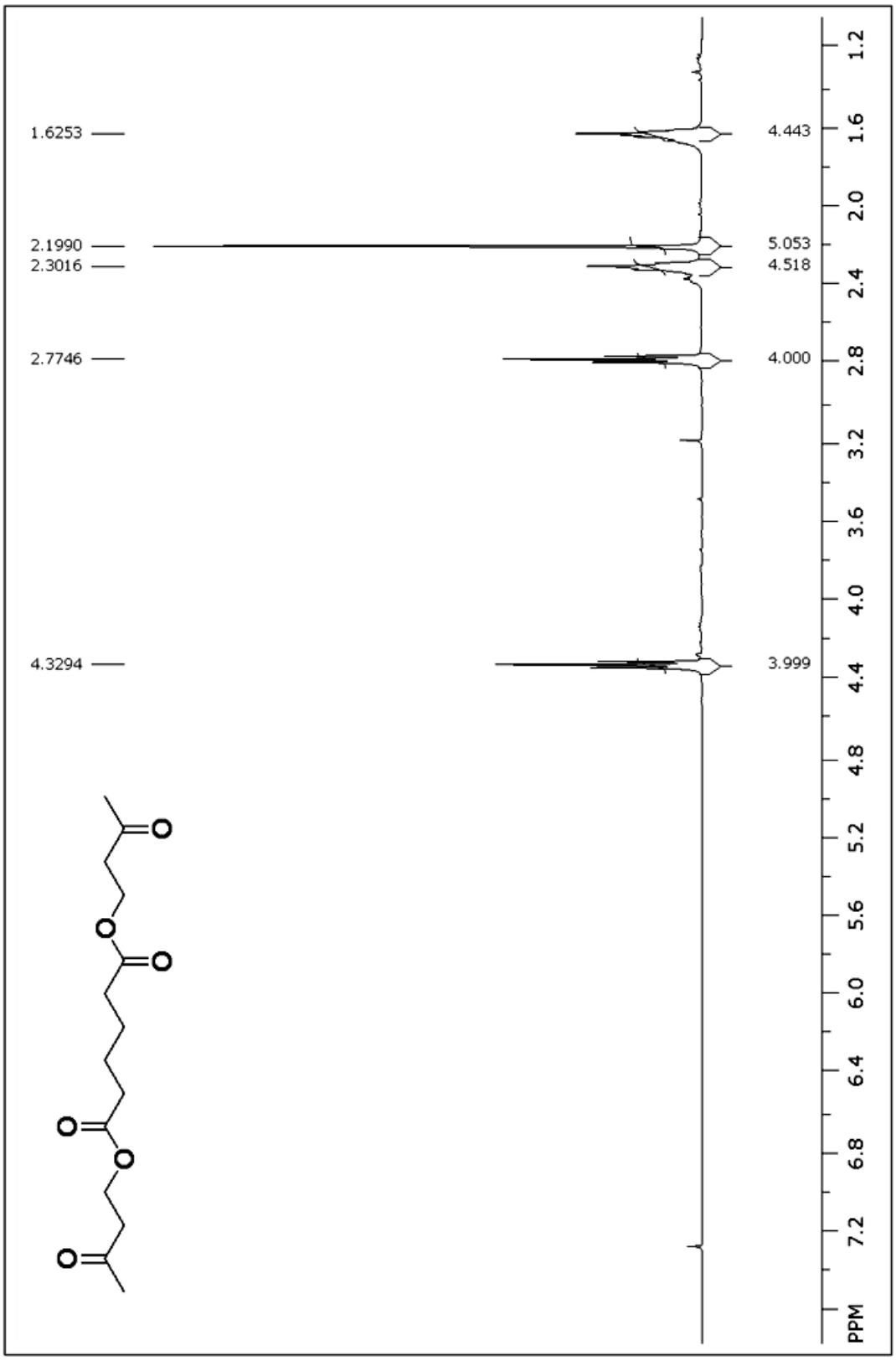

^{1}H NMR for 2,16-Heptadecanedione

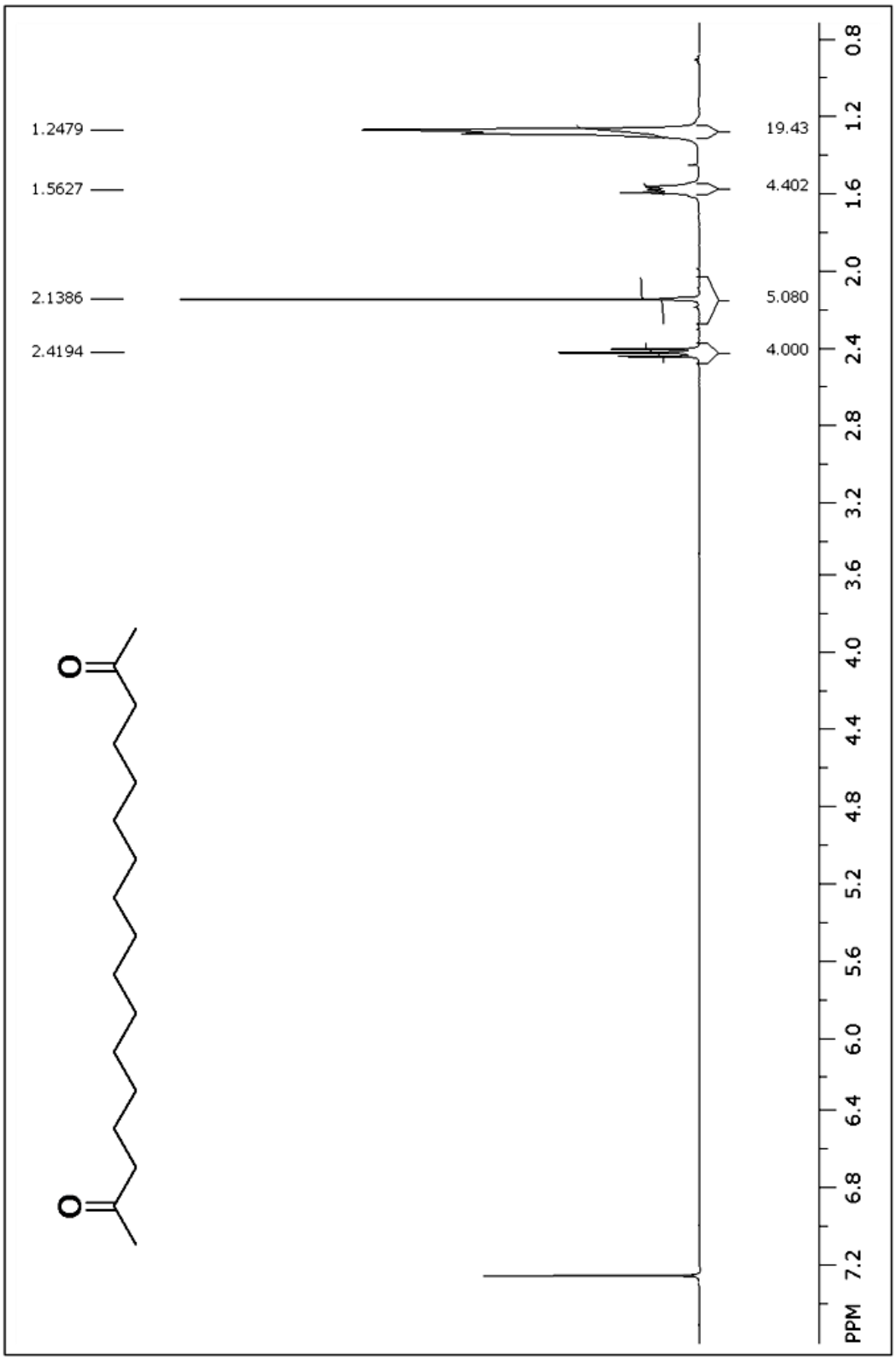

^{13}C NMR for 2,16-Heptadecanedione

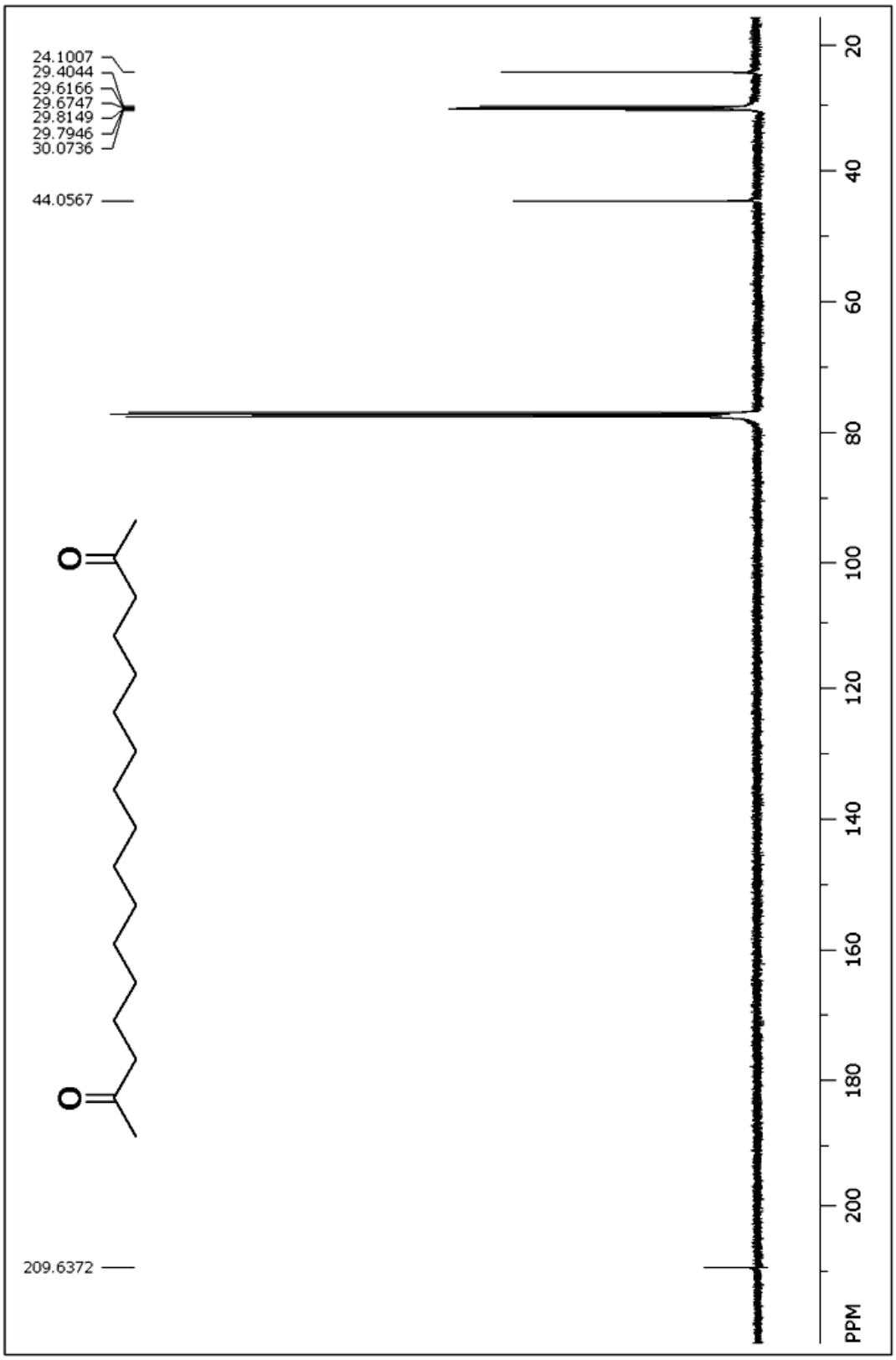

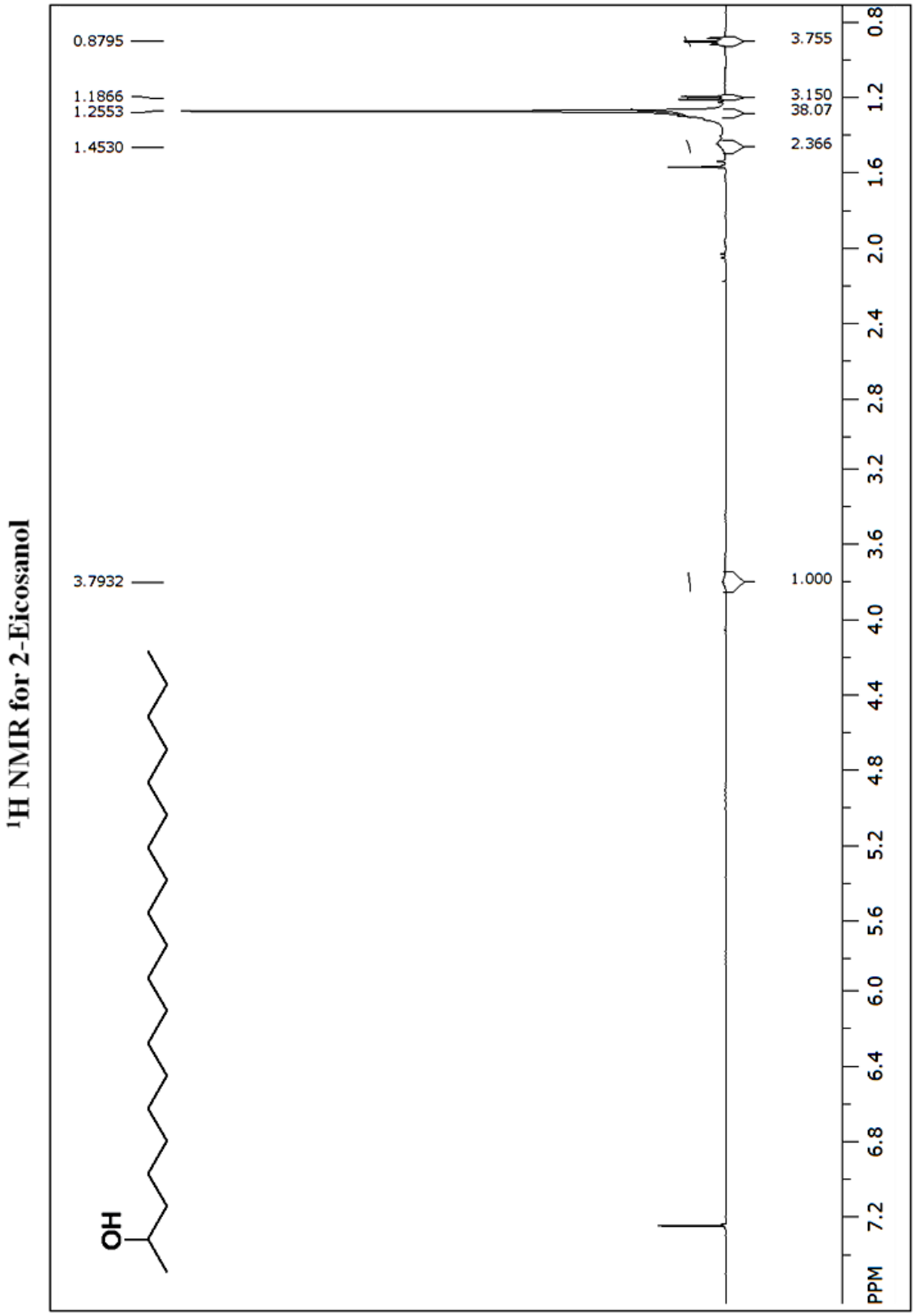

^{1}H NMR for 2-Eicosanol

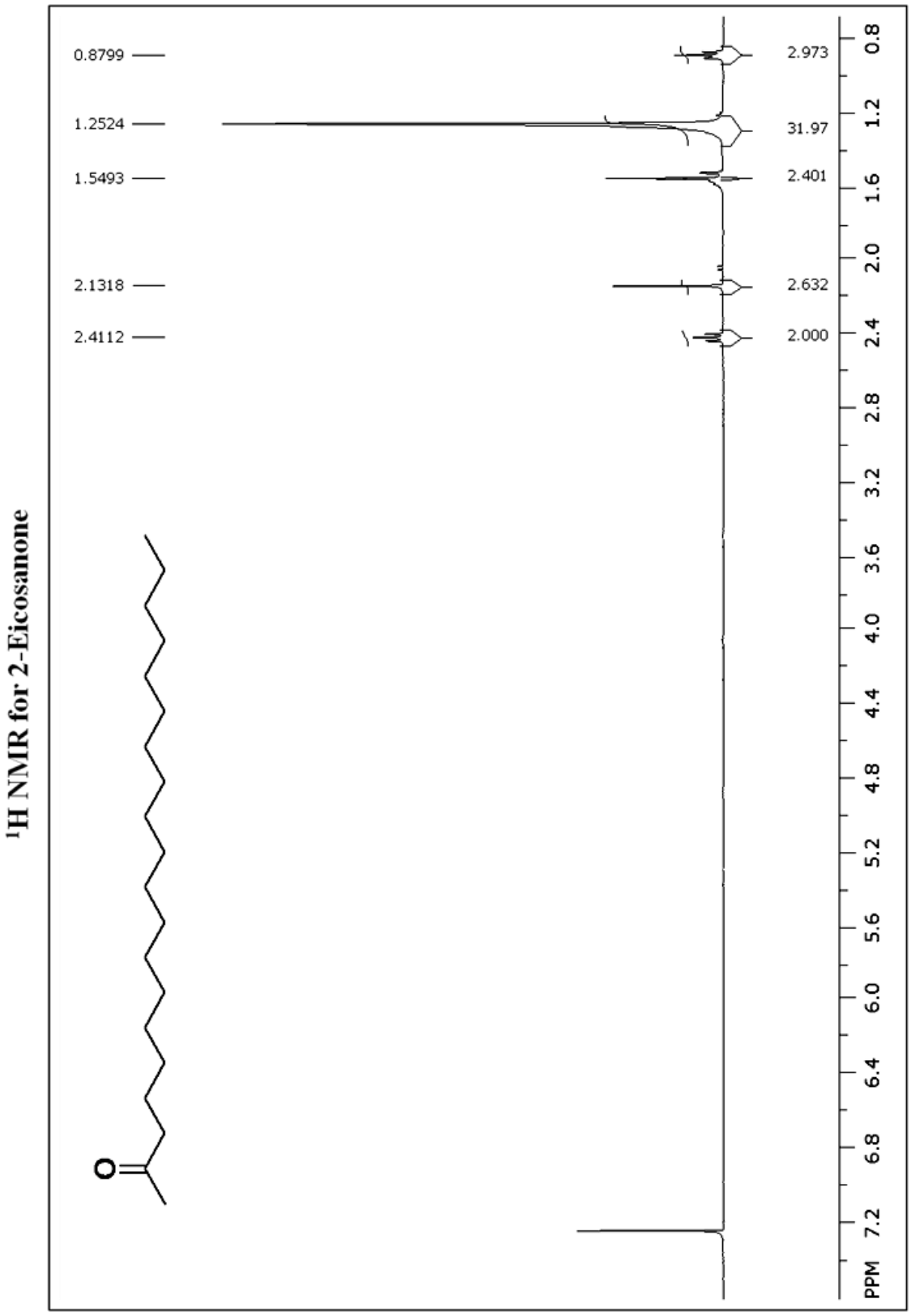

^{1}H NMR for 2-Eicosanone

^{13}C NMR for 2-Eicosanone